Reconstruction of the Behaviour of the Laurentide Ice Sheet using Satellite Imagery

Christopher D. Clark

Thesis submitted for the degree of:
Doctor of Philosophy

Department of Geology and Geophysics
Grant Institute

University of Edinburgh
July 1990

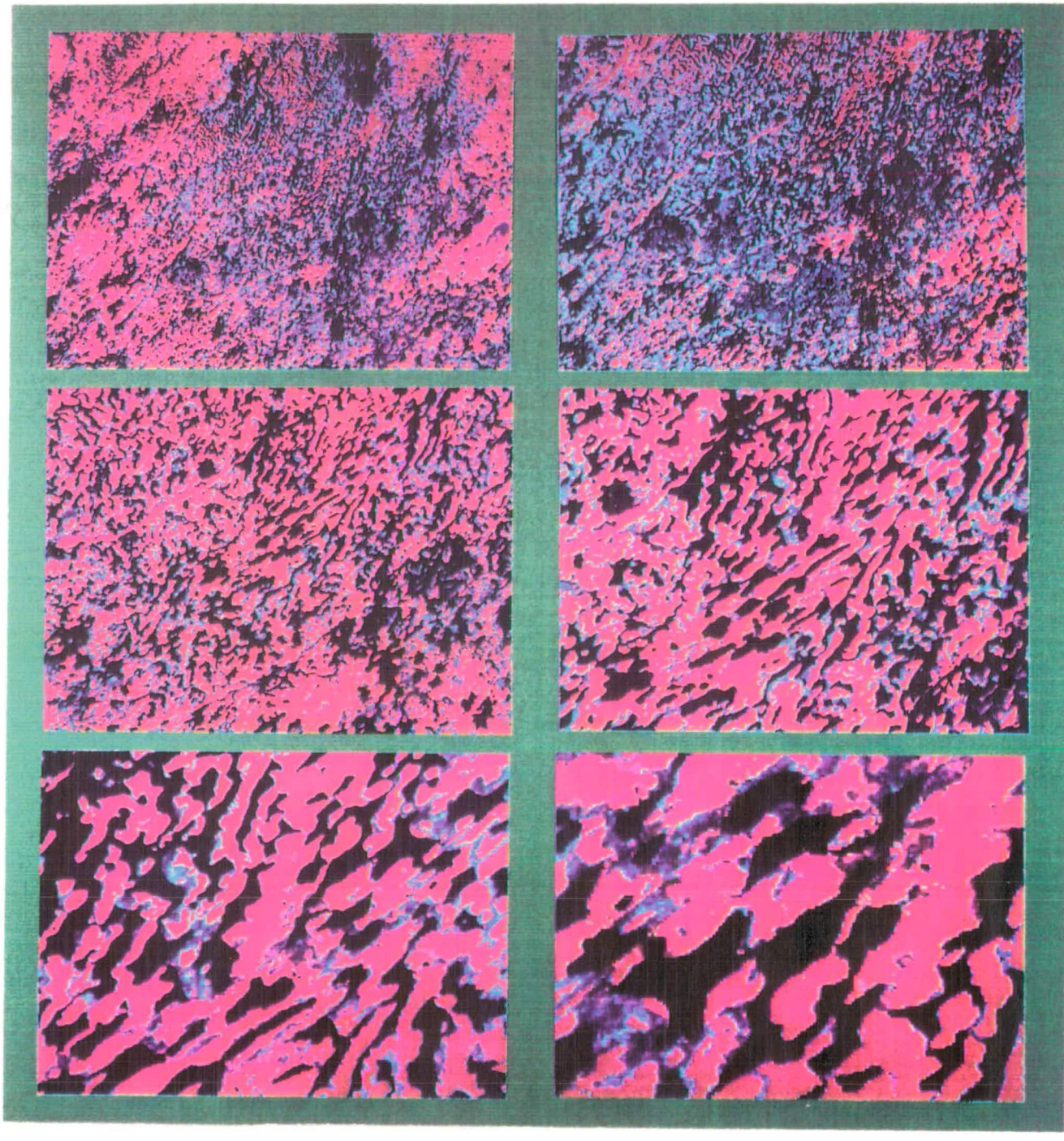

Frontispieces:

Cross-cutting pattern of drift lineations viewed from satellite. The six images show progressively zoomed extracts of a Landsat TM image: scale for top left image is 70 km across; bottom right, 5 km. Image processing (false colour composite, with a partial density slice at high intensities) was performed on a GEMSTONE 35 system.

Drift lineations produced by the flow of an overriding glacier. Oblique air photograph looking east from near Simpson Bay, southern Victoria Island, Arctic Canada.

Declaration:

This thesis has been composed by myself and the work within it is my own, except where otherwise referenced.

Chris Clark.

CONTENTS

Abstract

Examination of Landsat imagery of the bed of the last North American (Laurentide) Ice Sheet has revealed a previously undetected pattern of glacial streamlining. Superimposed, cross-cutting, sub-parallel sets of glacial lineations of the order of 2-50 km in length are found to be widespread. They are assumed to reflect successive phases of sustained ice flow, revealing major changes in the geometry of ice sheet flow.

Using six scales of remotely sensed imagery to map the lineations, and establish their cross-cutting relationships, permits relative ages of continent-wide ice flow phases to be determined.

Comparison of the principal ice flow sets with established stratigraphies suggests that the inferred shifts in ice flow occurred during the last (Wisconsinan) glacial cycle. The configuration of ice flow indicates that ice divides migrated by the order of a thousand kilometres.

The evolution of the Laurentide Ice Sheet through the Wisconsinan is reconstructed. There is evidence that during the Early Wisconsinan, ice sheet formation in Keewatin may have been independent of that in Labrador-Quebec, and that these two ice masses coalesced to form a major Early Wisconsinan ice sheet. The palaeo-ice flow evidence indicates that this ice sheet configuration consisted of a trans-Laurentide divide aligned NW-SE across Hudson Bay. Subsequently, the western sector decayed whilst the eastern dome remained stable (Middle Wisconsinan). An ice dispersal centre in the west reformed and fused with the eastern ice mass to form the Late Wisconsinan Ice Sheet. Decay of this ice sheet is well known from existing analyses.

The probability of strong coupling between ice sheet topography and atmospheric circulation suggests that the major changes in Laurentide Ice Sheet geometry must have been associated with large-scale atmospheric circulation changes. The corollary is that the high mobility of mid-latitude ice sheets may help explain the non-linear response of glacial climates to the insolation changes produced by external forcing.

Chapter 1

Introduction

Chapter 1

Introduction.

The largest ice sheet to grow and decay during the Quaternary climatic fluctuation between glacials and interglacials was the North American Ice Sheet. This ice sheet is first introduced, and then its global significance examined. Strategies for reconstructing such an ice sheet are briefly discussed. These include the utilisation of geological evidence provided by; glacial isostasy, palaeo-ice margins, glacial dispersal of indicator erratics, till fabric analysis, and linear ice flow indicators. The discovery and mapping of a hitherto unrecognised pattern of palaeo ice flow, and its relevance to the reconstruction of the last North American (Laurentide) Ice Sheet is introduced.

1.1 The Laurentide Ice Sheet and its global significance.

A large ice sheet complex covered much of North America during the last major cold phase (Wisconsin glaciation) of the Pleistocene Epoch. That part, stretching from the Queen Elizabeth Islands of Arctic Canada in the North, to the mid-western United States in the South, and from the eastern slopes of the Canadian Cordillera in the West to the continental shelf beyond Labrador in the East, is known as the Laurentide Ice Sheet, (see figure 1). It covered an area of approximately $1x10^7$ Km^2. Hughes *et al.* (1981) have estimated its maximum volume to have been $34.8x10^6$ Km^3. This is larger than the present volume of the Antarctic Ice Sheet.

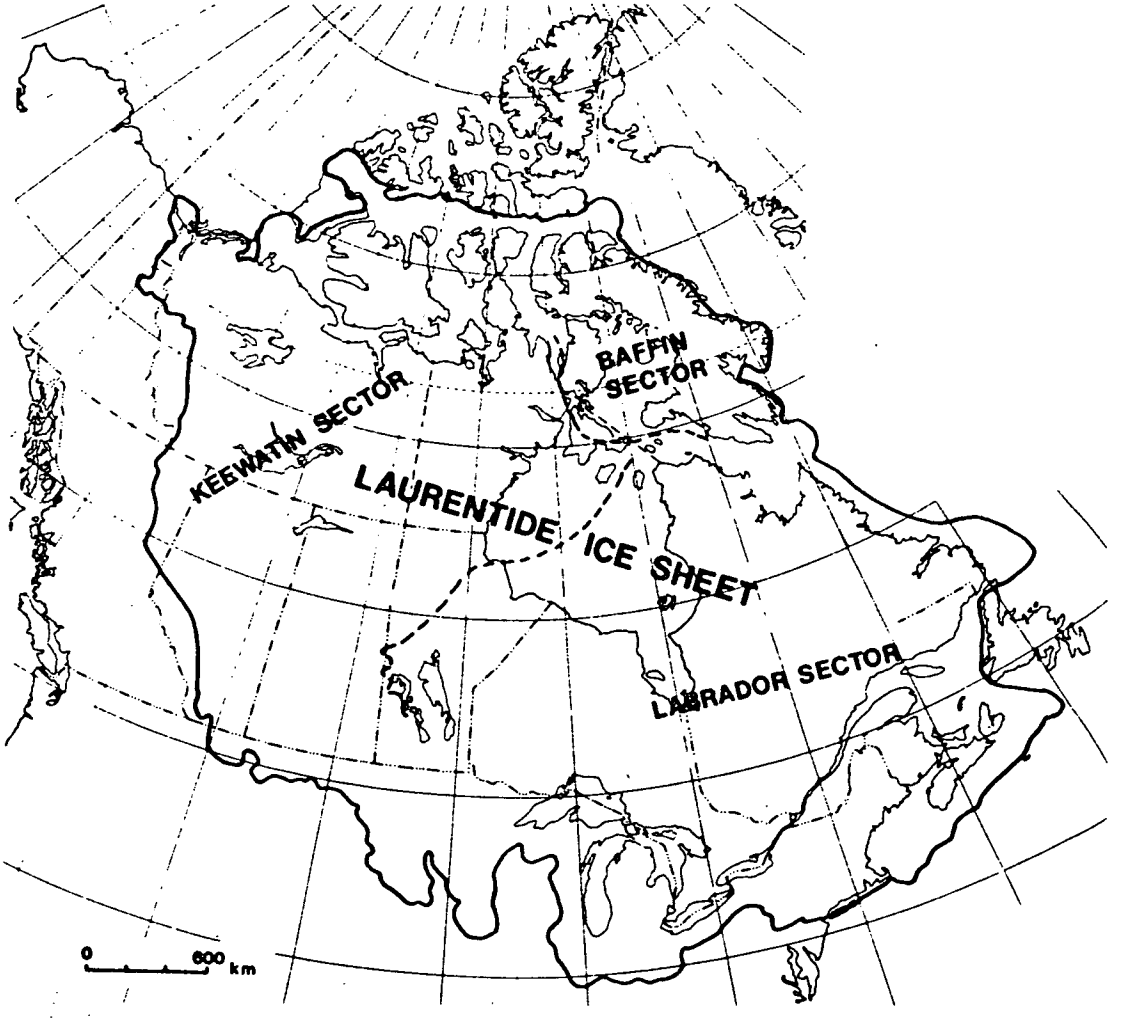

Figure 1. *Area covered by the Laurentide Ice Sheet (from Fulton and Prest, 1987).*

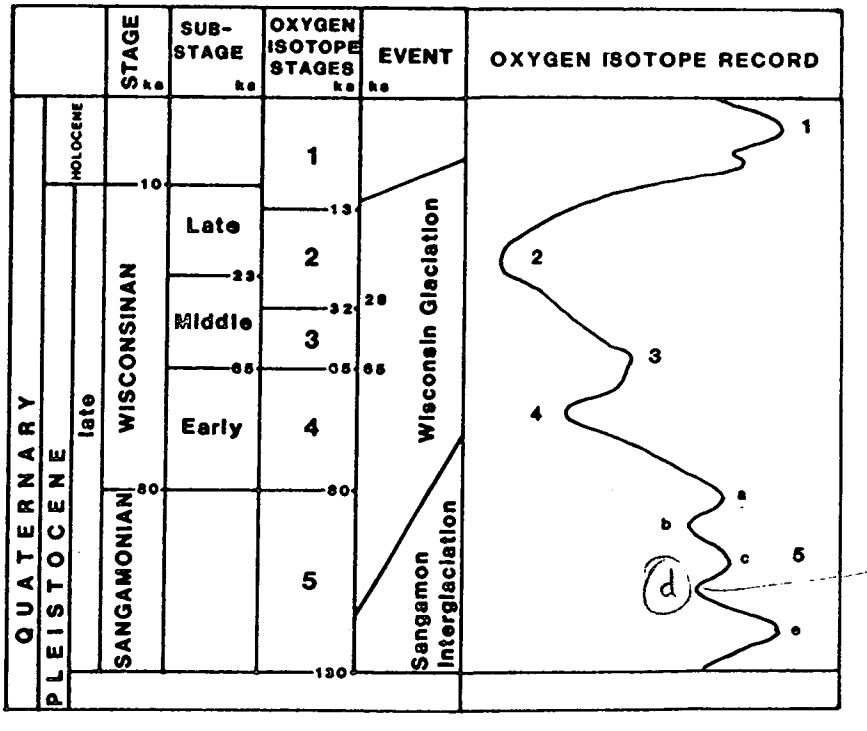

Figure 2. *Chronostratigraphic framework of the last glacial-interglacial cycle (from Fulton and Prest, 1987). The oxygen isotope signature (core v28-238, Shackleton and Opdyke, 1973) provides a proxy record of changing global ice volume.*

Initiation of the Laurentide Ice Sheet is thought to have occurred at around 120 thousand years before present (Ka BP). By 18 Ka BP it is believed to have grown to its maximum extent. Retreat resulted in its almost complete disappearance by 6 Ka BP. A tiny fragment of the former ice sheet remains as part of the Barnes Ice Cap on Baffin Island (Hooke, 1976). The chronostratigraphic framework for Canada for the last glacial-interglacial cycle, as defined by Fulton and Prest (1987), is used throughout this thesis and is illustrated in figure 2.

The Laurentide Ice Sheet covered much of North America for a period of about 100,000 years, profoundly re-arranging the surface, and leaving a distinctive geologic and geomorphic legacy. However, the Ice Sheet also had a significant influence on global climate (the coupled atmosphere-ocean-ice sheet system). Herein lies its wider significance.

The oxygen isotope ratios obtained from benthic foraminifera from deep sea cores are believed to produce a proxy record of global ice volume, (Shackleton and Opdyke, 1973, see figure 2). Postulated ice volumes of the world's major ice sheets, both at the present day and at the maximum of the last glacial period are indicated in the table below.

	VOLUME (10^6 km^3)		GLACIAL-INTERGLACIAL CHANGE	
ICE SHEET	PRESENT	ICE AGE MAXIMUM	VOLUME (10^6 km^3)	% OF TOTAL
Laurentide	0	34.8	34.8	66%
Eurasian	0	13.3	13.3	25%
Antarctic	30.0	34.0	4.0	7%
Greenland	2.6	3.5	0.9	1%

[Based on Flint (1971); Drewry (1982); Oerlemans and Van der Veen (1984)]

It is clear that the main net change in ice volume between the last glacial and interglacial

is due to the Laurentide Ice Sheet and that, therefore this must be the primary modulator of the curves of oxygen isotope records. Changes in Laurentide Ice Sheet volume are recorded in ocean chemistry from deep sea cores as widely spaced as the Pacific, Atlantic, and Caribbean Oceans.

The existence of a large ice sheet over North America provides two main inputs to the general circulation system; increased area of high albedo, and an orographic perturbation of the planetary wave system (Rossby waves). The albedo effect provides a strong positive feedback mechanism, intensifying glaciation beyond the bounds predicted by orbital forcing alone (Birchfield and Weertman, 1983). Planetary waves are regarded as being primarily controlled by orography (Charney and Eliassen, 1949; Bolin, 1950). Ruddiman and Raymo (1988) believe that the Tibetan plateau and the North American Cordillera provide the main controls on Rossby wave formation during interglacials. The summit height of the Laurentide Ice Sheet extended up to 3.5 Km (Denton and Hughes, 1981). This is between one third and one fifth of the height of the topopause and therefore, as Kutzbach and Wright (1985) and Broccoli and Manabe (1987) have shown, the presence of a large ice sheet acts as a major tropospheric perturbation breaking up the interglacial pattern of zonal westerly flow, and splitting the jet stream around the southern and northern margins of the Laurentide Ice Sheet. The equatorward advection of cold air forced by ice sheet topography provides strong feedback by helping to preserve winter snow cover, increasing the land-ocean temperature gradient, and thereby influencing sea-ice extent, sea surface temperature, cyclone tracks and precipitation patterns (Ruddiman and MacIntyre, 1981; Muszynski and Birchfield, 1987).

In the study of climatic change on a 100,000 year time scale the Laurentide Ice Sheet is a crucial link in the ice-ocean-atmosphere system that cannot be ignored.

Looking to the future of our Earth's climate, it is important that we gain an understanding of how our contemporary ice sheets, in particular the West Antarctic Ice Sheet, are likely to modulate the current climatic trend, and affect global sea level (Fastook, 1984). Because the timescale of scientific discovery is at least three orders of magnitude less than the timescale of large ice sheets, we are unlikely to be able to ascertain the temporal dynamics of our contemporary ice sheets simply because we cannot observe them for long enough. This problem may be solved by studying the Laurentide Ice Sheet, which through the geological and geomorphic evidence it left behind, provides a key to reconstructing its behaviour on a timescale compatible with its life-span. It is hoped that this thesis and associated publications (Clark and Boulton, 1989; Clark, 1990; Boulton and Clark, 1990a; Boulton and Clark, 1990b) will contribute to our knowledge of how ice sheets behave over timescales of tens of thousands of years, and how they modulate climate and maybe ultimately our future.

1.2 Strategies for Ice Sheet Reconstruction.

Given that large, mid-latitude ice sheets grow in response to global cooling and provide an important modulating effect on the climatic change that initiates them, it is important that we understand the behaviour of ice sheets as a precursor to understanding the actual mechanisms of climatic change on a 1,000,000 year timescale.

Research over the last century has produced information that permits us to reconstruct fragments of the behaviour of the Laurentide Ice Sheet in time and space. There are models for the whole of the ice sheet for specific time-slices, mostly based at the presumed maximum extent at 18 ka. Many assume steady state dynamics, and often

simplify the geologic input, i.e. margin positions determined by geologic evidence have been assumed synchronous, or drumlins indicating ice flow directions have been assumed to have formed synchronously at 18 ka.

Most published models of the Laurentide Ice Sheet portray different representations of ice sheet form and dynamics; there is no consensus. I believe these differences may be explained by the varying emphasis placed on the four primary parametric inputs to ice sheet models: glacial geology; glaciological theory; glacial isostasy; and palaeoclimate.

The following sections critically describe the geologic inputs that have been used in reconstructing the Laurentide Ice Sheet.

1.2.1 Glacial Isostasy.

Raised shorelines are common around the coast of Canada, especially in the Hudson Bay area. They occur as ridges parallel to the coast, up to 80 Km inland and 120 metres above present sea level. Emergence of these shorelines chronicles the isostatic recovery of the lithosphere since the disappearance of the Laurentide Ice Sheet. Where prominent shorelines of the same age can be found in different areas, it is possible to construct an isobase map which indicates the pattern of postglacial rebound (see figure 3, Andrews, 1970). The map shows maximum rebound to the S.E. and N.W. of Hudson Bay, and these areas have been taken to represent the loci of maximum loading by the ice sheet. Geophysicists have applied the shoreline isobase data to complex models of lithospheric response, and have produced reconstructions of the surface form and mass of the Laurentide Ice Sheet (Peltier, 1981, Peltier *et al.* 1978, Clark, 1980). A reconstruction

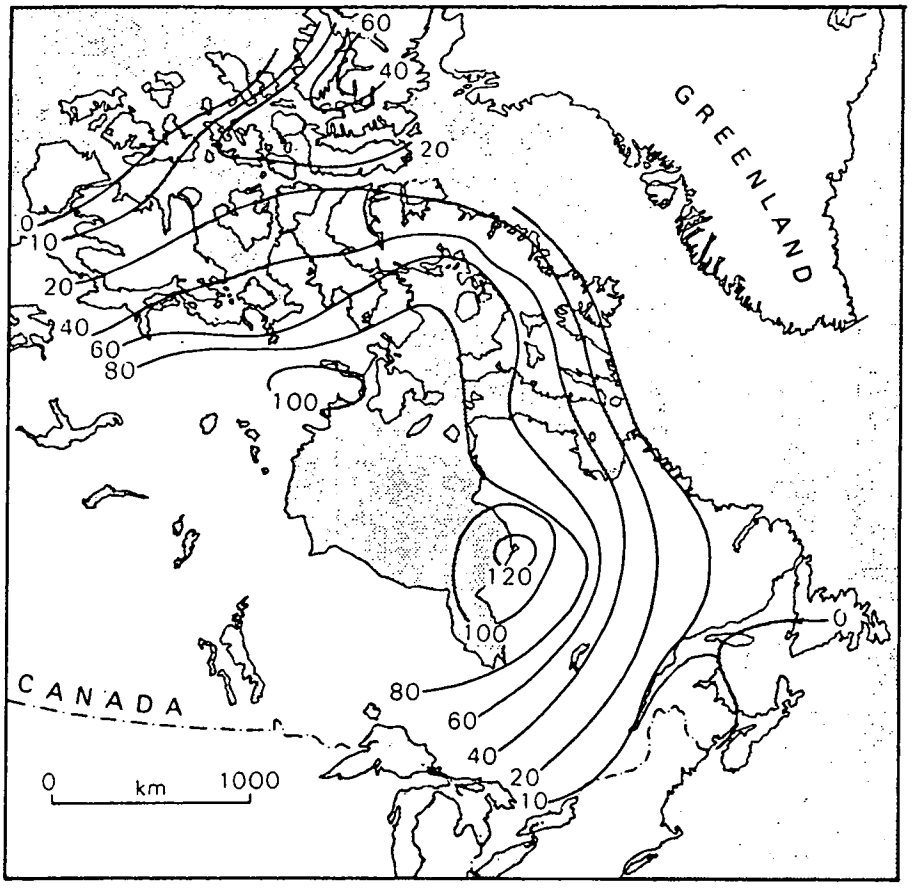

Figure 3. *Isobase map documenting the pattern of shoreline emergence (in metres) since 6000 years BP (after Andrews, 1970)*

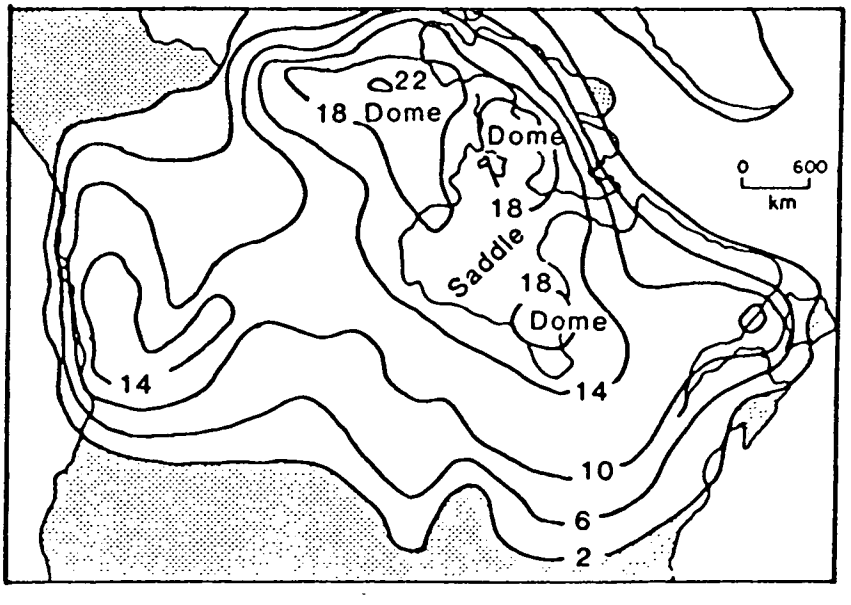

Figure 4. *Ice thickness (contours in hundreds of metres) of the Laurentide Ice Sheet at 18 ka BP, as reconstructed by the isostasy-based ICE-3 model of Peltier (1981).*

called ICE-3, produced by Peltier (1981) is illustrated in figure 4 and shows the modelled centres of mass, or ice domes of the Laurentide Ice Sheet.

However, ice domes can migrate and as isobase data only reflects average loading integrated over time, it follows that a unique solution for ice sheet reconstruction is not possible.

Although definitive reconstructions of the Laurentide Ice Sheet are not considered possible solely through glacio-isostatic modelling, they still have an important part to play in ice sheet reconstructions. Progressive flexure of the lithosphere beneath an ice sheet can alter the relative areas of ablation and accumulation so as to change the mass balance and thereby lead to a change in ice sheet volume, and it can also affect the susceptibility of the ice sheet to marine drawdown.

1.2.2 Palaeo-ice margins.

End moraines mark glacier extent at the time of moraine formation. Geochronometric techniques have enabled some moraines of the Laurentide Ice Sheet to be dated (Bryson *et al.* 1969; Prest, 1969; Flint, 1971; Dyke and Prest, 1987). In these cases the perimeter of the Ice Sheet is fixed in both space and time, thus forming an important reference point for ice sheet reconstructions.

Bryson *et al.* (1969) and Dyke and Prest (1987) produced maps of morainic systems of the Laurentide Ice Sheet, and used available dates to produce interpolated isochrones for the retreat of the ice sheet from its maximum position (see figure 5). Most of the

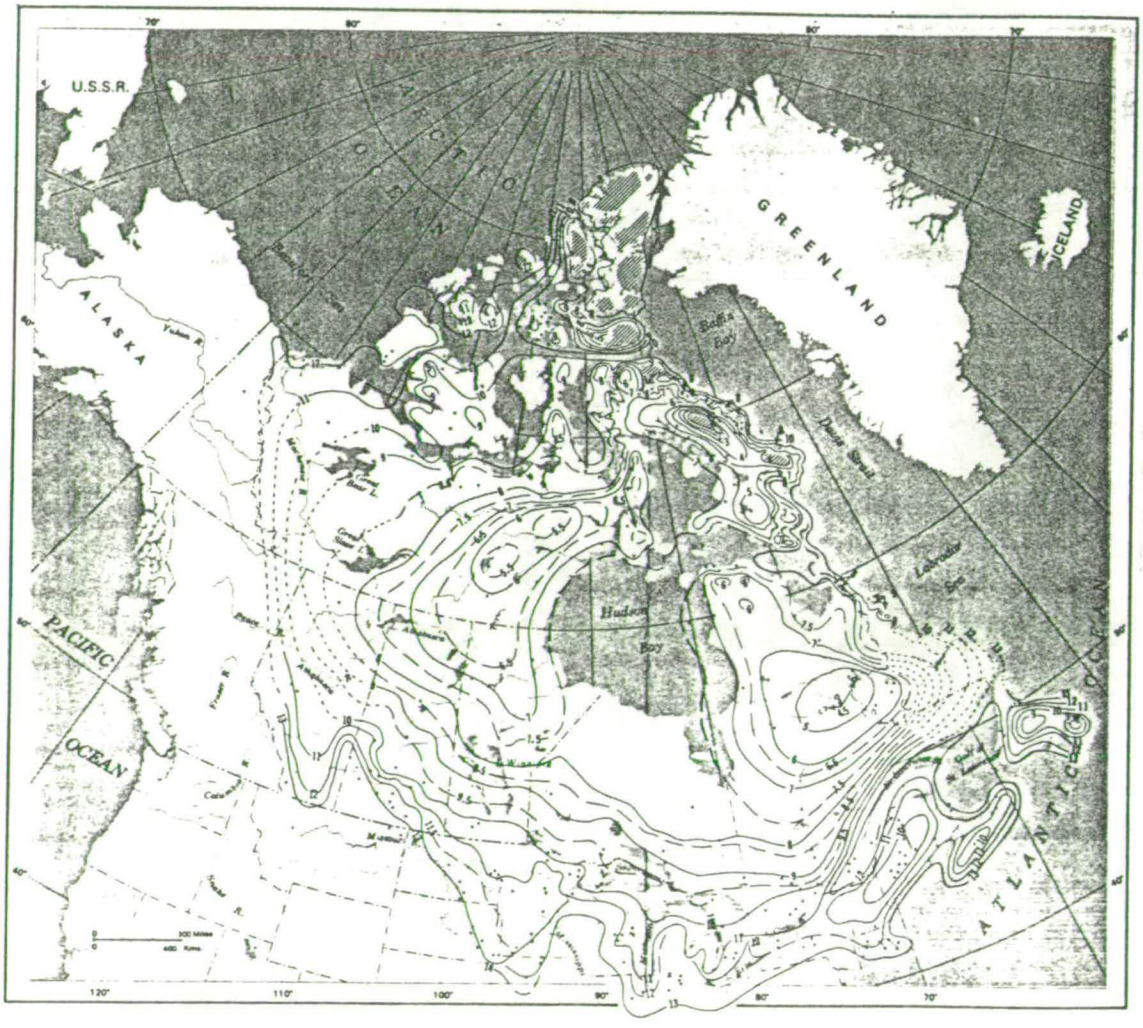

Figure 5. *Radiocarbon isochrones of the retreat of the Laurentide Ice Sheet. Isochrone location is based on radiocarbon dates, coastline location, moraine orientation, and other field evidence. (from Bryson et al, 1969).*

morainic evidence is either for the maximum extent, particularly in the American Mid-West and the Yukon, or for some readvance moraine systems which formed at about 10 ka BP. A large degree of interpolation was required to produce their reconstruction, as limits of ice extent which are both spatially and temporally fixed, are sparse. However it is the most recent synthesis for Laurentide Ice Sheet retreat, and incorporates all of the currently available dated stratigraphies.

The earliest mathematical models of the surface form and dynamics of the Laurentide Ice Sheet were applied to its assumed maximum extent as marked by moraines. Using this approach Sugden (1977) calculated basal ice velocities and thermal characteristics of the ice sheet. The surface form of these first generation ice sheet models (e.g. Sugden, 1977; Denton and Hughes, 1981) are illustrated in figures 6 and 7. They used the most extensive Wisconsinan moraine systems and assumed them to be synchronous with the volume maximum at 18 Ka BP.

However, research on the stratigraphy and age context of deposits around the ice sheet margin have since shown that the maximum extent in all sectors was not synchronous, but occurred at different times at different locations (Grant, 1977; Stalker, 1977; Rampton, 1982; Clayton and Moran, 1982; Fullerton and Colton, 1986; King and Fader, 1986; and Bonifay and Piper, 1988). This invalidates the first generation of models. The asynchrony of the margin positions is discussed in detail by Boulton (1979) and Dyke and Prest (1987).

Even if margin positions for a particular time slice were known I argue that it would not be possible to determine a unique configuration of ice domes and divides from this data

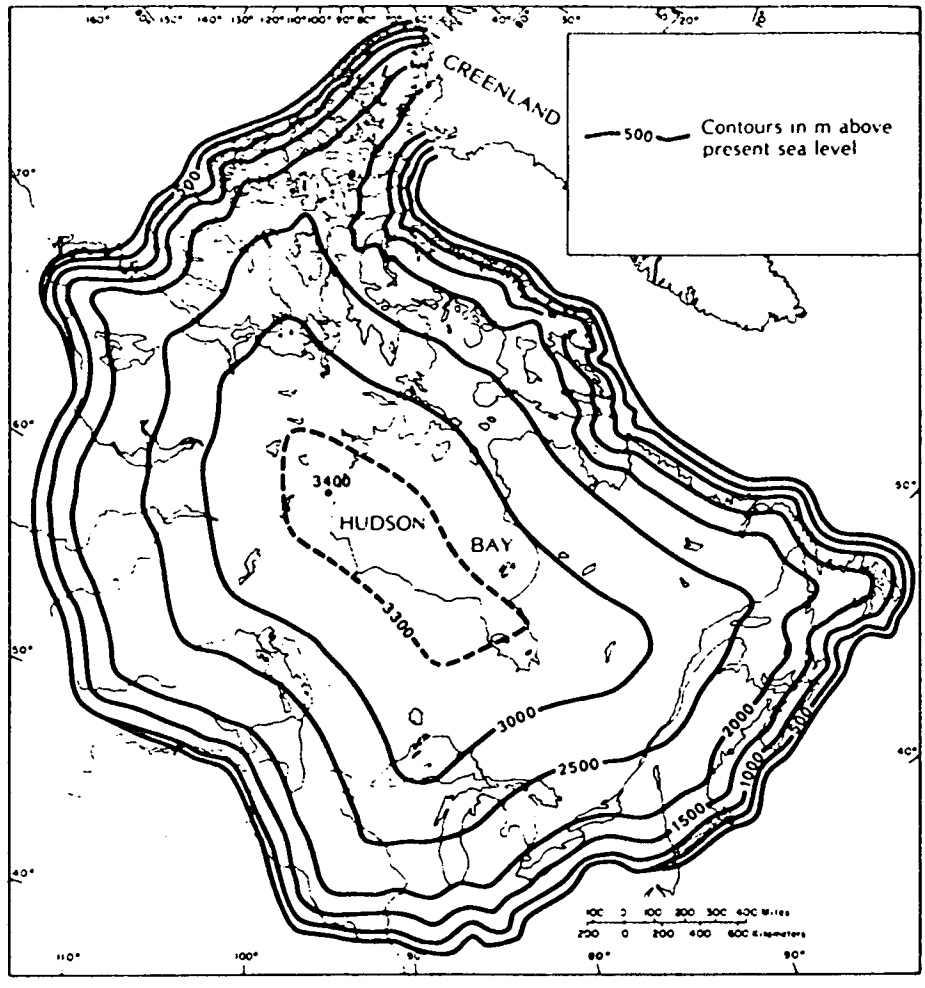

Figure 6. *Modelled surface morphology of the Laurentide Ice Sheet at its maximum Late Wisconsinan extent (from Sugden, 1977).*

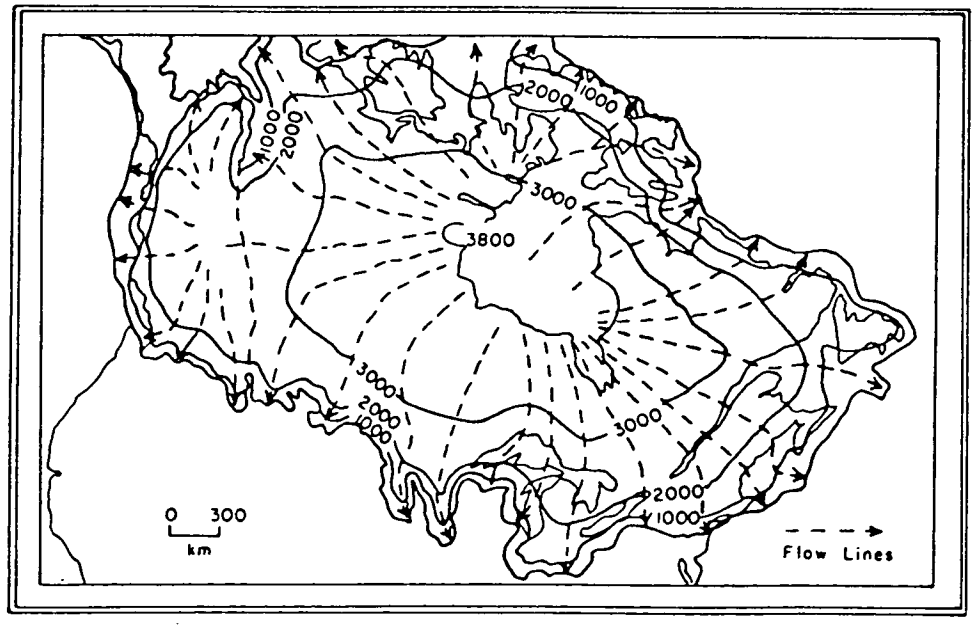

Figure 7. *Modelled surface morphology and ice flow lines of the Laurentide Ice Sheet at its maximum Late Wisconsinan extent. (from Denton and Hughes, 1981).*

alone. Modern ice divides (e.g. on the Antarctic Ice Sheet or Vatnajokull) do not bear simple relationships to the margins of ice sheets.

1.2.3 Glacial Dispersal of Indicator Erratics.

Following de Saussure (1796), who coined the phrase *terrain erratique* to describe material of distant origin overlying areas of local bedrock, the term erratic is widely used in glacial geology to describe the same phenomenon. Indicator erratics (Fairbridge, 1968), are those foreign materials (from millimetres to tens of metres in size) that have a distinctive enough lithology for them to be traced to their original source.

Erratics are typically distributed in narrow fans with the apex positioned at the outcrop and material spreading out in the direction of glacier flow (Peach, 1909). There is normally an exponential decrease in frequency of erratic material away from the source area. However, erratics from the Canadian Shield have been traced for distances of over 1200 Km (Flint, 1971).

Erratic evidence can help in the reconstruction of flow lines within an ice sheet. To my knowledge no model or reconstruction of the Laurentide Ice Sheet has been solely based on erratic dispersal patterns, but they have been used to support or refute reconstructions. Shilts *et al.* (1979), and Shilts (1980) used the observed erratic pattern, coupled with the length of time required for transportation, to refute the previous school of thought (Flint, 1971; and Denton and Hughes, 1981) regarding the single-domed Laurentide Ice Sheet configuration. They combined erratic dispersal data with other indicators of ice flow (striae, drumlins etc.) and presented an alternative view of ice sheet configuration (multi-

dome) (see figure 8). Boulton *et al.* (1985) developed a mathematical model that simulated erratic dispersal under a single domed ice sheet and discovered dispersal pathways strikingly different to those formed in reality, further disproving the validity of the single dome model.

The difficulty in making ice sheet reconstructions from erratic evidence is twofold:

1) evidence is lithology/location dependent, and thus spatially restricted, i.e. not ice sheet-wide.

2) transport of erratics may have occurred in two or more successive phases of ice movement, and the flow direction may have been different for each phase. In these cases the apparent erratic dispersal paths may be hiding more complex multi-phase flow directions, and yet simple uni-phase flow lines may be erroneously inferred.

Solutions to this second problem may be found by using erratic data in conjunction with other ice flow evidence. A recently developed technique, the Total Transport Distance (TTD) method (Salonen, 1986; Bouchard and Salonen, 1989 and *in press*), may be able to differentiate between multi-phase and uni-phase dispersal events. This method using average transport distances at specific sites was tested on dispersal trains thought to have formed as a result of the Cochrane re-advance surge (uni-phase) and the main Late Wisconsinan ice flow (multi-phase, multi-directional) in the James Bay Lowlands. If this technique enables other uni-phase and multi-phase dispersal paths to be differentiated, it may alleviate the problem of interpreting successive movements of erratics.

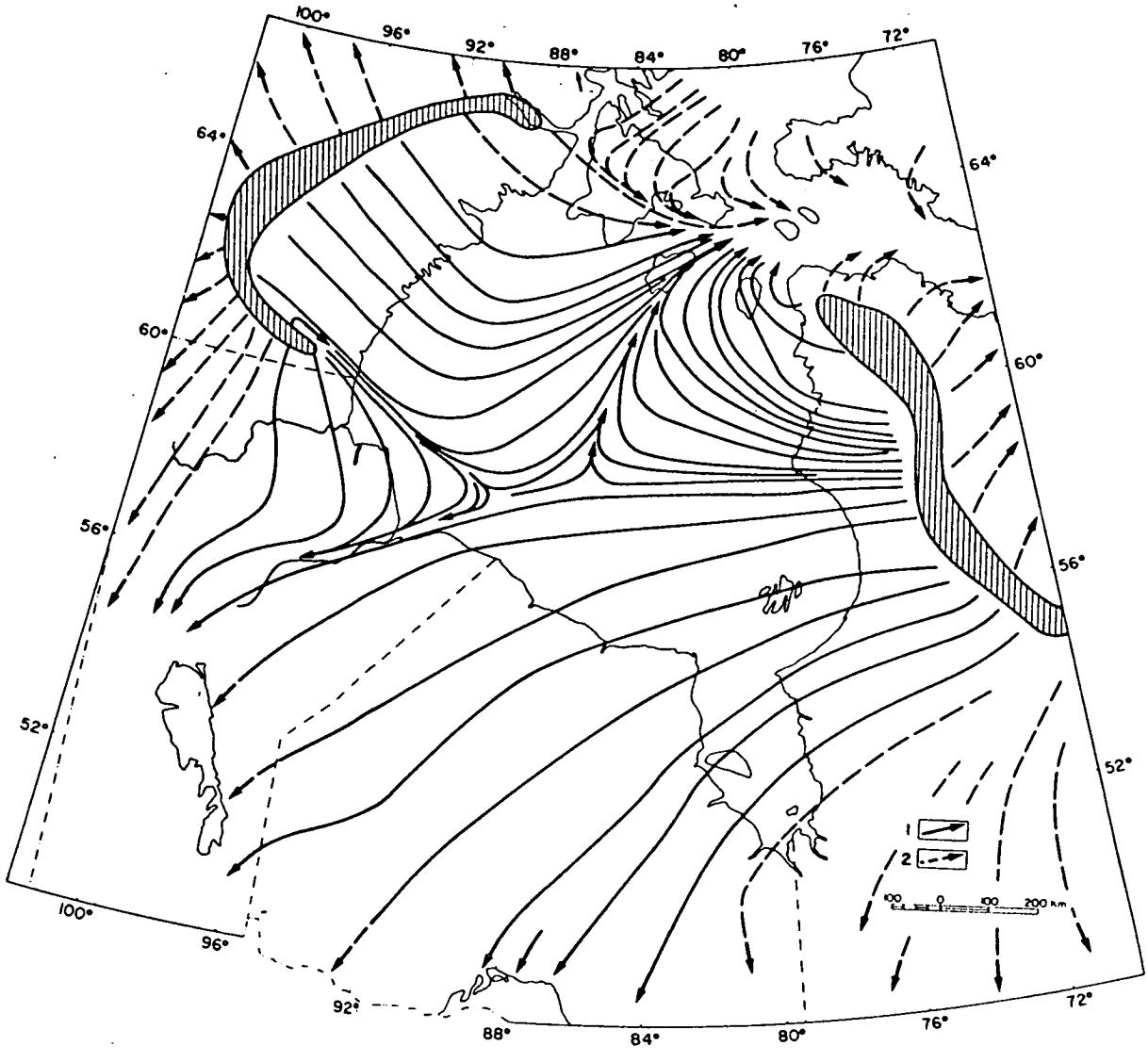

Figure 8. *Reconstructed ice flow lines and ice divides of the central portion of the Laurentide Ice Sheet (Shilts, 1980). 1 = flow lines based on ice moulded lineations and, or erratic dispersal patterns. 2 = flow lines based on trends shown on the Glacial Map of Canada (Prest et al, 1968).*

1.2.4 Till Fabric.

Till clasts often show a preferred orientation related to the direction of ice movement (Miller, 1884; Holmes, 1941; and Glen *et al.* 1957). Field measurement of till fabrics has enabled many workers to reconstruct former ice flow directions. It is a particularly useful technique when dealing with multiple till sequences, because ice flow directions for each till can be determined from a single section (e.g. Dredge and Nielson, 1985).

However, the time-consuming nature of till fabric analyses has meant that few sites can be investigated when compared to the size of the ice sheet. They must be regarded as point data from a large spatial continuum, and require a framework to structure them. For this reason it has not been a useful technique for reconstructing continental scale ice movements and has been restricted to local studies (up to a few hundreds of Kilometres).

Other problems associated with fabric analyses are that subsequent ice flows may cause a re-orientation of previously deposited tills (this is discussed in more detail in Section 3.3). It is also crucial that the till in question is positively identified as a lodgement till. Flow tills for example may also display a fabric, but one that has no relation to the regional ice flow direction (Boulton, 1971).

1.2.5 Linear Ice Flow Indicators.

Linear morphological forms aligned parallel to former ice flow direction are common. They exist on a number of scales from striae, which are typically centimetres in length, through to flutes and drumlins, which are of the order of tens and thousands of metres in length.

Striae.

Striae document former ice flow directions, and sometimes occur as cross-cutting sets representing multi-phase ice movements (e.g. Virkkala, 1960; Stromberg, 1972; Vorren, 1977; and Veillette, 1986).

In an area south of James Bay, Veillette (1986) made 300 measurements of cross-striated sites revealing three directions of ice flow, and ascertained their relative age. This evidence was examined in conjunction with published work on the stratigraphy and erratic dispersal patterns of the area. He concluded that a west-southwest flow direction was of an Early Wisconsinan or pre-Wisconsinan age, and that a south-southwest ice flow direction represented glacier movement during the last glacial maximum. A further, southeast flow was assigned to the final deglaciation of the area. To discuss these changes in direction of ice flow, Veillette resorted to previously hypothesized models of the Laurentide Ice Sheet to provide a framework in which to operate. He was able to demonstrate major shifts in ice flow and to relate them to regional erratic movements. Unfortunately, valuable work such as this is only available for a local area (300 by 500 Km), and so it is only possible to modify current views on ice sheet configuration, rather than to use striae as a basis for a temporally integrated ice sheet reconstruction.

Many have been sceptical about the theory that several orientation sets of striae may reflect regional changes in ice flow. Their concern is due to the potential (as pointed out by Demorest, 1938) for complex and synchronous patterns of basal ice flow to occur around local bedrock protuberances. As a consequence many field-workers have only recorded the dominant direction, explaining differently oriented striae as being due to local topographic effects. Veillette (1986) has shown that the differently oriented and less obvious striae do in fact form coherent and integrated flow directions. The corollary to

this is that the local bedrock protuberance argument (Demorest, 1938) has probably been responsible for a large loss in ice flow evidence (i.e. the unrecorded striae).

Drumlins, Megaflutes and Flutes.

Drumlins, flutes and mega-flutes are morphological terms for streamlined linear sedimentary ridges produced parallel to former ice flow. Flutes have typical spacings of 1-10m, with length of 10^2-10^3m; drumlins and megaflutes have spacings of 10-10^3m, and lengths between 10^2-10^3m (drumlins), and 10^2-10^4m (megaflutes). The scale of these palaeo ice flow indicators allows them to be readily observed on air photographs.

In comparison with the other indicators of former ice flow already discussed, drumlins, flutes and megaflutes provide a much more powerful tool for ice sheet reconstruction because they are contiguous, and so less interpolation is required (c.f. striae). Former ice flow direction can also be identified from air photographs and so can be used to acquire an almost continent-wide pattern of ice flow. This is extremely important because information on former ice flow is then on a scale similar to that of the Ice Sheet. The disadvantages of few investigated sites for field-based studies does not apply here. Prest *et al.* (1968) were aware of this potential for ice sheet reconstruction and undertook the enormous task of mapping drumlins and flutes from air photographs for the whole of Canada. Figure 9 shows the mapped drumlin orientation and distribution for the western portion of Arctic Canada. These lineations were incorporated on the Glacial Map of Canada (Prest *et al.* 1968, MAP 1253A), which has provided a basis for many subsequent reconstructions of the Laurentide Ice Sheet.

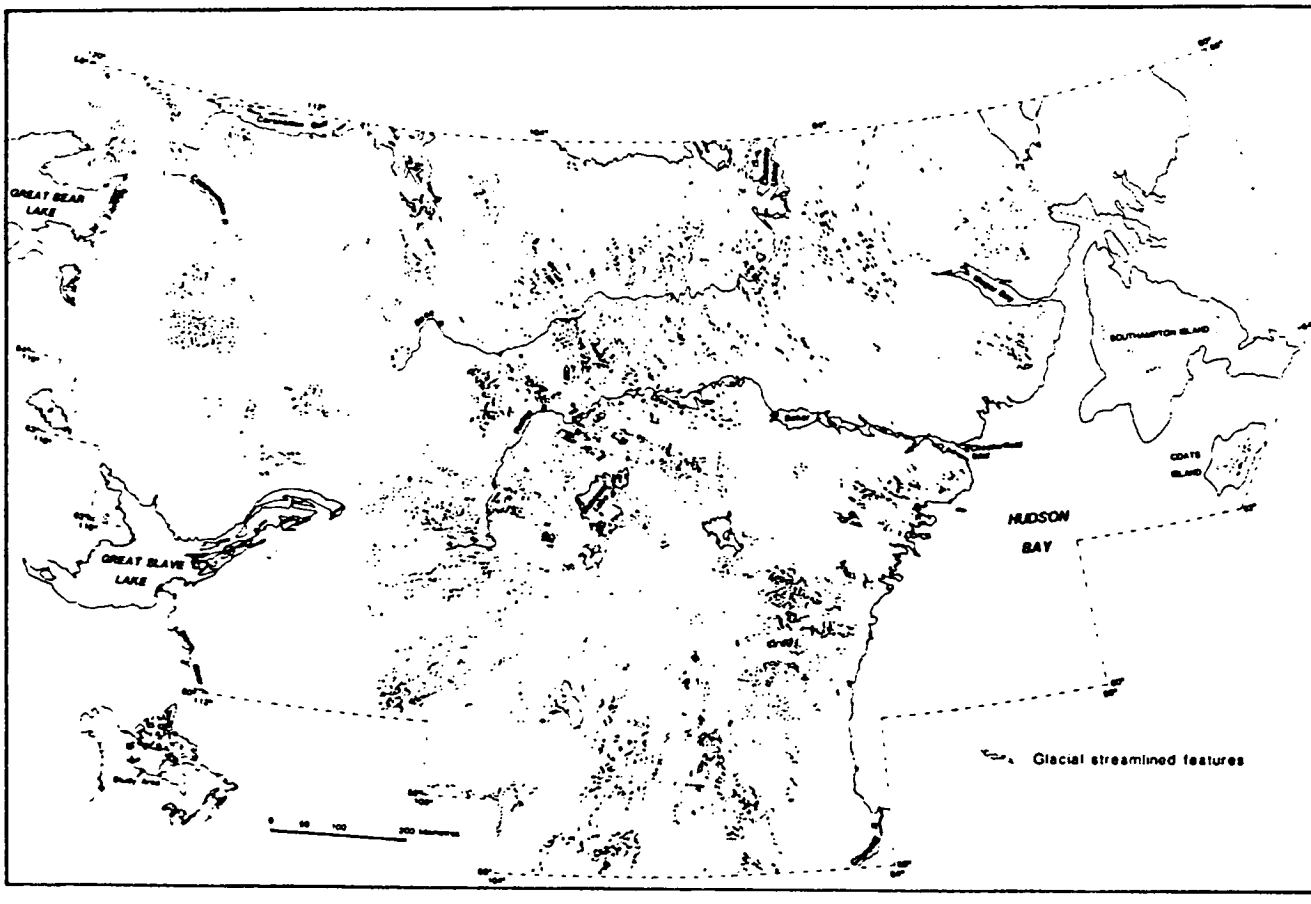

Figure 9. *Distribution of drumlins and other ice moulded drift lineations for the Keewatin sector of the Laurentide Ice Sheet (from Shilts et al, 1987).*

The age of the drumlins are unknown, but the following logic was applied by Prest (1984):

1) Drumlin genesis only occurs under fast moving ice.

2) When the Laurentide Ice Sheet was at its maximum extent, basal ice velocities were high enough to mould drumlins.

3) When the Ice Sheet was in retreat the ice velocities were too low to form new drumlins and the erosive power too small to disrupt the existing pattern.

Given that the observed drumlin pattern formed roughly synchronously with the Late Wisconsinan glacial maximum (18 Ka), Prest (1984) was able to draw ice sheet flow lines based partly on drumlin orientation and partly on the assumption that the margin lay normal to the flow direction. This reconstruction of flow pattern, ice dome configuration and margin position is illustrated in figure 10.

Using a different set of assumptions regarding the date and synchroneity of formation of the drumlin pattern, Boulton *et al* (1985) produced a very different reconstruction. They noted that basal velocities are highest just behind the glacier terminus, and therefore assumed that the majority of drumlins were formed beneath the retreating glacier margin. In this way the continent-wide pattern of drumlins was not interpreted as a roughly synchronous flow stage, but as a radially time-transgressive pattern. The drumlins that formed near the maximum extent dated from 18 ka, and within this belt they formed a concentric succession of sub-marginal flow patterns, with the youngest drumlins being formed under a much smaller ice sheet at 6 ka (see figure 11).

The advantage of using drumlins and flutes for ice sheet reconstructions lies in their ability to provide ice sheet-wide flow patterns. However, as discussed above, different

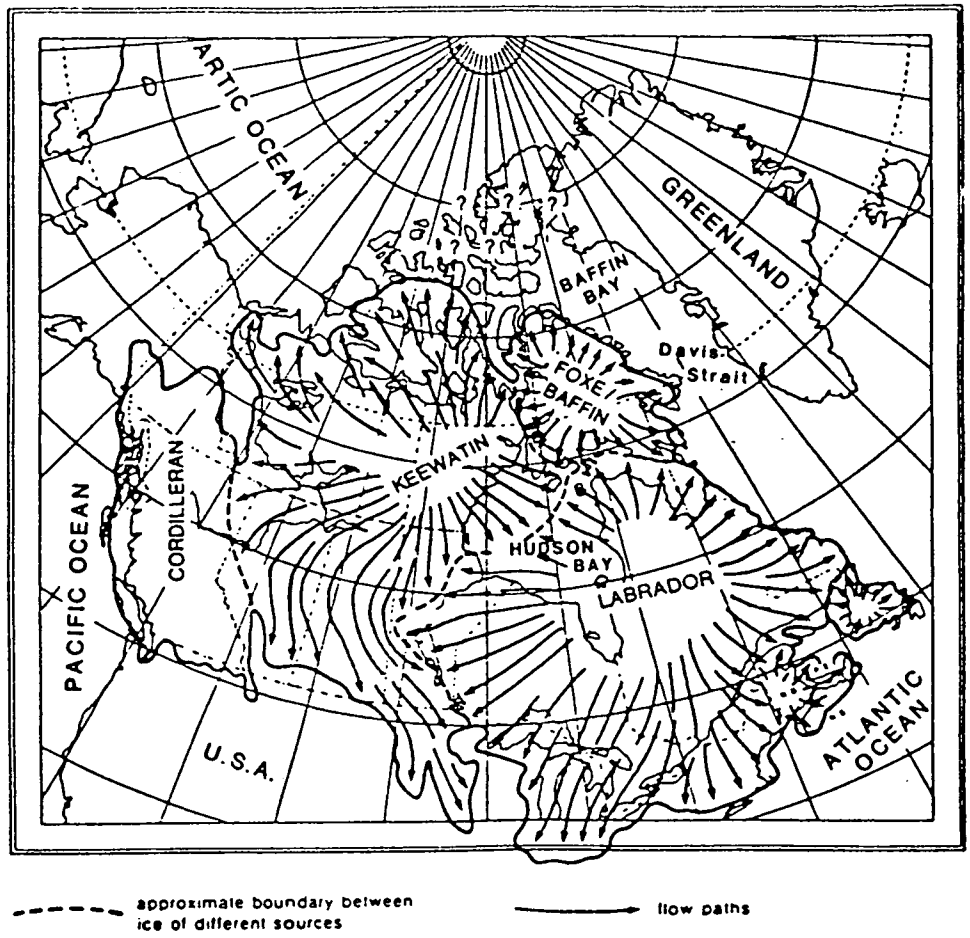

Figure 10. *Simplified flow pattern and ice dome configuration of the Laurentide Ice Sheet at 18 ka, as reconstructed from drumlin orientations by Prest (1984). (from Andrews, 1987).*

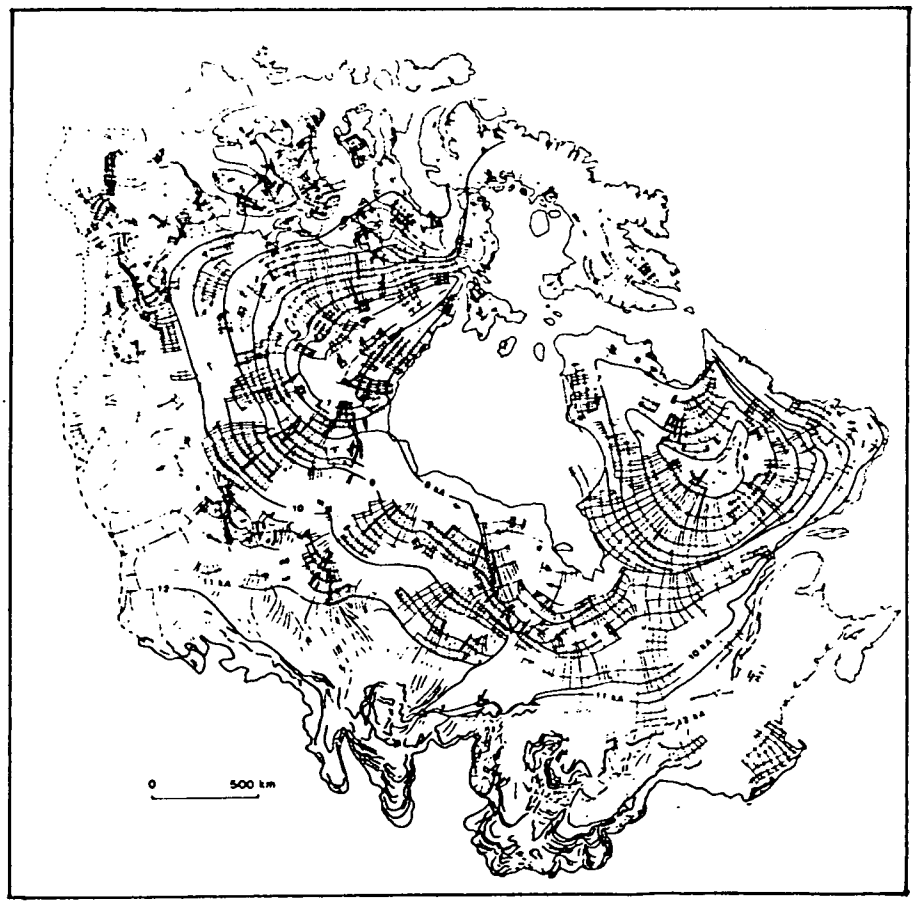

Figure 11. *The radial pattern of ice moulded lineations mapped by Boulton et al (1985). This pattern was presumed to be related to ice sheet decay, which is illustrated by isochrones calibrated by radiocarbon dating.*

views of their relative ages leads to quite different conclusions; one model of maximum glaciation and one of deglaciation.

1.3 New Discoveries of Palaeo-Ice Flow Patterns.

Detailed examination of the glacial geomorphology portrayed on Landsat images has led to two major discoveries:

A) MEGA-SCALE GLACIAL GRAIN:

The first discovery is that a hitherto unrecognised pattern exists and is widespread within glacially streamlined drift. I refer to this pattern as the **mega-scale glacial grain**. The discovery of this grain represents an important breakthrough in that it documents former directions of ice flow in a way that is far more extensive than that expressed by drumlins and flutes alone.

B) CROSS-CUTTING RELATIONSHIP.

The second discovery relates to the topological pattern displayed by these large palaeo-ice flow indicators. During the course of mapping the mega-scale glacial grain, it became apparent that in many cases, what at first appeared as a confusing background noise, was in fact the degraded form of a former ice flow pattern. On closer inspection it was discovered that mega-scale glacial lineations and the overall mega-scale glacial grain frequently show cross-cutting relationships, both with themselves and with other glacial lineations of a different scale (e.g. drumlins and flutes). Crossing drift lineations necessarily imply different directions of ice flow at different times. The nature of the cross cuts shows the re-orientation of elements of pre-existing lineations into new lineation sets. This is extremely important as it allows their relative chronology to be

ascertained, and hence provides information on changing directions of ice flow occurring at different times within the life of the ice sheet.

The recognition of the mega-scale glacial grain and its cross-cutting nature indicates that there is a pattern of palaeo-ice flow that constitutes a new and important tool for the reconstruction of the Laurentide Ice Sheet. In comparison with the techniques for reconstruction previously outlined in Sections 1.2.1 - 1.2.5, this data is potentially more powerful in that it provides a spatially more complete coverage and, by the very nature of the cross cutting relationships, numerous time slices through the life of the Ice Sheet.

In a review paper on the reconstruction of Pleistocene ice sheets, Andrews (1982) concludes that "there is a need for more detailed glacial geological studies to understand better the shifts in flow directions and regimes during a glacial cycle". This thesis documents the mapping and interpretation of the mega-scale glacial lineation pattern covering Canada. The data resulting from this has the potential to provide:

1) A spatially extensive framework at various time slices on which to base and extrapolate other forms of evidence (e.g. striae, erratic dispersal, geochronometrically dated sites)

2) A basis of data and theory on which to construct an integrated model of the dynamics of the Laurentide Ice Sheet through the last glacial cycle.

Chapter 2

Nature of the Mega-Scale Glacial Grain

Chapter 2

Nature of the Mega-Scale Glacial Grain.

The character of the mega-scale glacial grain and its cross-cutting nature is described and illustrated in the following two sections, and by reference to selected case studies.

2.1 Mega-Scale Glacial Grain.

Most of formerly glaciated Canada displays a mega-scale glacial grain. Photoplates 1 and 2 show extracts of Landsat mosaics which clearly illustrate this large scale texture. Even AVHRR imagery with its ground resolution of only (>) 1.1 km is able to display the grain (Photoplate 3).

The co-linear texture or grain that is apparent on satellite images is characterised by repeated parallel lineations contiguously arranged and forming distinctive sets. The lineations are often apparent as obvious sediment ridges (Photoplate 1; photo a), or from linear lake boundaries (Photoplate 1; photo b), or river patterns (Photoplate 2).

At the scale of Landsat imagery the appearance of a grain within glacial drift can be attributed to two components:

1) Streamlined glacial landforms composed of drift can be detected on a scale larger than can be readily observed on conventional air photographs. They can exist as continuous

Photoplate 1: *Extracts of Landsat mosaics illustrating the mega-scale glacial grain. East-west dimension is 140 km.*

photo a: *SW-NE mega-scale glacial grain composed of obvious sediment ridges. Larch River area, Quebec (NTS 24D).*

photo b: *SW-NE mega-scale glacial grain expressed by linear arrangement of lake boundaries. Reindeer Lake region, Manitoba (NTS 64L).*

a

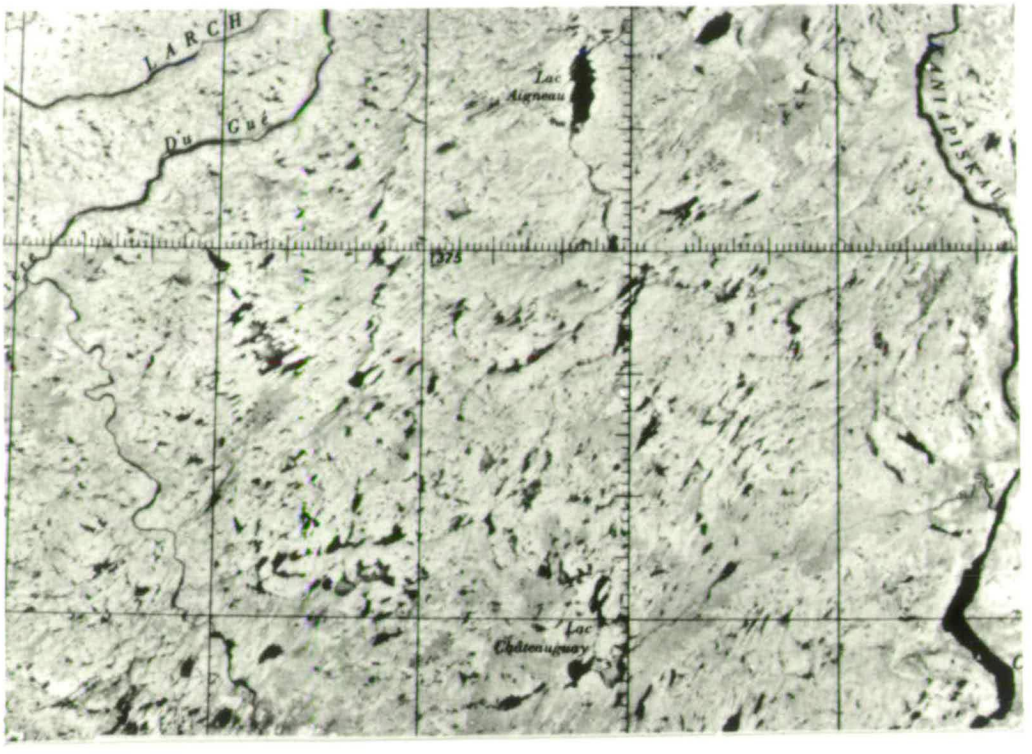
LARCH
Du Gué
Lac
Aigneau
Lac
Chibougamau

b

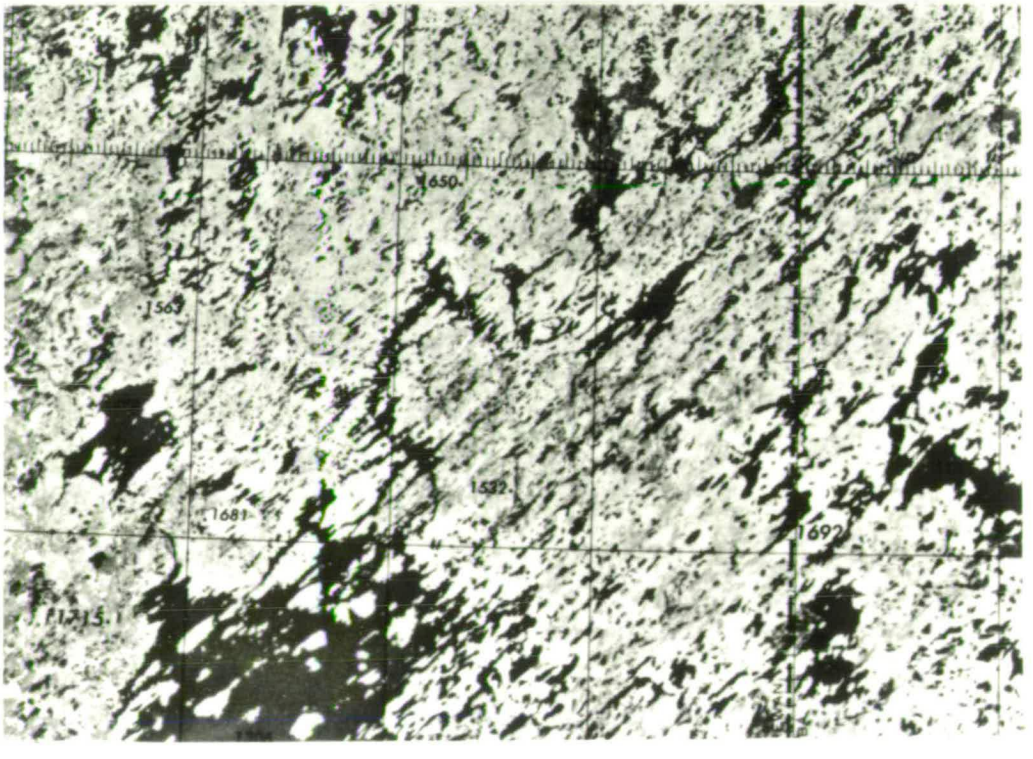
1650
1569
1532
1681
1692

Photoplate 2. *Mega-scale glacial lineations oriented NNW-SSE, some of which are over 50 km in length. Extract of Landsat mosaic of the Attawapiskat River region, James Bay Lowlands (NTS 43C+F). East-west dimension of image is 140 km.*

Photoplate 3. *NOAA satellite image illustrating that even when viewing such large areas (700 km across) it is still possible to detect the mega-scale glacial grain. A radial pattern emanating from the NE corner of the image is visible. This digitally-processed image consists of AVHRR channels 2, 3 + 5 (blue, green, + red), with an applied edge enhancement by convolution filtering. The area covered is that east of Lake Athabasca.*

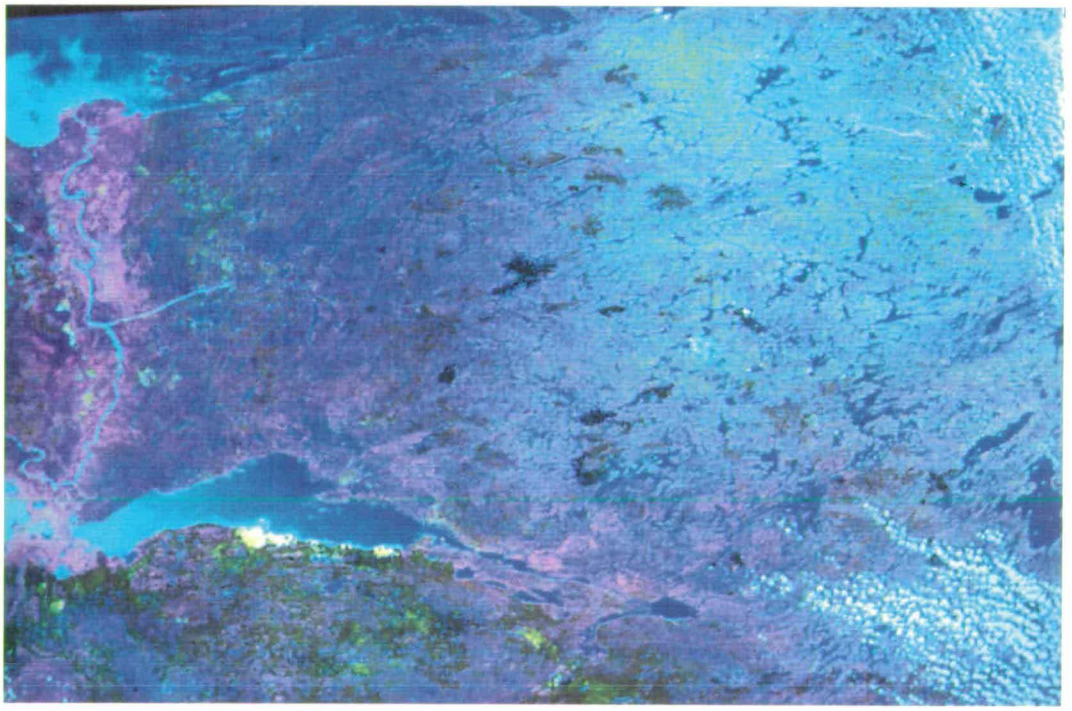

linear forms much greater in length than drumlins or mega-flutes, and often reach over 50 km in length (see Photoplate 2). These features I refer to as **mega-scale glacial lineations**. A strong NNW-SSE mega-scale glacial grain is illustrated in Photoplate 4. Individual mega-scale glacial lineations of 20-30 km in length are visible on the Landsat image, with one of the lineations reaching 80 km. Typical spacings are of the order of 3 km. The air photograph shows part of this area. Its limited size does not allow the mega-scale glacial lineations to be easily detected, although they do exist and are just visible. Widely-spaced fragments of streamlined elements had hitherto not been recognised as such at air photograph scale, and their discovery on Landsat images has shown them to be widespread for the area covered by the Laurentide Ice Sheet.

Mega-scale glacial lineations can be observed as individual forms, but over wider areas can be regarded as representing a grain. Compare the two images on Photoplate 5, the first of which covers a wide area and displays an obvious grain and the second which clearly illustrates individual mega-scale glacial lineations.

2) The larger field of view afforded by Landsat images enables other smaller streamlined glacial landforms such as drumlins and flutes to be viewed as a grain rather than as individual forms (compare the photos in Photoplate 6).

The size of mega-scale glacial lineations and the spatial extent of the grain (covering most of Canada) provide a basis for determining former ice flow directions on a continent-wide scale. In comparison with drumlins and flutes which tend to occur as discrete fields, the grain is more extensive and thus provides a more complete record of ice flow. Interpretations based on bedrock striae, which are typically centimetres in

Photoplate 4. *Mega-scale glacial lineations that are clearly seen at the scale of Landsat imagery are often difficult to detect on air photographs of the same area.*

photo a: *Strong NNW-SSE trending mega-scale glacial lineations. Landsat mosaic of part of the James Bay Lowlands (NTS 42M).*

photo b: *Air photograph of a small part of the Landsat image (marked by a box) in which the lineation pattern is not so easy to detect.*

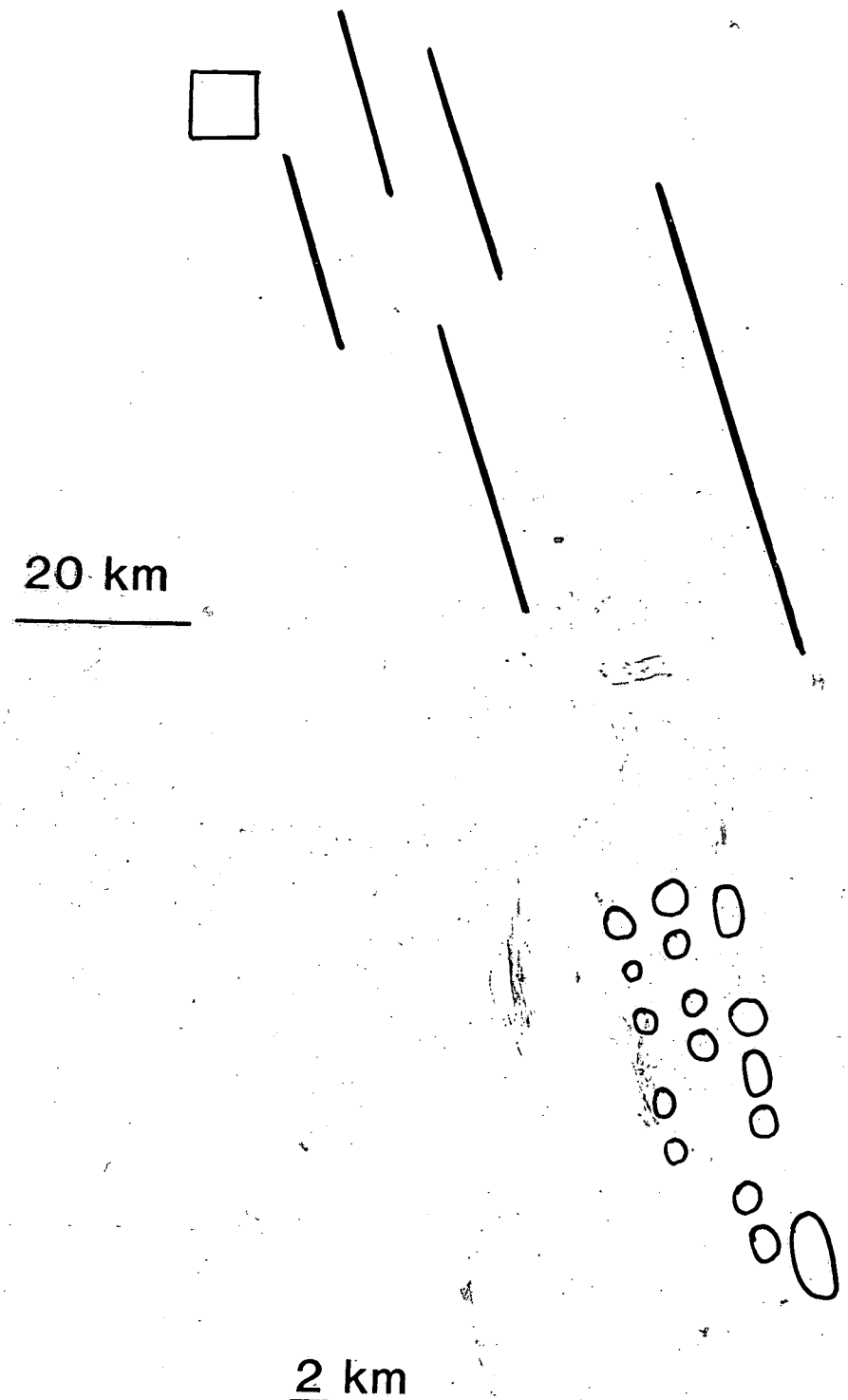
20 km
2 km

a

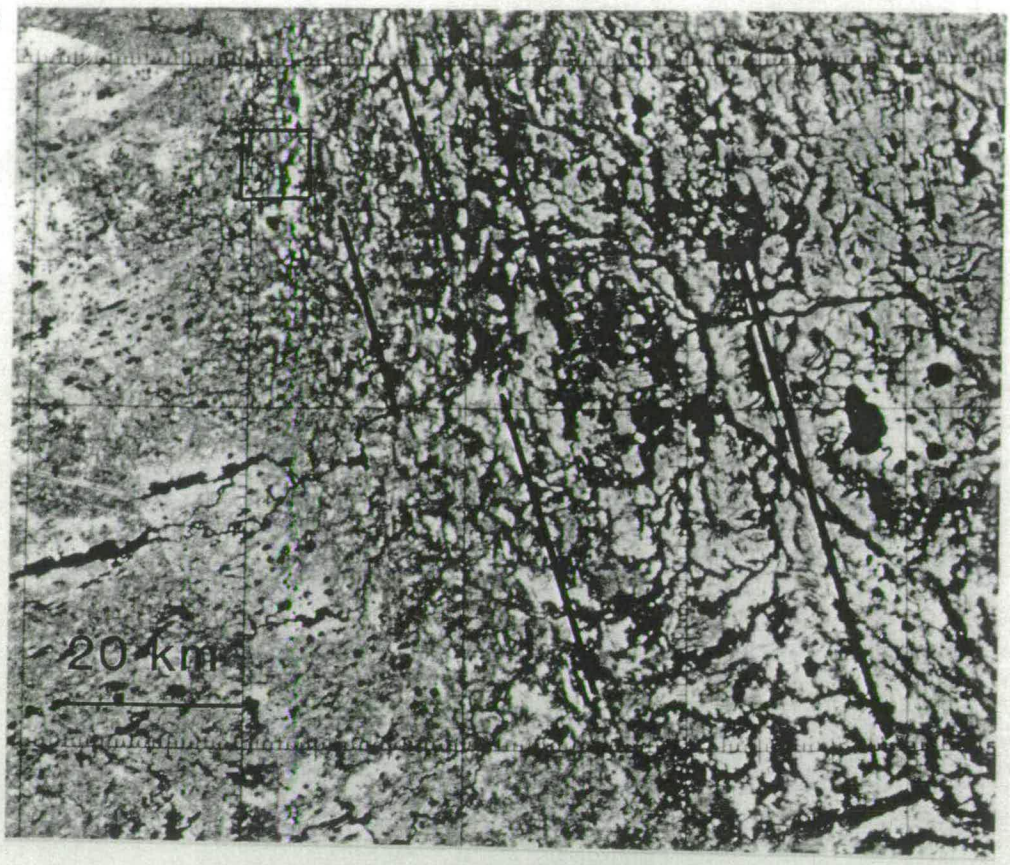

b

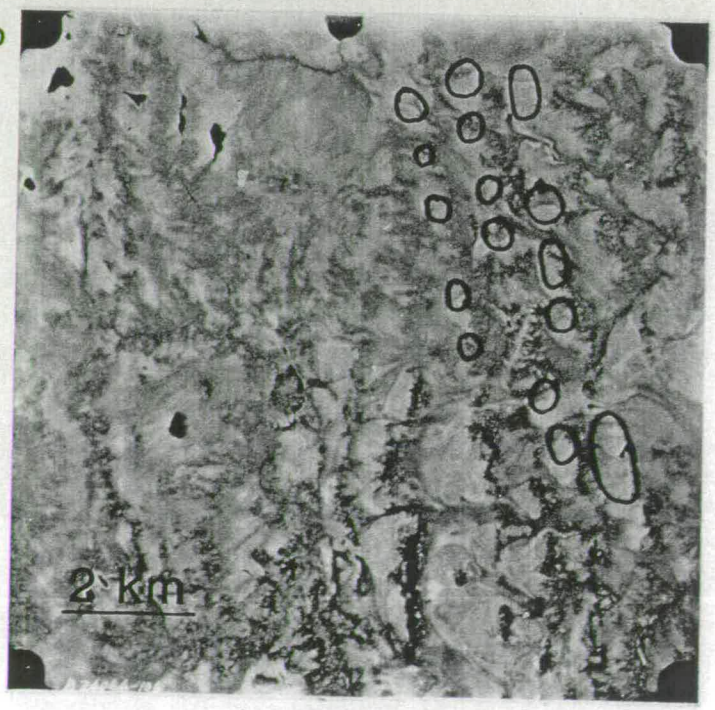

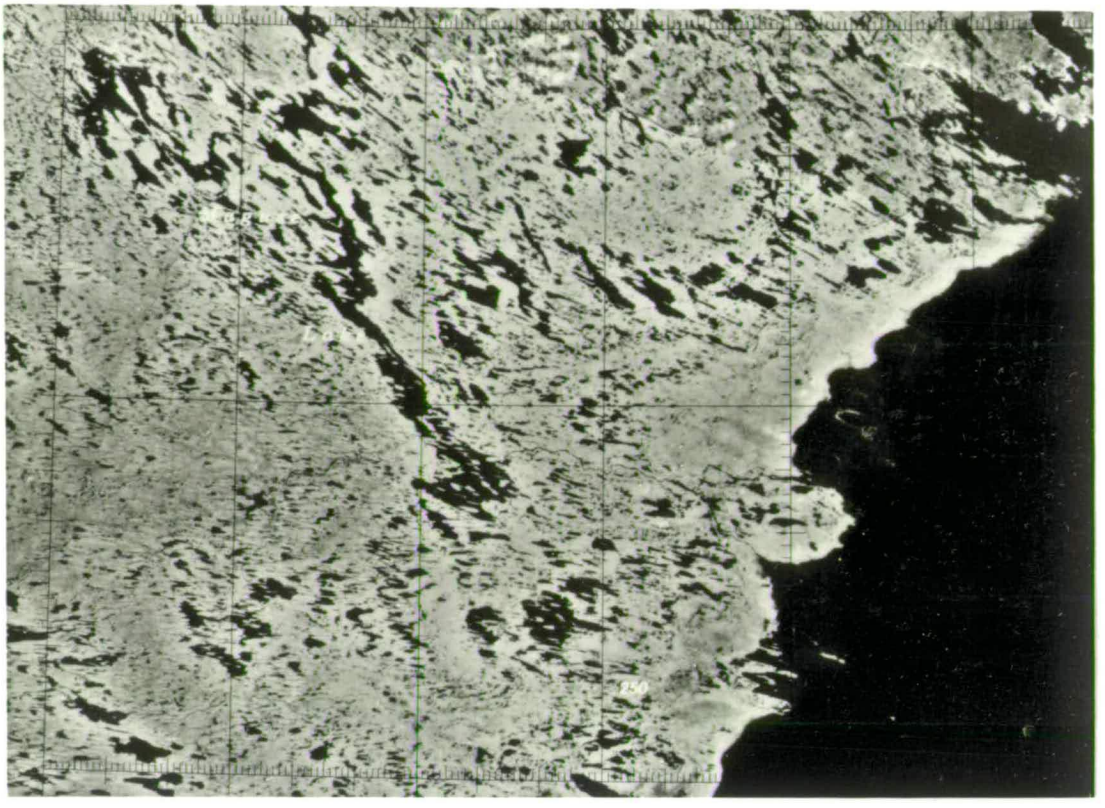

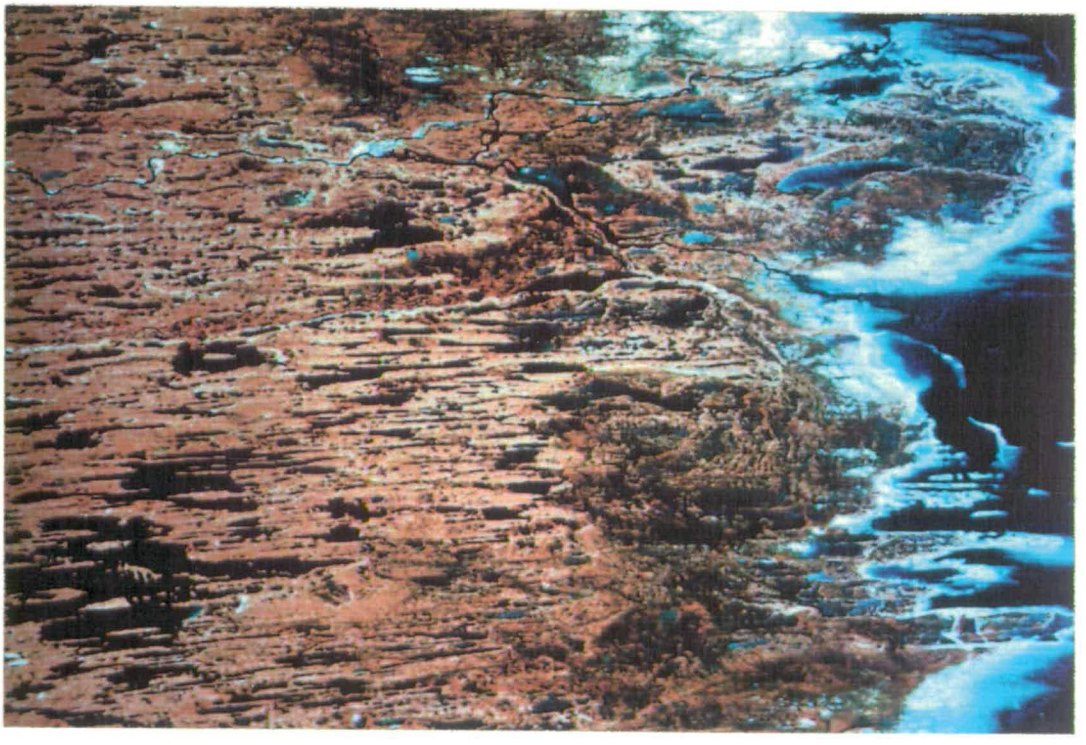

Photoplate 6. *The appearance of a grain, representing ice flow, on Landsat images can often be seen to be composed of individual drumlins on air photographs of the same area.*

photo a: *Extract of a Landsat mosaic displaying a NW-SE mega-scale glacial grain. Thelon River region (NTS 66C).*

photo b: *Air photograph of a small part of the Landsat image (area marked by a box) showing individual drumlins.*

20 km

1 km

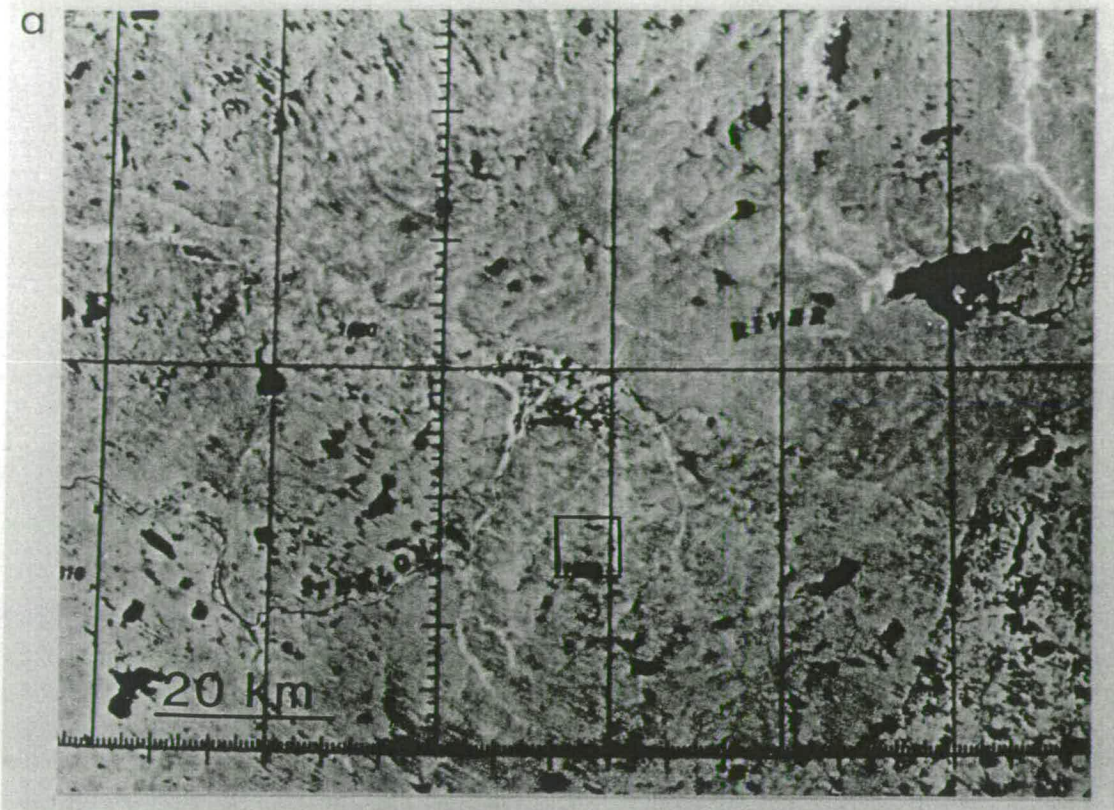
a
20 km

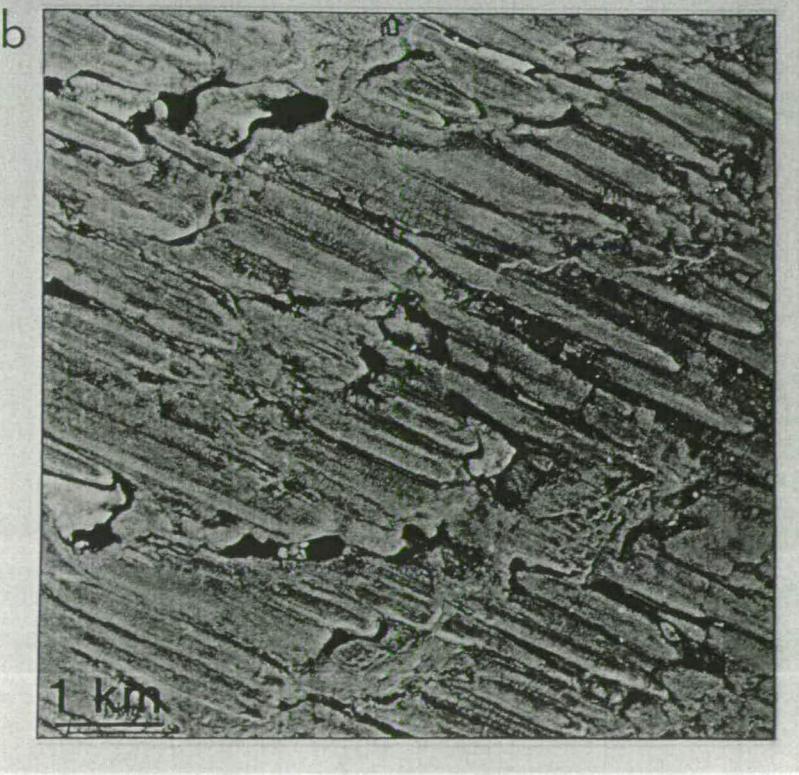
b
1 km

length and often separated by up to hundreds of kilometres, involve a great deal of freedom of interpretation when inferring gross ice flow patterns. This is in contrast to the mega-scale glacial grain which, by its frequently contiguous or overlapping nature, defines ice flow in an unequivocal manner.

2.2. Cross-Cutting Drift Lineations.

It was discovered that what, at first, appeared as a confusing background noise in the mega-scale glacial grain was in fact another set of drift lineations intersecting the primary grain at a different orientation. Cross-cutting relationships between differently oriented lineation sets are found to be widespread within Canada (and Fennoscandinavia). Sometimes as many as four different superimposed orientations of lineations are preserved.

The assumption that has hitherto been prevalent amongst glacial geologists: that the most recent ice flow direction remoulded all of the underlying drift and obliterated all previously produced orientations is thus incorrect. Superimposed and cross-cutting sets of drift lineations do exist and therefore record multiple phases of palaeo-ice flow in different directions.

Relative age determination.

It is not possible to determine the relative age of two cross-cutting sets by assuming that the most recent ice flow direction always produces the dominant or freshest looking lineation pattern. This assumption is invalid, and can easily be falsified by reference to

examples. It is only possible to reliably determine the sequence of ice flow phases by reference to the detailed geomorphic relationship between the lineation sets.

The nature of the cross-cutting relationships frequently shows the re-orientation of elements of pre-existing lineations into new lineation sets. I presume this to be achieved by remoulding of drift from the original lineation into a pattern produced by a more recent and different ice flow direction.

Two forms of relative age indicators are found:

1) SUPERIMPOSITION: where one set of streamlined lineations are visibly superimposed upon another differently oriented set.

2) PRE-EXISTING LINEAMENT DEFORMATION: deformation during a more recent phase of ice movement often alters the form or continuity of a pre-existing lineation, thus revealing the relative age.

The age relationships of crossing lineation sets were only determinable using high resolution satellite images for the clearest of examples. It was generally necessary to use air photograph mosaics or individual air photographs to ascertain relative ages reliably.

The nature of cross-cutting relationships and the determination of relative age is illustrated by reference to the following four case studies.

Case Study One

Case study 1; Victoria Island.

The Landsat image of the southern-most portion of Victoria Island (Photoplate 7) displays two clear cross-cutting sets of glacial lineations. The main area of cross-cutting is marked on the overlay, although glacial lineations are visible over most of the image. Previous air-photo mapping of this area (Prest 1969) did not resolve the cross-cutting pattern, but instead ascribed a diverging flow to account for the different orientations, i.e., not allowing the flow patterns to cross-cut. It is clear that the different orientations of lineations are not spatially separate and do cross-cut. For the lineations in the centre of the image the geomorphic relationship between the two cross-cutting sets allows their relative age to be determined. This is illustrated by means of the schematic sketch below.

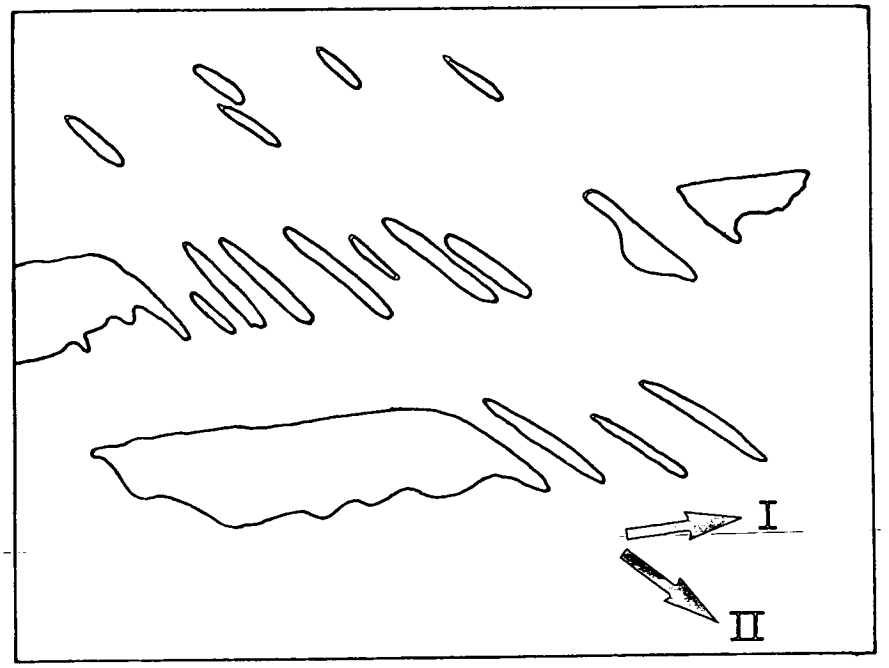

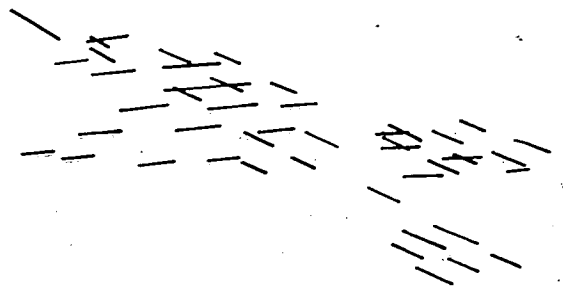

20 km

Photoplate 7. *Extract of a Landsat mosaic of the southern most part of Victoria Island (NTS 77D).*

Photoplate 7. *Extract of a Landsat mosaic of the southern most part of Victoria Island (NTS 77D).*

Case Study Two

Case Study 2; Boyd Lake vicinity, Northwest Territories.

Photoplate 8 illustrates how cross-cutting patterns seen on Landsat images can be interpreted in terms of relative age using air photographs.

Photo-a is part of a Landsat mosaic showing a strong NE-SW mega-scale glacial grain that is cross-cut by lineations aligned WSW-ENE. The latter is most clearly seen cross-cutting the former in the southwest quadrant.

Individual air photographs, from within the marked area of cross cutting, allow the relative chronology of the two lineation sets to be ascertained. Air photograph b illustrates how the relative chronology can be determined by means of **superimposition**. Drumlins of WSW-ENE orientation are visible superimposed upon the mega-scale glacial lineations of orientation SW-NE, thus determining the relative age (southwesterly flow followed by west-southwesterly). The actual direction of flow is indicated by drumlin form (stoss upstream) and in this case erratic and striae indication of southwesterly ice movement (Lee 1959).

Pre-existing lineation deformation is illustrated in air photograph c. The SW-NE lineations have undergone subglacial deformation and sediment translocation, realigning elements of the original lineations to the subsequent WSW-ENE orientation. Deformation such as this causing breaching and attenuation of pre-existing lineations clearly indicates the relative age of the ice flow phases.

Photoplate 8. *Extract of a Landsat mosaic and air photographs of the Boyd Lake region, NWT (NTS 65E).*

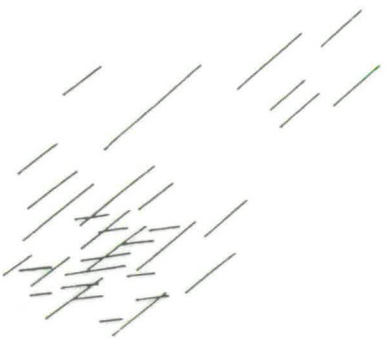

30 km

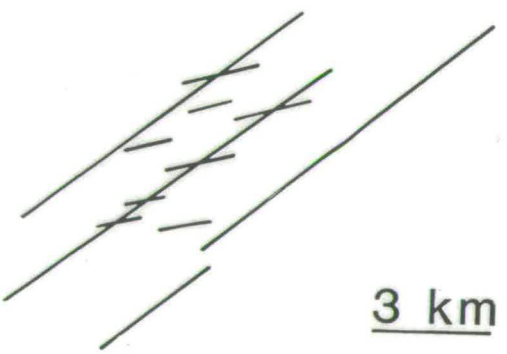

3 km

3 km

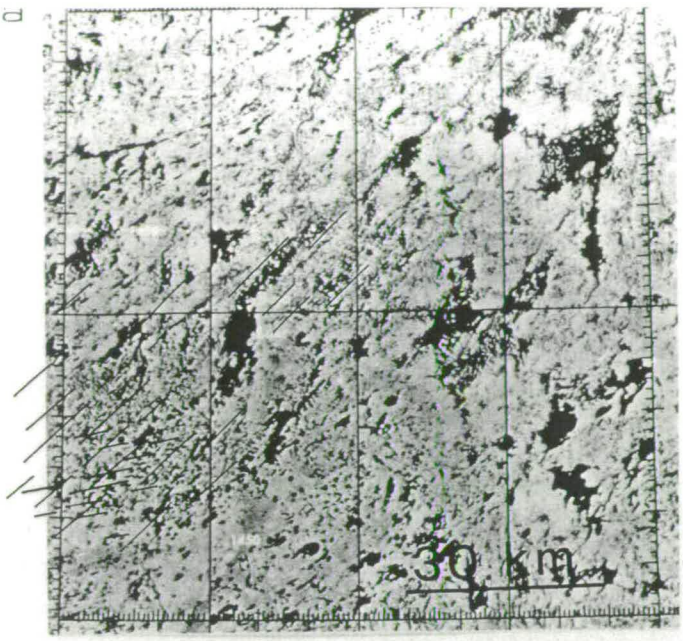
a
30 km

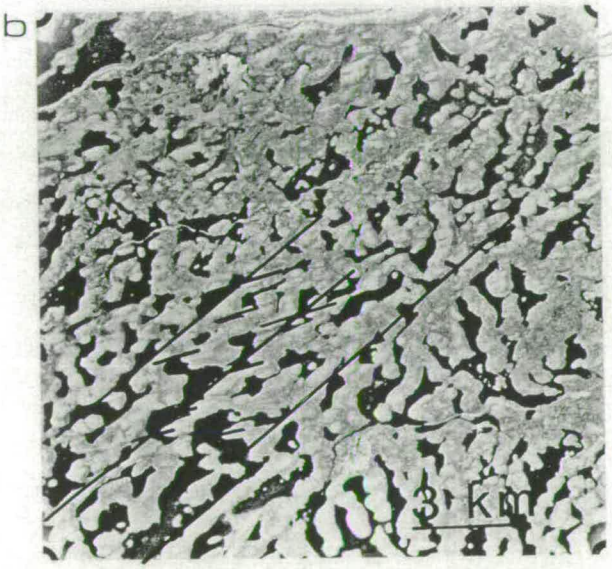
b
3 km

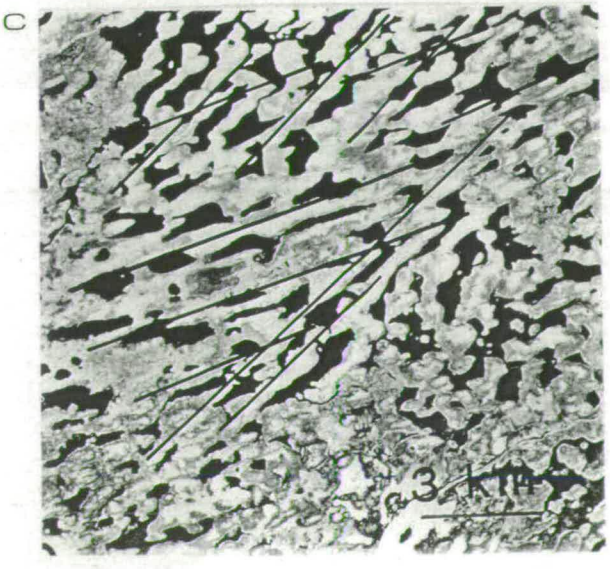
c
3 km

Case Study Three

Case Study 3; Engemann Lake vicinity, North Saskatchewan.

The cross-cutting pattern mapped from the Landsat mosaic (Photoplate 9 and overlay) was defined mostly by lake boundary alignment. However, patterns of intersecting sediment ridges are visible on the air photograph mosaic (Photoplate 10) on which it is easy to determine the relative age. The pre-existing lineations (NNE-SSW) were deformed by a later ice flow creating new lineations aligned ENE-WSW.

Note that the relative dominance, or "freshness" between the two sets of lineations on the Landsat and air photo-mosaic are different. The NNE-SSW orientation is dominant on the Landsat image, and the ENE-WSW pattern on the air photo-mosaic, this illustrates that criteria such as dominance or apparent freshness of a flow cannot be used to determine relative age.

The air photograph (Photoplate 11) illustrates the geomorphic relationship between the two lineation sets. Mega-scale glacial lineations of low spatial frequency oriented NNE-WSW are seen to have been deformed by a subsequent ice flow from the ENE. This deformation has been achieved by attenuation of sediment from the primary lineations to form secondary lineations of a higher spatial frequency. The relative age and the polarity of the later flow is thus indicated.

Photoplate 9. *Extract of a Landsat mosaic of the Engemann Lake vicinity (NTS 74J).*

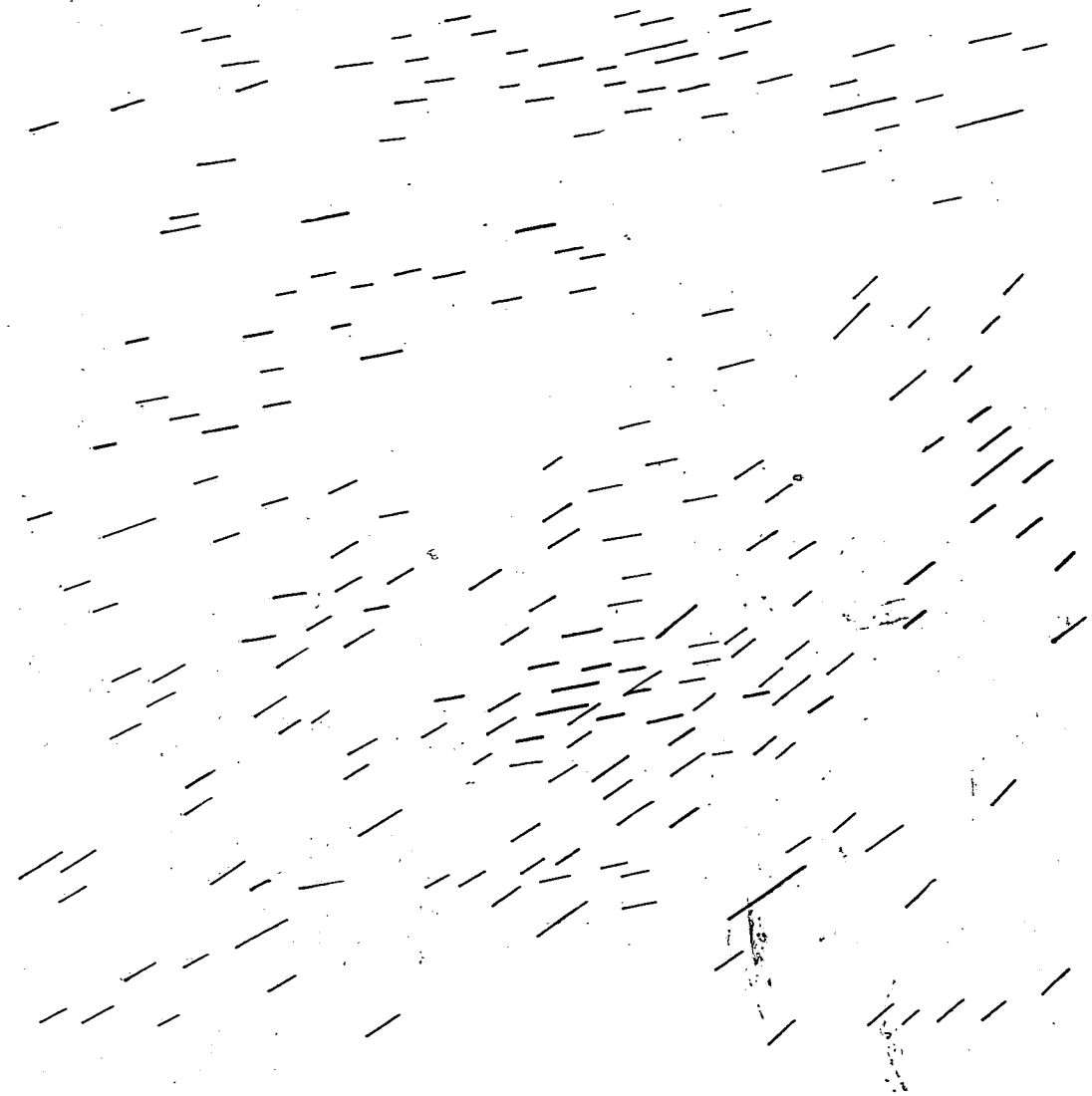
30 km

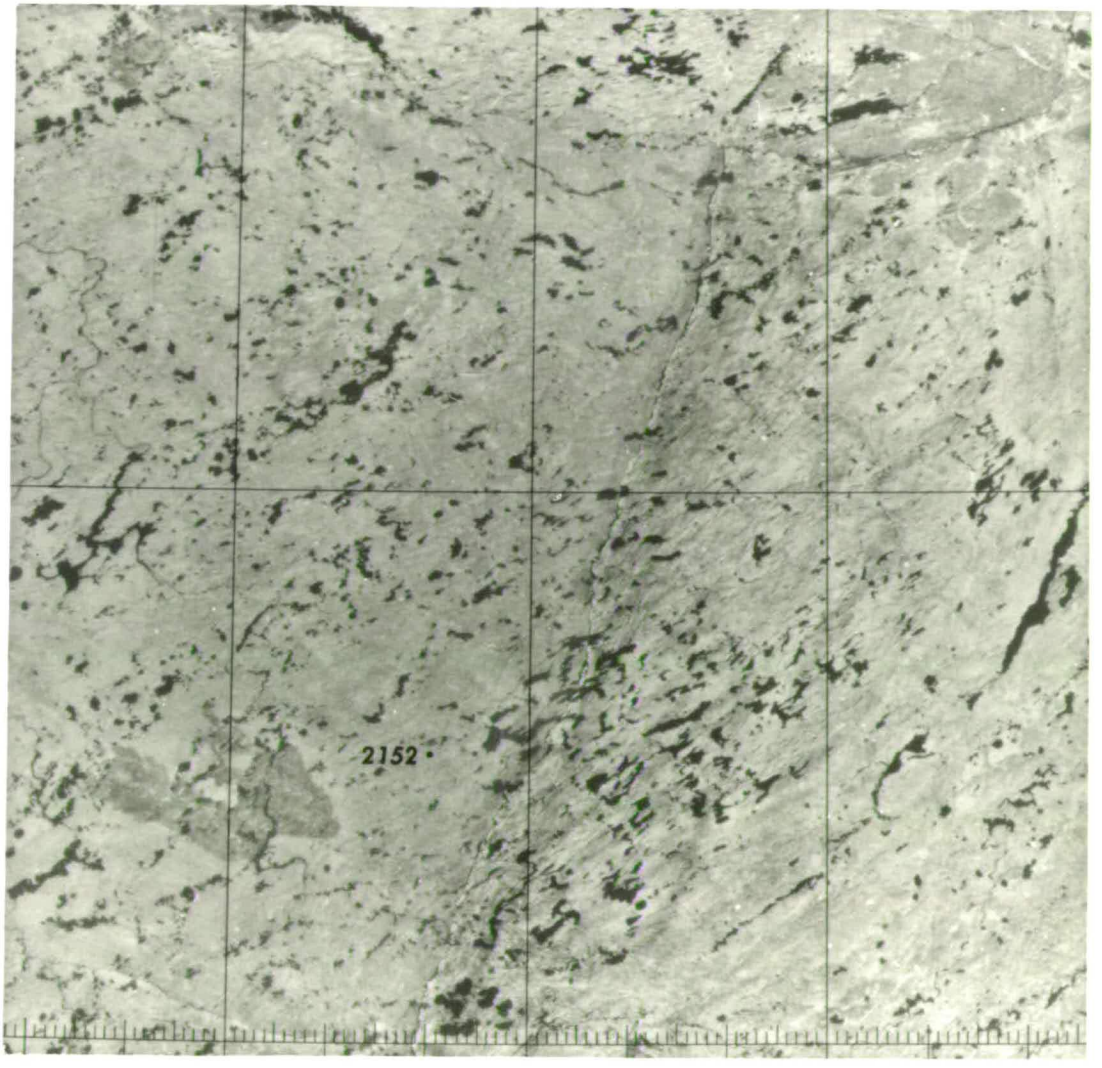
2152

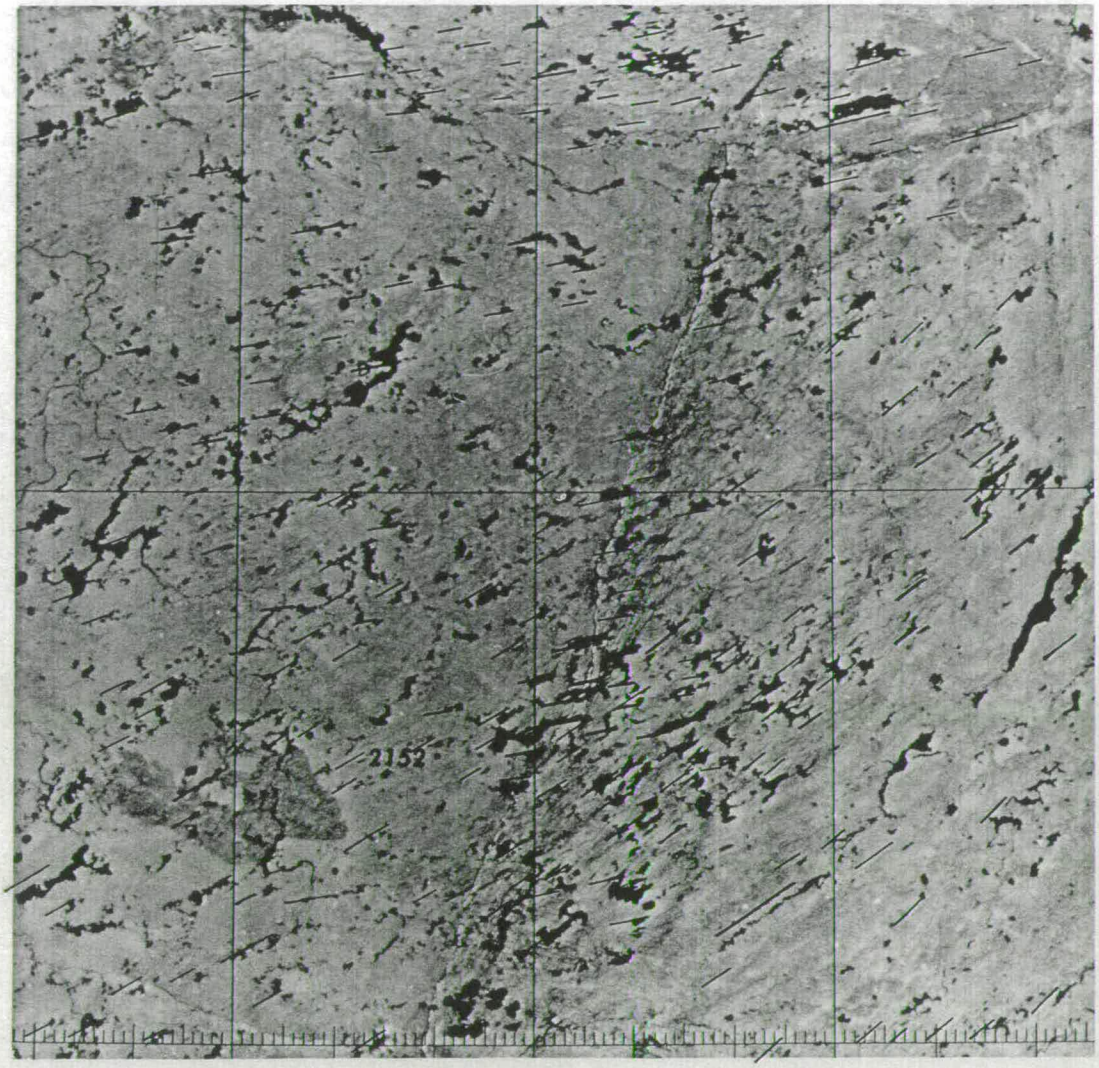

30 km

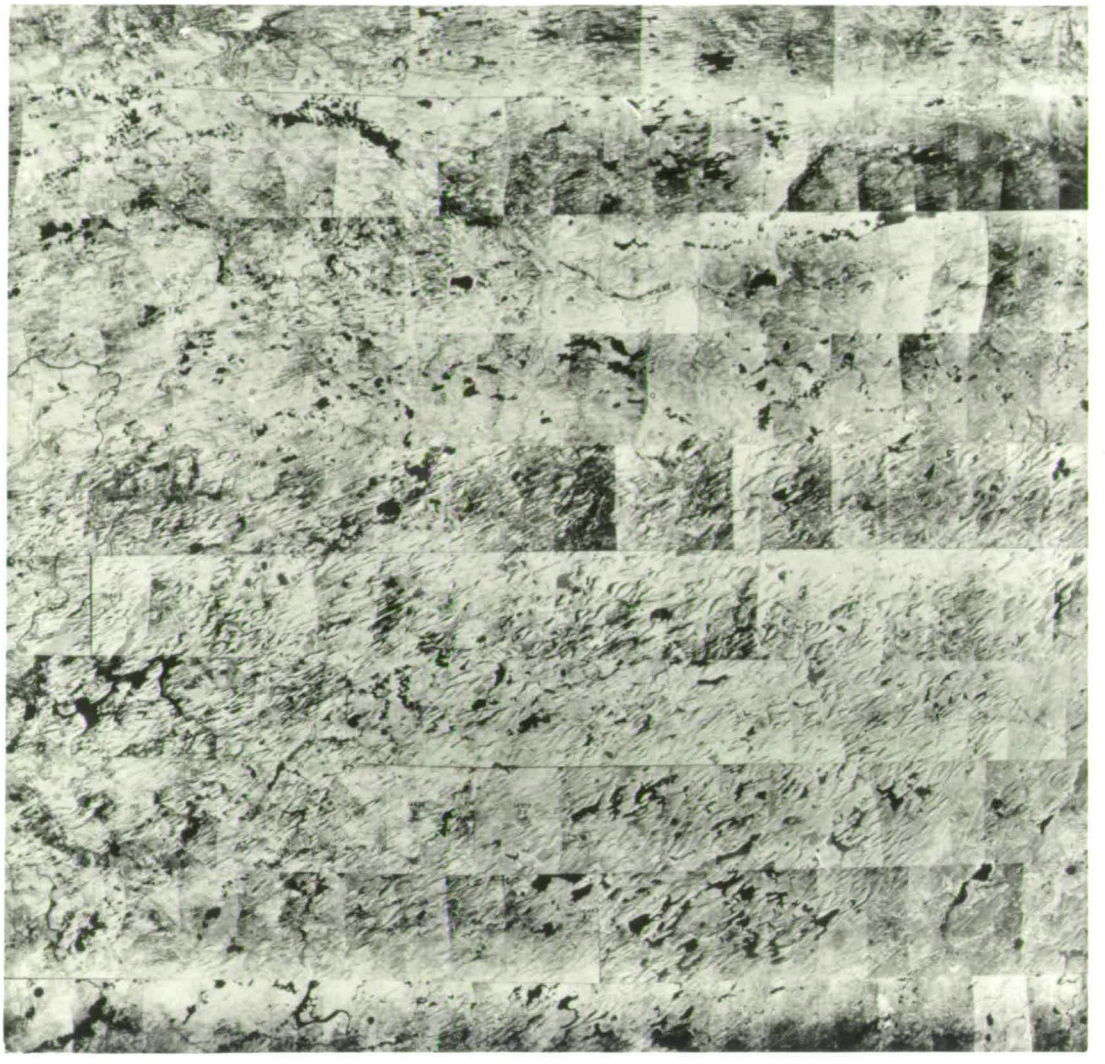

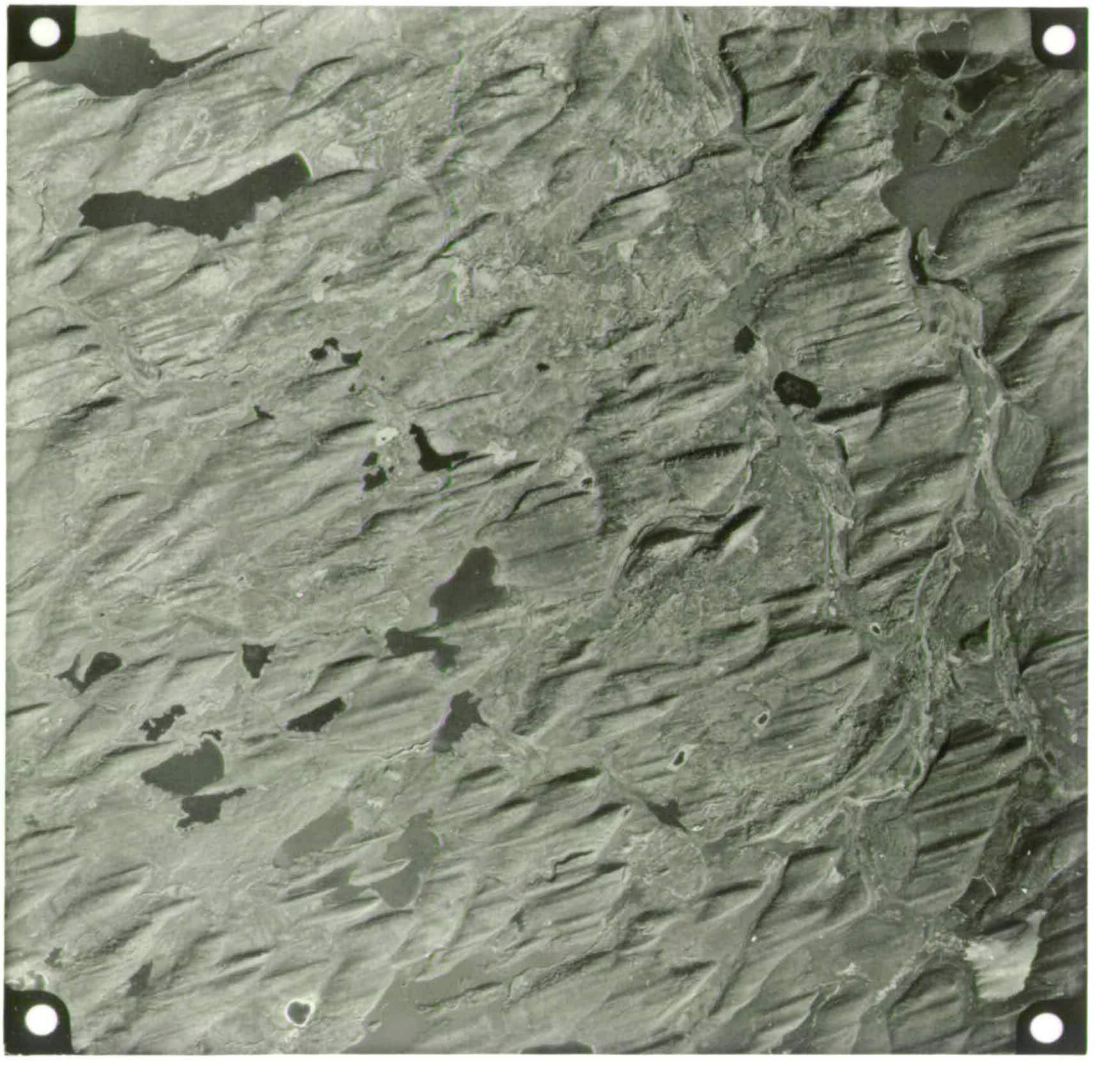

Case Study Four

Case Study 4; North of Coppermine River, Northwest Territories.

The oblique air photograph shows a field of drumlins outlined by water. The arrangement of many of the drumlins show them to lie superimposed on other lineations of a different orientation. Including the obvious curving drumlin field, three or possibly four different orientations of lineations are visible. The conventional air photograph shows the superimposed relationship between the drumlins and larger glacial lineations.

On the Landsat image the actual relationship between the lineation sets is not clear, but the identification of differently oriented lineation sets is possible.

Photoplate 12. *Images of a complex drumlin field north of the Coppermine River, NWT (NTS 87B).*

photo a: *oblique air photograph.*

photo b: *conventional air photograph.*

photo c: *extract of Landsat mosaic.*

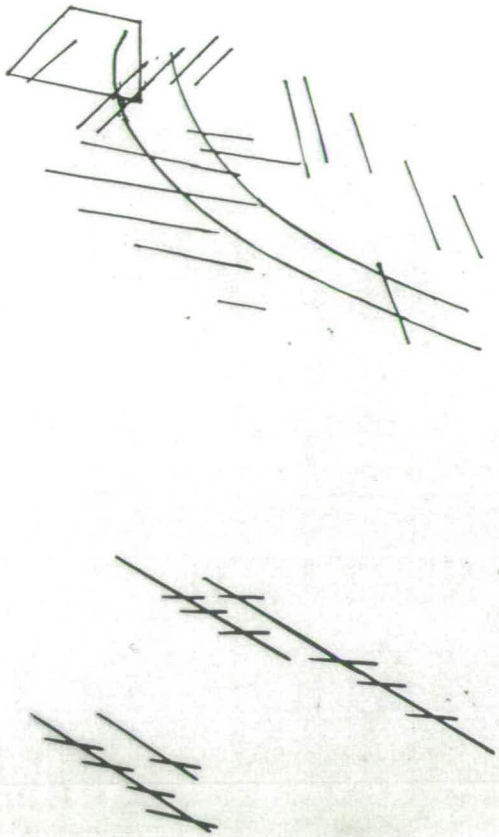

3 km

20 km

a

b

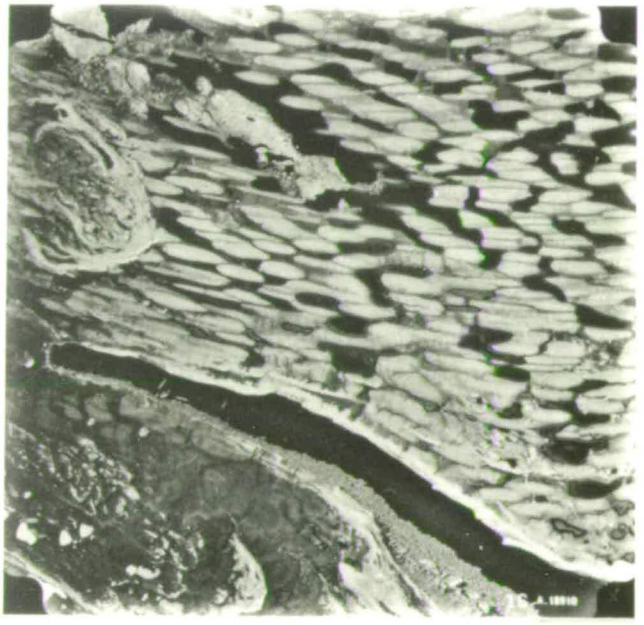

c

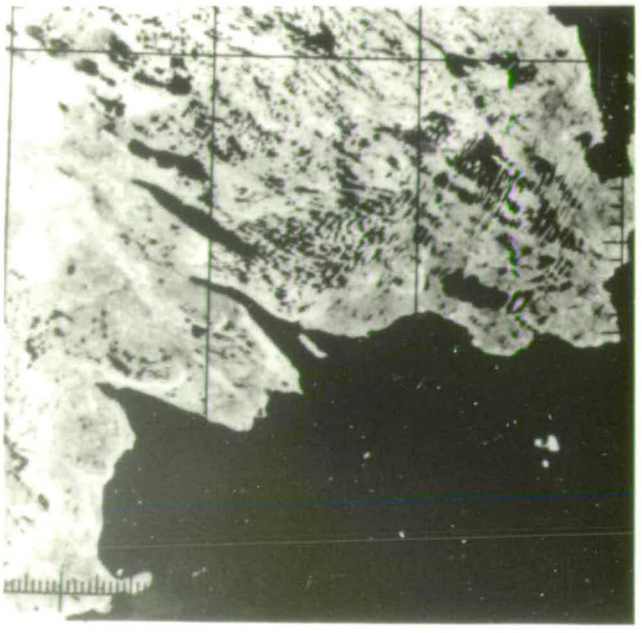

a

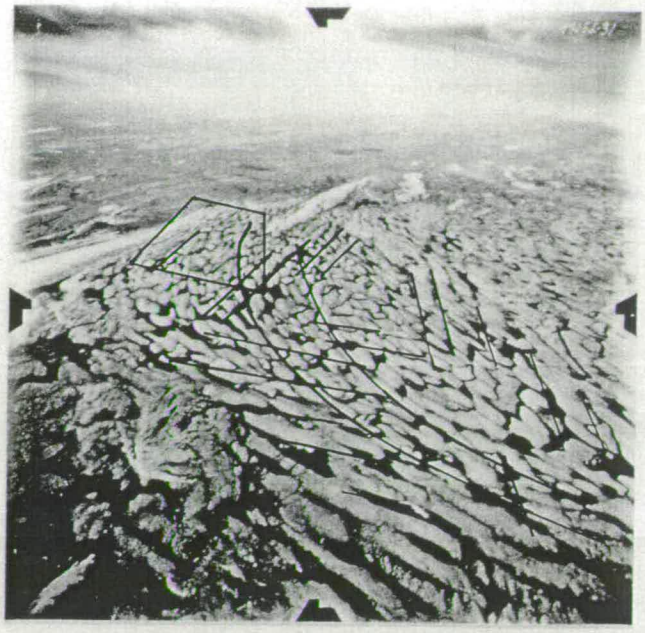

b

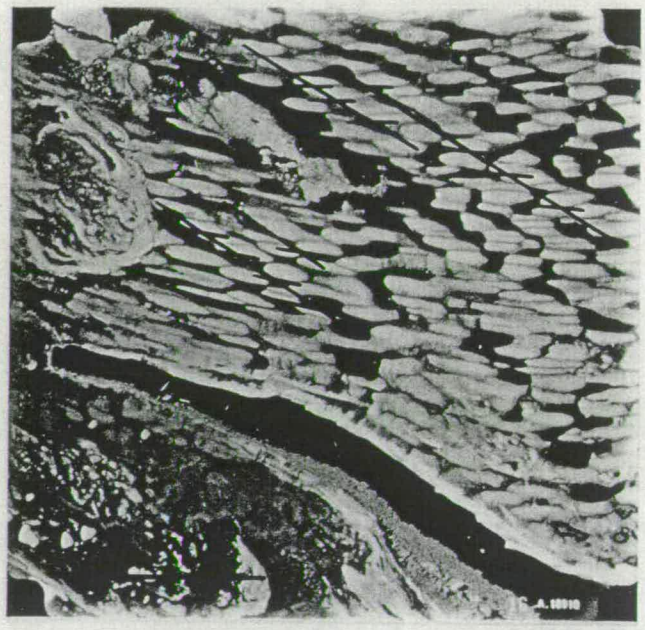

c

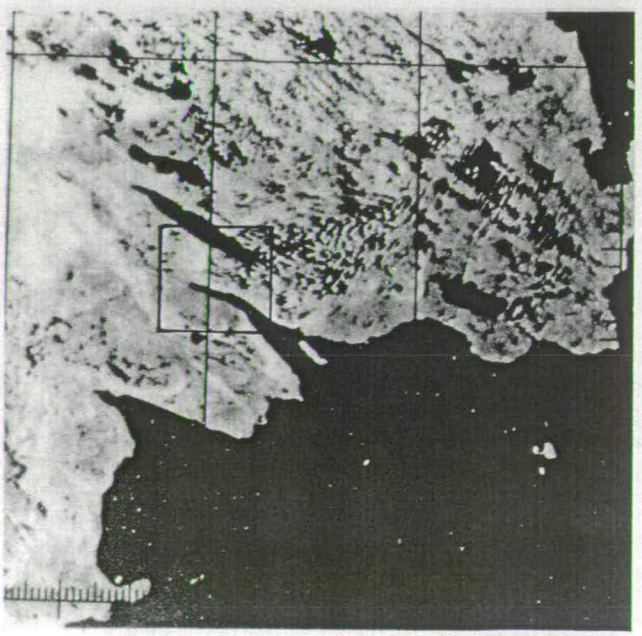

Chapter 3

Implications and Theory

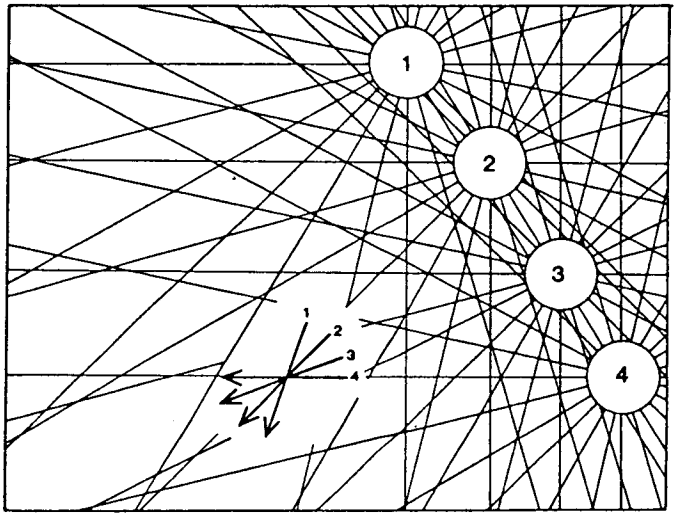

Chapter 3

Implications and Theory.

The relevance of cross-cutting lineations to the reconstruction of the behaviour of the Laurentide Ice Sheet is discussed in this chapter. An outline of glacial lineation formation theory, and consideration of the relationship between lineations and till fabrics is also presented.

3.1 Implications of Cross-cutting Patterns for Ice Sheet Behaviour.

Drumlins and megaflutes mapped on a continent-wide scale from air photographs (Prest, 1969) and Landsat images (Newsome, 1986) have been used to infer the configuration and topography of the Laurentide Ice Sheet at its maximum extent (Prest, 1984) and during its retreat phase (Boulton *et al.* 1985). In both cases major assumptions regarding the formative age of the mapped drumlins were required. Prest (1984) regarded the lineations to have formed roughly synchronously with the glacial maximum, and Boulton *et al.* (1985) assumed them to have formed in a radially time-transgressive manner during the retreat phase of the Ice Sheet.

The discovery that these hitherto mapped glacial lineations form only a small subset of a much larger group of cross-cutting lineations invalidates the assumptions of synchroneity presented by Prest (1984) and limited asynchroneity by Boulton *et al.* (1985). Different

cross-cutting lineation sets must be of different ages, and therefore indicate a change in flow geometry through time.

Numerous superimposed ice flow sets of varying ages and orientations can be interpreted in two ways:

1) they may be a reflection of changing patterns of ice flow during the history of a single ice sheet,

2) they may record ice flow patterns produced by ice sheets during successive glaciations.

The age of formation of the lineations is thus crucial in determining which interpretation is valid. Glacial drift lineations in Canada have always been regarded as of Late-Wisconsinan age on the assumption that only the last phase of lineation formation survives. This assumption is clearly incorrect as many older sets of lineations do survive subsequent overriding

Turbulent or meandering flow does not occur in ice, and therefore the change in flow directions documented by cross-cutting lineations can only arise from a change in the location of ice dispersal centres or ice divides.

The major changes of ice divide location demonstrated in this thesis may have occurred during the history of a single ice sheet, or may reflect different divide locations during different glacial periods. As in Chapter 6 it will be demonstrated that many of the

identified ice flows were formed during the history of a single ice sheet, it is thus appropriate to discuss the geometry of changing ice divides.

In theoretical consideration of how ice divides migrate we can generate patterns that, once recognised in the lineation record, allow us to reconstruct ice divide movements. A series of rapid ice divide shifts between relatively stable positions will create a number of superimposed radial patterns (figure 12). Radial flow lines emanating from different ice dispersal centre locations will intersect at angles of approximately ninety degrees close to the dispersal centre. These are the positions on the ground that would experience a strong change in flow direction. At greater distances from the ice dispersal centre, the upstream angle between intersecting flow lines will be less. Within glacially streamlined sediments strong changes in flow directions will be more easily recognised on satellite images than minor angular changes. It therefore follows that areas close to ice divides will provide the clearest evidence for reconstructing the migration of divides and domes.

Cross-cutting patterns of glacial lineation therefore indicate that the centres of mass of the Laurentide Ice Sheet have migrated, and thus provide a tool for the reconstruction of such major glacier-topographic changes.

3.2 Lineation Genesis and Theoretical Distribution.

A full discussion of the processes that lead to the creation of linear subglacial drift bedforms is beyond the scope of this thesis. However, a brief consideration follows concerning their generation, and more importantly, the spatial patterns they display.

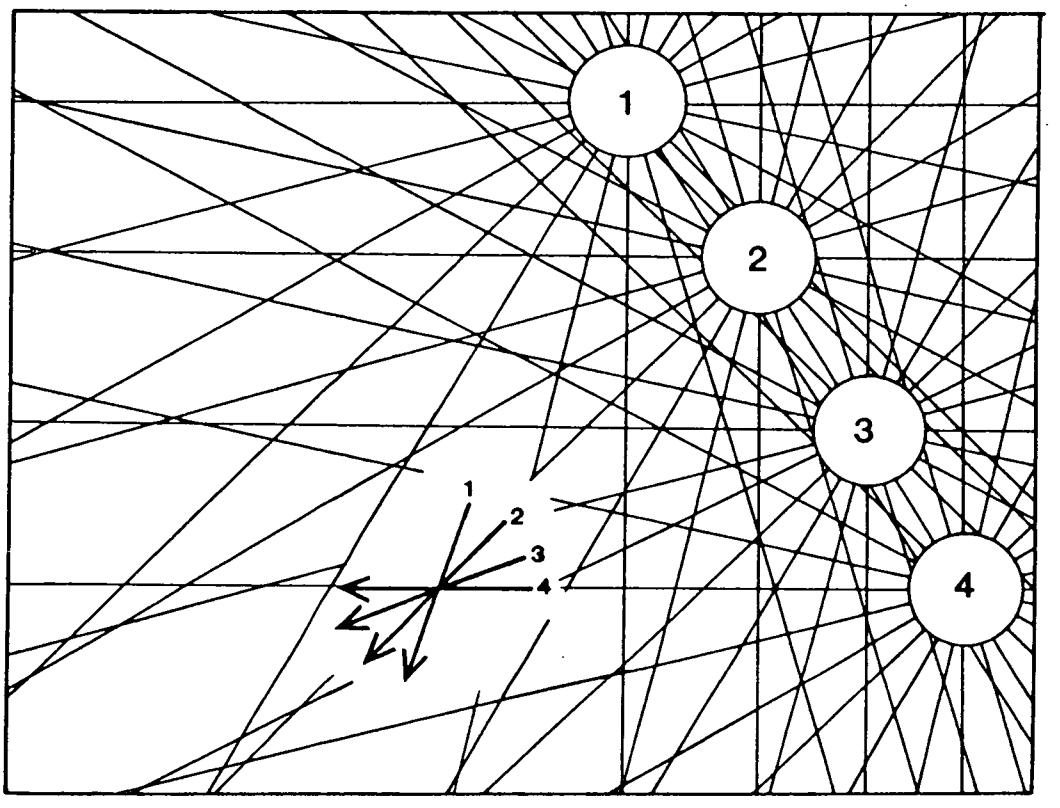

Figure 12. *A series of rapid ice divide shifts between relatively stable positions (1 to 4) creates a number of superimposed radial patterns.*

The movement of ice over a sediment substrate often produces streamlined linear bedforms aligned parallel to flow on a variety of scales. The inaccessibility of currently subglacial environments precludes detailed investigation, and consequently, theories about the processes of formation of glacial lineations are based primarily on features which, having formed subglacially, are now exposed subaerialy. This has inevitably led to a wide variety of explanatory theories. Processes invoked for drumlin genesis have been: sediment deformation (Smalley and Unwin, 1968; Boulton, 1987), basal lodgement (Fairchild, 1907; Boulton, 1982), depositional meltout (Shaw, 1980), and fluvial deposition in subglacial cavities (Shaw, 1983; Dardis and McCabe, 1983; Sharpe, 1985). In the formation of glacial lineations, it may also be that different processes operate on different scales. For example flutes can form by sediment flow into incipient grooves in the lee of lodged boulders (Boulton, 1976), and so this process is limited by boulder size. An alternative view to this multi-process, multi-scale form, is that glacial lineations are scale invariant (perhaps between 1 metre and 50 kilometres), and might best be described by fractal geometry. This would imply a single process operating over the entire scale range. However, this view is considered unlikely in that natural spatial frequencies of glacial lineations seem to have spectral power concentrated at specific frequencies (Clark and Boulton, 1989; Clark, 1990).

If subglacial deformation can create long drift lineations, what are the theoretical spatial patterns that might arise?

A threshold basal shear stress will exist below which no deformation and therefore no streamlining will occur. If velocity is assumed to be a proxy for shear stress, it is logical to presume that the length of a streamlined lineation will be proportional to the velocity and duration of the flow of ice that produced it:

$$L_{(x,t)} = \int_0^t V_{(x,t)} dt.$$

where L = maximum lineation length,

V = basal ice velocity,

x = distance,

t = time

This reduces to $L \leq Vt$. Figure 13 illustrates this relationship. On the basis of these assumptions a transect from an ice sheet centre to ice margin should resemble figure 14. Basal velocities at the ice divide are zero and working outwards along the transect reach a threshold at which streamlining begins. At this point short lineations may develop if sediment rheology is favourable. Basal velocity increases to a maximum at a position a few tens of kilometres behind the ice margin. This is the position where the potential length of streamlined lineations will be at their greatest. Two points should be noted about this simple model:

1) The portrayed lineation length should be regarded as the maximum length it could reach. Sediment characteristics provide a limiting factor.

2) It is only a model of the geological imprint "at an instant" within the life of an ice sheet.

To overcome this second problem it is necessary to integrate the effects of the basal velocity over ice sheet residence time. Temporally symmetric growth and decay of a

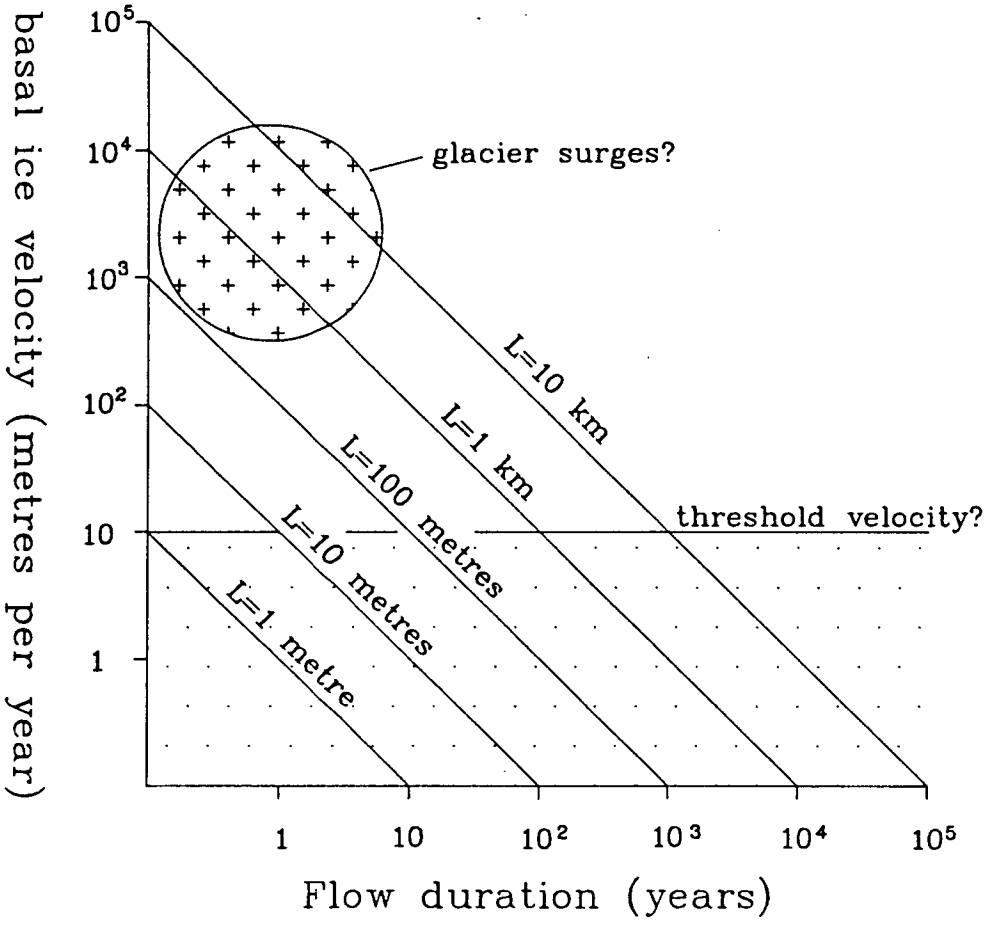

Figure 13. *Theoretical maximum lineation length (L) as a function of ice velocity and flow direction. Lineations of a certain length may form under fast moving ice over a short period of time (e.g. a surge), or under slow moving ice, over a long period.*

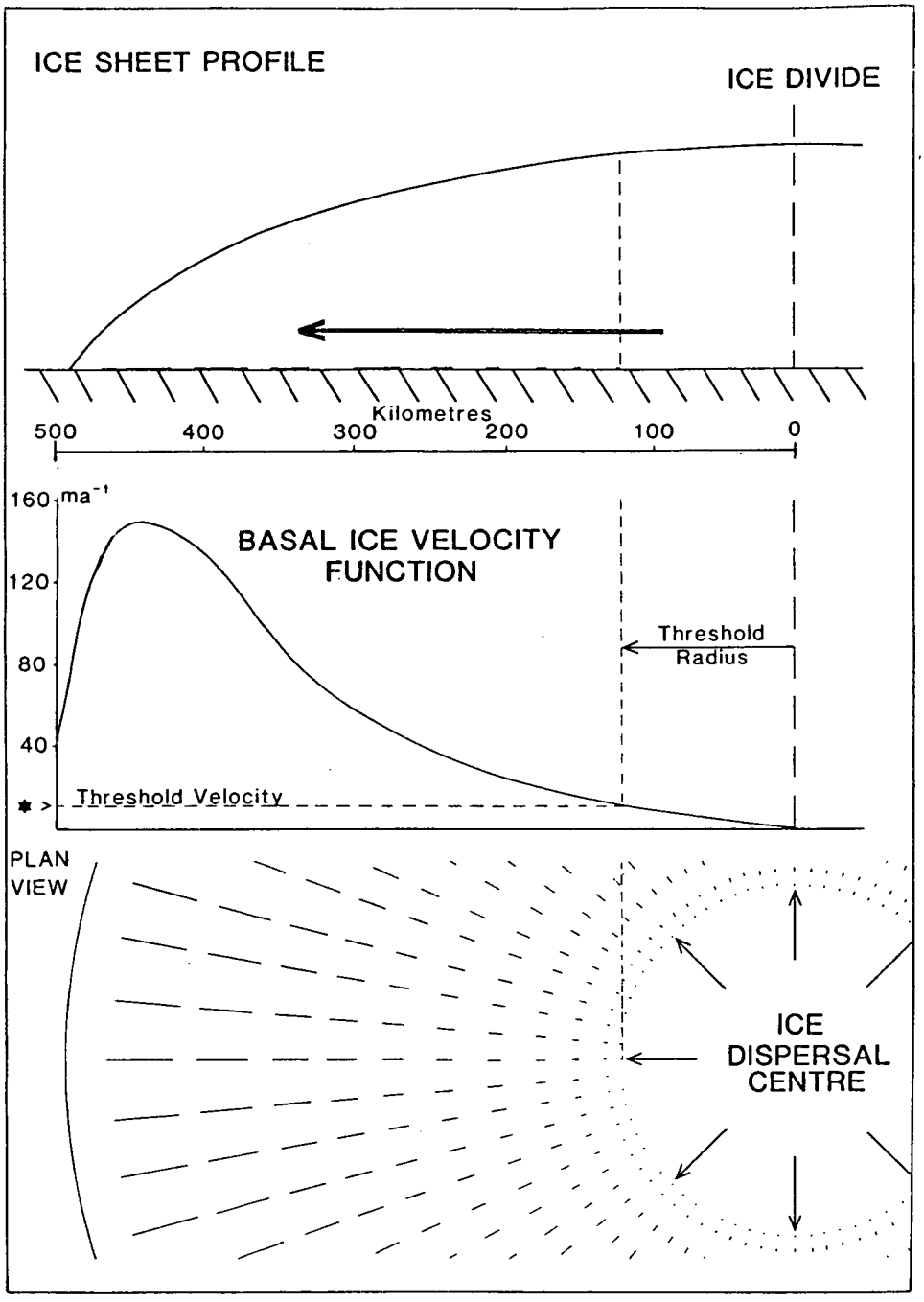

Figure 14. *Illustration of how lineation lengths may vary beneath an ice sheet. A threshold basal velocity set at 10 m/a produces a protective radius of 125 km, within which no lineations form.*

single-domed ice sheet emanating from, and retreating to, a fixed centre was assumed. This allowed a residency curve, plotted as time against ice sheet span, to be constructed (figure 15a). This illustrates the duration of ice cover (and flow) at any point in the ice sheet transect. The modelled velocity distribution (velocity against ice sheet span) for different sizes of ice sheet (Hindmarsh, *pers comm*), can be taken to represent stages in ice sheet growth and retreat (figure 15b). This was integrated over time, using the assumed residency curve to produce a theoretical envelope of maximum potential lineation length (figure 15c). In this simple model maximum lineation lengths are produced appropriately 0.7 of the maximum half-span of the ice sheet away from it's centre, i.e. maximum lineation length is predicted to occur just under three quarters of the distance away from the ice sheet centre to margin.

The concept of a threshold basal velocity for ice moulding, and the attendant threshold radius (figure 14) implies that ice divide regions act so as to protect underlying sediments; although it is likely that explicit modelling of the extent and characteristics of a protective ice divide region would also have to include the thermal regime (frozen or melting bed), which is intimately related to the velocity parameter. If it is true that ice dispersal centres have a significantly large protective area (as I suspect), then many previously interpreted ice divide positions, such as the reconstruction of the Keewatin divide by Lee (1959) and Shilts *et al.* (1979) must be erroneous, as they show drumlins and flutes extending almost to the divide (figure 16a). An alternative explanation that would create the same geologic record is illustrated in figure 16b. When the ice dispersal centre was at position A, no lineations were created within the threshold radius, and the sediment within it and any previous lineations were protected. Beyond the threshold radius, the length of lineations increased with distance from the ice dispersal centre. When the ice dispersal centre migrated to position B, the strong lineations produced at

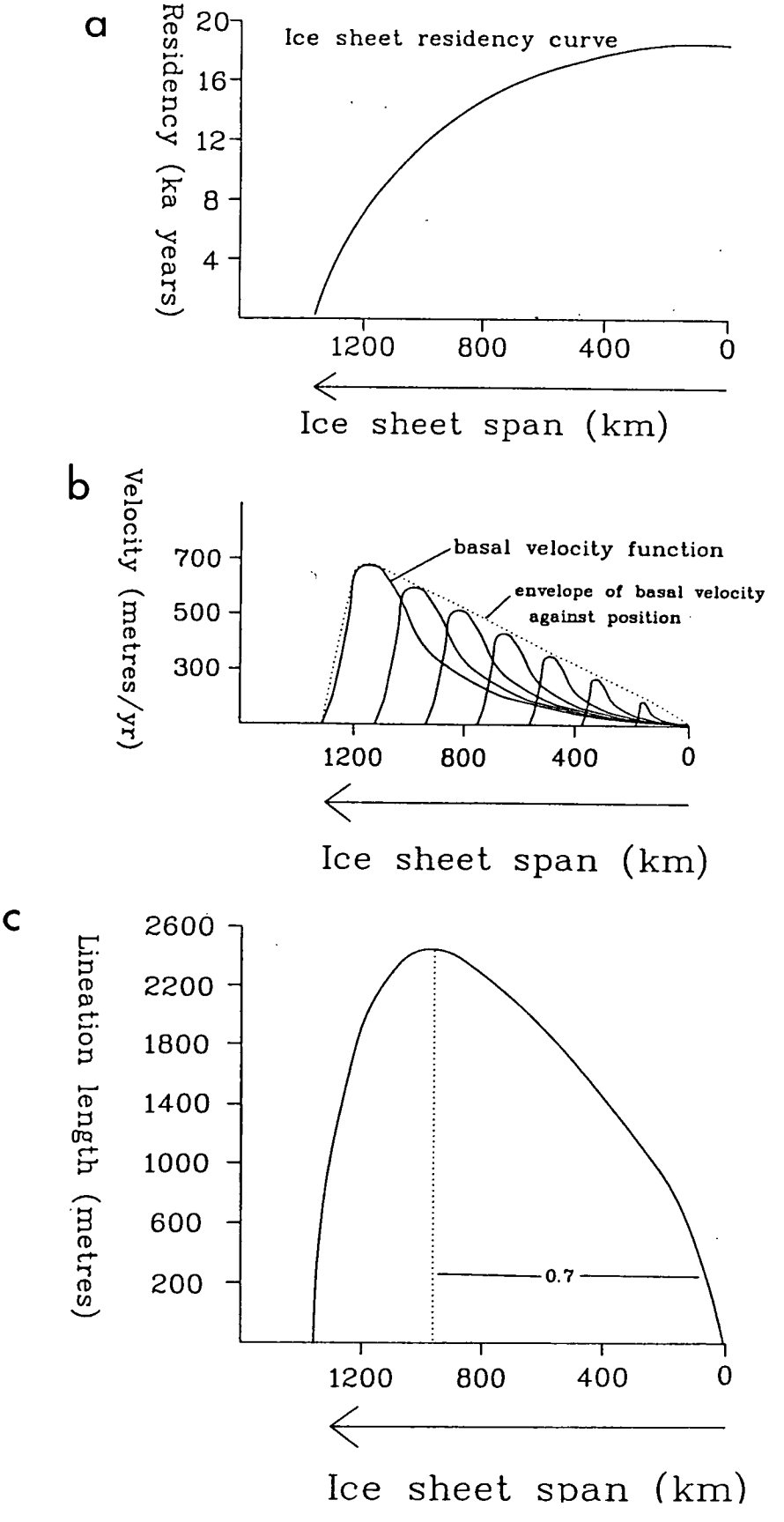

Figure 15. *Theoretical model integrating basal ice velocities, along a transect, over the life-span of an ice sheet (see text). Maximum lineation lengths are predicted to occur 0.7 of the maximum half-span of the ice sheet away from it's centre.*

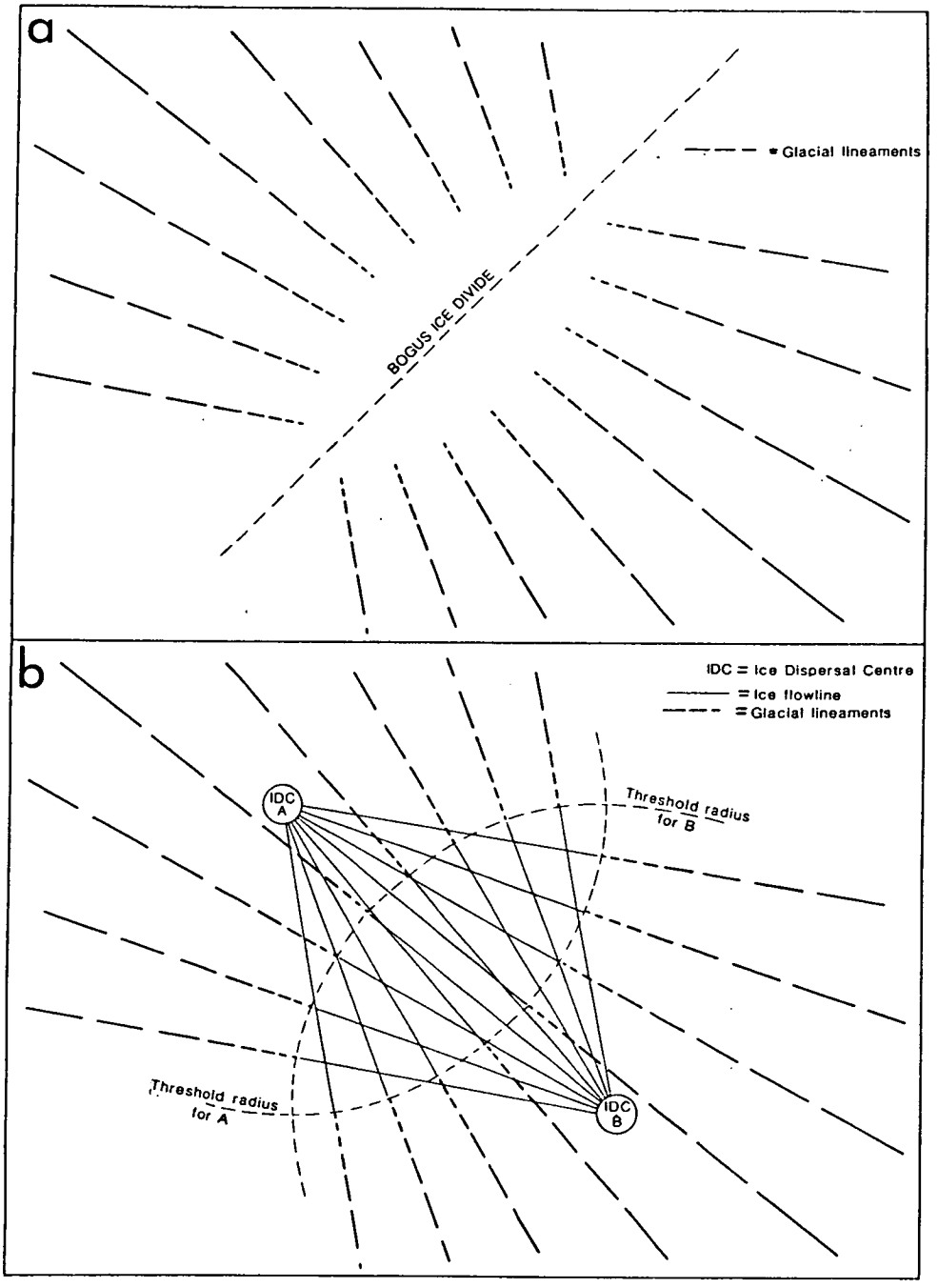

Figure 16. *Alternative explanations of ice sheet behaviour that create the same lineation pattern.*

a: *"Traditional" ice divide explanation. Note however that lineations extend almost to the divide.*

b: *Alternative, and favoured explanation involving a migrating ice dispersal centre.*

position A lay within the new threshold radius, and were therefore preserved. Lineations from position B were created beyond its threshold radius, producing the pattern shown in figure 16b. I suggest therefore that the ice divide marked in figure 16a represents a misinterpretation of the data, which is better explained by a migrating ice dispersal centre.

If ice flow patterns change, where are the lineations produced during the earlier flow phase most likely to survive, and how will they be related to lineations of the later phase? The regime at the glacier sole can be divided into four zones according to the potential to reorganise the glacier bed (figure 17):

ZONE A; In the ice divide region, basal ice velocities are so low that no deformation of pre-existing lineations occurs.

ZONE B; higher basal ice velocities allow some modification and reorientation of elements of pre-existing lineations. However, the first flow direction remains dominant.

ZONE C; still higher basal ice velocities produce modification of the older lineations to such a degree that they become fragmentary. Lineations produced by the second flow direction dominate.

ZONE D; maximum basal ice velocities just behind the ice margin produce such strong deformation that the older lineations are obliterated and replaced by the new ones.

This suggests that dominant lineation patterns are not necessarily the most recent.

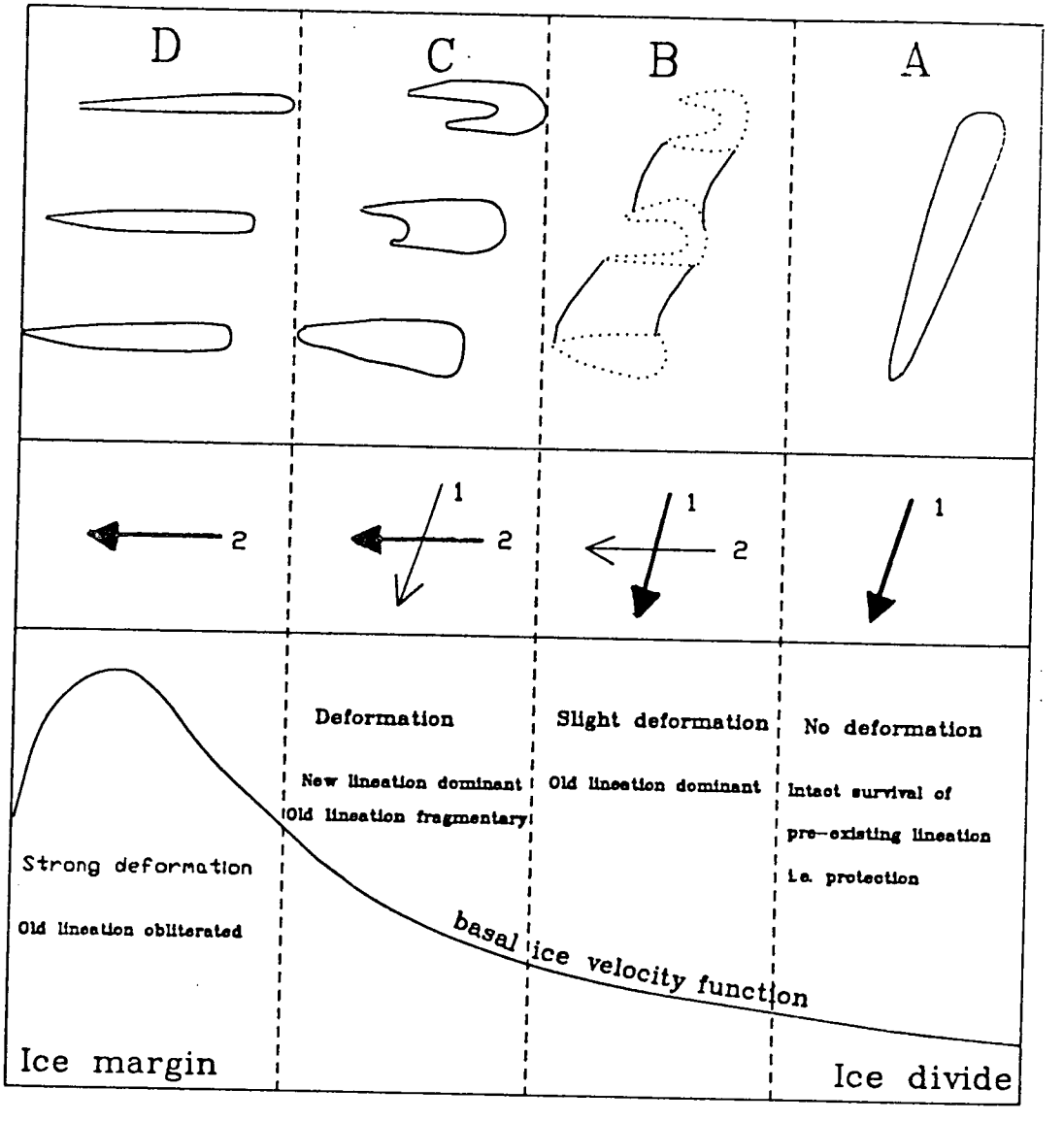

Figure 17. *Varying degrees of alteration to pre-existing lineations as a result of a shift in flow direction (see text).*

[A fully time-integrated simulation of the above model requires the duration time for the flow to be taken into account as well as the deforming potential].

3.3 Lineation and Till Fabric Relationships Produced by Shifting Ice Flow.

If complex sequences of ice flow phases occurred over large parts of Canada, as argued in this thesis, then do we find evidence for this in till fabric studies?

It is assumed that till fabric orientations will be roughly parallel to the major linear features within which they occur. If ice flow direction changes, the greatest reorganisation of fabric will occur where there is the greatest reorganisation of mass, and thus new linear features will have new fabrics and old undeformed lineations or till will tend to preserve old fabrics. The focus of deformation that is intrinsically implied by individual lineation genesis should produce strong clast orientations within the lineation, relative to the surrounding till.

Given these assumptions, what are the likely lineation-fabric outcomes that might result from a shifting pattern of ice flow? Two major options exist, dependent upon whether the glacier-bed is operating under a depositional or erosional regime. If it is primarily depositional then the import and deposition of new sediment will create a superimposed layer of till. This new layer should display the fabric orientation of the ice flow that deposited it, and so will be in contrast to the direction of flow indicated in the underlying till. The till lithologies may also be different, reflecting the change of source area. So for the depositional regime, shifting ice flow produces a series of superimposed tills each

displaying its own fabric orientation corresponding to the direction of ice flow that deposited it. There are many examples of such arrangements (described in Chapter 6). For shifting ice flow with an erosional regime the situation is more complex. If ice flow direction changes during a phase of continuous till deposition or in which it is eroding the underlying till then I believe there are five possible outcomes (see figure 18). It may completely reorient the fabric to the new direction, reorient only part of the till, possibly leaving a complex or bi-modal fabric orientation, or if deformation is strong enough the substrate may develop major linear features. If glacial lineations develop, the clast fabric within them should parallel their trend, but the surrounding till may either display the same orientation or retain the fabric of the previous ice flow direction. These five generalised options are displayed in figure 18. Options no. 2 and 5 are the only ones in which multiple directions of ice flow are likely to be recorded in the till fabric. I suggest that this is partly the reason why many till fabric analyses do not appear to show multiple phases of differently oriented ice flow.

It is suggested in this thesis that some linear features are so large as to be undetectable on the ground. It is therefore vital that the large-scale geomorphic pattern should be elucidated in order to interpret regional ice flow using fabric orientations. Interpretations not doing so are likely to produce only partial and confusing reconstructions.

Theorised options 2 and 5 have been detected by till fabric analysis. MacClintock and Dreimanis (1964) examined excavations of the St Lawrence Seaway, which displayed two tills; the lower till member (Malone Till) derived from ice flowing NE-SW and attributed to the "Wisconsin ice age", and an upper till member (Fort Covington Till) which was deposited by a readvance of Late Wisconsinan ice flowing towards the SE. They report "puzzling fabrics (were) found in the Malone Till". Abnormal fabrics

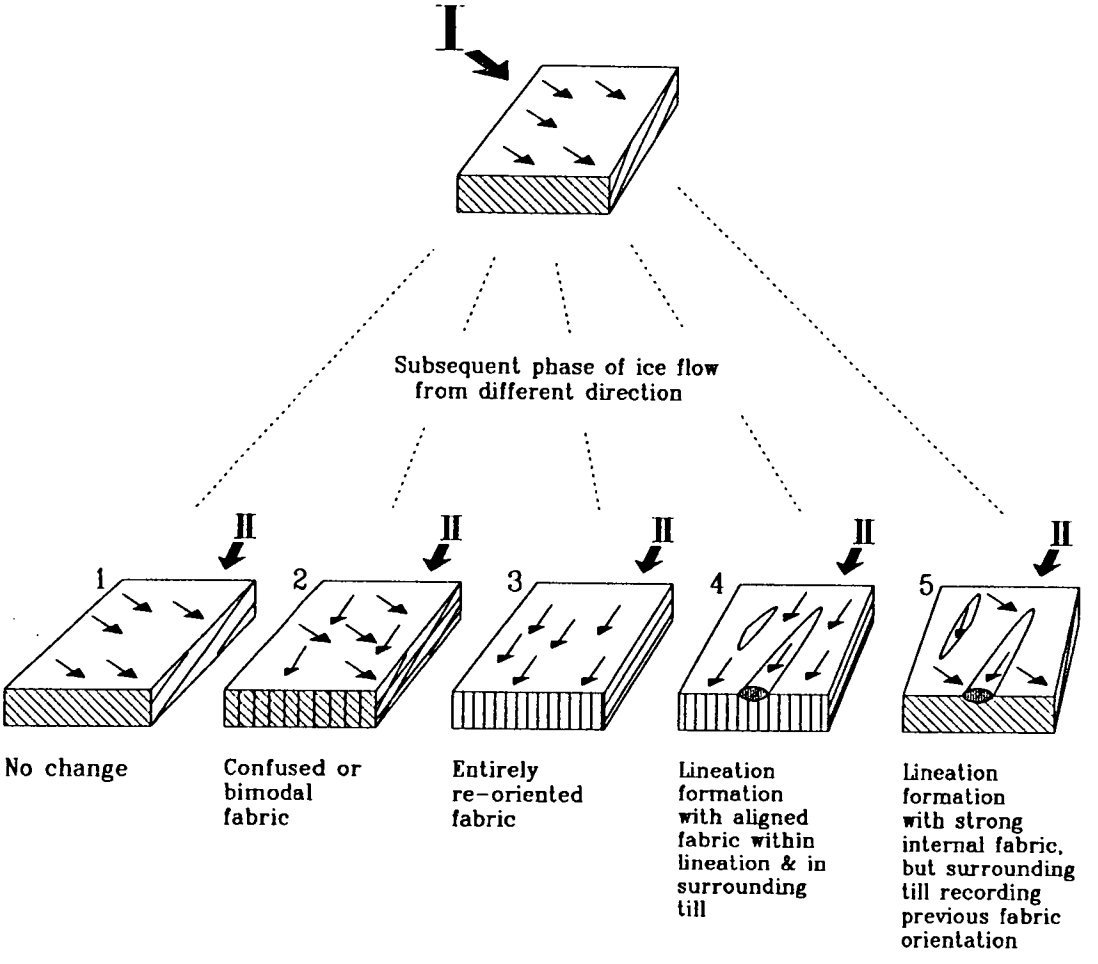

Figure 18. *Possible fabric-lineation relationships resulting from two phases (I and II) of ice flow (see text).*

indicating flow towards the SE were found in this till, which otherwise displayed an overall fabric indicating ice flow towards the SW. Fabric diagrams from different locations also showed a bi-modal distribution of orientation; a main SE maximum and a smaller SSW maximum. They suggest that this shows "a gradual reorientation of a SW to a SE fabric; and that the rearrangement has not been completed, as a considerable number of pebbles have been left aligned through the sector between the former SW maximum and the new SE one". Cross-cutting striae in the vicinity also show the same two directions. This evidence of a bi-modal till fabric documenting a gradual reorientation of clasts by changing ice flow directions represents my option no.2 (figure 18).

MacClintock and Dreimanis (1964) also found evidence which I regard as an example of my option no.5: glacial lineations containing fabrics parallel to their trend in a surrounding till which displays an altogether different fabric orientation. They describe reorientation of clasts and deformation of till occurring in a linear zone 200 feet wide and 30 feet deep within the Malone Till (this is the lower till deposited by ice flowing to the SW). This linear zone is oriented parallel to the ice advance of the later Fort Covington Till (SE flowing ice). They describe the shape of the reoriented portion as resembling a groove or gouge. This description seems to indicate the existence of a linear zone of deformation (shears and drag folds are also present) which could be a mega-scale glacial lineation identified on purely sedimentological grounds.

The implication of this fabric variability within till is that studies of individual or closely-spaced sites may give an erroneous impression or partial story of regional ice flow. Because of their limited spatial coverage they may record only one direction of ice flow. I suspect that many fabric diagrams have been compiled that show widespread or bi-modal orientations, but have been regarded as anomalous and have thus remained un-

interpreted. Only those with clear uni-modal maxima have been used to provide information on ice flow.

What are the likely clast fabric orientations within an area which contains two cross-cutting lineations? This is an important area of research that constitutes a future phase of analysis. Its results may allow a re-interpretation of much till fabric evidence and provide more complete palaeo-ice flow information. It is of particular importance as it provides the link between major large-scale lineation studies (this thesis) and detailed stratigraphic and dated sections. At present we can only theorise about the nature of the detailed relationship of fabrics to mega-scale lineations. The only certain result of two stage ice flows which produce cross-cutting relationships, is that clast orientations within the youngest lineation will parallel its trend. The fabric within the older lineation and in the surrounding till could be either aligned parallel to the old or new flow direction or reflect a mixture of both.

Research on a smaller scale indicates a further order of complication within the fabric-lineation relationship. Rose (1989) investigated flutes superimposed at a different orientation upon megaflutes in north Norway, and discovered firstly that although clast orientations in flutes do broadly parallel the flute axis, there is a slight convergence and divergence of flow present. If this type of flow pattern also produced mega-scale glacial lineations, we would expect large convergences and divergences and thus need to allow for this variability when examining associated fabric orientations. More importantly, Rose was able to show that three fabric orientations exist in the cross-cutting lineations. Firstly, there is strong preferred fabric within and parallel to the megaflute, except for a so-called erosional zone that lies immediately adjacent to the superimposed flute. In this zone fabrics were reoriented parallel to the superimposed flute. The fabric orientations

and strengths vary according to their exact position within the zone. The third orientation present is the fabric displayed within the superimposed flute itself, which is broadly parallel to the flute, but with the aforementioned convergence and divergence.

It is important to discover if the fabric-lineation relationship recorded by Rose (1989) holds true for lineations of much greater size, as it has important implications for stratigraphic interpretation. For example, if sections were examined at different positions in and around a cross-cutting lineation pattern, different "regional ice flow" reconstructions could emerge from each.

Chapter 4

Strategy Adopted for Mapping Ice Flow

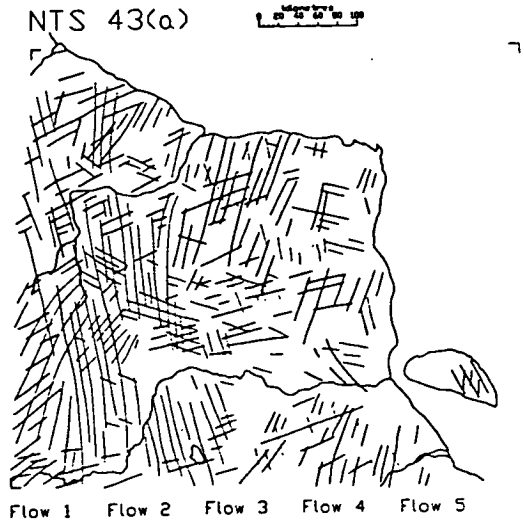

Chapter 4

Strategy Adopted for Mapping Palaeo-Ice Flow.

This chapter describes the detection and mapping of glacial lineations. Firstly, the importance of scale of remotely sensed imagery is discussed, and the characteristics of the six types of imagery that were used is outlined. Glacial lineation mapping and relative chronology determination, within a system devised to provide internal corroboration, is described. The way in which gross ice flow patterns were derived from individual lineations is outlined. Ice flow patterns were then digitised and compiled as a final mosaic of continent-wide flow sets.

4.1 Remote Sensing Scales.

It was argued in the previous chapter that glacial lineations exist over a wide range of scales. It is thus important that an equally wide range of remote sensing scales are used in order to capture a large and scale-unbiased data set.

Each scale of remotely sensed image can be regarded as a spatial frequency filter, which filters the natural spatial frequencies into discrete ranges which have high-frequency boundaries determined by resolution and low-frequency boundaries controlled by the instantaneous working area (IWA). A conventional air photograph, for example, at a scale of 1:50,000 has a potential resolution of 1.5 m and an IWA of 13 by 13 km, while a Landsat MSS image has a resolution of 80 m and IWA of 185 by 185 km. Detectable

frequencies clearly need to be of wavelengths which are significantly smaller than the IWA. Comparison of the images in Photoplate 13 illustrates that each remote sensing scale samples only one of the three natural frequency ranges typical of glacially-streamlined landforms. If the air photograph (photo a) is used to map ice flow direction, the dominant drumlin pattern will be discerned, giving a flow orientation of 254 degrees, but the orientation of lower frequency elements will be missed. The Landsat scene (photo b) shows a very clear orientation at 225 degrees, but the higher spatial frequency orientation at 254 degrees is virtually filtered out. Comparison of both scales allows orientations at both spatial frequencies to be discerned. For example, once low frequency forms are detected on Landsat images they can often be traced across air photographs where they were previously undetected. It is important that if a pattern is just discernible at one scale of imagery, then it should be pursued to a more suitable scale and investigated.

Mapping at one scale enables only part of the natural data set, which reflects former ice flow, to be captured. In order to accommodate this problem my analysis of drift lineations in Canada has utilised 6 different scales: air photographs, air photo mosaics, Landsat TM and MSS, MSS mosaics and AVHRR imagery. These IWA and resolution parameters are related to the presumed modes of spatial frequency of glacial lineations in figure 19. The characteristics of each type of imagery are outlined in the following table:

	RESOLUTION	INSTANTANEOUS WORKING AREA (IWA)
Air photographs:	1.5 metres	13 x 13 km
Air-photograph mosaics:	15 metres	50 x 75 km
Landsat Thematic Mapper (TM):	30 metres	185 x 185 km
Landsat Multi-spectral Scanner (MSS):	80 metres	185 x 185 km
Landsat (MSS) mosaics:	80 metres	500 x 500 km
NOAA, AVHRR Advanced Very High Resolution Radiometer:	1100 metres	3000 x 3000 km

Photoplate 13. *Different scales of remote sensing sample different spatial frequencies of ice flow landforms. An air photograph and Landsat image are illustrated for comparison.*

Photo a; *air photograph in which the dominant drumlin pattern is easily discerned indicating a flow orientation of 254°. Location of air photograph is marked as a box on the Landsat image.*

Photo b; *extract of a Landsat image which clearly displays a mega-scale glacial grain trending towards 225°. Area shown is that around Boyd Lake Northwest Territories, (NTS 65E).*

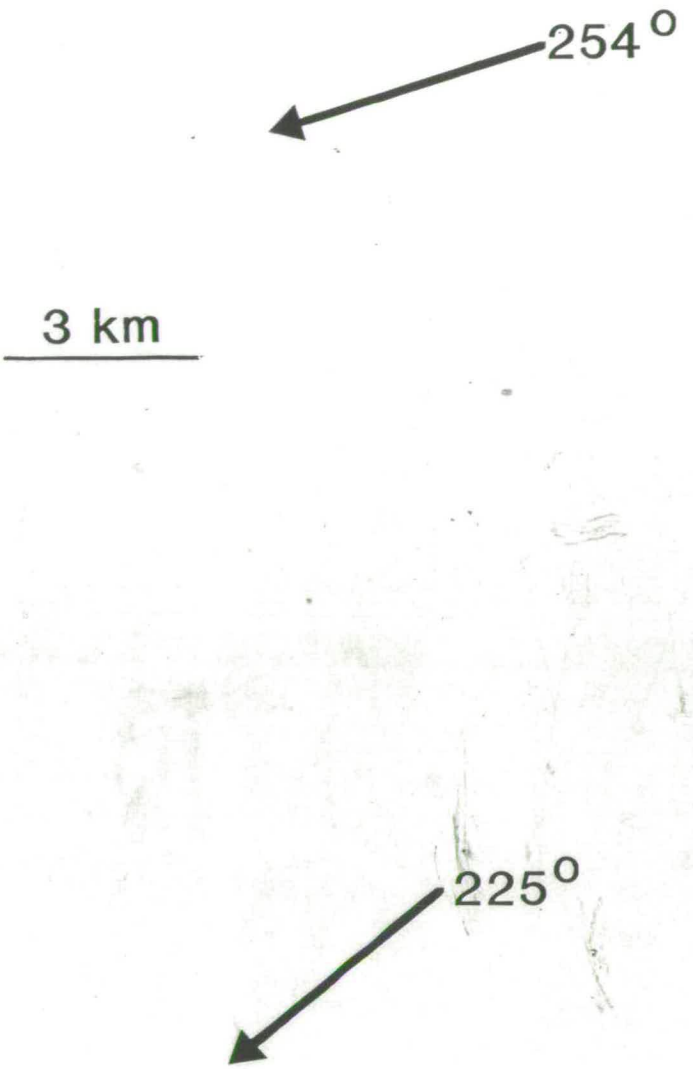
254°
3 km
225°
30 km

a

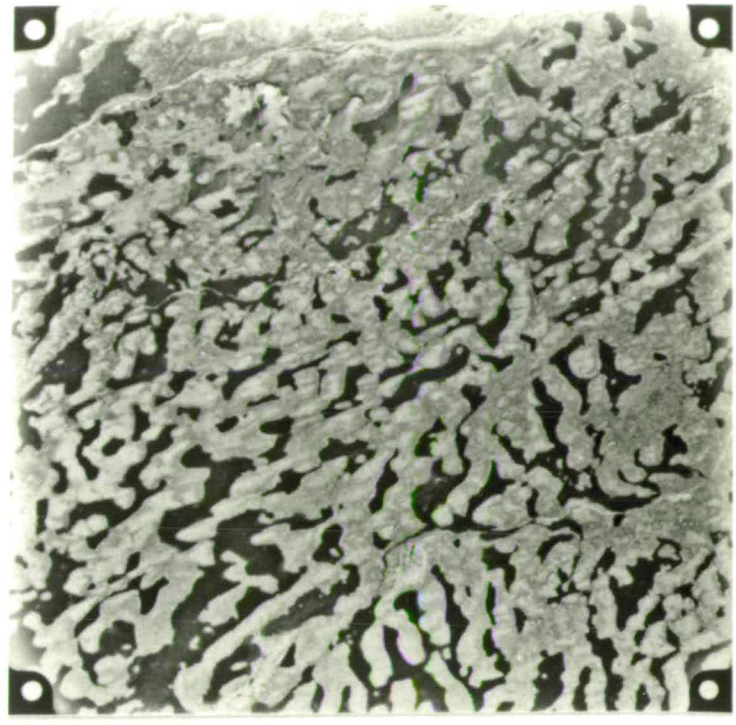

b

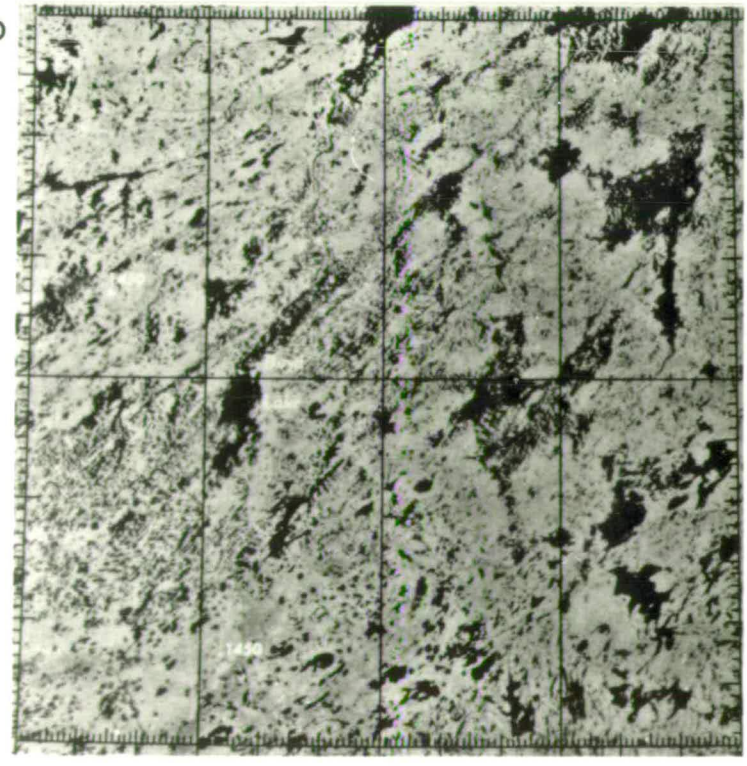

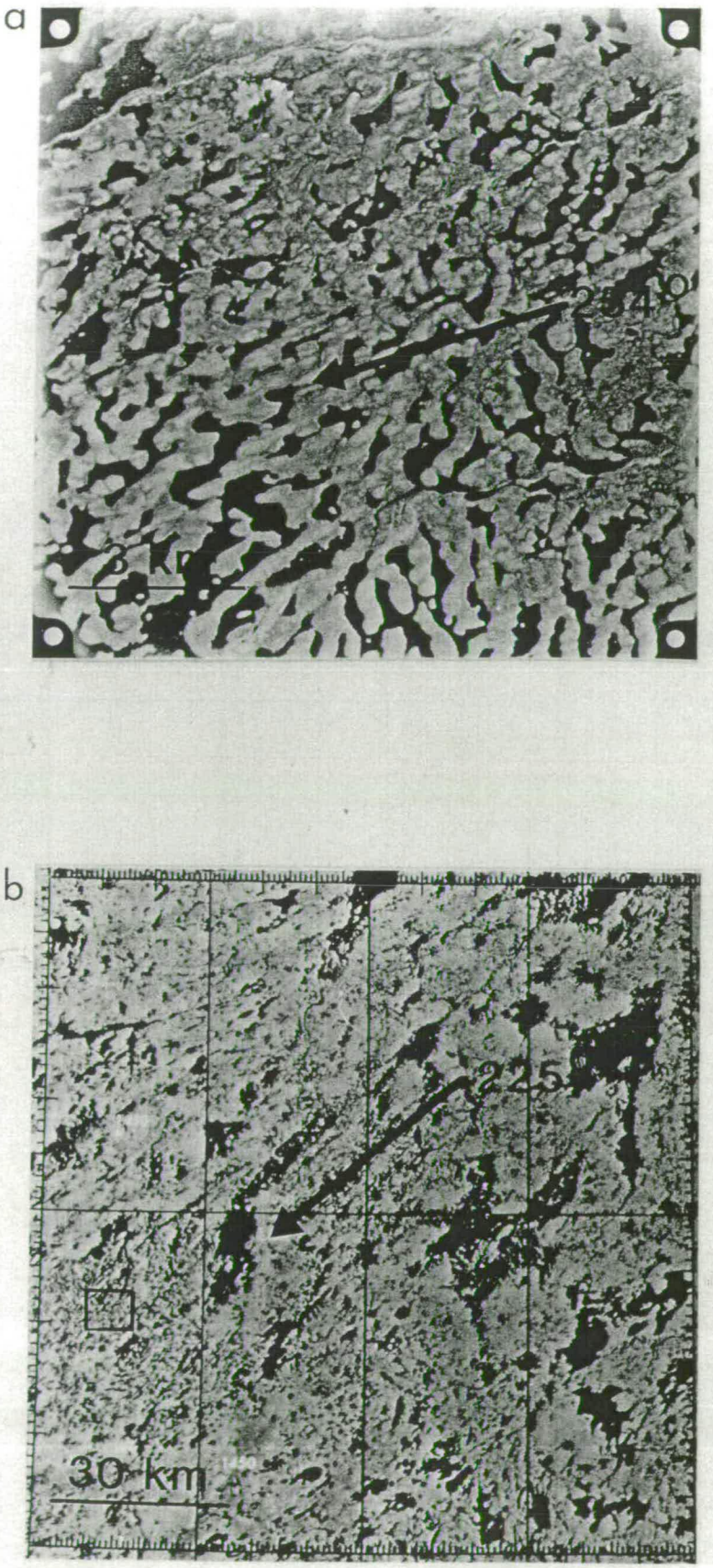
a
b
30 km
30 km

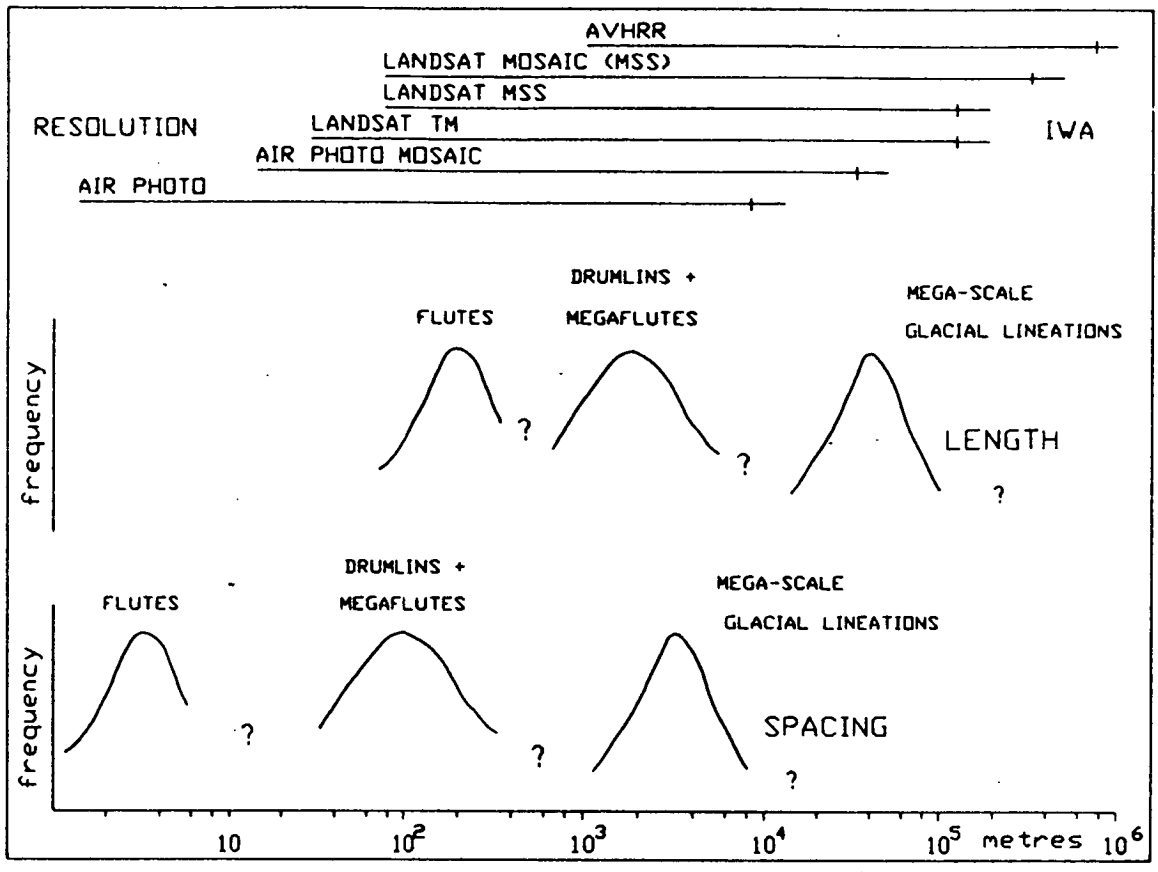

Figure 19. *The resolution and instantaneous working area (IWA) of remote sensing media used in this thesis compared to presumed modes of spatial frequency of glacial lineations.*

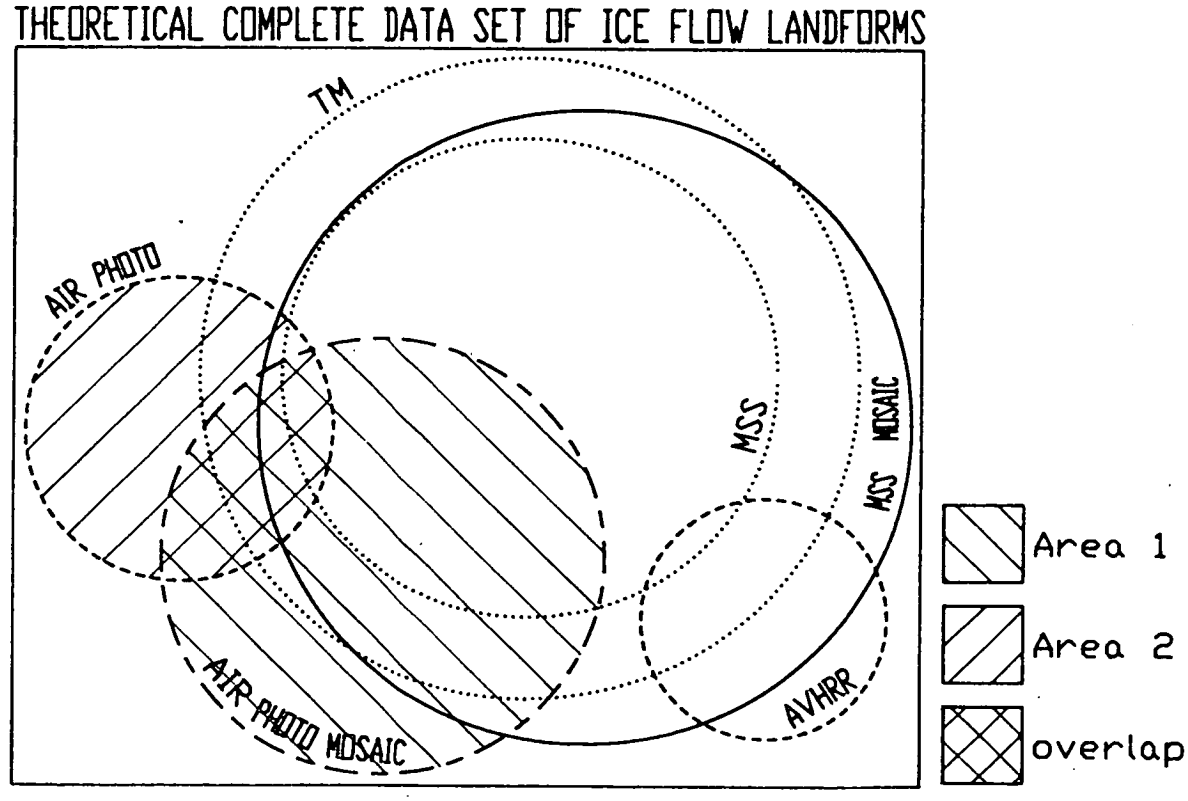

Figure 20. *Venn diagram illustrating the relationship between the overlapping spatial frequency ranges sampled by remotely sensed imagery, and the ice flow data they appear to capture (see text).*

In figure 20, I relate the overlapping spatial frequency ranges of these data sets to the ice flow data they appear to capture by means of an adapted Venn diagram. The box represents a theoretically complete data set of ice flow landforms and the circles correspond to the remote sensing scales that were used, with the area of each circle representing a subjective estimate of the proportion of data that can potentially be captured at that scale. The Venn diagram illustrates the interplay between resolution and IWA in influencing the detection of natural frequencies as the scale of sampling increases. Air photographs capture only a fraction of the available information about palaeo-ice flow, and so this fraction is represented by a circle of small area in the Venn diagram. For air photo mosaics, the IWA is considerably increased, thus allowing lower frequency landforms to be detected. This increase in data capture is represented by the area shaded 1. High frequency flute patterns however, will be lost because of the coarsening of resolution from 1.5 to 15 m. Area 2 shows this loss of data. The region of overlap between the circles is the proportion of data that is discernible at both scales. The Landsat MSS and TM circles are positioned concentrically, as they have the same IWA, but the resolving power of MSS is considerably less. Mosaics of Landsat MSS cover a 500 by 500 km area which allows very large features to be easily identified. AVHRR imagery of larger IWA and decreased resolution is able to pick out only the lowest frequencies and is particularly valuable in large scale regional interpretations and for detecting very low frequency patterns (e.g. Johnston *et al.* 1989). However, a great deal of AVHRR-derived information is duplicated by Landsat mosaics, illustrated in the Venn diagram by the large degree of overlap and the small area representing acquisition of new data. The remainder of the area outwith the circles and inside the box indicates the existence of still uncaptured information. The AVHRR scale of 1000's of kilometres is at the same order of magnitude as the Ice Sheet and thus excludes the possibility of missing any extremely low frequency ice flow patterns.

An exception to this might be lineations that are themselves very narrow (less than a pixel width), but display extremely low spatial frequency (spacing of 100's of kilometres). Forms such as these are considered unlikely in that there seems to be a high correlation between lineation width and spacing, i.e. flutes tend to be narrow and closely spaced, drumlins broader and more widely spaced. This relationship is probably a result of limited sediment supply and would be expected to hold throughout the whole range of lineation scales. The missing information is at the scale of centimetres and metres. Ice flow indicators at this scale tend to be isolated and, unlike lineations seen at Landsat scale, do not spread contiguously over large distances. Small scale lineations are thus difficult to group into discrete flows making it difficult to infer gross ice sheet flow patterns.

The interaction between the scales of remote sensing media and the frequency of variation in glaciogenic landforms led me to devise the following sampling strategy: widespread mapping at two basic scales; Landsat mosaics (1:1 000 000) and air photograph mosaics (1:250 000 to 1:800 000), coupled with careful examination of AVHRR, MSS and TM individual scenes and air photographs for selected areas. The areas covered by each type of imagery are indicated in figure 21.

Figure 21. *Coverage of different types of remotely sensed imagery used for examination and mapping of glacial lineations. The Canadian, National Topographic System (NTS) is superimposed for reference.*

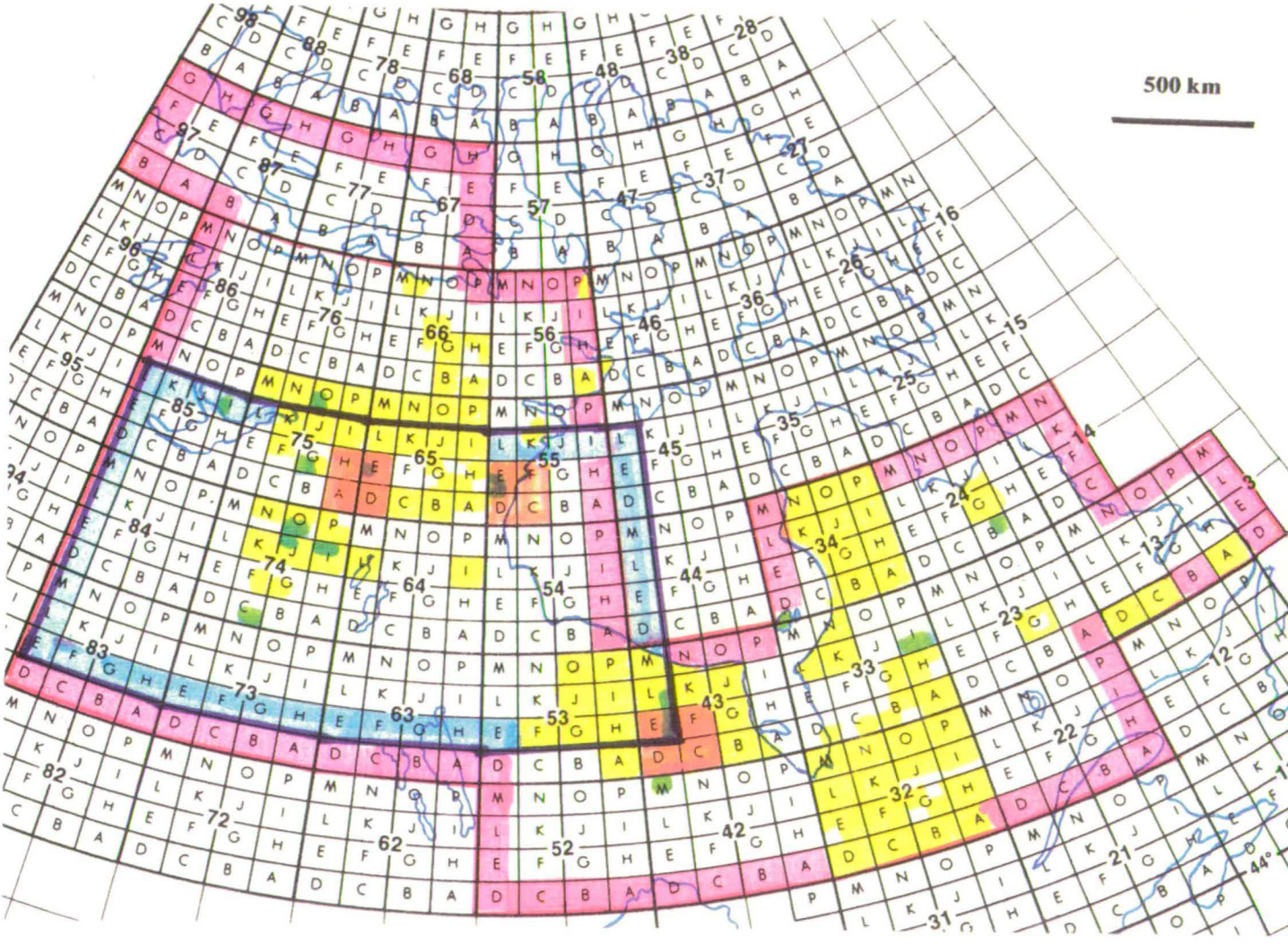

; aerial photographs

; air-photograph mosaics

; Landsat images; Multispectral scanner (MSS), or Thematic mapper (TM)

; Landsat mosaics

; NOAA Advanced Very High Resolution Radiometer (AVHRR)

4.2 Basic Mapping Technique.

4.2.1 Method for Internal Corroboration.

The National Topographic System (NTS) of Canada is a system of quadrants which allows areas rather than points to be easily referenced (without recourse to latitude and longitude coordinates). All imagery and interpreted maps have been referenced according to this system (see figure 21).

In this thesis ice flow features have been mapped by visual appraisal. On remotely sensed imagery the appearance of glacial lineations varies in degree of clarity from extremely strong high-amplitude signatures to weaker and more subdued patterns. As illustrated in Chapter 2, the older lineations tend to be more dissected, degraded and subdued. Although these are harder to identify, they are critical indicators of multi-phase ice movement.

In most areas the patterns of glacial lineations are clear and easily recognised, but the weaker patterns are often near to the boundary of interpretability. The mapping strategy must therefore maximize the identification of such weak forms, and provide a means to test the subjectivity of interpretations. This was achieved by mapping from Landsat and air photograph mosaics in NTS quadrants, without knowledge of their location, or attention to the orientation of the image. All drift lineations thought to be produced parallel to ice flow were mapped, irrespective of their orientation, frequency or compatibility with current ideas regarding regional ice flow direction. Once complete, the interpreted quadrants were compiled as a mosaic, so as to test the cross-quadrant

continuity of lineations. Strong continuity was taken to confirm the original interpretations. Where there was poor continuity across boundaries the lineations were regarded as suspect (i.e. over-interpreted) and were therefore rejected. In the majority of cases, lineations correlated well across numerous quadrant boundaries, producing integrated co-linear sets over 100's to 1000's of kilometres. This was the case, even when original interpretations were thought to be speculative and with images from different times of the year and with varying sun elevations.

I believe such methods of internal corroboration provide an extremely useful test when dealing with large and inaccessible areas where external confirmation is not available.

4.2.2 Glacial Lineation Mapping from Landsat Mosaics.

Landsat mosaics were acquired of almost the whole area of mainland Canada thought to have been covered by the Laurentide Ice Sheet. The mosaics were prepared by the Surveys and Mapping Branch, Department of Energy, Mines and Resources, Ottawa, and together comprise approximately 400 Landsat scenes (from the Landsat-1 mission between 1972-1974) spliced together and presented as 33 NTS blocks at a scale of 1:1,000,000. Photoplate 14 illustrates a 30% reduction of one of the Landsat mosaics. The images are all monochrome renditions of band 6, with a simple linear contrast stretch applied. Cloud cover is minimal (less than 5% of the total area). Band 6 (0.7 - 0.8 μm) or 7 (0.8 - 1.0 μm) are the most suitable bands for lineation detection. This is because they both detect vegetation and moisture differences, and show strong shadow effects. Lineations defined by topography cast shadows, and those that have no surface

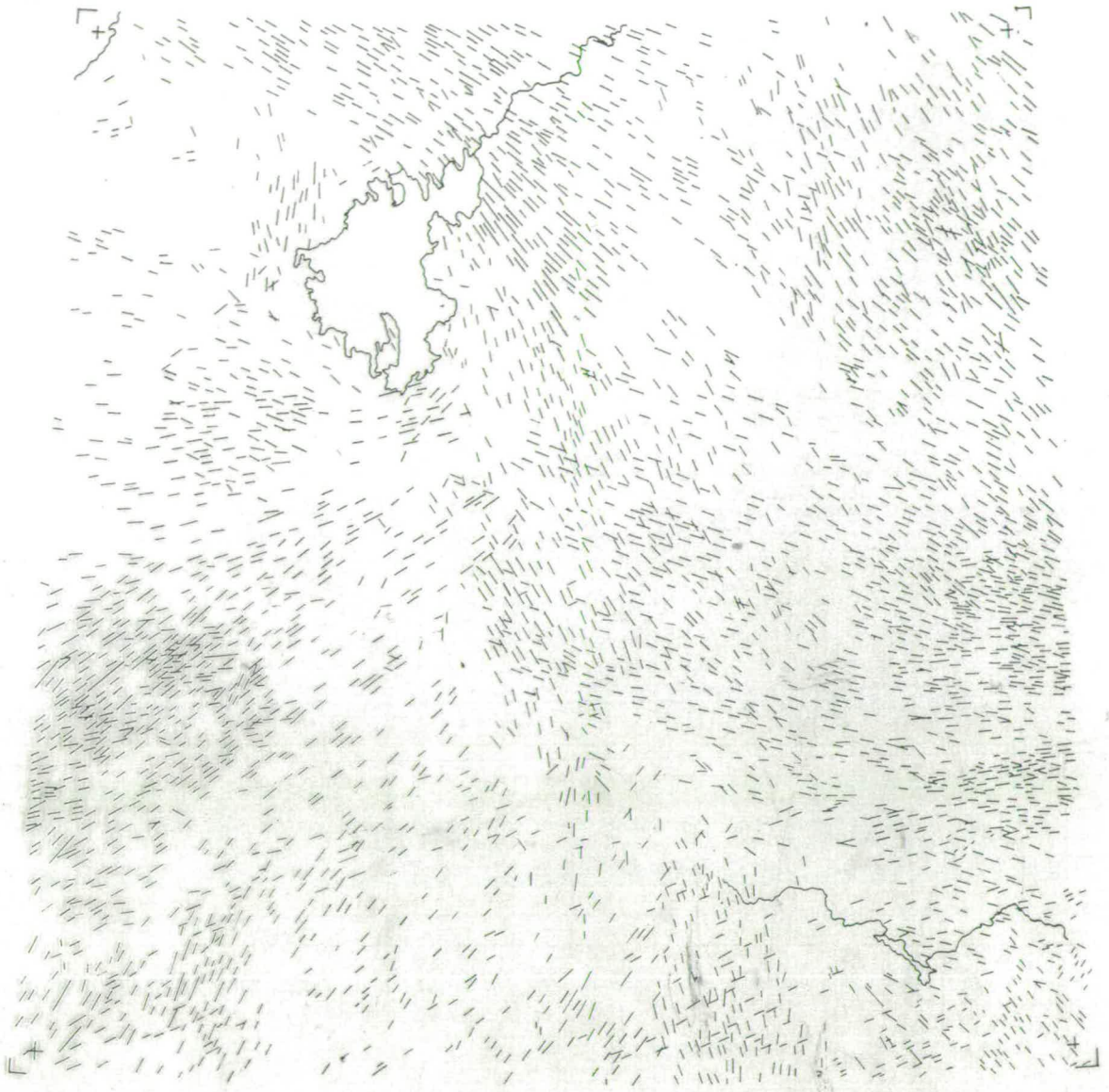

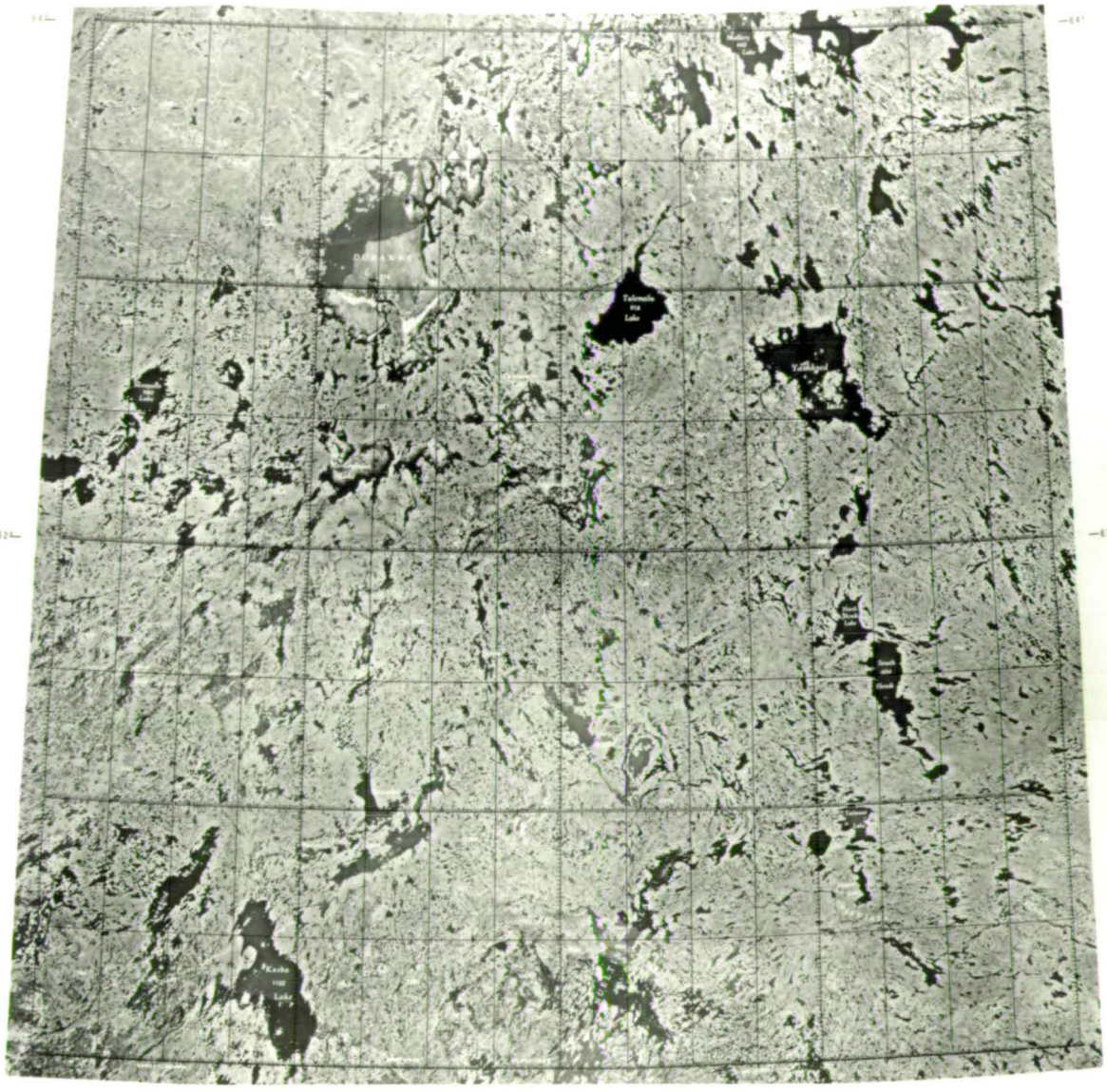
Talemaila
ma
Lake

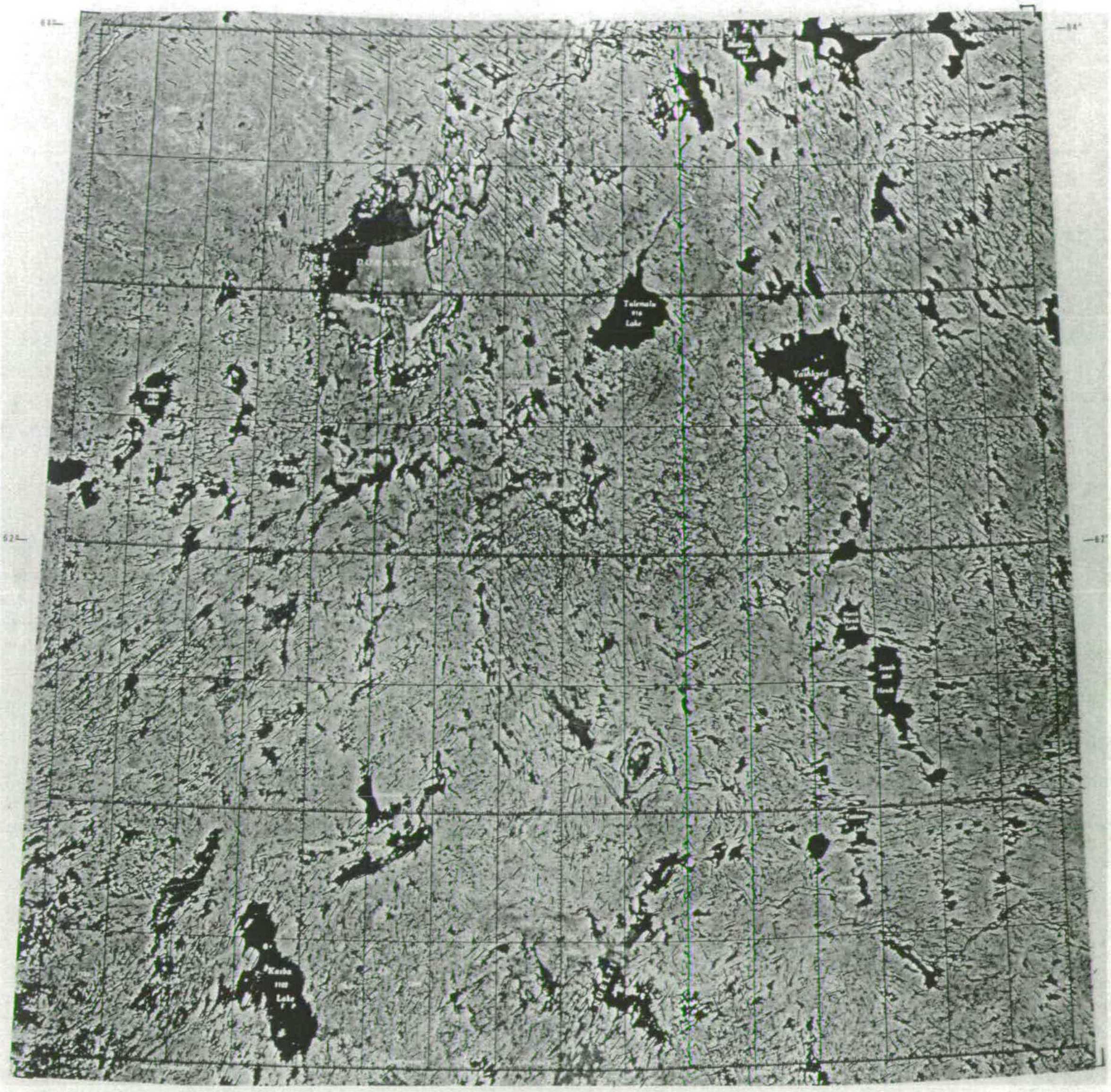

expression but are defined by variation in sediment character can be detected by drainage (soil moisture) and vegetation preference.

The perception, detection and mapping of glacial lineations is not a conscious procedure using the notional characteristics described above (they constitute the reasons why) but by identification of sharp tonal contrasts in the imagery forming straight lines. In Photoplate 15 a section of a Landsat mosaic is presented at the working scale used for mapping. The millimetre (= km) scale of tonal contrasts within the image clearly illustrates the nature of glacial lineations.

The mega-scale glacial grain was mapped by laying acetate sheets over the photo-mosaics and by marking on the orientations of the lineations. Because of the large number of lineations and the high spatial frequency they often display, coupled with the poor definition tonal contrast provides for resolving individual features, it was considered futile to mark on singular geomorphic forms. If individual lineations were marked, the subsequent scale-reduction of the mapped sheet would render many areas as a dense mass of uninterpretable black ink. For these reasons the representation of the glacial lineations, which can be regarded as forming a grain (of varying spatial frequency) were mapped by using straight lines aligned parallel to the lineation trend, and repeated enough times to portray the grain and to mark its extent. The length of the line was made proportional to the perceived length of the lineation, although this was prone to a degree of subjectivity. However, the line lengths do help to characterise particular lineation sets.

Substantial effort was spent in mapping each NTS block, and the orientation of the image was frequently altered in an attempt to minimise any preferential bias in interpreting specific directions.

Photoplate 15. *An extract of a Landsat mosaic (NTS 65N) presented at the scale used for mapping (1: 1000 000). East-west dimension of image is 130 km.*

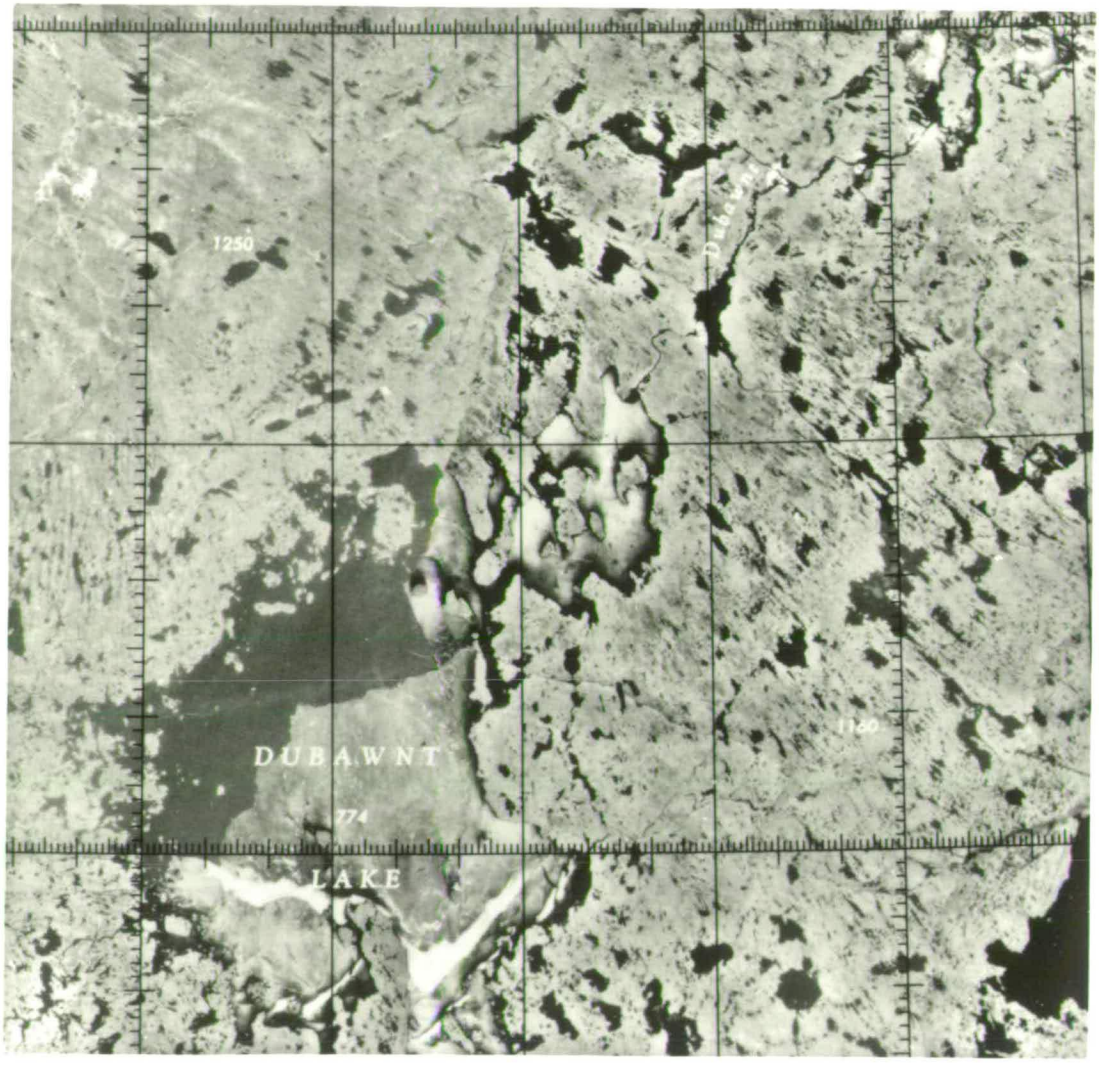
1250
DUBAWNT
774
LAKE
1180

A possible source of sampling bias is the effect of sixth-line banding or drop-out in the imagery. Photoplate 16 shows an enlarged extract of a Landsat mosaic, which clearly illustrates this problem. Landsat images are composed of lines of pixels that are scanned perpendicular to the direction of travel of the satellite. Unfortunately radiometric drifting of the six onboard sensors on the early Landsat missions often resulted in every sixth line being either lighter or darker than average (Kalush, 1979). This effect is present throughout the Landsat mosaics used for mapping in this thesis. It has the potential to enhance lineations parallel to the scan lines. It is hoped that an awareness of this background grain in the imagery has limited the sampling bias that it might otherwise have created. In practice, after many hours of interpreting, the "sixth-line dropout" effect becomes invisible in much the same way as a cracked windscreen does when driving a car.

The consistency of the mapping procedure was tested by re-interpreting NTS quadrant 32, ten months after interpreting the original. Individual lineations obviously varied, but the produced pattern of ice flows was identical.

An example of an interpreted overlay is presented with Photoplate 14. It was decided that analysis of this and other data would be carried out at a working scale of 1:2,000,000. This required all the acetate sheets of mapped ice flow to be photographically reduced by 50%.

Photoplate 16. *An extract of a Landsat mosaic illustrating the systematic (WNW-ESE) background grain or noise, that is the result of sixth line banding. East-west dimension of image is 50 km.*

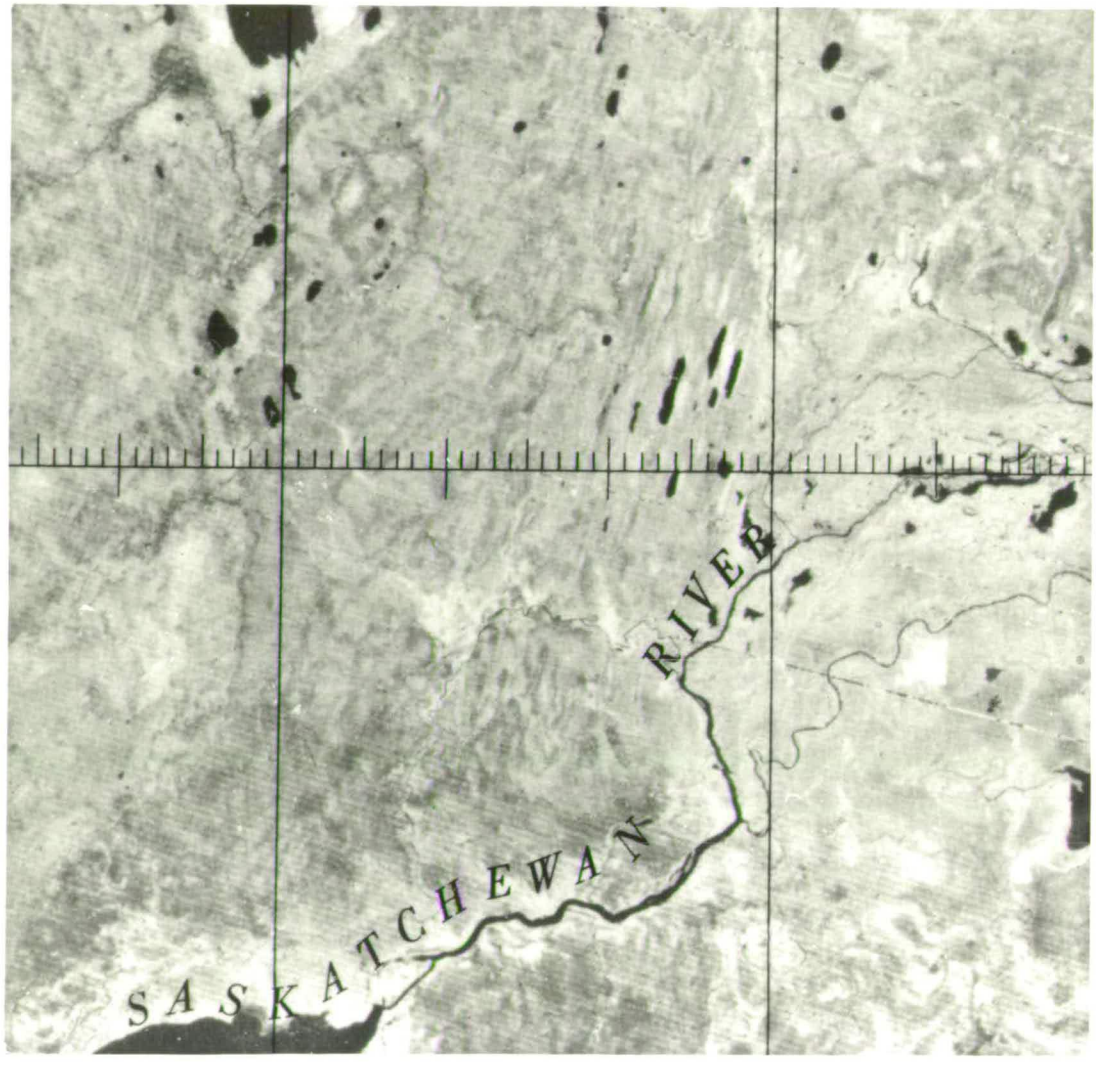
SASKATCHEWAN RIVER

4.2.3 Glacial Lineation Mapping from Air Photograph Mosaics.

Many hundreds of air photograph mosaics were acquired from the Department of Energy, Mines and Resources, Canada. They were chosen to cover critical areas for the development of a relative chronology of cross-cutting lineations apparent on Landsat images. The coverage is indicated in figure 21. Over 500 mosaics representing approximately 75,000 individual air photographs were acquired. They vary in scale between 1:250,000 to 1:800,000 and are not geometrically corrected to any topological control system.

A slightly reduced air photograph mosaic is illustrated in Photoplate 17. The boundaries of each air photograph are clearly visible, but are easily ignored when interpreting. An overlay of interpreted glacial lineations is included in Photoplate 17. Mapping was performed using the same grain representation criteria as described in the previous section for Landsat mosaics. The only difference was that interpretation lines were drawn with a heavier line weight to permit the greater size reduction required to bring them to the working scale.

Once complete, the precise scale of each mosaic was measured and calculated and the corresponding acetate overlay photographically reduced to the allotted working scale of 1:2,000,000. This scale reduction produced an image the size of a postage stamp. These were pasted together into NTS blocks so as to be compatible with the Landsat interpretations. Figure 22 is an example of one such NTS block.

Photoplate 17. *Air-photo mosaic composed of approximately 130 individual air photographs. An overlay of mapped lineations is included. East-west dimension of image is 60 km.*

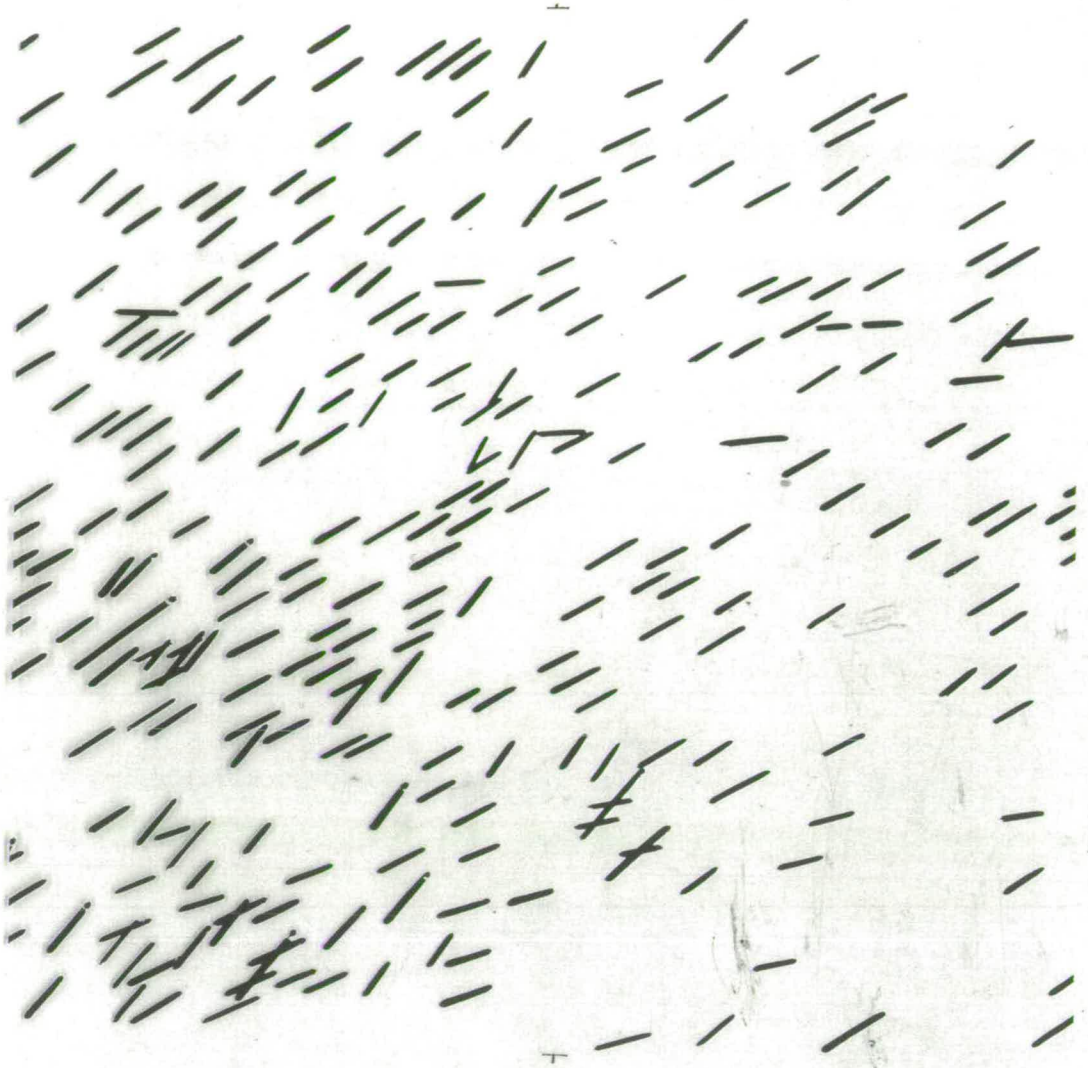

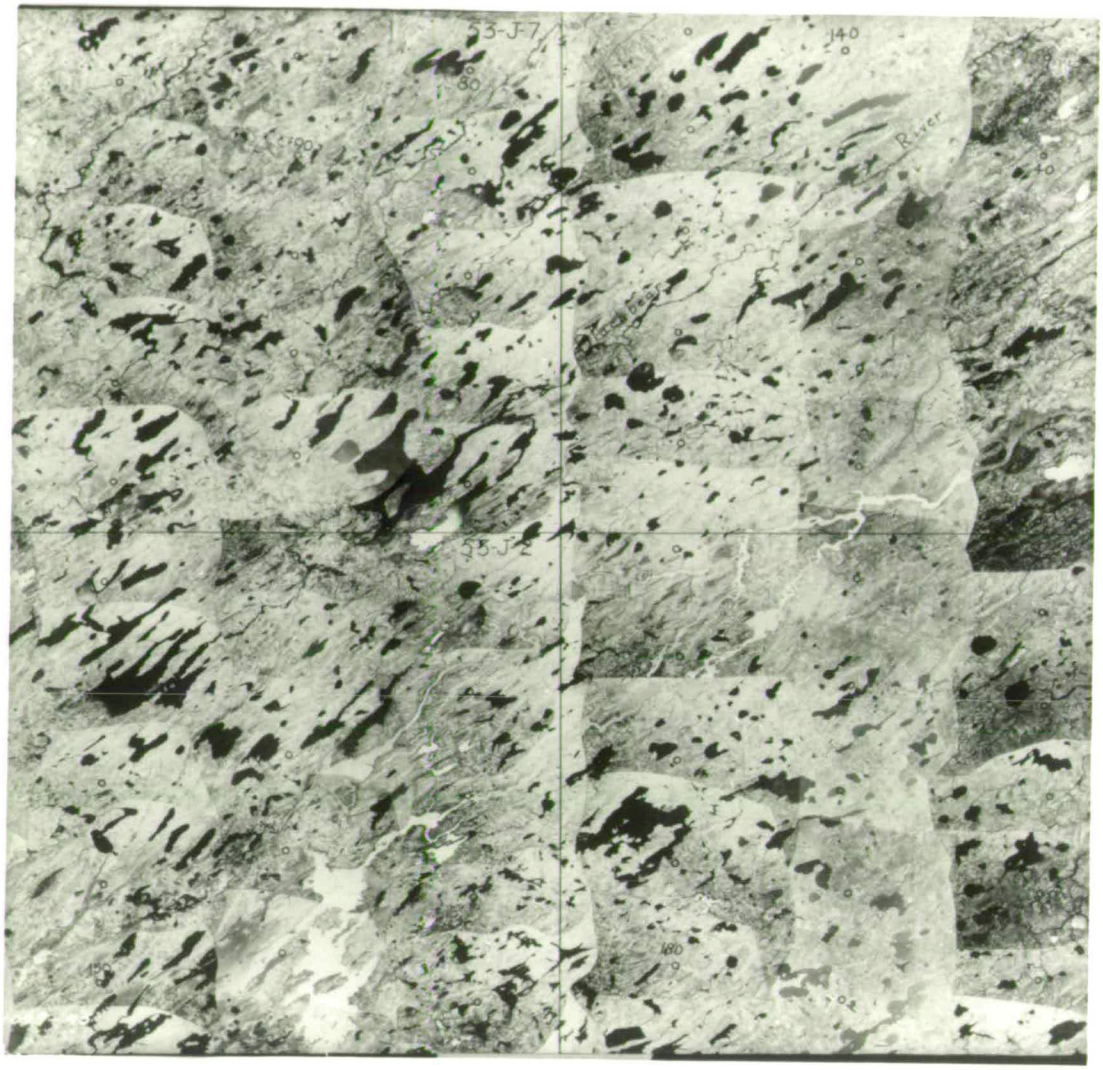
33-J-7
140
River
33-J-2
180

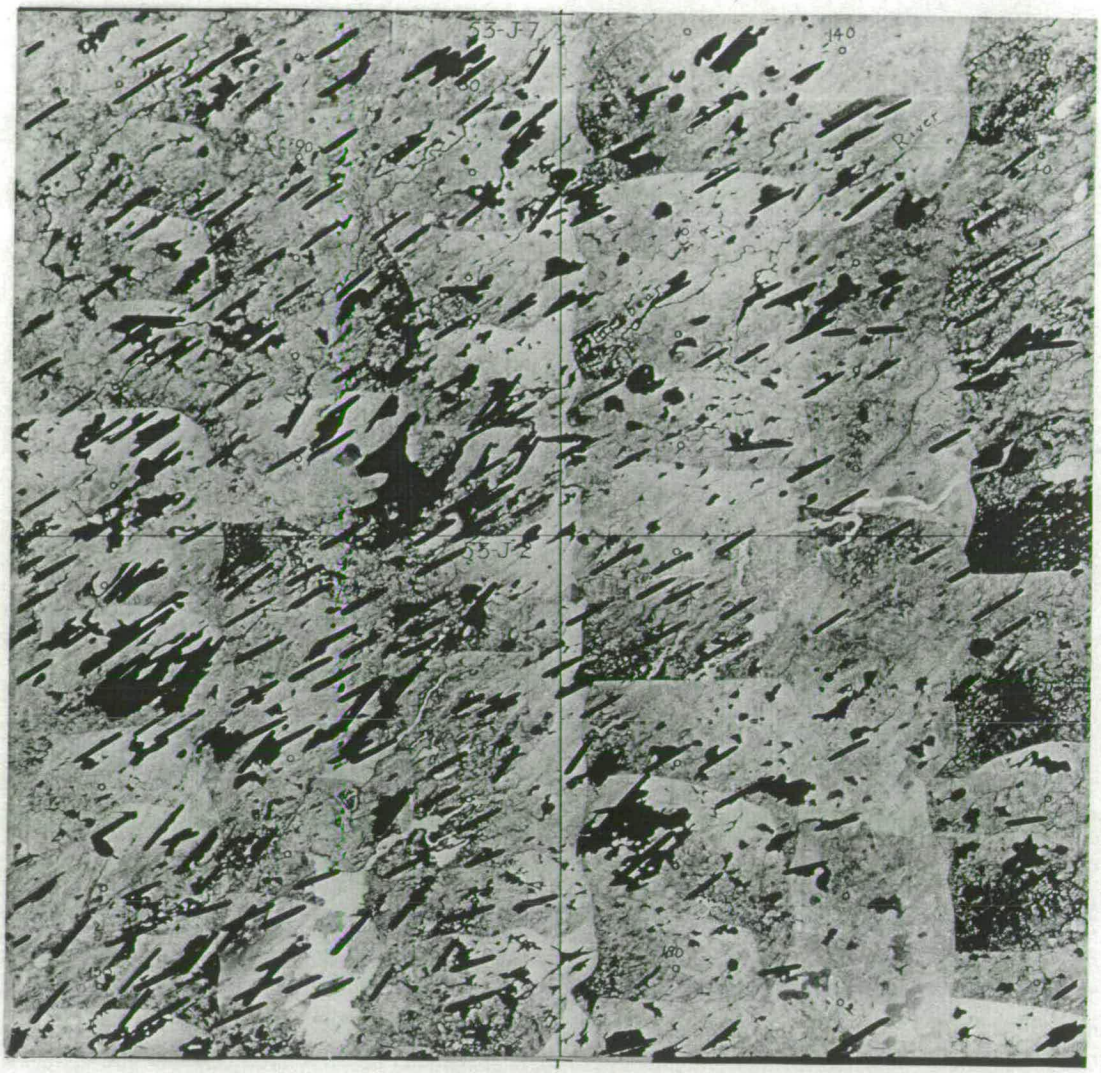
53-J-7
140
River
53-J-2
180

Figure 22. *A mosaic of mapped lineations compiled as an NTS quadrant. Each small square contains lineations that were mapped from different air-photo mosaics, which were then photographically reduced in size and pasted together.*

4.2.4 Influence of Non-Glacial Structures.

The mapping of glacially produced drift lineations can be problematic in areas of extensive bedrock exposure. This is especially true if there is a strong inherent pattern of bedrock lineation. When predominantly bedrock areas were mapped, great care was taken to avoid recording structural bedrock lineaments. However, many structural patterns have been enhanced by glacial erosion, and a small number of lines were drawn to represent this. On the Canadian Shield structural patterns are extremely complex in contrast to the straight and parallel glacially-produced drift lineations (see Photoplate 18). This makes the task of differentiating the two patterns simple. However, dyke swarms often display a similar pattern to glacial lineations, i.e. they form sub-parallel sets extending over many tens of kilometres with a similar spatial frequency and degree of curve. Knowledge of the location of major dyke swarms allowed this potential for confusion to be avoided (see Section 4-3-2). Other non-glacial linear structures which may sometimes be confused with glacial lineations are: beach and lake strandlines; river and gully patterns, and oriented permafrost lakes (Hall and Ormsby, 1983). They are however, isolated cases and are readily identified when overall ice flow patterns are reconstructed (see Section 4.3).

4.2.5 Relative Chronology Determination.

It is often possible to determine the relative ages of cross-cutting lineation sets (see Chapter 2). Knowledge of their relative age is of great importance because it provides a history of change in ice flow for that location, and together with other locations, may

Photoplate 18. *Contrast between drift glacial lineations in the southern half of the image and complex structural geological patterns in the northern half. Extract of a Landsat mosaic of the area east of Lake Athabasca (NTS 74O). East-west dimension of image is 220 km.*


NORTHWEST TERRITORIES
SASKATCHEWAN
Fond du Lac
Richards Lake
Riou Lake
Pasfield Lake

form a pattern that constrains possible ice divide positions. The resultant large-scale patterns may permit us to reconstruct changes in ice sheet configuration through time.

After mapping the lineation pattern on an air photograph mosaic, a relative chronology index card was produced. It was compiled using the following criteria:

1) ORIENTATION AND FREQUENCY OF OCCURRENCE: The interpreted pattern of lineations were summarised in a rose diagram. Lines on the index card were drawn parallel to each flow direction, with the length of line representing a subjective estimate of the dominance of each orientation.

2) RELATIVE CHRONOLOGY: The relative ages of lineations forming cross-cutting sets is determined by examining their geomorphic relationship to each other. If one lineation set can be observed either superimposed upon, or to have deformed and attenuated a differently oriented set, then it must represent the younger flow. By this method the relative chronology of differently oriented flows was ascertained and the relative age relationship recorded on the index card using Roman numerals (i.e I, II), figure 23. In this way it is possible to build up relative age sequences.

It was noted that the degree of certainty of relative age determination varied. For this reason a system of degrees of certainty was introduced to the assessment of relative age. A three level star system was used:

***: clear and unequivocal relative age determination.

**: probable relative age determination.

*: possible, but uncertain, relative age determination.

3) POLARITY: Detailed examination of individual components of the grain (including drumlins and flutes) often allowed the polarity of the flow to be ascertained. Strong

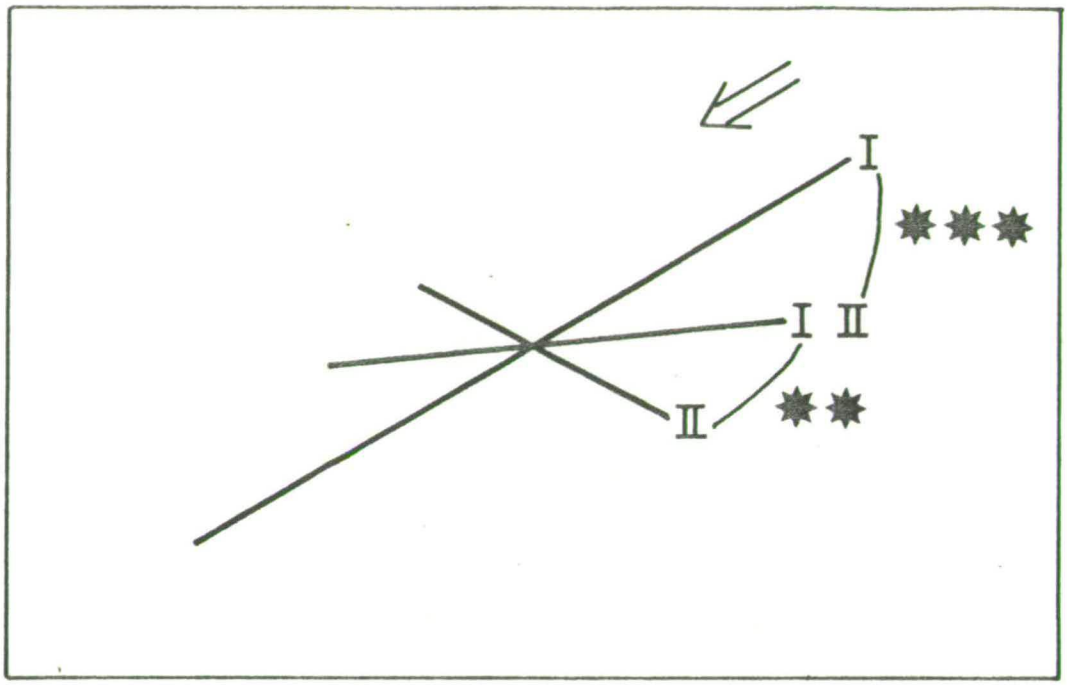

Figure 23. *Example of a relative chronology index card. Lines are drawn parallel to lineation sets, with line length representing a subjective estimate of the dominance of each orientation. Relative ages between different orientations of flow are recorded by Roman numerals, with stars used as an estimate of certainty (see text).*

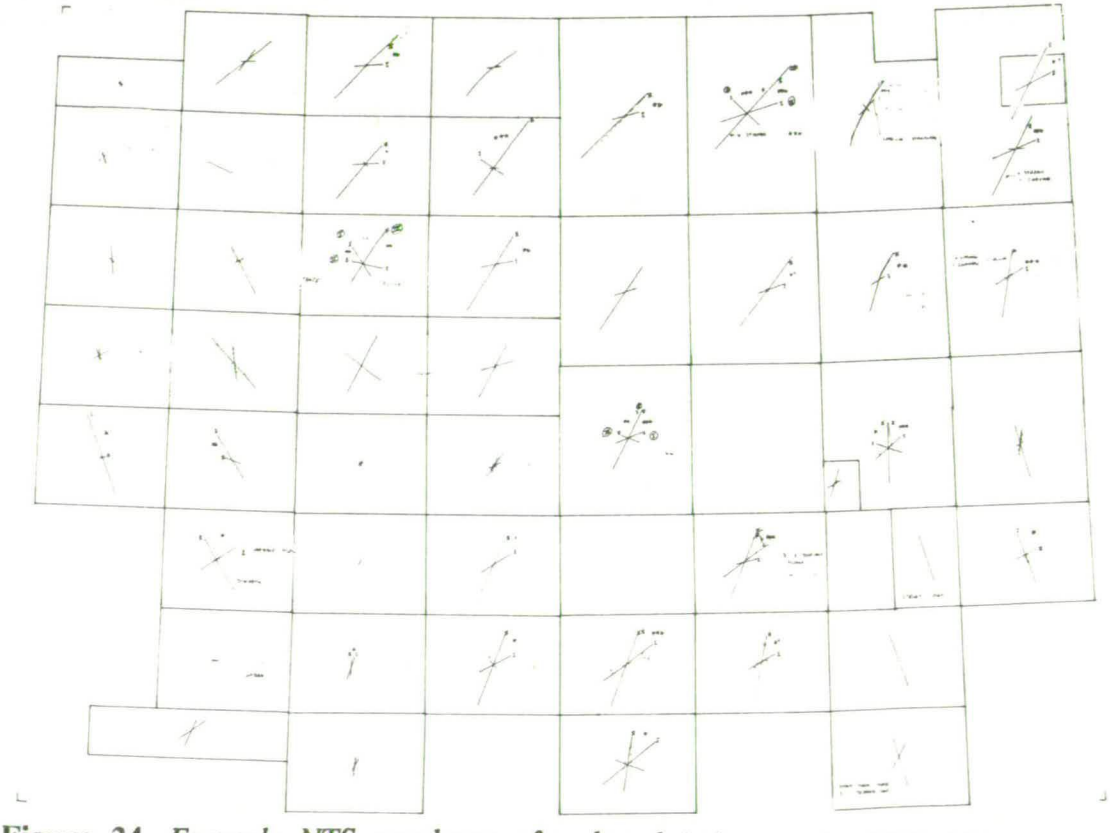

Figure 24. *Example NTS quadrant of reduced index cards (NTS 32). East-west dimension is 450 km.*

deformation of pre-existing lineation sets also revealed the polarity of the later flow. In both these cases the direction was marked on the index card by an arrow.

Determination of relative chronology and polarity was aided by the use of individual air photographs of large scale, when they were available (see figure 21 for coverage). In no instances did reference to single air photographs contradict interpretations made at mosaic scale.

To enable the relative chronology index cards to be used in conjunction with the maps of interpreted lineations, they were reduced in size and pasted together in NTS blocks (see figure 24). These were then photographed onto transparent acetate sheets for use as overlays.

4.3 Technique for Palaeo-Ice Flow Derivation.

4.3.1 Collation of Data.

To facilitate the adopted quadrant-by-quadrant approach, all data was filed according to its NTS quadrant number (representing a ground area of approximately 500 by 500 km). Each file has maps at the scale of 1:2,000,000 and contains:

1) Landsat-derived lineation map (on paper and transparent overlay).

2) air photo-mosaic derived lineation map (on paper and transparent overlay).

3) map of relative chronology index cards (on transparent overlay).

4) map of surface cover; defined as drift, drift/bedrock, or bedrock (on transparent overlay).

5) map of generalised structural geology (on transparent overlay).

6) map of dyke swarms, when present (on transparent overlay).

Inclusion of items 2 and 3 depended upon air photo-mosaic coverage (see figure 21). Maps for items 4, 5 and 6 are enlarged sections taken respectively from National Atlas of Canada, (map 37-38); tectonic map of Canada, (GSC map 1251A); and diabase dyke swarm of the Canadian Shield, (GSC map 1627A). An example of each of the above maps for NTS quadrant 65 (Dubawnt Lake area, North West Territories) is displayed in figures 25- 30.

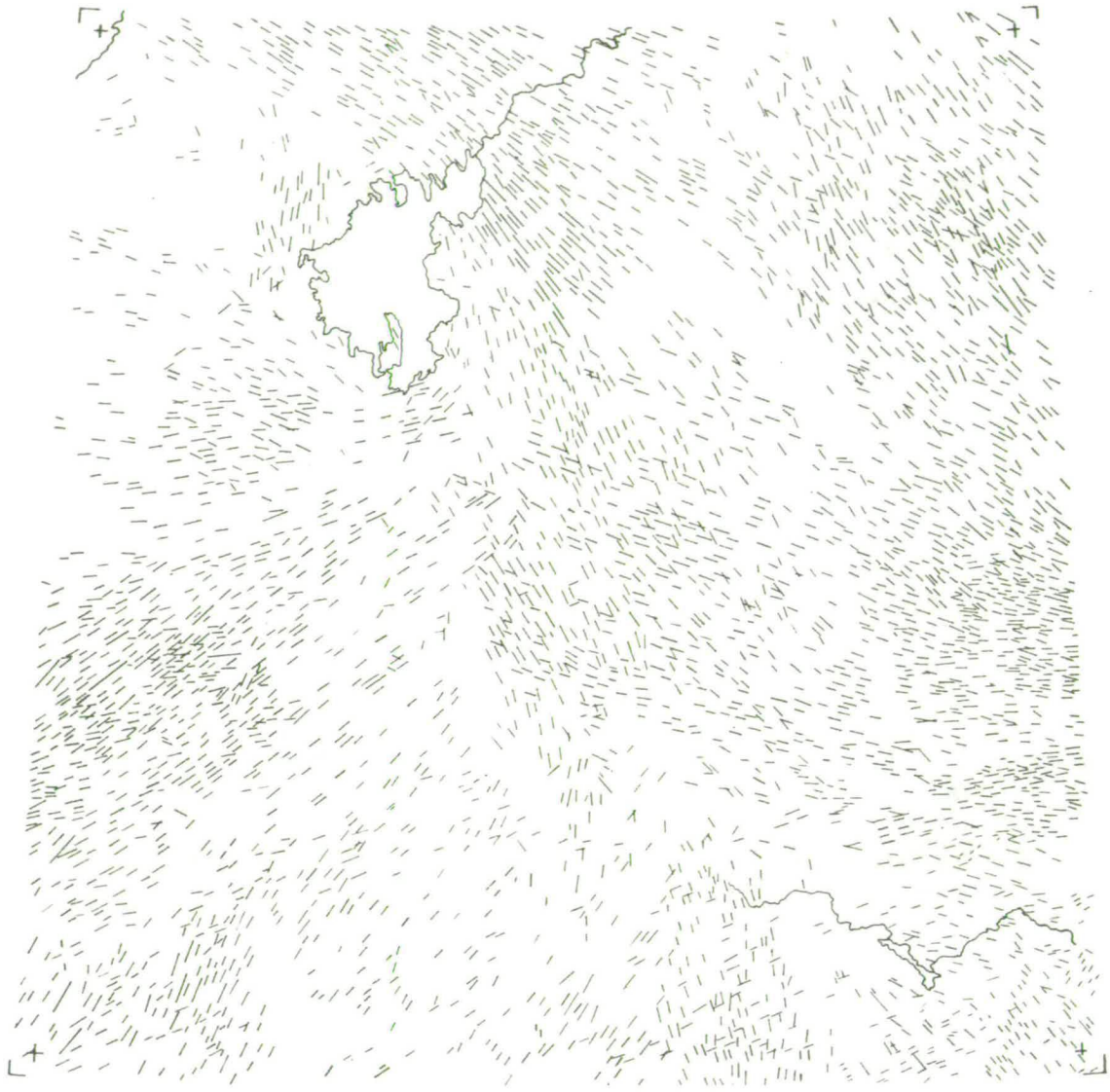

Figure 25. *Example of lineations mapped from a Landsat mosaic (NTS 65). East-west dimension is 450 km.*

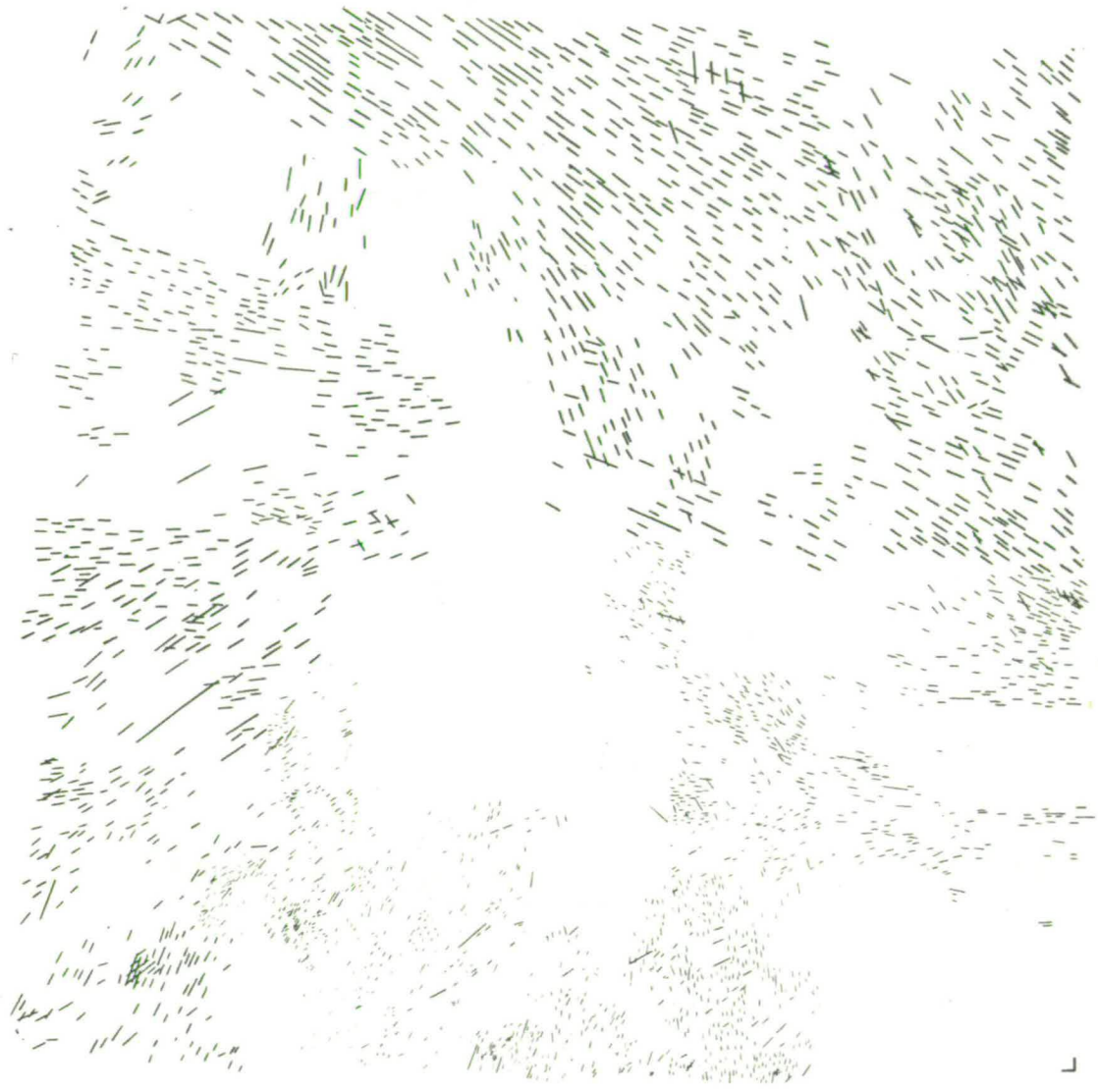

Figure 26. *Example of lineations mapped from many air photo mosaics (NTS 65). East-west dimension is 450 km.*

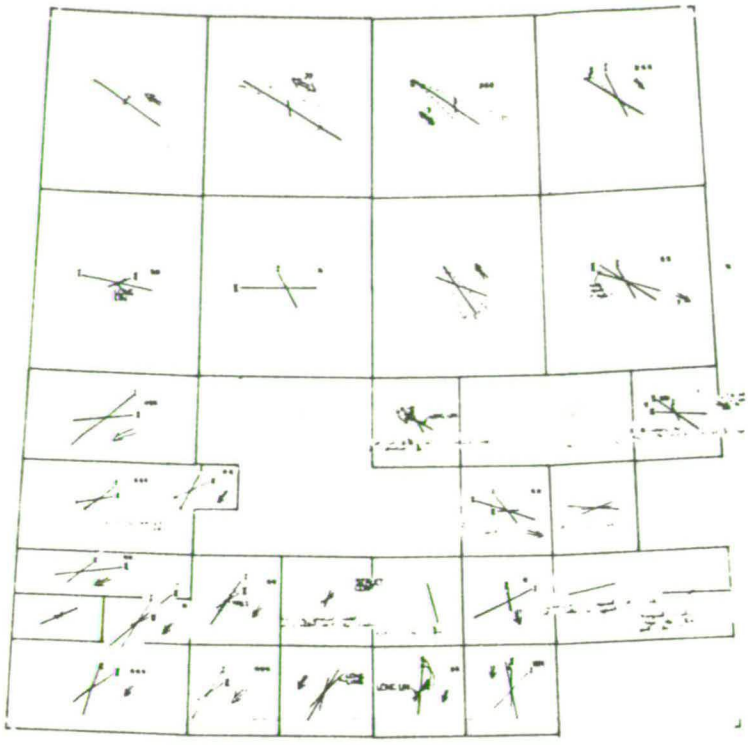

Figure 27. *Example mosaic of relative chronology index cards for NTS 65. East-west dimension is 450 km.*

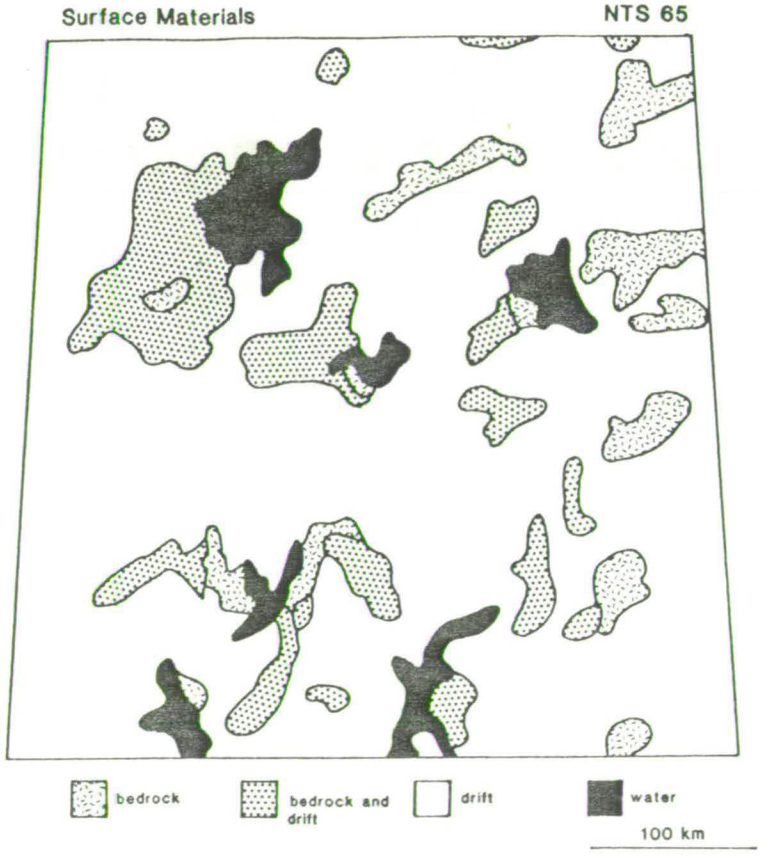

Figure 28. *Map of surface materials for NTS 65. East-west dimension is 450 km.*

Figure 29. *Map of simplified tectonics of NTS 65. East-west dimension is 450 km.*

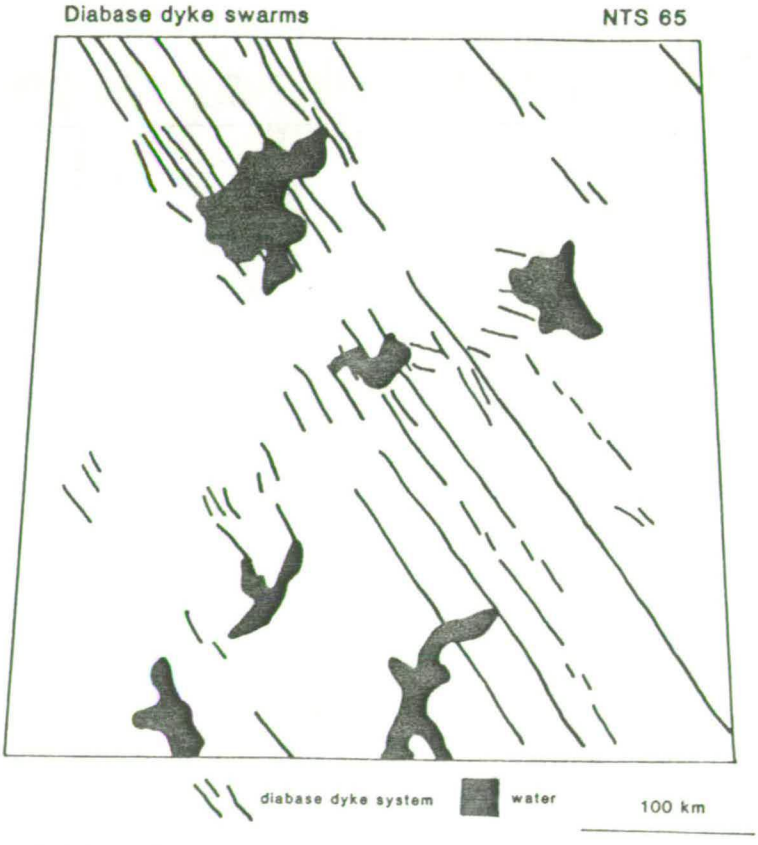

Figure 30. *Map of dyke swarms of NTS 65. East-west dimension is 450 km.*

4.3.2 Identification of Ice Flow from Landsat-derived Lineation Maps.

The majority of the mapped lineations form coherent and overlapping sub-parallel patterns which permit continuous lines to be drawn which summarise the lineation trends. These represent ice flow lines. Figure 31 illustrates the derivation of flow lines from lineation patterns. The most obvious and dense patterns of lineations permit us to draw closely spaced and continuous ice flow lines, and therefore reconstruct the spatial pattern of flow with confidence. More fragmentary and sparse lineation patterns yield less continuous and wider spaced flow lines, and hence less extensive integrated flow patterns. Flow lines are only drawn where lineations exist to define them, they are not extended or extrapolated through areas devoid of lineations.

Integrated groups of parallel flow lines reveal widespread patterns of flow that I refer to as ice flow sets. Figure 32 shows the identified ice flow sets for NTS 65. Many isolated lineations cannot be grouped into ice flow sets, and thus remain unsummarised (compare figure 25 with figure 32). Only lineations representing major ice flow events are therefore mapped. In the majority of cases flow sets are of large extent (100's kms) and are easily defined. Small isolated groups of flow lines can sometimes prove problematic. Their spatial separation makes them hard to correlate with other flow sets. If an isolated group of flow lines is compatible in terms of ice flow with a major nearby ice flow set, it is included in that set. If however the orientation is glaciologically incompatible with a nearby flow set (e.g. flows at right angles to each other) then the group remains isolated. Where many cross-cutting ice flow sets are present, and some isolated groups of flow lines exist, a unique solution is not always accessible. In the interests of objectivity, if no unique solution existed, as many alternative compilations of flow sets were made as

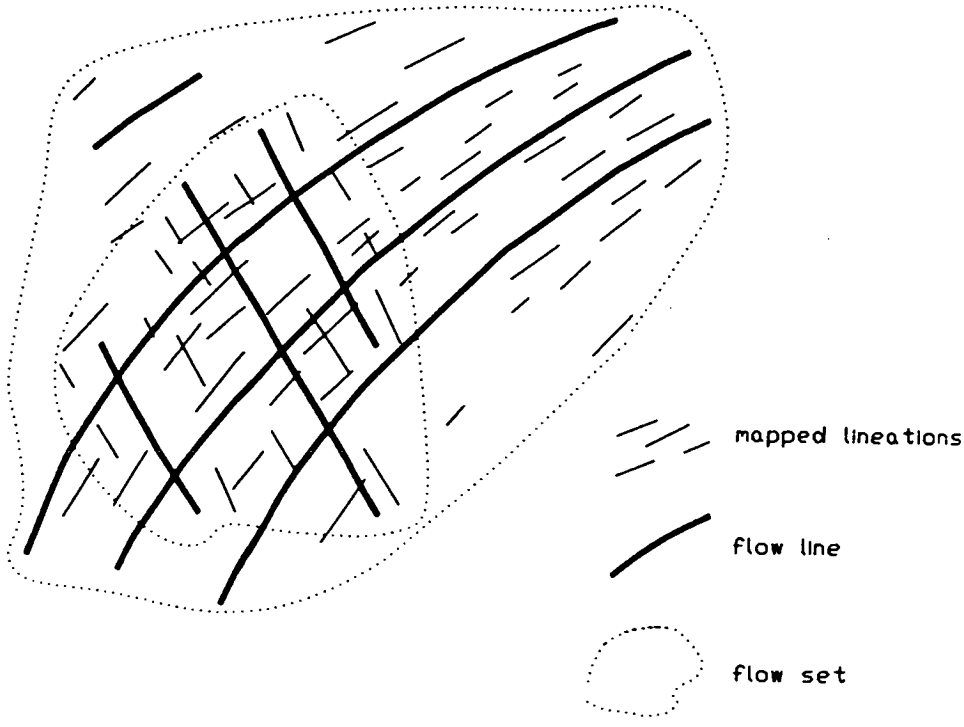

Figure 31. *Illustration of how ice flow lines and flow sets are derived from individually mapped lineations.*

Figure 32. *Interpreted ice flow lines grouped into colour-coded flow sets for NTS 65 (compare to figure 25, which shows the individually mapped lineations that this pattern is derived from).*

NTS 65(a)

kilometres
0 20 40 60 80 100

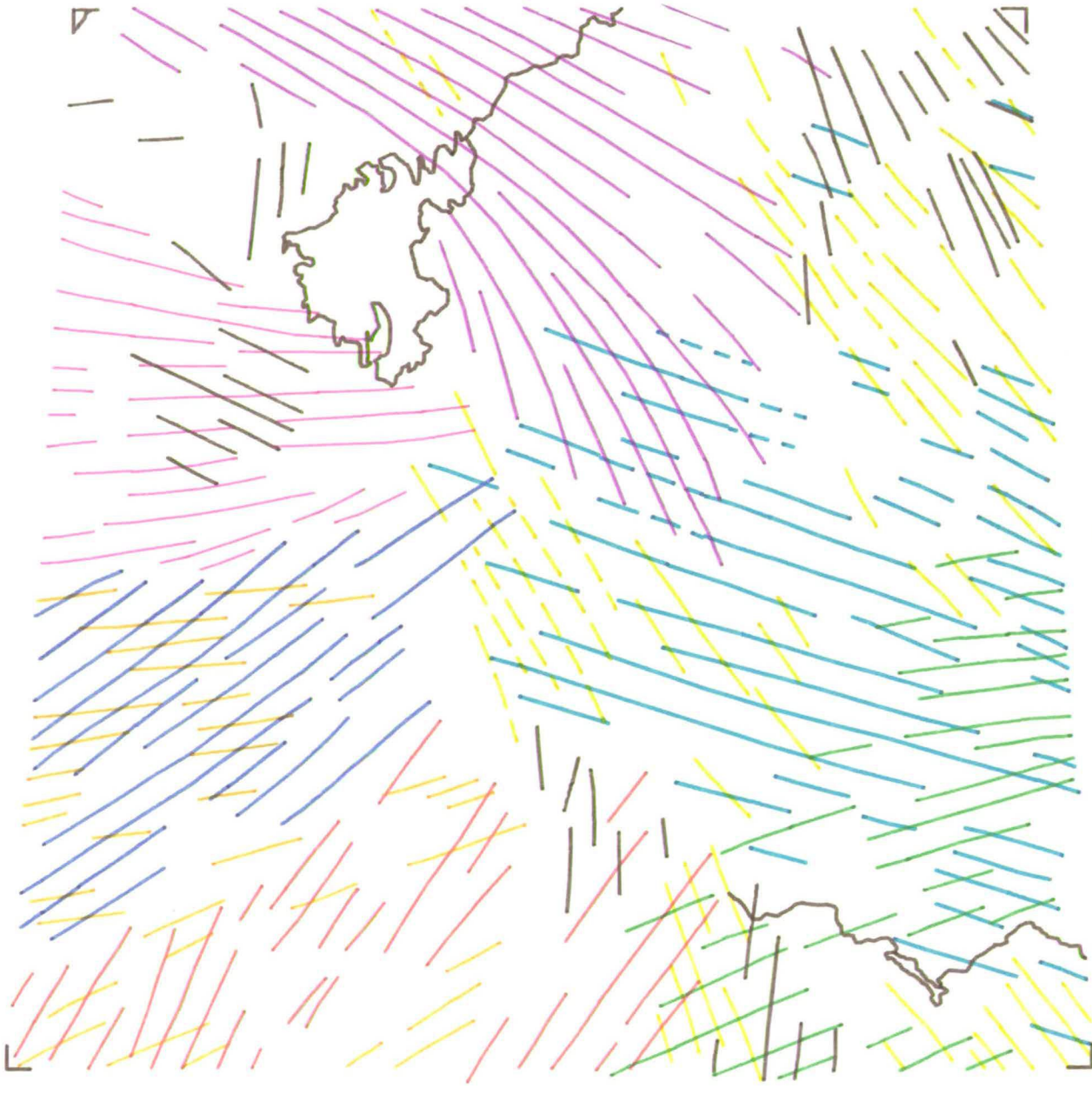

Flow 1 Flow 2 Flow 3 Flow 4 Flow 5
Flow 6 Flow 7 Flow 8

possible. The maps in the appendix show colour-coded ice flow sets for each NTS quadrant, and include these alternative compilations (e.g. NTS 65, a.b.c.). A method for discriminating between these alternatives, (using neighbouring quadrants), is described in the next chapter.

Maps of surface sediment, generalised structural geology, and diabase dyke swarms were individually laid over the maps of ice flow sets. This was a final check to determine whether ice flow sets might have been confused with bedrock lineaments. On some occasions inferred flow patterns were rejected because of a suspicion that they might reflect bedrock structure rather than drift lineations. Bedrock structure was rarely a cause of error, but for dyke swarms, which display a similar scale of pattern as that of ice flow, these were more frequently confused with drift lineations. In some instances predominantly bedrock areas displayed lineations that paralleled strong glacial lineations in adjacent drift areas. In these cases, and situations where it appeared that geological structure was preferentially enhanced in a specific direction, ice flow lines were represented as dashed lines. In all cases of possible structural influence, reference was made to the original Landsat images and to any air photograph mosaics or individual air photographs. This usually resolved the ambiguities.

4.3.3 Identification of Ice Flow Sets from Air-Photo Mosaic Derived Lineation Maps.

In quadrants where air photo-mosaics were available, the summary of ice flow was carried out by the same process as described in the previous section. The discrete flow

sets were colour coded to correspond to the flows identified on the Landsat-derived maps. Comparison of flow summaries of lineations detected on Landsat imagery to those detected on air photo mosaics shows there to be a high degree of similarity. The most notable difference is usually in the relative dominance of individual flows, although sometimes new higher frequency patterns are detected.

The ice flow sets recorded on the Landsat-derived lineation maps were treated as the master copy. They were amended as necessary by any extra information provided by air photo-mosaic ice flow summaries.

4.3.4 Determination of Relative Chronology of Ice Flow Sets.

This section describes how the relative chronologies ascertained from air photo-mosaics, which represent purely localised indicators of palaeo-ice flow, were used to determine the relative ages of the major ice flow sets. This involves translation of palaeo-ice flow information from the scale of air photo-mosaics (10's of kms) to the scale of the ice flow sets observed on Landsat images (100's of kms). This is a necessary step in the procedure for acquiring continent-wide palaeo-ice flow patterns.

The maps of relative chronology index cards were laid over the ice flow patterns derived from air photo-mosaics. This methodology is illustrated in figure 33, which shows how the relative ages of the red, blue and green ice flow sets were determined by recording the colour sequence in each box (representing each air photo-mosaic). The list of colour sequences and the star system of relative age confidence are shown in the lower part of

Figure 33. *Each small box represents the flow lines and relative ages recorded from individual air photo mosaics. Compiled together, as opposite, they provide the means by which overall flow set chronology can be determined.*

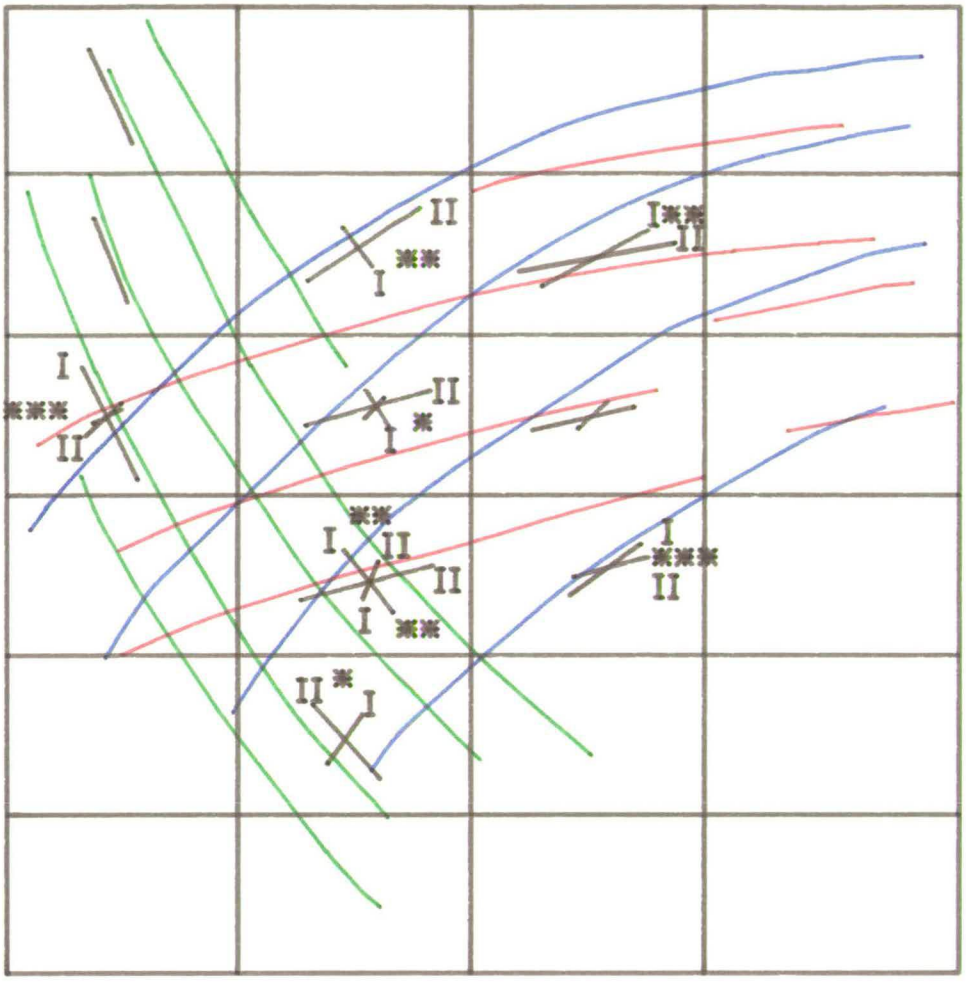

I II ***

I II **

I II ***

I II *

I II **

I II **

I II ***

I II *

Therefore relative age = I II III

figure 33. These colour sequences show the relative age of the ice flow sets as: green followed by blue, and then red. Similar age relationships are repeatedly revealed, and although contradictions do sometimes occur, these are heavily outweighed by repetitive relationships of high confidence. However, because of the potential error in determining relative ages (hence the use of the star system), a statistically-based system of deriving relative age sequences of ice flow sets was used.

It was hoped that a technique for topological sorting could be found, and that this would also provide a statistic relating the confirmations to contradictions within the system, therefore providing an indication of confidence of the final relative age sequence. The relevant literature was searched for a technique that may have been used in analogous situations (e.g. analysis of cyclic alluvial sediments: Powers and Easterling, 1982; Gingerich, 1969), but none was found to be suitable. Therefore, I devised a simple method that is described below.

Using NTS 32 as an example, four ice flow sets were identified: red, blue, green and magenta. These coloured ice flow sets allow six possible dual relative age relationships: red-blue, red-green, red-magenta, blue-green, blue-magenta, and green-magenta. Relative age hypotheses for each of these were considered, i.e. does red pre-date blue, or blue pre-date red? The list of relative age determinations were used to decide which hypotheses were correct. In order to quantify this procedure it was necessary to give the different levels of confidence (the three-level star system) weightings or scores. The following weightings were used:

*** 100

** 60

* 10

Three star determinations are unequivocal and receive a weighting of 100. Relative to this, I regard two star determinations as ones of strong probability and assign them a score of 60. One star determinations are given a weighting of 10 to represent their uncertain nature.

The tabulated scoring system for NTS 32 is shown in figure 34. For the hypothesis that green pre-dated red there are 7 three star determinations, 4 two star determinations, and 6 one star determinations, totalling a score of 1000. For the alternative hypothesis (red pre-dating green) there are 2 one star determinations providing a score of 20. Thus, in deciding which hypothesis is most likely to be correct, I compare the score of 1000 to 20 and conclude that the first hypothesis (green pre-dating red) is most likely.

This was done for the six dual colour relationships and provided 5 relative age sets. There was no evidence for the green-magenta relationship. The above process produced the following age relationships:

green	before	*red*
blue	before	*red*
blue	before	*magenta*
magenta	before	*red*
blue	before	*green*

From these it is possible by logical reasoning to derive a combined age sequence:

green, *blue*, *magenta* | before *red*, and *blue* before | *magenta*, *green*

therefore *blue* before | *magenta*, *green* | before *red*

This allows two final age sequences:

blue magenta green red, or

blue green magenta red.

The statistic of confidence I developed indicates 95% 'probability' for both of these sequences. The choice between the 2 sequences cannot be solved until all the NTS quadrants are compiled as a mosaic and neighbouring quadrants compared.

The system I have illustrated here by reference to NTS 32 was applied to all NTS quadrants with relative chronology evidence. The relative age relationships for some quadrants

NTS 32

I II **	I II **	I II *
I II *	I II **	I II *
I II ***	I II *	I II ***
I II **	I II **	I II *
I II ***	I II ***	I II *
I II ***	I II *	I II ***
I II *	I II **	I II *
I II ***	I II ***	I II *
I II *	I II **	
I II ***	I II ***	

Relative age hypotheses	*** 100	** 60	* 10	Score	Result
I II	700	240	60	1000	I II 98% n=19
I II			20	20	
I II	200	60	10	270	I II 82% n=5
I II		60		60	
I II	100	60		160	I II 100% n=2
I II				0	
I II				0	I II 100% n=1
I II		60		60	
I II				0	? n=0
I II				0	
I II			20	20	I II 100% n=2
I II				0	

1590 n=29

contradictions=80/1590

=5%

provided a unique sequence of relative ages, and for others three or four possible sequences. The advantage of this tabulated system is that it allows the relative age determinations to be easily referred to at a later stage, providing a concise indication of confidence in each relationship.

No three star contradictions were found. Contradictions were usually from one star determinations, and only represented less than 5% (relating to my scoring system) of the total score. This indicates that my relative ages were highly consistent for many hundreds of air photo-mosaics, and if internal corroboration such as this is to be believed, shows that the relative age data is not erroneous.

4.4 Creation of a Digital database.

The methodology process described so far has resulted in the evidence of palaeo-ice flow being represented by 30 maps (NTS quadrants), each with between 2-8 colour-coded flow sets. Some quadrants have up to four alternative flow configurations (see maps in the Appendix). Relative age information is contained on 15 of 30 of the quadrants. Comments written at the time of interpretation, pertaining to the nature of lineaments, their relative age, influence of bedrock geology, extent of drift cover and correlation between Landsat and air photo-mosaic interpretations are also included with each NTS quadrant.

A result of interpreting each NTS quadrant in isolation is that the colour coding of flows is unique to each map. To facilitate the final objective of deriving continent-wide palaeo-ice

flow patterns, the thirty maps were required to be assembled as a single mosaic. Once assembled, flow sets which linked across boundaries from map to map, needed to be grouped into contiguous co-linear sets and identified as single colours.

It was realised that this manipulation of complex flows into continent-wide integrated sets with associated re-allocation of colours and re-drafting, was a considerable task (see next chapter). Digitisation of the flows provided the potential for the repetitive manipulations and redrawing required, thus reducing this task to a manageable level.

The remainder of this section deals with the strategy adopted for creating a digital database of palaeo-ice flow. The actual derivation of continent-wide patterns of palaeo-ice flow is dealt with in the next chapter.

The following computing facilities were used:

* two RM NIMBUS personal computers,
* a TDS digitising tablet and mouse,
* computer aided drafting software; AUTOCAD, supplied by AUTODESK INC.
* Hewlett Packard colour pen plotter,
* 30 floppy diskettes.

In a pilot project, ice flow lines forming coloured flow sets were digitised and manipulated to ensure that the AUTOCAD software was capable of performing the required functions. This was also used as a vehicle for planning the overall digitising strategy, which is outlined below.

Each NTS quadrant map was treated as a BLOCK, with the sw corner representing the

origin, and the co-ordinates of the other corners calculated in millimetres. A Cartesian grid was computed containing all of the NTS quadrants, this provided the framework for the final mosaic.

All ice flow lines were digitised as POLYLINES (i.e. lines treated by AUTOCAD as a single ENTITY, even though they are composed of individually digitised Cartesian co-ordinates). However, in order to be able to manipulate the flow lines as discrete groups or sets, each flow set was digitised as a separate LAYER. This enabled each flow set to be treated as an ENTITY, and turned ON or OFF, and for colours to be easily changed. Careful choice of file names for each layer (e.g. F1_32a, F2s_32a) and corresponding text (Flow 1; F1T_32a, etc.) allowed WILD-CARD manipulations to be used with great effect in the final mosaic. This saved an enormous amount of time and effort. When the colour of a certain flow was changed using WILD-CARD specification, the colour of the text key (Flow 1 etc.) also changed accordingly. Dashed lines were used for flows of uncertain integrity, and the corresponding LAYER file name given the subscript s. The coastline, rivers and lakes were also digitised on different layers, as were the corner marks, scale and sheet title. This enabled their appropriate inclusion/exclusion at different scales of presentation. All NTS quadrant sheets are presented as AUTOCAD plots in the Appendix.

The total mosaic of NTS quadrants was compiled by INSERTing each file as a BLOCK into one large file (1.49 Mb). Some x and y axes stretching was required to make the best fit (the original Landsat mosaics are not geometrically exact). Figure 35 shows the total mosaic of interpreted quadrants. Note that each quadrant has its own unique colour coding. However, it is obvious that most of the flows join up across quadrant boundaries, and it is the task of the next chapter to describe how the colours and file names were manipulated so as to derive a final palaeo-ice flow reconstruction of Canada.

Figure 35. *Total mosaic of interpreted quadrants. Each quadrant has a unique colour-coding of ice flow sets.*

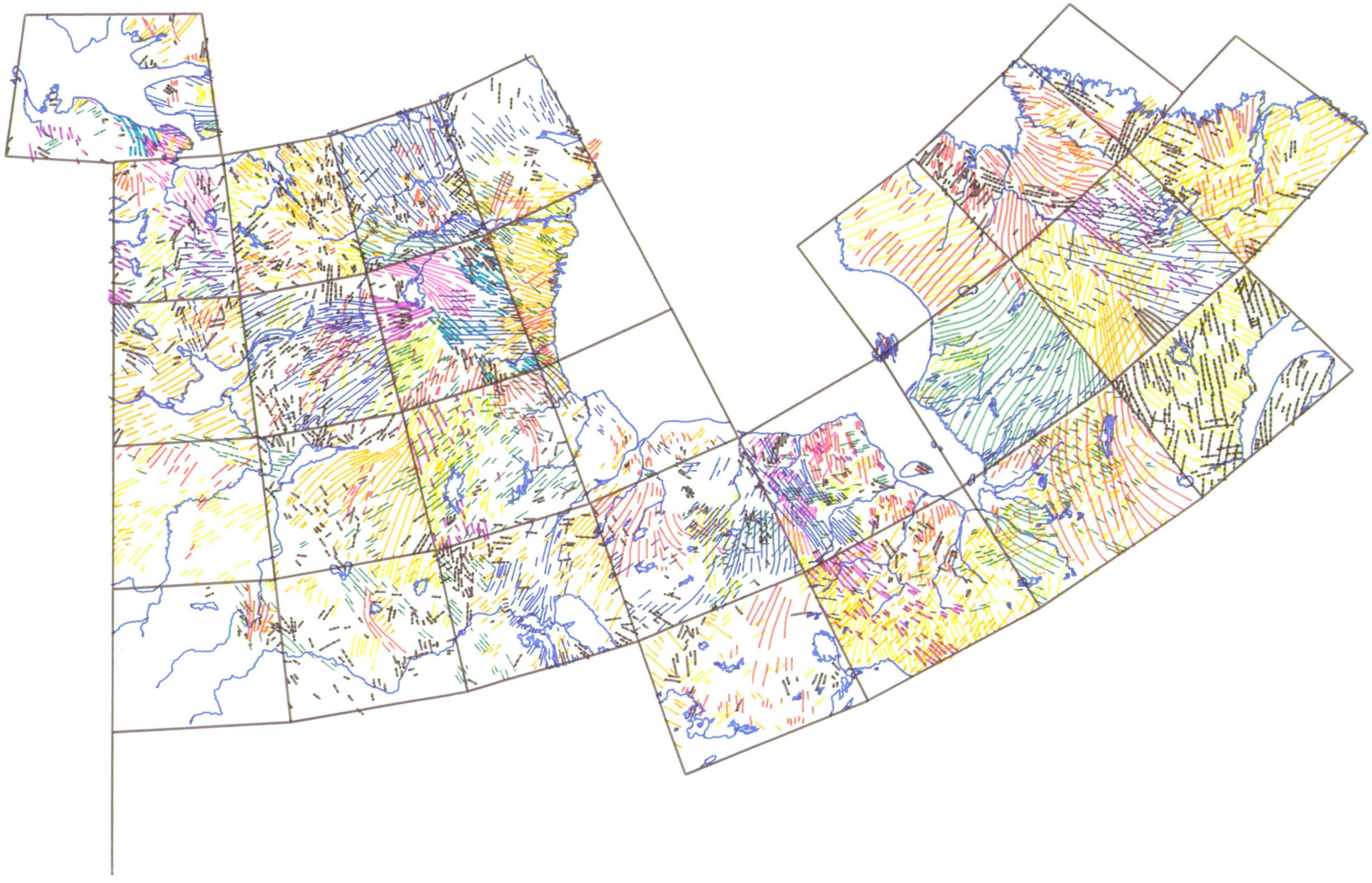

Chapter 5

Continent-wide Ice Flow Patterns and their Relative Chronology

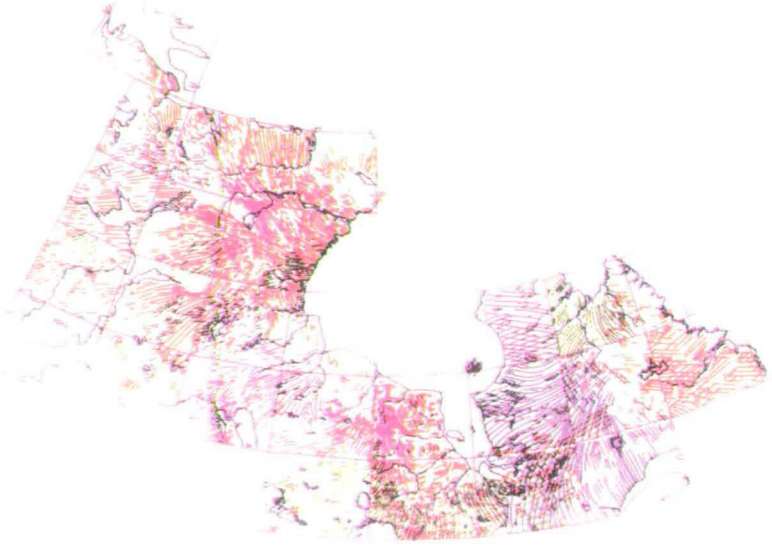

Chapter 5

Continent-wide Ice Flow Patterns and their Relative Chronology.

Arrangement of the assembled palaeo-ice flow sets into continent-wide patterns of ice flow is described, and the time sequence of flows established. All permutations of possible flow configurations which are compatible with glaciological theory and relative age are examined. A sequence of flow stages is suggested.

5.1 Spatial Organisation of Ice Flow Data; the Identification of Discrete Flow Sets.

Continent-wide integrated ice flow sets were derived from the quadrant-specific flow sets illustrated in the mosaic in figure 35. This was achieved by comparing flow sets in neighbouring quadrants. Flow sets from different quadrants which together form coherent and glaciologically viable patterns, were grouped into higher order flow sets. These I call discrete ice flow sets, as they represent distinctive, demarcated patterns of ice flow. It is apparent from figure 35 that discrete ice flow sets extend over many quadrants, and for distances of up to 1000 kilometres. Digitisation of ice flow data (described in Section 4.4) into a primitive type of "Geographic Information System" (GIS) allowed quadrant-based ice flow sets to be grouped into continent-wide discrete ice flow sets.

Ice flow sets identified within quadrants (figure 35), are now correlated between quadrants. In adjacent quadrants very strong co-linear flow sets are found in which lineations pass from quadrant to quadrant. These clearly form part of a large scale discrete ice flow set. For example, it was clear that a spatially extensive discrete ice flow set existed to the west of Keewatin (figure 36, DF1). The flow sets that form part of this pattern are:

F3_85	F2_84
F4_75b	F1_65a
F5_65a	F3_74
F2_65a	F2_64a
F2_73	

where, F3_85 is the computer-based flow name meaning flow 3 on NTS quadrant 85. Each of these flow names constitutes a separate LAYER in the GIS module. To enable them to be manipulated as a single discrete flow, all of the individual flow names (or LAYERS) were RENAMED to DF1 (discrete flow 1) with the quadrant-bounded flow sets being denoted by DF1_85, DF1_75b, etc.

As major flow patterns were identified and grouped into discrete flow sets (DF1, DF2, DF3, etc) their LAYERS were TURNED OFF within the system (making them invisible on the computer VDU), thus reducing the complexity and enabling easier identification of other patterns. This process was continued until no further major ice flow patterns remained, although many uncorrelated residuals still exist.

Discrete ice flow sets were numbered DF1 - DF39, although some were subsequently merged making a total of 36. These groups are tabulated below, and are illustrated in

figure 36.

DF1 comprises: F4_75b F3_85 F2_84 F5_65a F2_65a F3_74 F2_73 F1_65a F2_64a F2s_73
DF2 does not exist.
DF3 comprises: F5_86 F2_85 F2_76 F7_8797F4_66 F7_65a
DF4 comprises: F4_86 F1s_76 F4_8797
DF5 comprises: F6_86 F3s_76 F5_66 F4_56 F5_56
DF6 comprises: F3_84 F5_75b F4_65a
DF7 comprises: F1_75b F1s_75bF1_84 F1_74 F2_83 F1mm_64a
DF8 comprises: F7_86 F8_8797
DF9 comprises: F6s_65aF6_65a F3_55 F4_64a
DF10 comprises: F2_66 F3_56 F2_55 F2s_66
DF11 comprises: F3_65a F1_55
DF12 comprises: F2_56 F1_46
DF13 comprises: F1_56 F1_66
DF14 comprises: F3_66 F8s_65a
DF15 does not exist.
DF16 comprises: F2_52 F4_53 F3_23 F2_32a F5_33b F2_43e F3_42a F2_32a
DF17 comprises: F5_43e F6_42a
DF18 comprises: F5_42a F4_43e F5_53 F4_42a
DF19 comprises: F5_63c
DF20 comprises: F2_42a F1_52 F4_33a F3_43e
DF21 comprises: F1_34 F1_32a F4_33b F1_22 F7_23
DF22 comprises: F1_43e F1_42a
DF23 comprises: F3_13 F4_23 F3_14 F3_24
DF24 comprises: F2_13 F2_14 F8_23
DF25 comprises: F5_23
DF26 comprises: F1_24
DF27 comprises: F6_43e F5_32a
DF28 comprises: F6_33b
DF29 comprises: F2_33b
DF30 comprises: F3_33b
DF31 comprises: F1_23
DF32 comprises: F2_22 F6_23
DF33 comprises: F7_43e F3_53
DF34 comprises: F8_65a F4_55 F5_54 F1_64a
DF35 comprises: F2_34
DF36 comprises: F2_63c
DF37 does not exist.
DF38 comprises: F3_63c F3s_63c F6_54 F7_64a F1_53
DF39 comprises: F3_73 F3_64a F3_54 F2_74

Note that the DF1-DF39 numbering is arbitrary and does not represent any chronological order.

Figure 36 also shows the residuals which were not considered of sufficient extent to constitute major discrete ice flow sets.

Figure 36. *The principal discrete ice flow sets (DF1-DF39) are illustrated in the following six pages. The seventh page illustrates residual flow elements which were not considered of sufficient enough extent to constitute major discrete ice flow sets.*

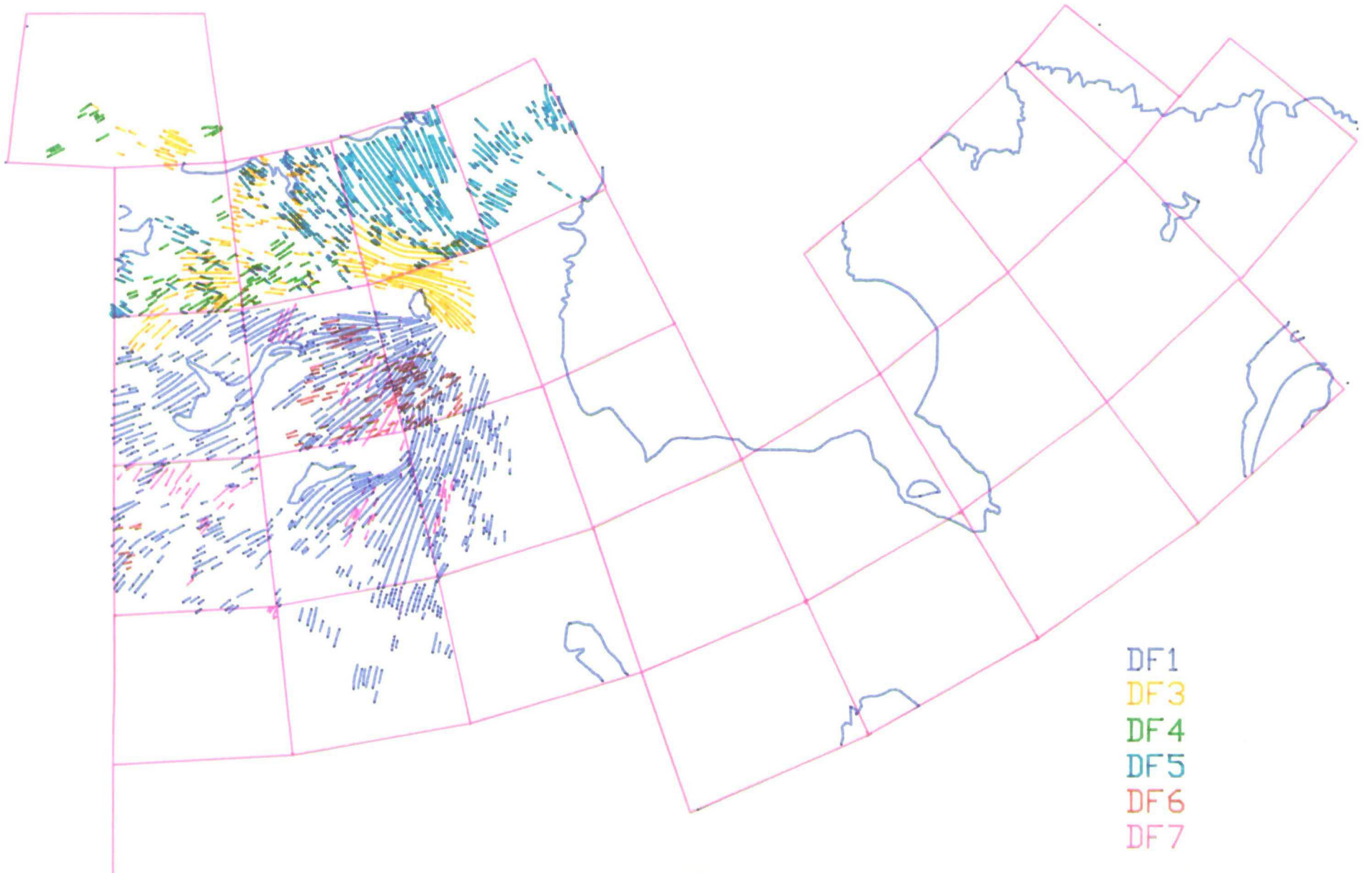
DF1
DF3
DF4
DF5
DF6
DF7

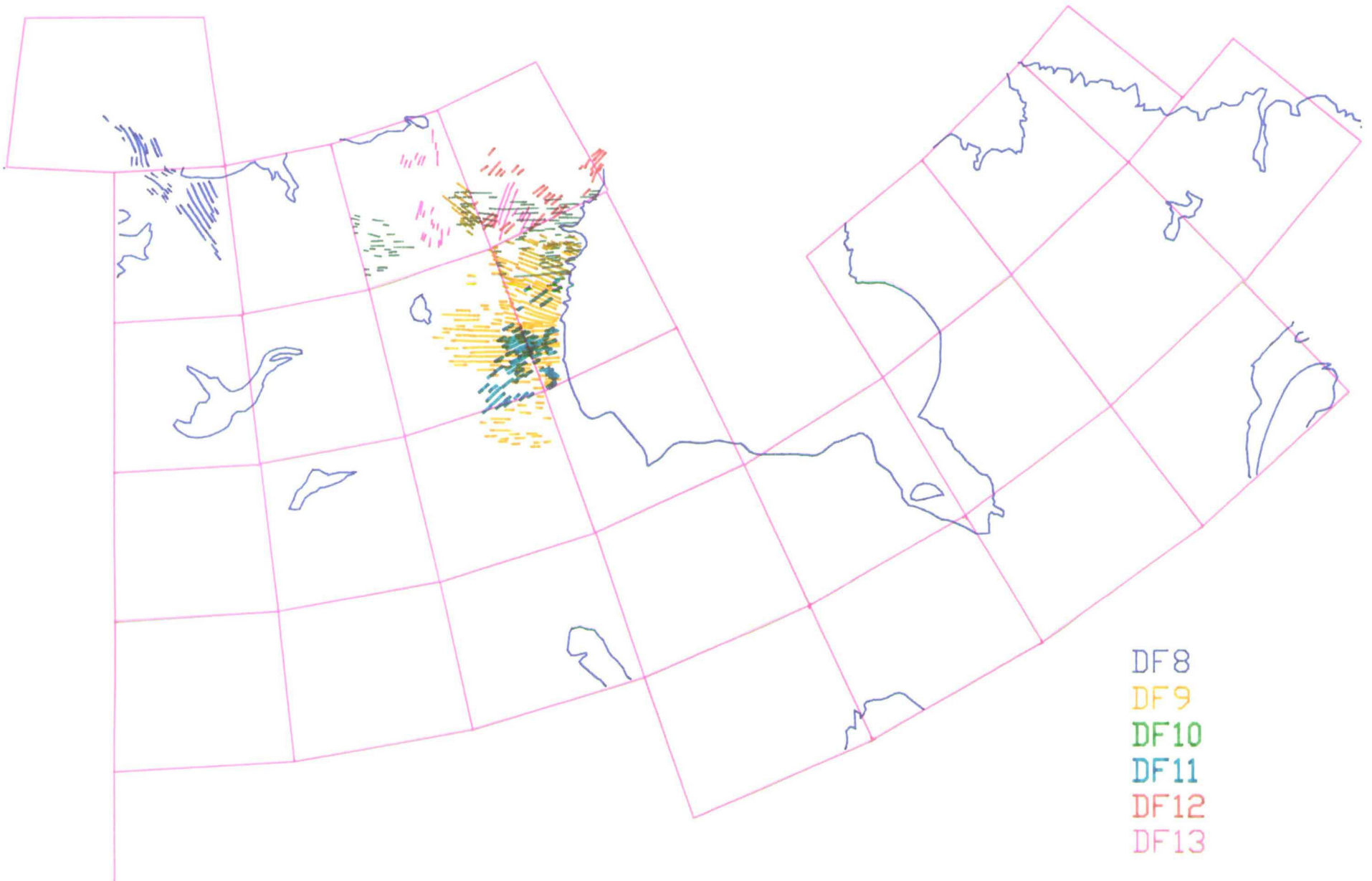
DF8
DF9
DF10
DF11
DF12
DF13

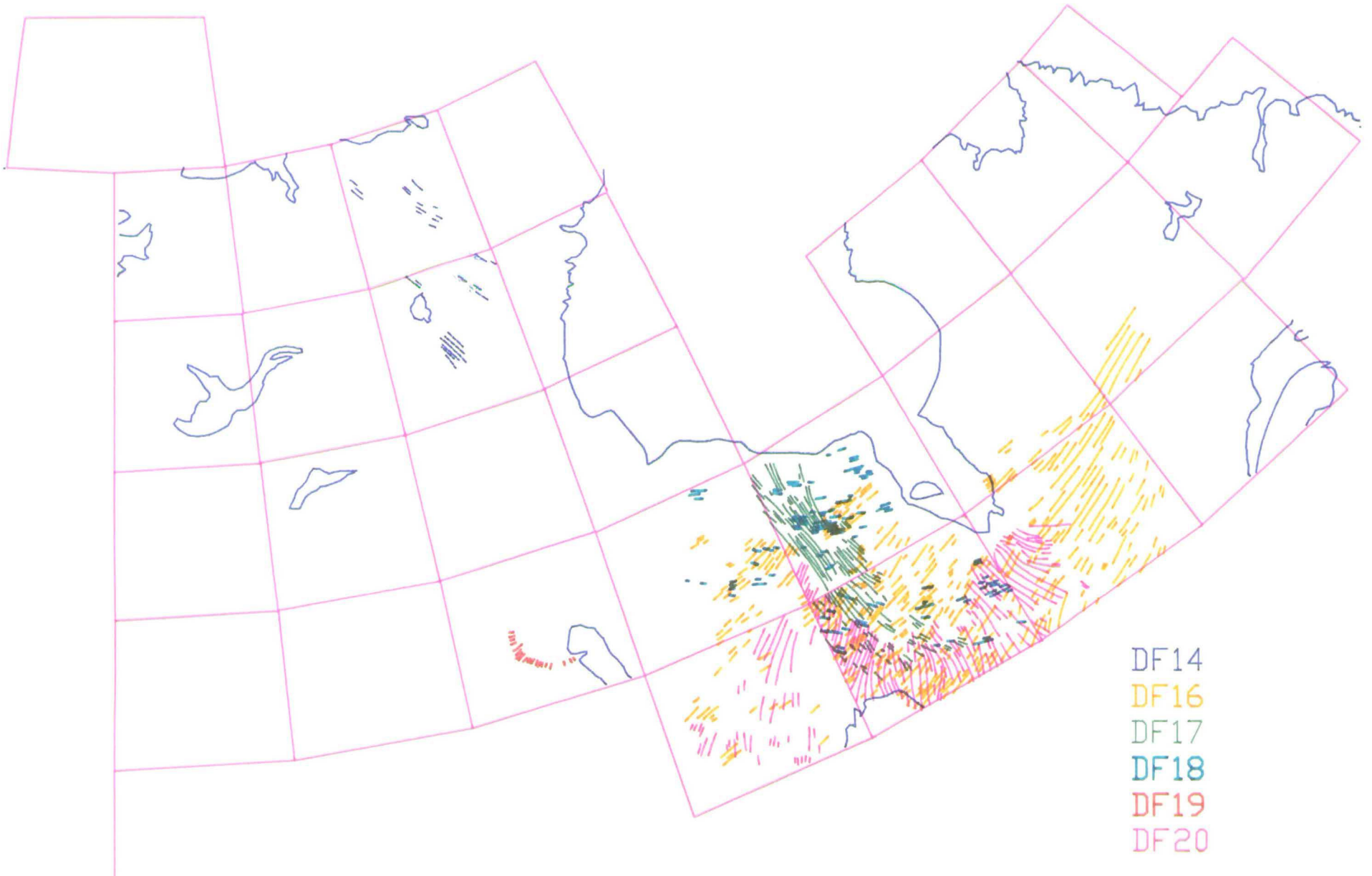
DF14
DF16
DF17
DF18
DF19
DF20

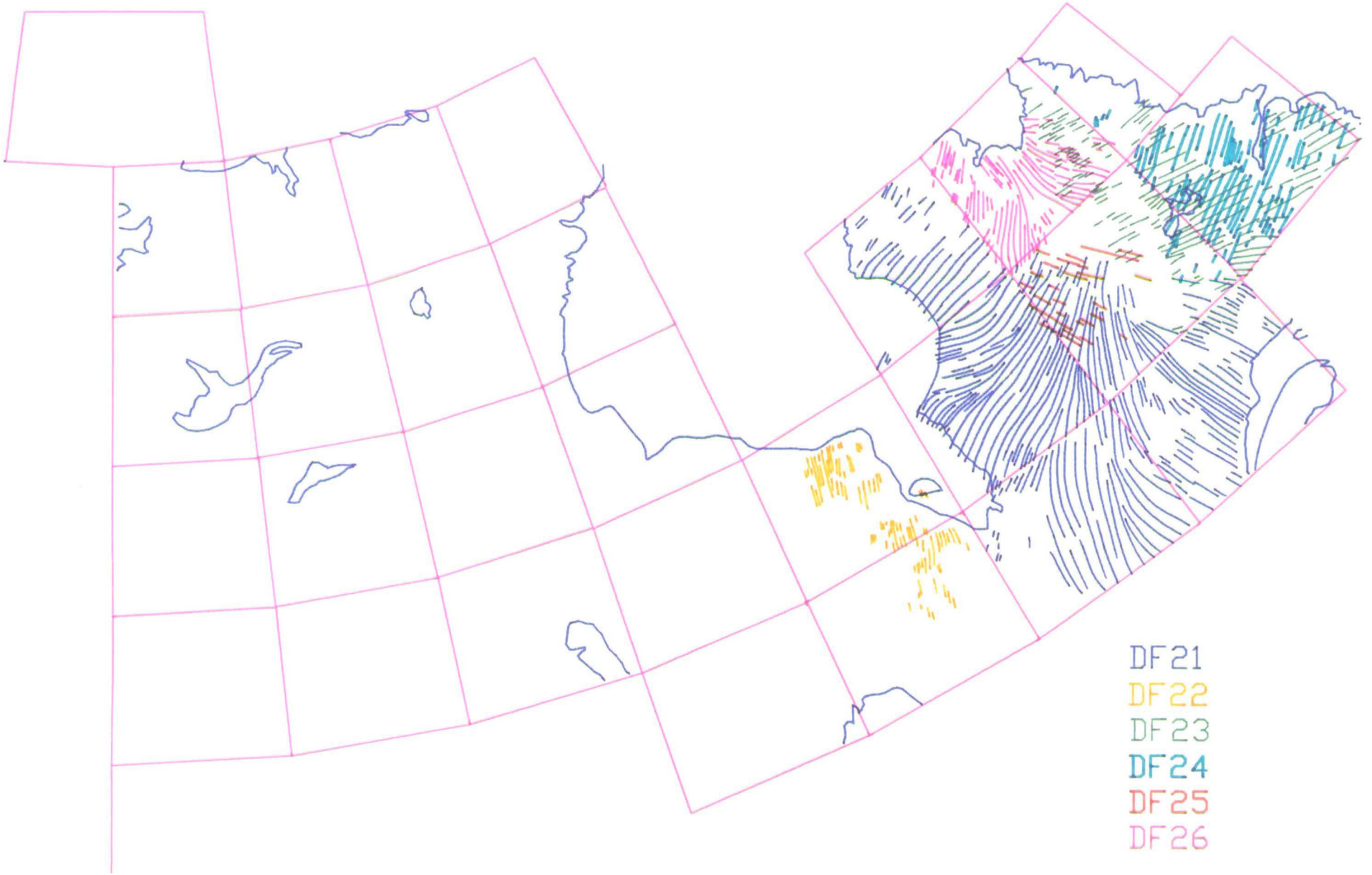
DF21
DF22
DF23
DF24
DF25
DF26

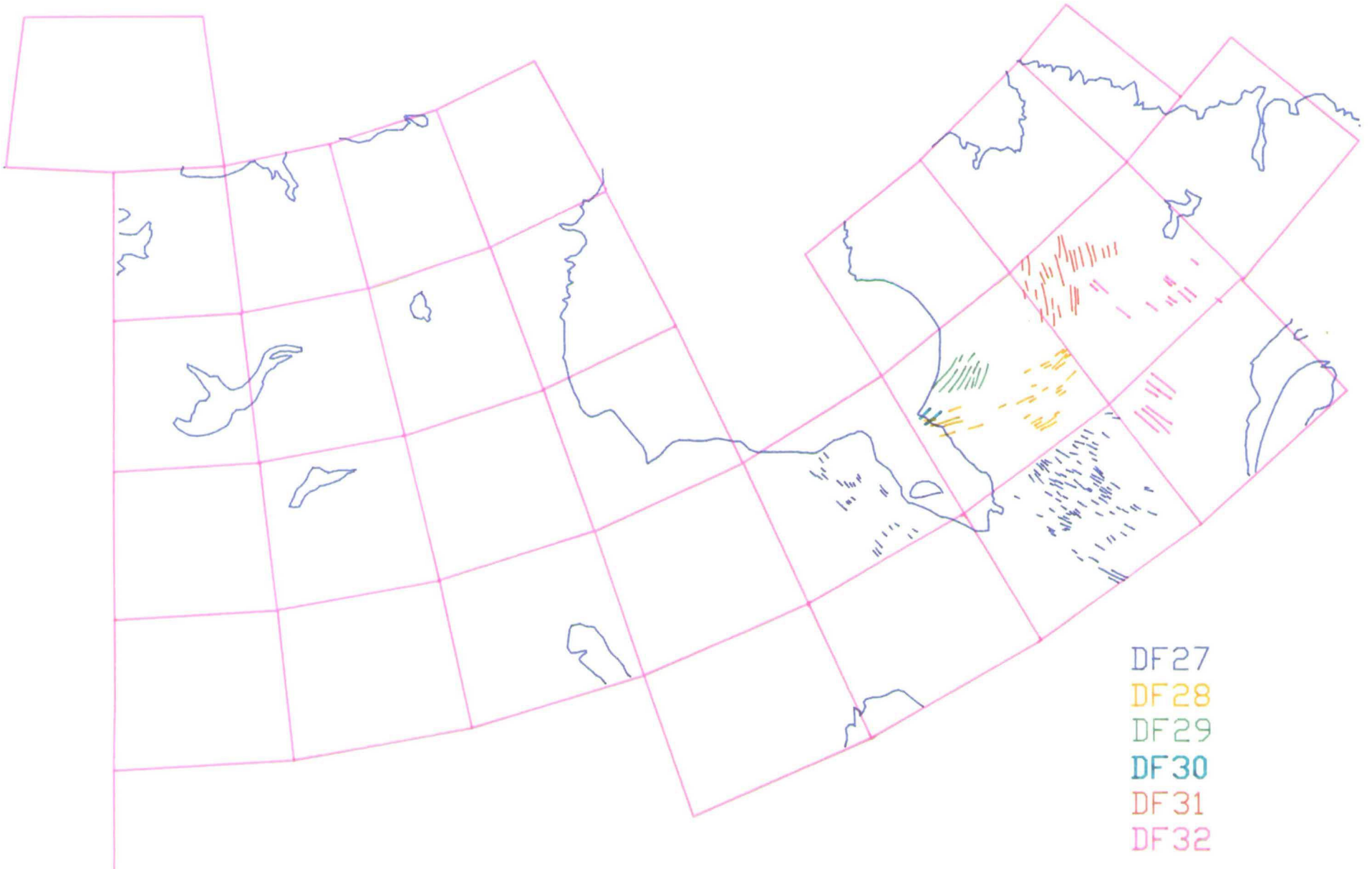
DF27
DF28
DF29
DF30
DF31
DF32

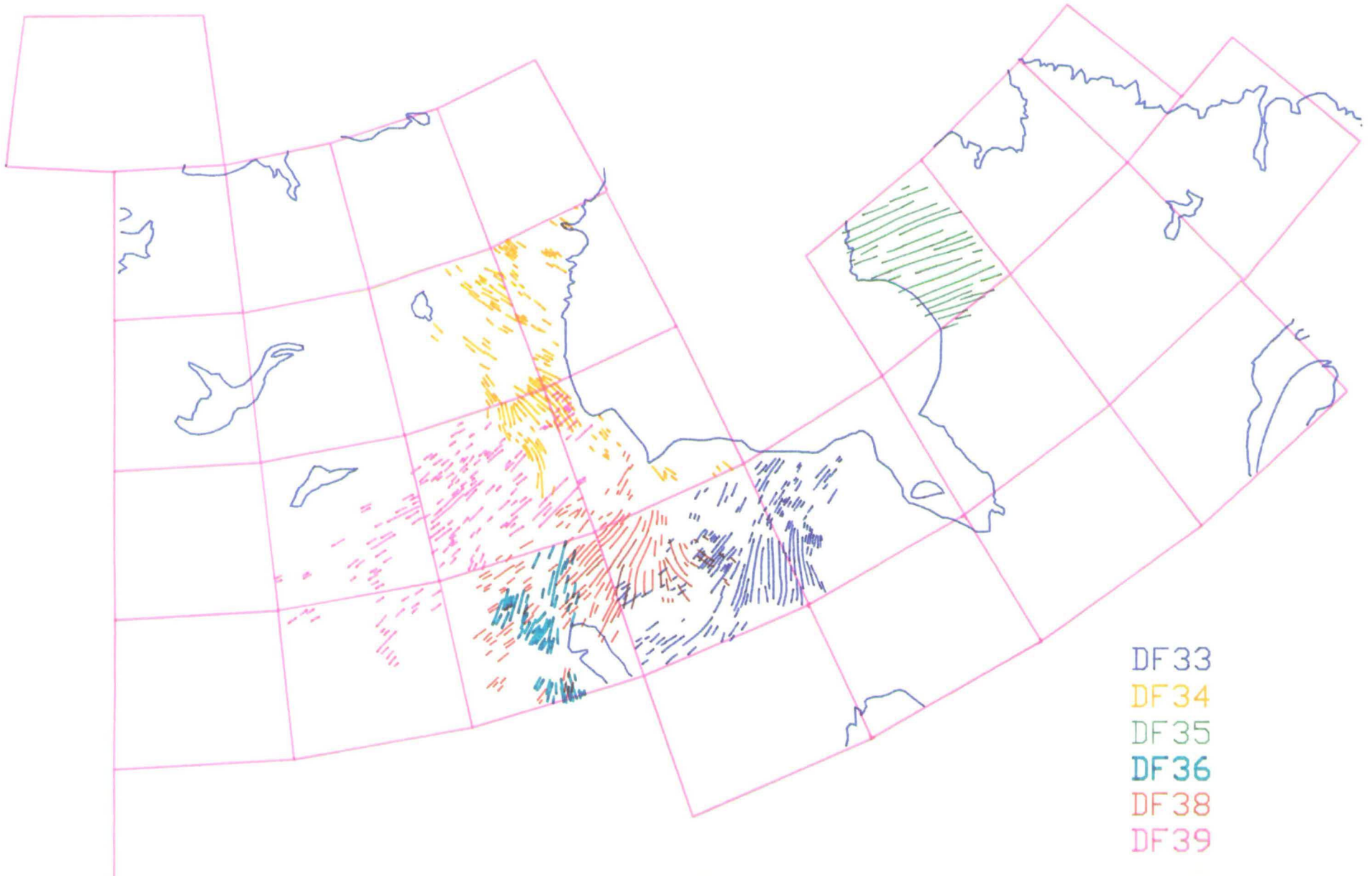
DF33
DF34
DF35
DF36
DF38
DF39

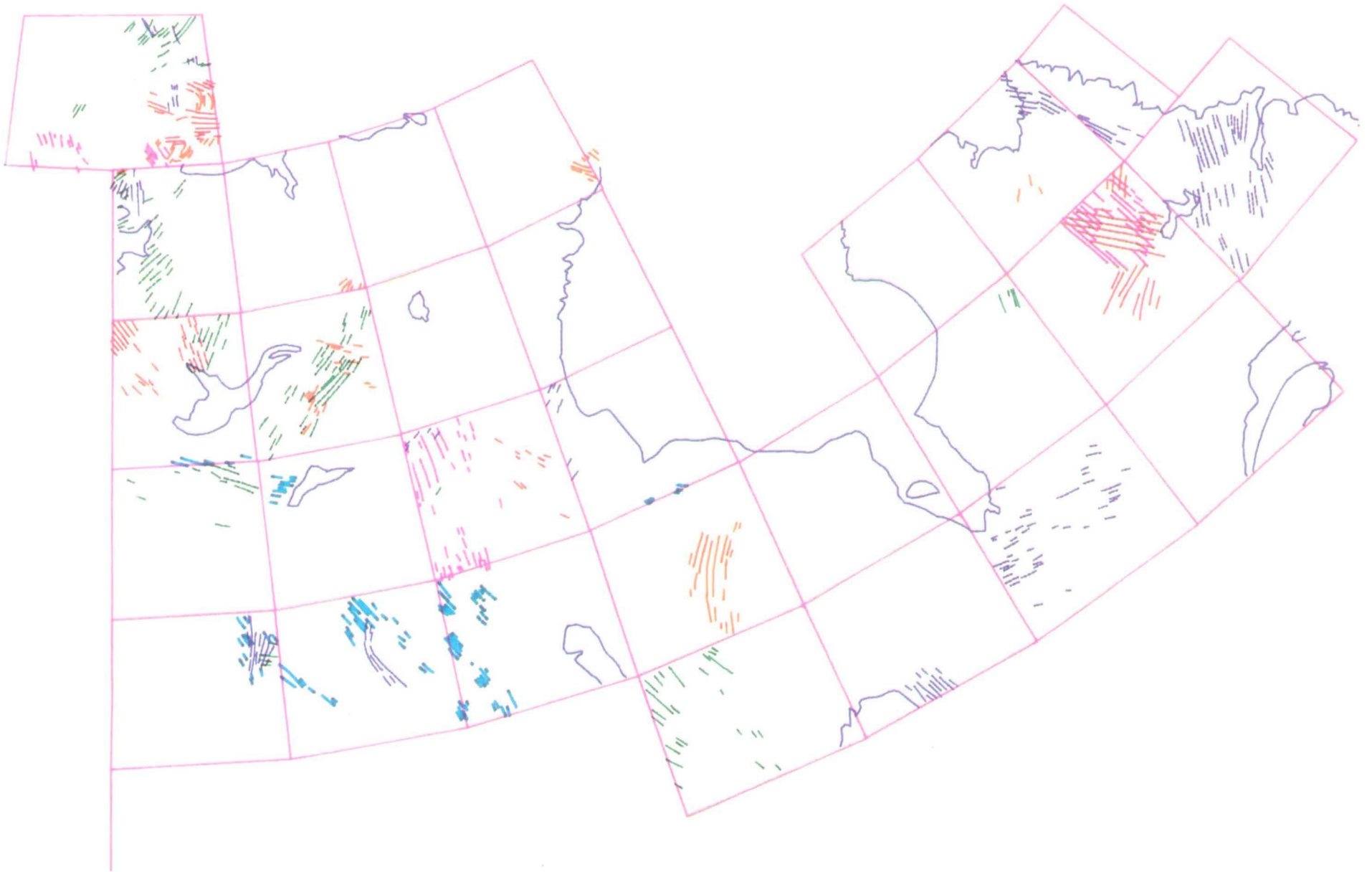

Many quadrants have more than one interpretation of ice flow sets (e.g. NTS 63 has three possible configurations; a, b, or c, see appendix). This is because a unique solution of ice flow configuration was not always possible (see Chapter 4). Part of the methodology of this stage of analysis was to assess which configuration best matched the flow patterns of adjacent quadrants. The following configurations provide the best fit with neighbouring quadrants, and are thus used from here on:

NTS 32a	NTS 63c
NTS 33b	NTS 65b
NTS 42a	NTS 64a
NTS 43e	NTS 75b

(see appendix for full listing and illustration of alternative configurations).

5.2 Temporal Organisation of Ice Flow Data; the Relative Chronology of Discrete Flow Sets.

In elucidating the evolving pattern of ice flow within the Laurentide Ice Sheet, it is necessary to determine the time sequence of the discrete flow sets identified in the previous section.

Relative age relationships have been determined for 15 of the 30 NTS quadrants, but at this stage are referenced according to the ice flow sets unique to individual quadrants (e.g. for NTS quadrant 13, F2_13 is known to pre-date F3_13). This information was thus required to be translated to the new frame of reference for palaeo ice flow, namely the discrete ice flow sets (DF1, etc). Therefore, flow set F2_13 pre-dating F3_13, became DF24 pre-dating DF23, and so on.

In a few cases it was found that one discrete flow set appeared to pre-date another in one quadrant and post-date it in another. This may mean that asynchronous flow sets have been included within a single discrete flow set, or that errors were made in original relative age determinations. The former may occur because ice flows of a similar direction may have occurred a number of times during separate phases of ice flow. For example, ice flow may have emanated from Hudson Bay at many different times during the time-span of the Laurentide Ice Sheet. The lineation imprint may record these different flow phases, but may appear as a single ice flow event. This was in fact the case for ice flowing out of Hudson Bay westward into Manitoba and Saskatchewan. Unequivocal relative age relationships with another flow of different orientation revealed two similarly oriented flows of different age. The identification (based purely on pattern) of this discrete flow set as a singular and extensive flow pattern was therefore erroneous. The relative age relationships revealed that it should be split into 2 spatially separate flows representing different phases of ice movement, but in a similar direction. It may be possible to distinguish such parallel flow sets of different age, by contrasting spatial frequencies and lineation lengths.

The translation of relative age data to the discrete flow sets (DF1, etc) and the minor pattern manipulations described above, led to the following temporal sequence of discrete ice flow sets:

older

↓

younger

		20	30	16			9	
24	23	18	21	21	22	35	11	39
23	26	16	29	29	20	21	12	1
		21						

older

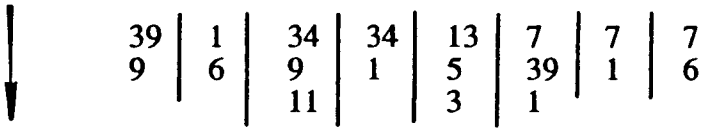

younger

Note: vertical lines separate flow sets whose relative ages have not been established. Links between these relationships allow the formulation of four entirely objective relative age clusters:

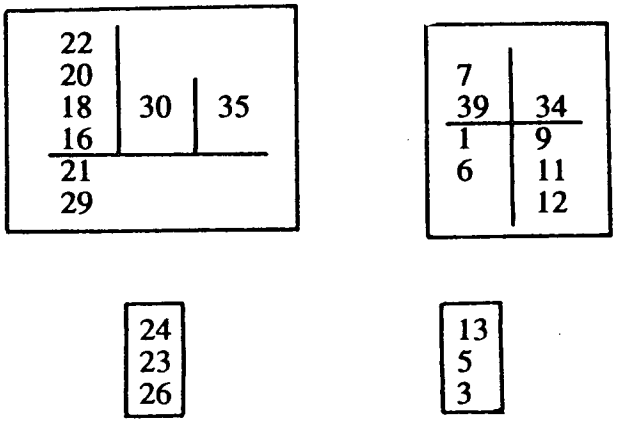

Numbers above or below each other represent younger-older relationships. Older at the top. Vertical lines separate flow sets whose relative ages have not been established. For example, DF30 is known to be older than DF21, but its relative age with DF22, 20, 18, or 16 is not known. The relative ages of the four clusters cannot be directly established.

Relative age information for the following discrete ice flow sets is not known: 4, 8, 10, 14, 17, 19, 22, 25, 27, 28, 31, 32, 33, 36, 38.

5.3 Space-Time Permutations; the Identification of Flow Stages.

Many discrete ice flow sets are of demonstrably different age, as evidenced by cross-cutting relations. They must therefore represent different phases of ice flow of the Laurentide Ice Sheet. However, relative age relationships cannot be directly determined from sets that are spatially separated. The possible synchroneity of these flows is examined in this section.

Flows that are not of demonstrably different age are compared with each other to investigate whether they could have formed part of the same ice flow pattern. For instance, although flow sets 13 and 3 (figure 37) cannot be distinguished on the basis of cross-cutting relationships, they are clearly incompatible with a synchronous flow pattern which could have produced both. In contrast, flow sets 5, 38 and 39 (figure 37) could reflect a roughly synchronous flow pattern emanating from an ice dome east of Keewatin. The simplest explanation of the data will be that in which all flows which could glaciologically be synchronous are assumed to correlate; an approach which will produce the smallest number of flow stages.

All glaciologically possible combinations of patterns were assessed using the computer display of discrete ice flow sets. Each discrete ice flow set was examined and any possible compatible flow sets recorded. Figure 38 illustrates the 25 compatible permutations that were found. Of the 25 permutations, six were rejected (figure 38, permutations: i,iii,ix,xxii,xxiii and xxv) on the grounds of proven non-synchroneity, drawn from the relative age clusters of the previous section. For example permutation xxv (figure 38) shows flow sets 6, 38, and 39 in an arrangement that could be roughly

Figure 37. *Discrete flow sets that relative age information permit to be of the same age are compared to ascertain whether they are glaciologically compatible and may thus represent roughly synchronous Flow Stages.*

top; *DF13 and DF3 could not represent a synchronous Flow Stage.*

bottom; *DF5, DF39, and DF38 represents a possible flow configuration. Relative age evidence does not exist to suggest that the flows are of different age. Pattern and relative age compatibility therefore allow these discrete ice flow sets to be grouped as a roughly synchronous Flow Stage.*

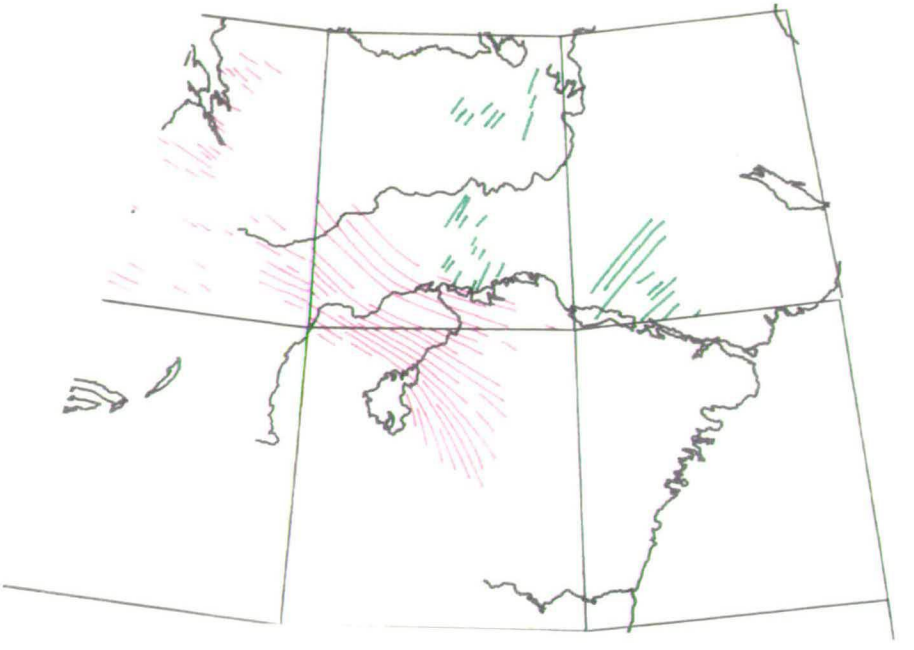

Green = DF13 Magenta = DF3

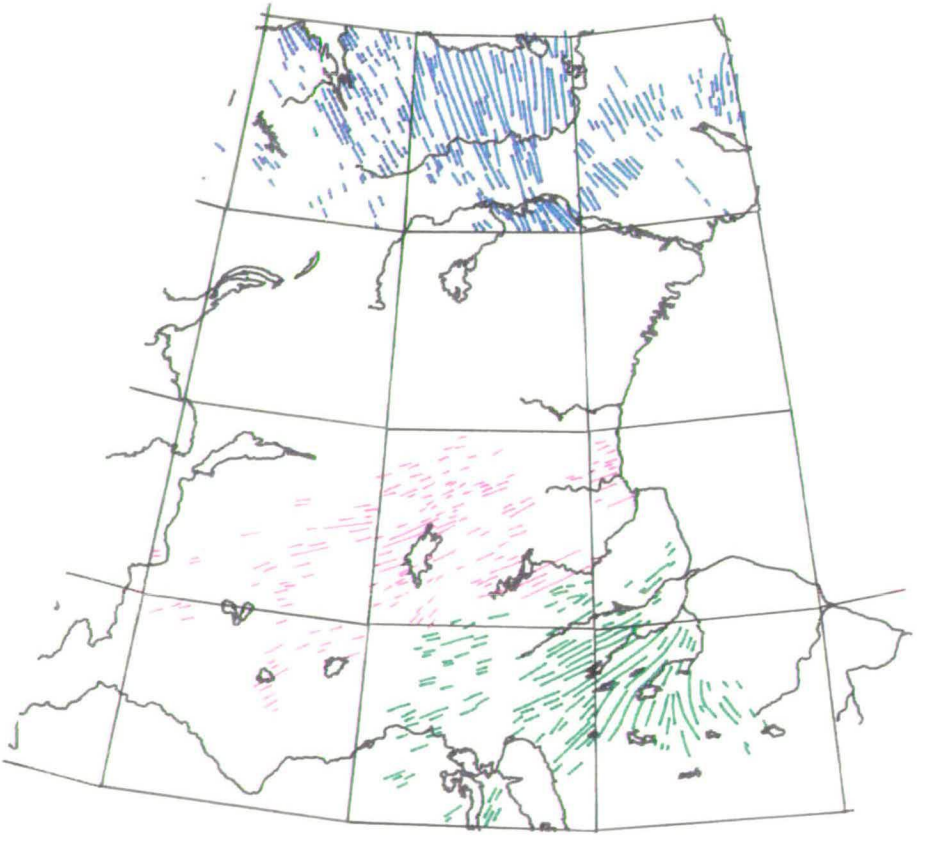

Blue = DF5 Magenta = Df39 Green = DF38

synchronous. However, reliable relative age indications with an overlapping flow set, show that 39 does in fact pre-date 6, and thus, cannot be synchronous.

The very strong lineation imprint on the so-called Pas Moraine of Lake Winnipeg (flow set 19) aligns broadly with discrete ice flow sets 36 and 38 (permutation xii and xiii). In detail however, neither flow set fits precisely. This upstanding sediment mass would be so susceptible to lineation formation, that it could have acquired a lineation rapidly, whilst the surrounding areas failed to do so. For these reasons permutations xii and xiii are rejected.

Closer examination of the patterns in figure 38, with particular regard to possible ice divide positions, led to a further number of permutations being rejected. It was apparent that the pattern displayed in permutation v is inconsistent with glaciological, and lineation-formation theory. The flow-lines show two splaying configurations; to the NW and SE, which implies that the ice divide must have lain between them. However, the lineations in both splaying patterns extend inwards, until they are virtually touching. This is not consistent with the existence of an ice divide, because basal velocities beneath an ice divide are approximately zero, and lineations are therefore not likely to form in this location. This suggests that two flows which formed either side of an ice divide must be separated by a zone free of contemporary lineations, suggesting that discrete flows 5 and 34 were not synchronous. Permutations v and xv are rejected for these reasons.

If permutation viii (flow sets 9 and 6) is to be considered as a synchronous ice flow pattern it is necessary for ice to have flowed westwards out of Hudson Bay. Directional indication in the form of drumlins however, shows that flow set 9 was formed by ice flowing into Hudson Bay, and so permutation viii must be rejected.

Figure 38. (following four pages). *25 permutations of discrete flow set configurations that are all considered to be glaciologically viable.*

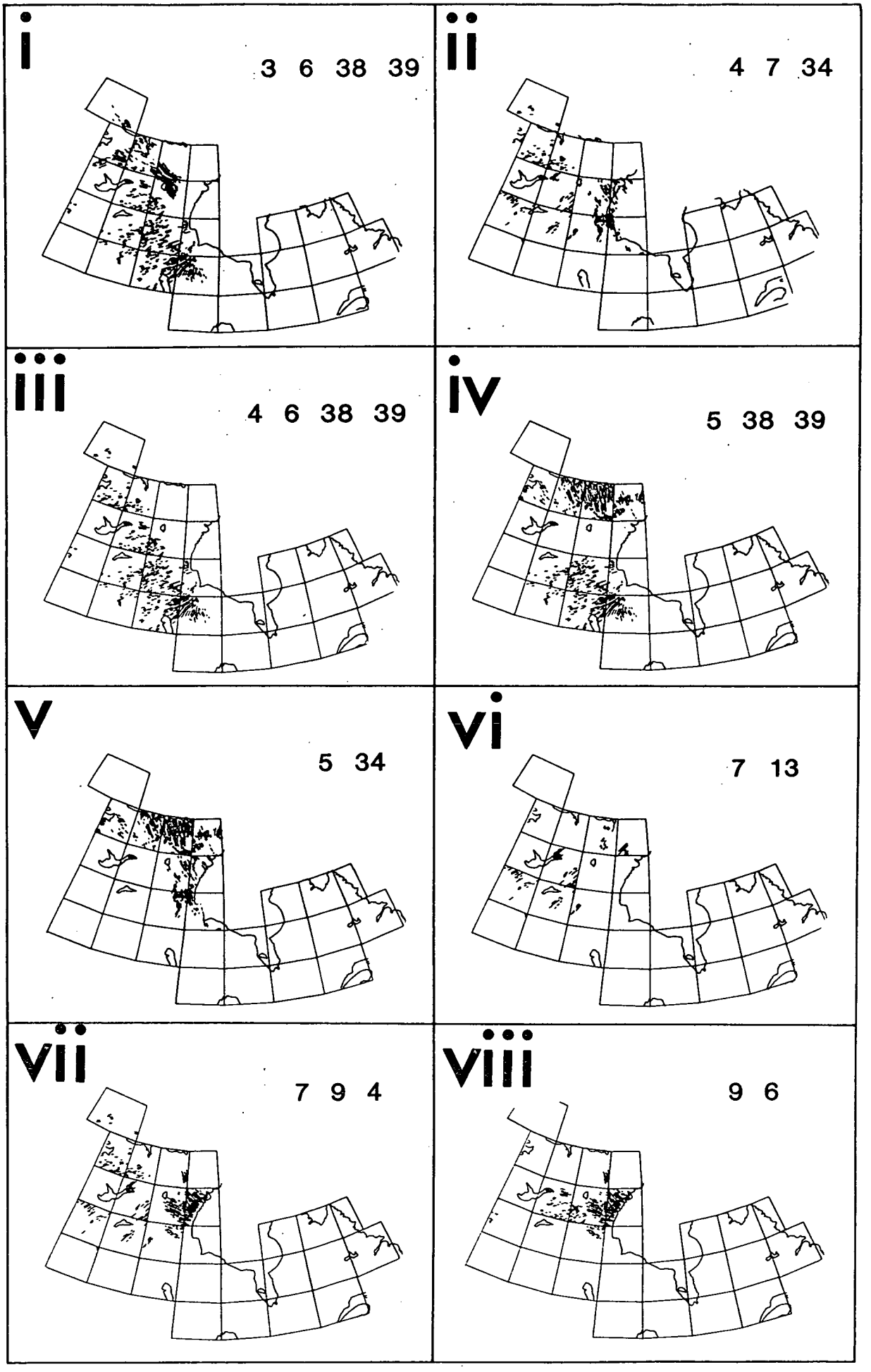
i
3 6 38 39
ii
4 7 34
iii
4 6 38 39
iv
5 38 39
v
5 34
vi
7 13
vii
7 9 4
viii
9 6

ix

11 6 39 12

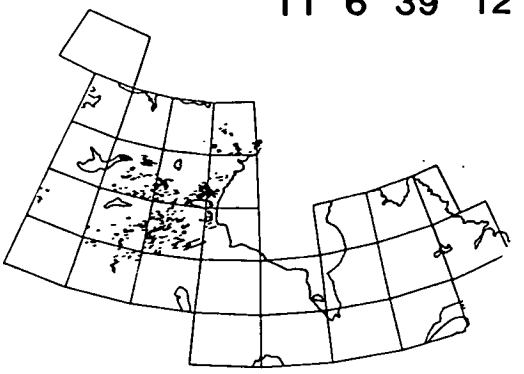

x

14 34

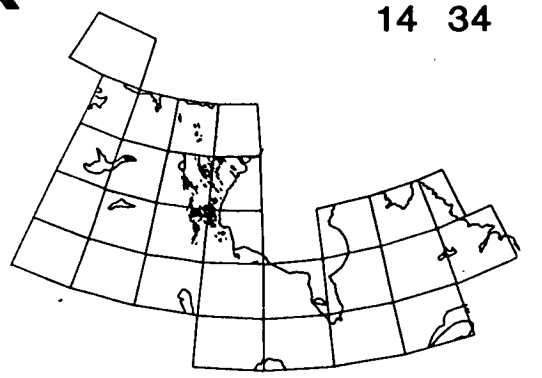

xi

16 24 35

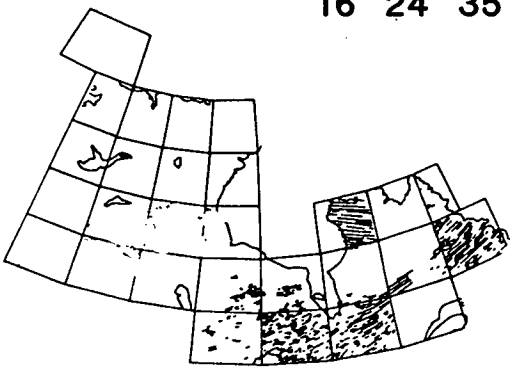

xii

19 36

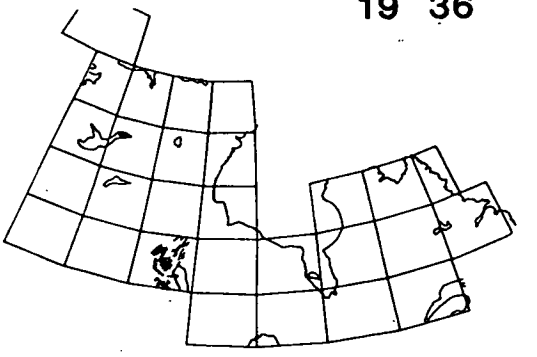

xiii

19 38

xiv

20 22

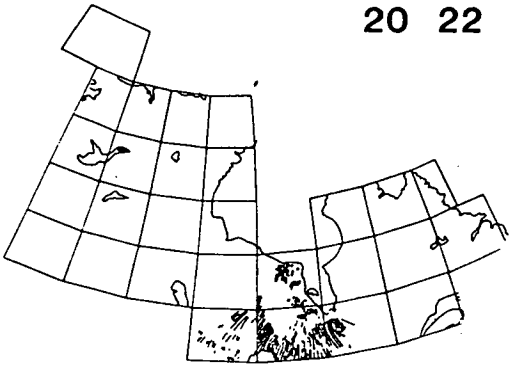

xv

21 26

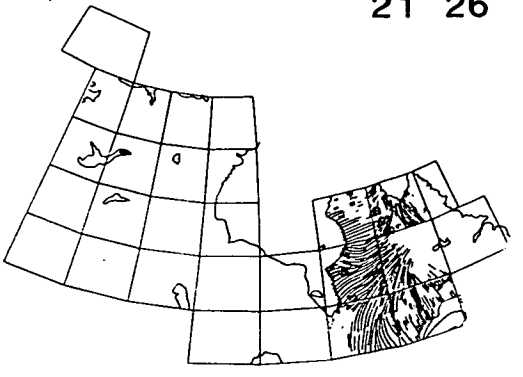

xvi

21 23

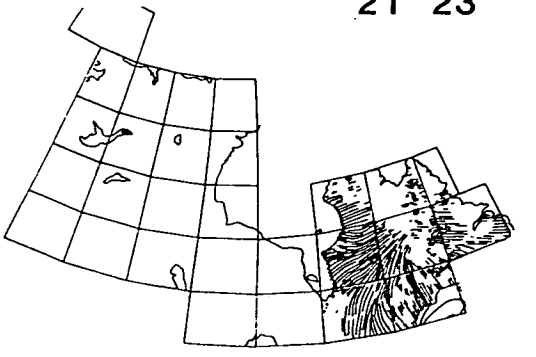

xvii

24 28

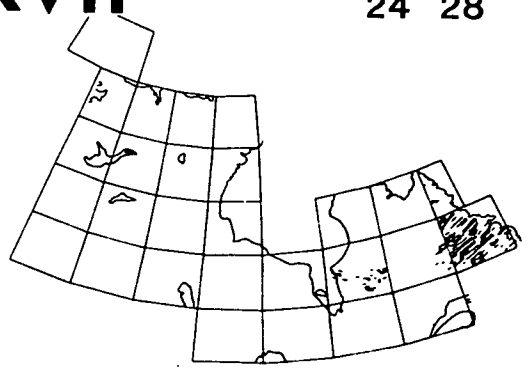

xviii

25 27

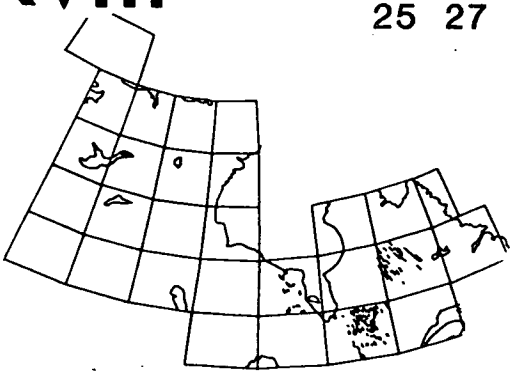

ixx

26 31

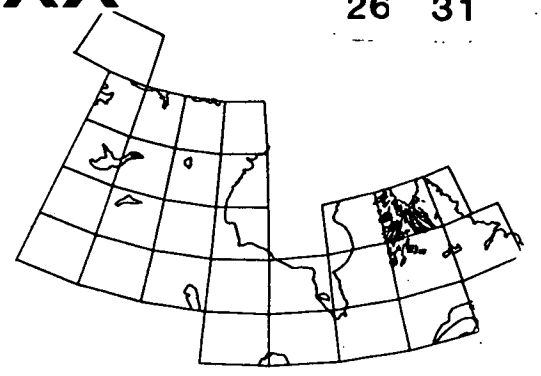

xx

27 32

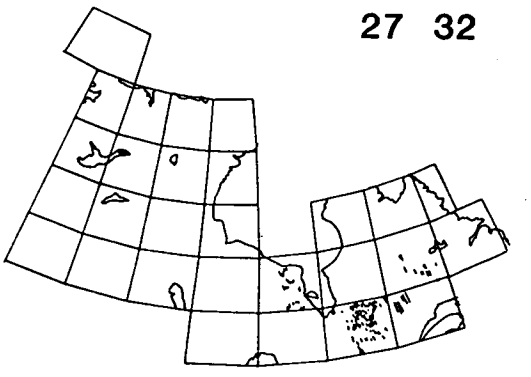

xxi

28 23

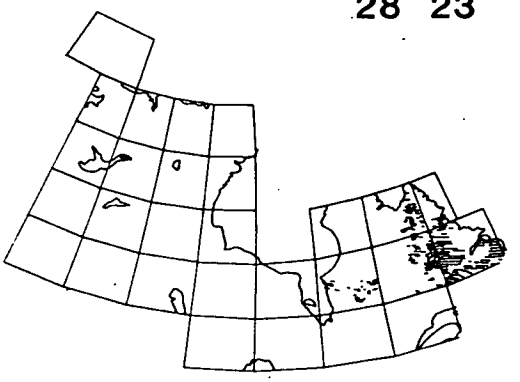

xxii

29 26 30

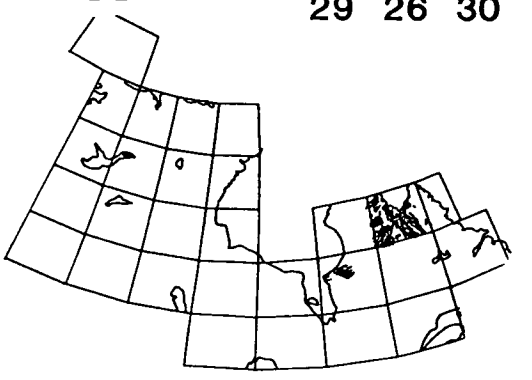

xxiii

29 30 31

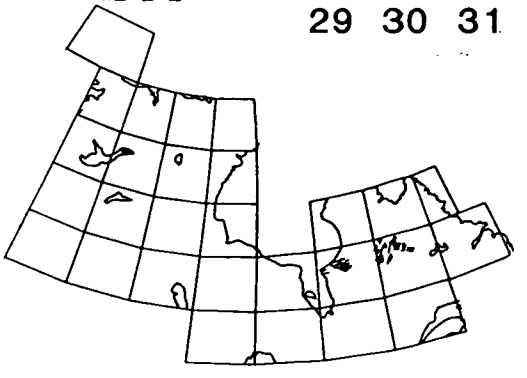

xxiv

35 23

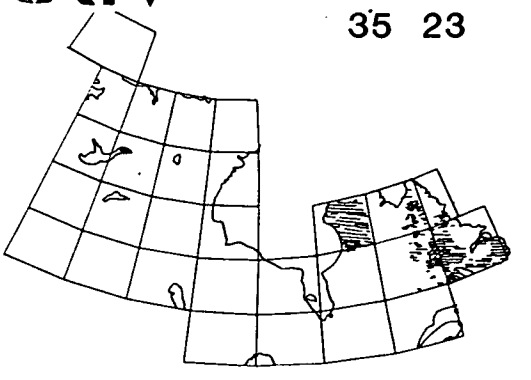

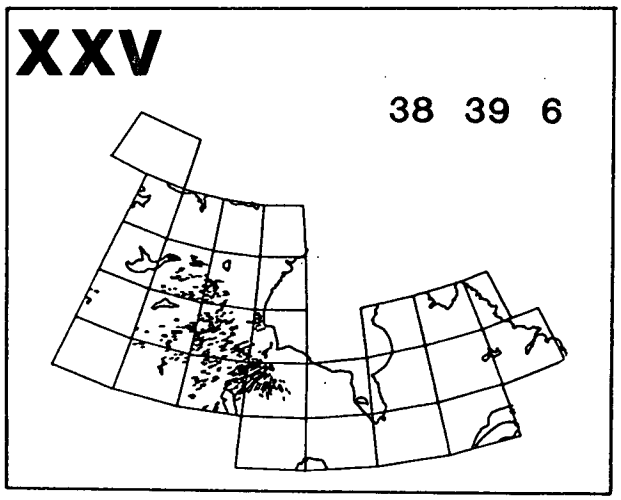
XXV
38 39 6

The combination of flow sets 13 and 7 to form a possibly synchronous flow configuration (permutation vi) seems likely in terms of pattern compatibility. But examination of the character of the lineations (spatial frequency, width, length, degree of degradation) from these sets shows them to be unusually dissimilar. In fact 13 is distinctly different from other ice flow drift lineations, in having much larger and broader lineations which, although severely degraded appear clearly on Landsat images and air photo-mosaics. A much greater antiquity than surrounding lineations is suggested by their appearance. Although generally, this type of "fresher = younger" reasoning is dangerous, I conclude that discrete flow 13 is probably older than 7 as this case is so striking. Permutation vi should therefore be rejected.

Of the 25 permutations, the following 14 are compatible; ii, iv, vii, x, xi, xiv, xvi, xvii, xviii, ixx, xx, xxi, xxiv, and xxv. The waters of Hudson Bay hide a major portion of the Laurentide Ice Sheet's former bed, and thus lineation sets are not recorded in this area. This tends to isolate lineation sets and relative age relationships into two separate data sets; one in Keewatin and the other in Labrador-Quebec. The four relative age clusters shown in Section 5.2 refer to either Keewatin or Labrador-Quebec flow sets, none are shared. The first and third clusters refer to Labrador-Quebec and the second and fourth to Keewatin flows.

Examination of the major patterns of flow in the west and east to consider how they may be correlated, leads firstly to the obvious visual compatibility of permutation xvi (flows 21 and 23) and flow set 1. These extensive flow patterns are illustrated in figure 39. This configuration produces a pattern which includes two separate ice domes, in which ice flow coincides with the pattern of lineations and moraines produced during the final

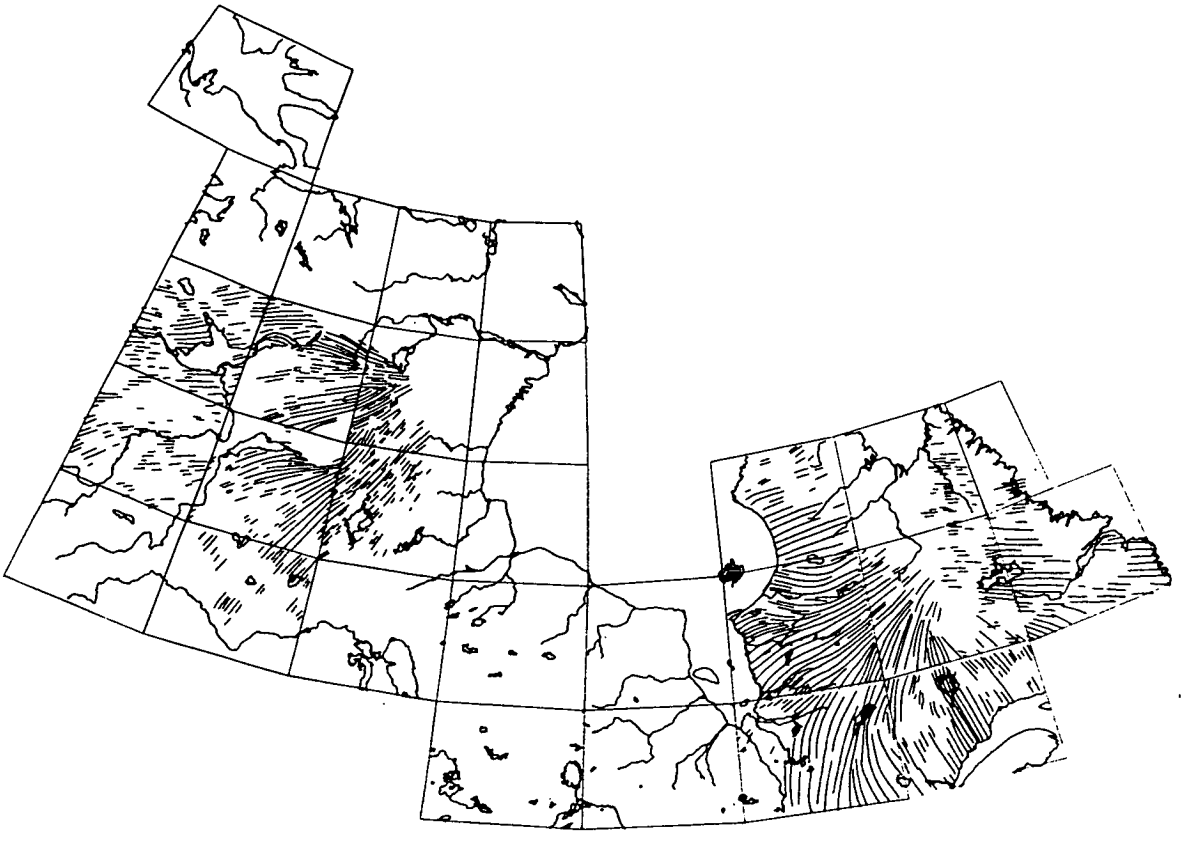

Figure 39. *Discrete ice flow sets 1, 21 and 23, producing a flow configuration indicative of two separate ice domes. This pattern is identical to that recorded by other workers (e.g. Dyke and Prest, 1987) which is widely regarded as representing the maximum configuration of the Late Wisconsinan Ice Sheet.*

retreat of the ice sheet (Dyke and Prest, 1987). This link between the eastern and western sectors of the ice sheet serves to combine the relative age clusters, producing the following relationships:

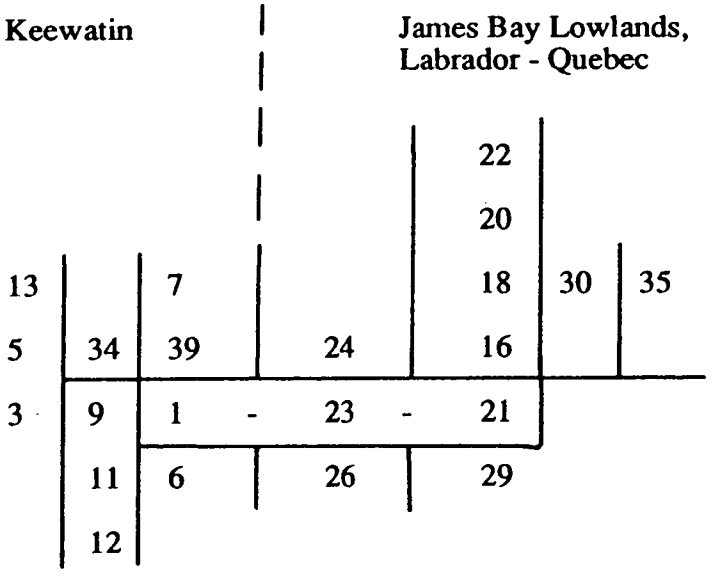

The recognition of the combination 1 - 21 - 23 as a synchronous flow pattern leads to rejection of permutation xxiv (35 and 23) or xxi (28 and 23).

The above new relative age table helps to determine which further flow patterns from the east and west might correlate. For instance two of the possible flow permutations in the west, 4 - 7 - 34 (ii in figure 38) and 5 - 38 - 39 (iv), cannot be correlated with 26 - 31 (ixx) in the east because the new structure in the relative age table shows the former to pre-date the latter.

The only further possible link between major flow patterns in the east and west sectors is between either 16- 24 - 35 and 5 - 38 - 39, or 16 - 24 - 35 and 4 - 7 - 34.

In order to assess which of the two trans-Laurentide correlations is the most likely, (16 - 24 - 35 and 5 - 38 - 39, or 16 - 24 - 35 and 4 - 7 - 34) both options were thoroughly

investigated in relation to the other patterns. The first alternative was found to represent the simplest combination. Examination of the lineation character also shows this combination to be more credible. The lineations of 16 - 24 - 35 and 5 -38 - 39 are similar in character (dimensions and spatial frequency) whereas 16 - 24 - 35 and 4 - 7 - 34 seem much less compatible. Adding this trans-Laurentide assertion of synchrony to the relative age cluster produces the following:

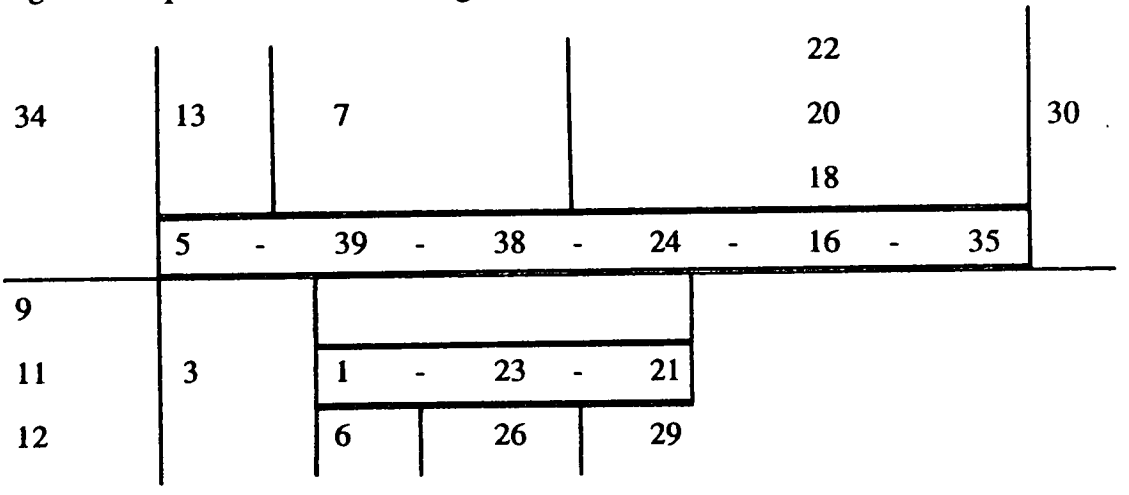

Future research should aim to establish additional constraints on correlations between flow sets, and hence produce a relative age cluster with less uncertainty (i.e fewer vertical lines), although this may prove very difficult.

The integrated trans-Laurentide flow sets (outlined in bold in the previous table) represent two flow stages within the history of the ice sheet. They act as a framework to which other less extensive flows can be related. Comparing identified flow patterns (figures 36 and 38) with the above relative age cluster allows intermediate flow stages to be derived.

Of the oldest recorded flow sets, 34 - 7 - 4 (ii in figure 38) is dominant. Its age relationship to 13 is unknown, but as previously discussed, the lineation character leads me to believe that 13 pre-dates 34 - 7 - 4. Flow sets 9 and 11 postdate 38 - 39 - 5 - 35 - 24

- 16 but their relationship to 1 - 21 - 23 is unknown. However, as the latter reflects the final pattern of flow during the decay of the Laurentide Ice Sheet, 9 and 11 must pre-date this.

In the James Bay lowlands flow sets 22 and 20 are so nearly congruent that they can be regarded as roughly synchronous. They pre-date 18 and 38 - 39 - 5 - 35 - 24 - 16, but there is no evidence of direct correlation with the older Keewatin sets.

The major discrete ice flow sets in Labrador-Quebec are well constrained in the two trans-Laurentide correlations; 38 - 39 - 5 - 35 - 24 - 16 and 1 - 21 - 23. Sets 26 and 29 are probably correlative and are known to post-date 1 - 21 - 23.

This temporal sequence of sets, established on a partly objective, partly subjective basis, is used to suggest a sequence of flow stages which provide a framework whereby widely spaced point information from stratigraphic sections can be integrated to develop a more complete history of ice sheet behaviour (see Chapter 6). These flow stages are listed below and illustrated in figure 40.

Flow Stage	Discrete flow sets
A	13
B	7 - 34 - 4
C	38 - 39 - 5 - 24- 16 - 35
D	9
E	11
F	1 - 21 - 23
G	3 - 6, 29 - 26, 17

For the flow stages A to G, ice divide positions are inferred. Note that this time-sequence of flows does not include all the identified flow sets. Remaining flow sets which cannot yet be incorporated within the relative age sequence may further refine or complicate this

reconstruction. Additional relative age information is required if they are to be incorporated.

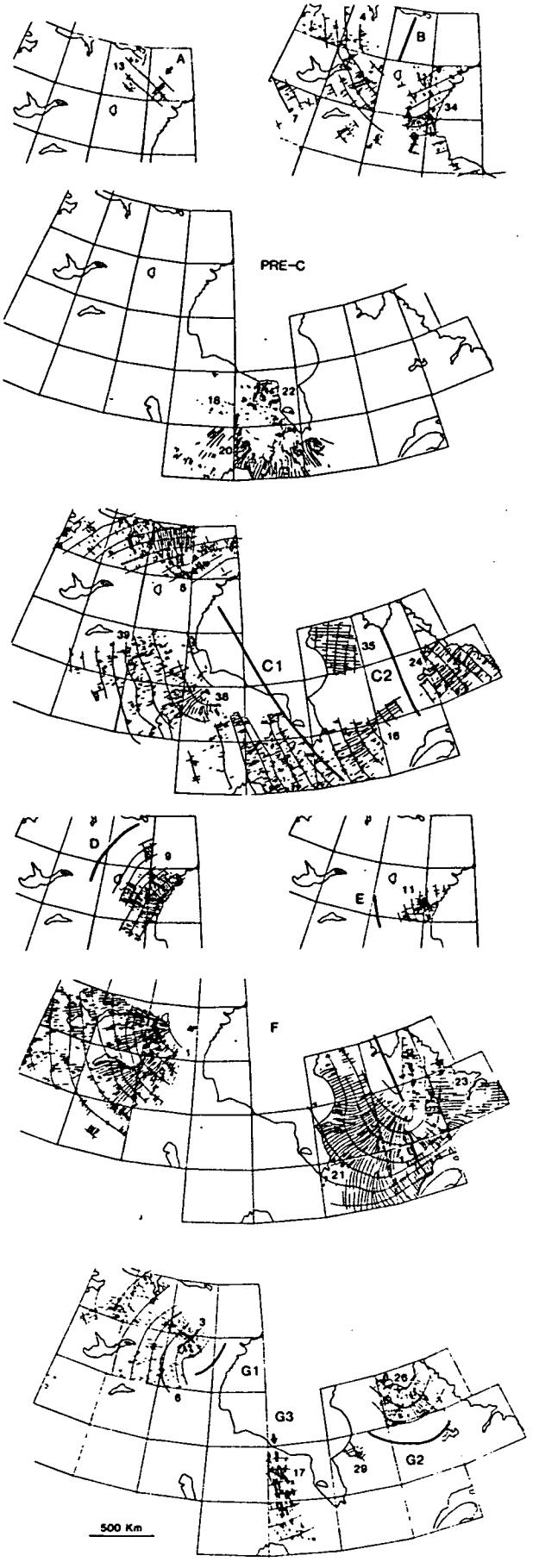

Figure 40. *Major Flow Stages reconstructed from discrete ice flow sets and their relative age relationships. Normals to the ice flow pattern are included to help define the morphology of the ice sheet surface. The postulated locations of ice divides are shown by solid lines. In Flow Stage C, an early divide (C1) and a later divide (C2) are distinguished.*

Chapter 6

The Evolution of the Laurentide Ice Sheet through the Last Glacial Cycle

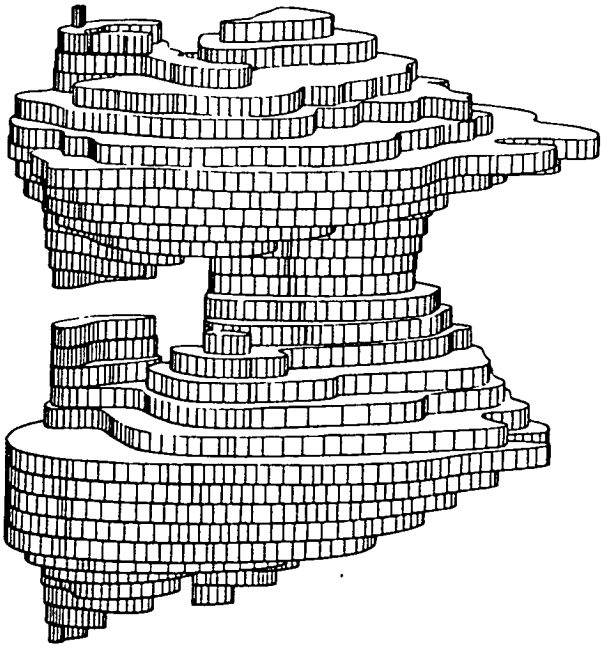

Chapter 6

The Evolution of the Laurentide Ice Sheet through the Last Glacial Cycle

The Flow Stages defined in the previous chapter are compared with published stratigraphic information in order to ascertain their ages. This permits reconstruction of major changes of ice sheet configuration through the Wisconsinan. A summary of the evolution of the Laurentide Ice Sheet is presented.

6.1 The Age of Flow Stages

The temporal sequence of flow stages described in the previous chapter are here compared with published data in an effort to ascertain their age. Stages F and G clearly correlate with the well known patterns produced during the maximum and decay stages of the Laurentide Ice Sheet (Bryson *et al.* 1969). Dyke and Prest (1987) produced a thorough synthesis of the evidence for ice sheet retreat provided by linear ice flow indicators, erratic dispersal patterns and moraines. From this they compiled a series of 11 palaeogeographic maps at time steps of a few thousand years (from 18 - 5 ka). Each map indicates the position of the ice sheet margin, and shows the configuration of ice divides and flow lines. By superimposing the flow lines of their 11 stages it was possible to compile a map showing areas in which ice flow directions changed during the retreat of the Ice Sheet. This map (figure 41) represents the theoretical imprint that the Ice Sheet could have made if lineations were formed and preserved for all stages of flow during Ice

Figure 41 *Major flow-lines plotted from Dyke and Prest's (1987) synthesis of Laurentide Ice Sheet Retreat. Stippled areas mark locations in which cross-cutting lineations may have formed during retreat of the Ice Sheet from its maximum position.*

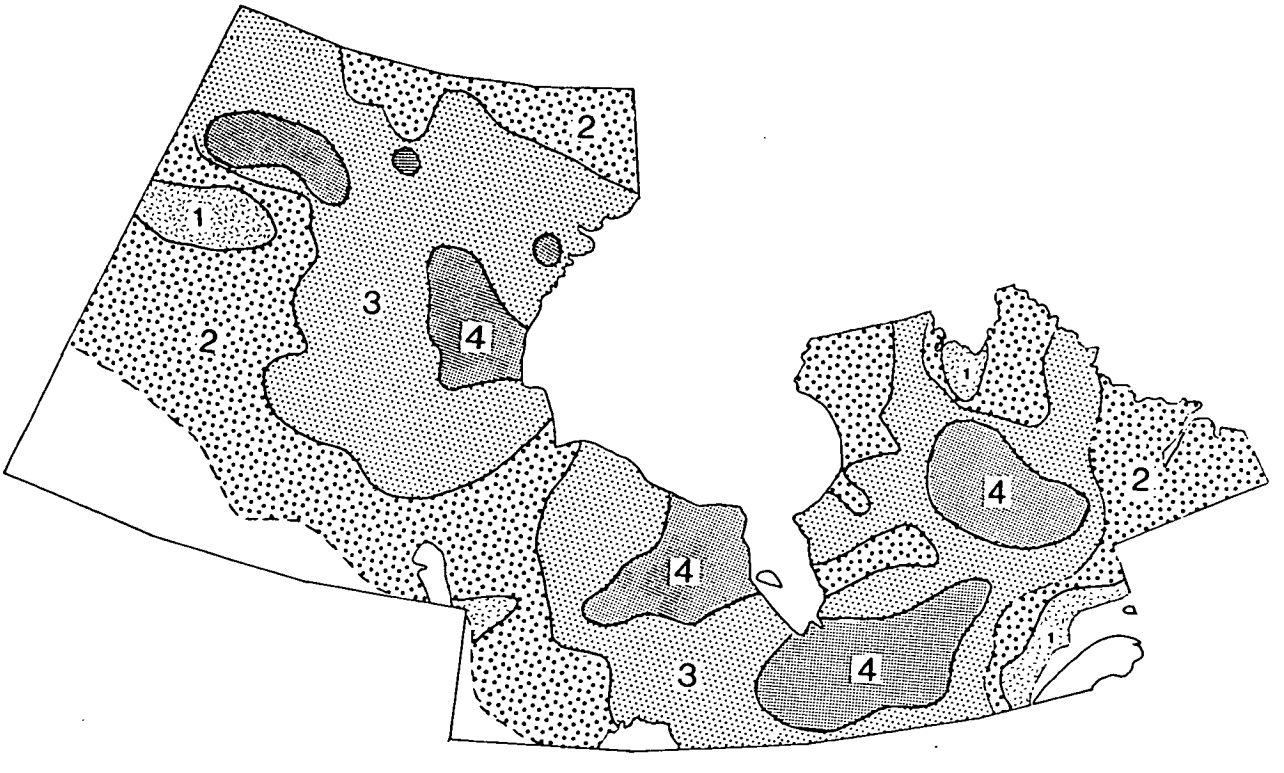

Figure 42 *Approximate cross-cutting "density" of lineation sets per unit area. Numbers indicate how many cross-cutting sets are present for that area.*

Sheet retreat. The Western Plains, a small area in Keewatin, and the area south of James Bay were the only regions in which strong changes in flow direction occurred and thus are the only locations capable of producing cross-cutting lineations during the retreat from the Ice Sheets maximum extent. Cross-cutting lineations are, however, much more widespread (figure 42). They must therefore record changes in ice flow prior to the Late Wisconsinan glacial maximum (18 ka). Flow Stages A - E and the residuals are in this category. Although they must pre-date 18 ka, it is not clear if they formed during the Wisconsinan stage or whether they include palimpsests of earlier Quaternary glaciations. Reference to dated stratigraphic sections partially helps resolve this uncertainty.

There is no direct method for determining the age of the identified flow sets. Fortunately however, there is a common link between records of ice flow and till stratigraphies; till fabrics. If fabric orientations are recorded in a section that can be dated, it thus enables phases of ice flow to be constrained in time. This produces an azimuth-age indicator i.e. ice flowing in a particular direction at a known date. Azimuth-age evidence sought from the published literature may be compared with the reconstructed Flow Stages in order to ascertain their age. For example, if there is only one till fabric orientation recorded at a particular site, and its direction matches with one of the mapped discrete flow sets for that area, it seems reasonable to assume that both directional phenomena relate to the same ice flow phase. This correlation thus fixes the discrete flow set in time. Correlations between lineations and till fabric are more convincing amongst stratigraphic sites in which multiple directions of fabrics are recorded. The stratigraphic position of the fabrics defines their relative age. If this relative age sequence exactly matches the relative age sequence of the mapped flow sets for the same area, it is reasonable to correlate them as the same ice flow events. In this way discrete flow sets, and the Flow Stages they

comprise, may be indirectly dated. This is not a new concept, it has been widely utilised to make use of striae evidence (e.g. Veillette, 1986; DiLabio, *et al.* 1988).

Regional studies of ice flow directions and till stratigraphy, incorporating dated deposits, are rare when viewed in the context of ice sheet span in time and space. The areas covered by regional studies that are described in the following, are illustrated in figure 43.

Dredge and Nielsen (1985) report a sequence of tills containing fabric evidence exposed in sections from Mountain Rapids and Limestone Rapids on the Churchill River, Manitoba (figure 44). The till fabrics record major shifts in ice flow direction which allowed them to deduce that ice both from the north and east has traversed the area during the Wisconsinan. Till lithologies, granitic versus carbonate, were also used to infer these changes. They report a sequence of three tills, the upper and lower of which contain orientation fabrics trending between 155^{o} - 185^{o}, with an intervening till whose fabric trends at about 250^{o}. A date of >32 ka was obtained for organic deposits immediately beneath the upper till, which they assign to the Late Wisconsinan. The two lower tills are believed to be of Wisconsinan age (Early or Middle). The sequence of three fabric orientations recorded by Dredge and Nielsen (1985, figure 44)) correspond with the local orientation sequences and relative ages of discrete flow sets identified in this thesis. Their lower till appears to correlate with DF34 (Stage B), middle till with DF38 and 39 (Stage C), and the flow directions in the upper till correspond to patterns of flow produced either in stage F or G.

In the Moose River Basin, west of James Bay, Skinner (1973) identified at least five till sheets separated by non-glacial sediments (figure 44). The sequence consists of the

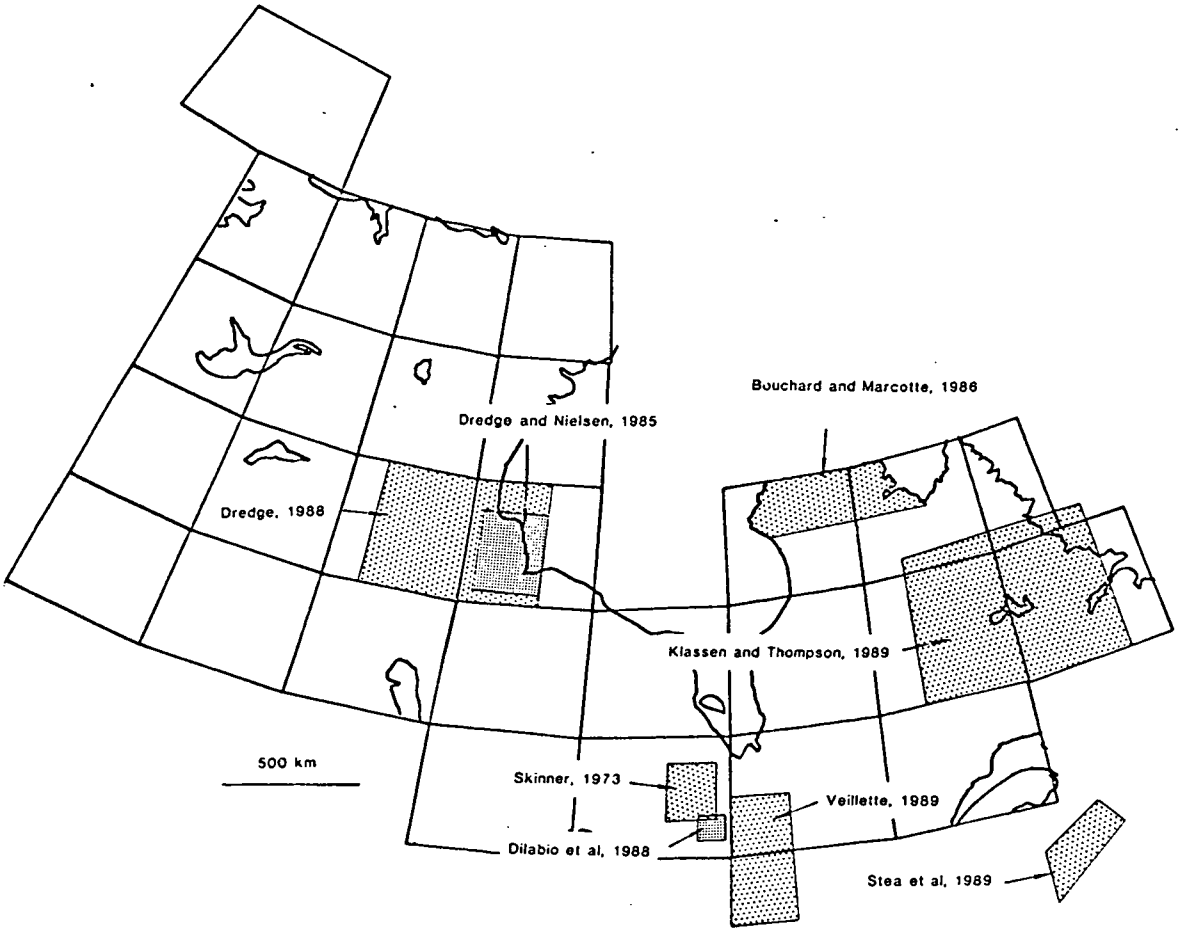

Figure 43 *Areas discussed in the text, for which shifting ice flow directions have been reported in the literature.*

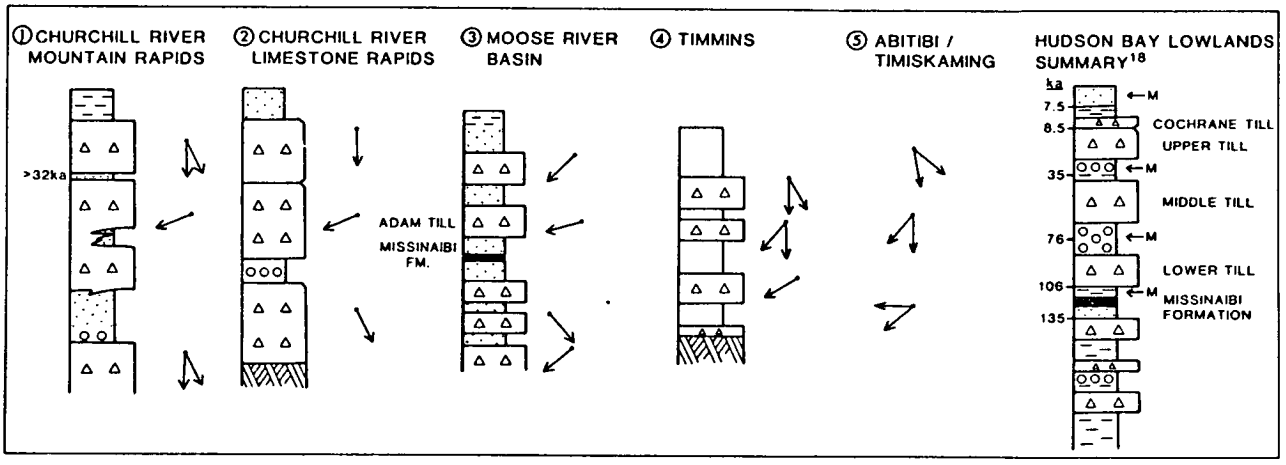

Figure 44 *Schematic stratigraphy of sites in the area immediately south of Hudson Bay (see figure 43). Arrows indicate the azimuth of ice flow as determined by till fabric or striae. Marine episodes are marked M. Sequences 1 and 2 from Dredge and Nielsen (1985); 3 from Skinner (1973); 4 from DiLabio et al. (1988); 5 from Veillette (1986); and the summary section from Andrews et al. (1983).*

Missinaibi Formation representing deposition during the last interglacial period (Sangamon) with three tills and intertill sediments beneath it and two tills above. The pre-Missinaibi sequence of tills are limited in spatial extent but record southwestward flowing ice. Above the Missinaibi Formation lies the Adam Till (WSW flow direction) and the Kippling Till (SW flow direction) separated by the Friday Creek non-glacial sediments. These latter sediments were regarded by Skinner as of Middle or Early Wisconsinan age. Shilts (1984) and Fulton *et al.* (1986) assign them to the Middle Wisconsinan, making the Adam Till Early Wisconsinan and the Kippling Till Late Wisconsinan. A particularly strong mega-scale glacial grain (DF16 - Stage C, figure 36) crosses the Moose River Basin. Its lineation trend matches best with the fabrics of the Adam Till. The southwesterly fabric orientation of the Kippling Till is compatible with the flow configuration my of Stage F, although lineations of this trend do not actually extend into the Moose River Basin.

In the Timmins area, 300 kilometres south of the Moose River Basin, DiLabio *et al.* (1988) utilised borehole information to compile a glacial stratigraphy which included four tills (figure 44). The uppermost glacial unit is the Cochrane Till which relates to a readvance of the decaying Ice Sheet margin at about 8 ka (Hardy, 1982; Dyke and Prest, 1987). Below this they describe the Matheson Till which overlies the Owl Creek Beds. These organic-rich beds contain pollen and beetles indicative of an interstadial or interglacial climate (Morgan and Morgan, 1980). Because radiocarbon dates from this unit are infinite (>37 ka; >51 ka) it is not clear whether these beds represent a Middle Wisconsinan interstadial, possibly related to the non-glacial conditions argued by Shilts *et al.* (1983), or to the last full interglacial (Sangamonian). Correlation between widespread striae reported by Veillette (1986) and the till stratigraphy provides a history of shifting ice flow directions. The Matheson Till is considered to have been deposited by

two ice flow movements; 150° - 180° and 180° - 220°. The first till beneath the Owl Creek Beds is correlated with an earlier set of striae indicating ice flow towards 240°. The pattern of discrete ice flow sets suggests the following correlations: DF16 (Stage C) with the first till beneath the Owl Creek beds, DF21 (Stage F) with the Matheson Till (Late Wisconsinan) and Flow Stage G3 with the Cochrane Readvance.

In the Abitibi - Timiskaming region Veillette (1986; 1989) examined over 2000 locations displaying bedrock striae, many of which were cross-cutting. The arrangement of the striated surfaces allowed the relative age of ice flow directions to be determined (Veillette, 1983; 1986). Three phases of ice movement are reconstructed from these data: PHASE 1: SW - W (230° - 270°); PHASE 2: S - SW (180° - 220°); PHASE 3: a more complicated deglacial flow pattern related to the deposition of the Haricana Moraine, with flow directions of 130° - 170° (S - SE) (see figure 44). Comparison of Veillette's (1989) ice flow reconstruction with the discrete ice flow sets mapped in this thesis (figures 35 & 36) shows a high degree of correspondence:

Veillette (1986,1989)		this thesis
PHASE 1		DF16 - Stage C
PHASE 2		DF21 - Stage F
PHASE 3		DF17 - Stage G3
	or	DF20 - Stage pre-C

DF20 is excluded as it contradicts the relative chronology determinations outlined in Chapter 5. The remarkable correspondence of ice flow indicators at such widely different scales (mega-scale glacial lineations versus striae) provides great promise for future work. Unfortunately Veillette's work on cross-cutting striae is unique, and further comparisons cannot yet be made.

In northern Manitoba, Dredge (1988) mapped the dispersal of drift carbonate over the Canadian Shield. She reported carbonates found in the matrix of a surface till some 260 km westwards of the Palaeozoic limestone bedrock which provides the source. This is indicative of sustained ice flow from the east, i.e. out of Hudson Bay. Granitic till (non-Hudson Bay source) is found overlying the calcareous till in places. Furthermore, flutes trending in a southward direction are found superimposed upon the calcareous till, and thus prove that a southward flow from a Keewatin ice centre (providing the granitic till) succeeded the westward flow from Hudson Bay (the carbonate dispersal phase). The reconstructed flow lines of Stage C show a pattern of ice movement emanating from Hudson Bay which could have produced the observed carbonate dispersal pattern. The superimposed southward trending flutes conform to the flow pattern produced during Stage F. The carbonate and granitic tills representing two major flow phases have not been dated, but their relationship to a presumed Late Wisconsinan moraine implies a Late Wisconsinan age for the Keewatin-derived flow and Early or Middle Wisconsinan for the Hudson Bay-derived flow (Dredge, 1988).

Andrews *et al.* (1983) have suggested an overall stratigraphy and chronology for late Quaternary events within the Hudson Bay Lowlands (figure 44), in which four major glacial events since the last interglacial are recorded by tills. They assert that the Wisconsinan history of the Laurentide Ice Sheet has been interrupted by three phases of marine incursion into Hudson Bay. This precludes the existence of a stable ice mass throughout the last glacial. Amino-acid analyses on marine molluscs from within the stratigraphic sequence of the Hudson Bay Lowlands has enabled them to constrain the ages of till deposition and associated glacial events (figure 44). Their lower till is suggested to be of Early Wisconsinan age, between 106 and 76 ka, which is correlated with Skinner's Adam Till and my Flow Stage C. Flow Stage F correlates with Skinner's

Kippling Till, DiLabio's Matheson Till and Veillette's second flow phase. These may be equivalent to the Middle or Upper Till in the schema of Andrews *et al.* (1983). However, the Kippling and Matheson Tills are widely regarded as Late Wisconsinan in age, equivalent to the upper till of Andrew's (Fulton *et al.* 1986; Steele, 1989). This reaffirms the Late Wisconsinan age of Stage F, a conclusion previously drawn from the similarity of the Stage F flow pattern with Dyke and Prest's (1987) Late Wisconsinan ice flow configuration. Flow Stage G3 appears to correlate well with the Cochrane Readvance into the James Bay Lowlands. This event occurred between 8.5 and 8 ka (Hardy, 1982).

Multiple phases of ice flow are also reported beyond the Hudson Bay Lowlands. Klassen and Thompson (1987, 1989) describe 7 phases of ice flow in the central Labrador - Quebec region (NTS 23 and 13). Three of these phases correlate well with discrete ice flow sets mapped in this thesis, but unfortunately there is no dating control. They do however regard all the flow phases, except the oldest, to represent events during the Wisconsinan. On the Ungava Peninsula (NTS 34), Bouchard and Marcotte (1986) report similar findings. They mapped a number of cross-cutting ice flow phases, indicating shifting ice centres, but are not able to date these movements. Using striae and glacial dispersal evidence in Nova Scotia, Stea *et al.* (1989) identified four major Wisconsinan ice flow events, each with a different flow pattern. Although Nova Scotia is outside the mapped area, it would appear that their Phase 1, which they regard as Early Wisconsinan, correlates well with my hypothesized Stage C.

In summary, it is apparent that over the last ten years multiple phases of ice flow have been reported from widely-spaced locations in Canada (figure 43). They provide "windows" through which the Laurentide Ice Sheet's history can be glimpsed and show a behaviour different from that recorded by the Glacial Map of Canada (Prest, 1968; Dyke

and Prest, 1987), which it is suggested reflects only part of the Late Wisconsinan behaviour of the Ice Sheet. Unfortunately most of the studies involving striae have little or no dating constraints. The most common from of chronological control is summed up by Klassen and Thompson (1987) in their remark: "because ice flow features recorded on outcrop surfaces do not show differential weathering, the phases appear to have been produced during a continuous ice cover and may represent changes during one or more stadials of Wisconsin Glaciation". In the Hudson Bay Lowlands however, radiocarbon and amino-acid dating within the context of a developed stratigraphy has enabled ice flow events to be constrained in time. Correlations which have been made with these sections leads to the conclusion that Flow Stages C to G belong to ice flow phases of the last glacial cycle (Wisconsinan). Although there is no direct evidence of the age of flow stages A and B (figure 40) it is likely that these may be build up phases of an Early Wisconsinan ice dome in Keewatin, immediately prior to a major Hudson Bay dome (Stage C).

6.2 Major Shifts of Ice Sheet Configuration through Time

Evidence has been presented to show that Flow Stages C to G were all produced by the Laurentide Ice Sheet during the last, Wisconsinan, glacial cycle, and that Stages C, D and E reflect phases prior to the Late Wisconsinan maximum (18 ka). It has also been suggested that Flow Stages A and B could belong to an early phase of the cycle representing the initiation and subsequent ice sheet build-up. The principal Flow Stages and the nature of the ice sheet whose behaviour they reflect are summarised below.

In most cases ice divide configuration and associated radial flow patterns represent an ice sheet whose centre of mass was relatively fixed, but which could have been expanding,

decaying or stable. However, it is only possible to account for Flow Stage C if the ice divides shifted dramatically during the course of the stage.

Flow Stage A (discrete flow set 13)

There is no direct evidence for the age of this flow, although it pre-dates discrete flows that form the stages B to G. The lineations may represent pre-Wisconsinan ice flow, but are tentatively suggested as reflecting earliest Wisconsinan ice sheet expansion from centres of initiation in northeast Keewatin or north Baffin Island.

Supporting evidence is found in published reports of fieldwork carried out in the area. There have been numerous reports of bedrock striae displaying the same orientation as the lineations of Stage A (Tyrrell, 1898; Bird, 1953; Taylor, 1956; Lee, 1959; Cunningham and Shilts, 1977). These have been labelled "old" striae (e.g. Tyrrell, 1898; Lee, 1959) in view of the fact that they pre-date the main, Late Wisconsinan, pattern of flow. Cunningham and Shilts (1977) found quartzite erratics in the Baker Lake region which indicates a major period of southward transport. "Old striae" supporting this flow phase are also found. Their preliminary interpretation was that it "could be that the Wisconsinan (or Late Wisconsinan) ice sheet grew with its centre of outflow in northern

Keewatin and that the centre migrated to the south and east to the vicinity of Baker Lake in the final phases of glaciation" (Cunningham and Shilts, 1977, p 313)

Snow-cover maps derived from satellite imagery permitted Williams (1978; 1979) to compute an energy balance model of potential glacierization for northern Canada. The model predicted that Baffin Island was the most probable site of ice sheet initiation, and that contrary to previous beliefs, northern Keewatin is just as susceptible to glacierization as Labrador-Ungava.

<u>Flow Stage B</u> (discrete flows sets 34-7-4)

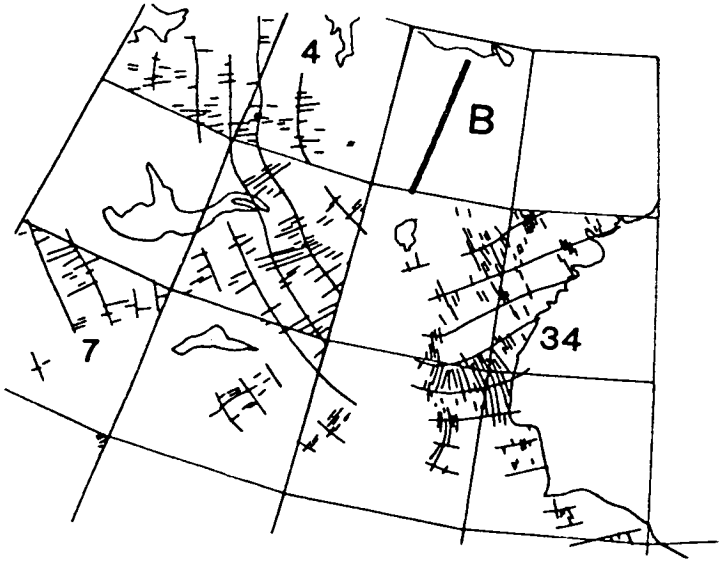

The pattern displayed by discrete ice flow sets 34-7-4 indicates probable existence of an ice dispersal centre located in northern Keewatin, with substantial expansion of ice into Manitoba and Saskatchewan. A north-south trending ice divide is inferred, although the data also suggests that subsidiary ridges may have been present which were oriented due west and south from the southern limit of the marked, main divide. This pattern corresponds to repetitive triple junctions of divide ridges observed in contemporary ice

sheets (Hindmarsh, *pers. comm*; Boulton and Clark, 1990). As expected (Chapter 3), lineations are not found in the ice divide areas of low basal-velocity.

Location of the Stage B ice dispersal centre is at least 400 km southwest of that in Stage A. If the two stages are consecutive, as is suggested, it represents a considerable migration of the ice divide. The coincidence of azimuth between DF34 and Dredge and Nielsen's (1985) fabric orientations of their lowest till, provides a tentative age constraint. They regard their lower till as Early or Middle Wisconsinan.

It may be noted that the Stage B ice dispersal centre is similar to the Late Wisconsinan Keewatin ice divide inferred by Lee (1959), Shilts *et al.* (1979) and Dyke and Prest (1987) and also my Stage D and F configurations. It seems that this location is a naturally favoured position.

<u>Pre-C Flow Stages</u> (DF18, 20 and 22)

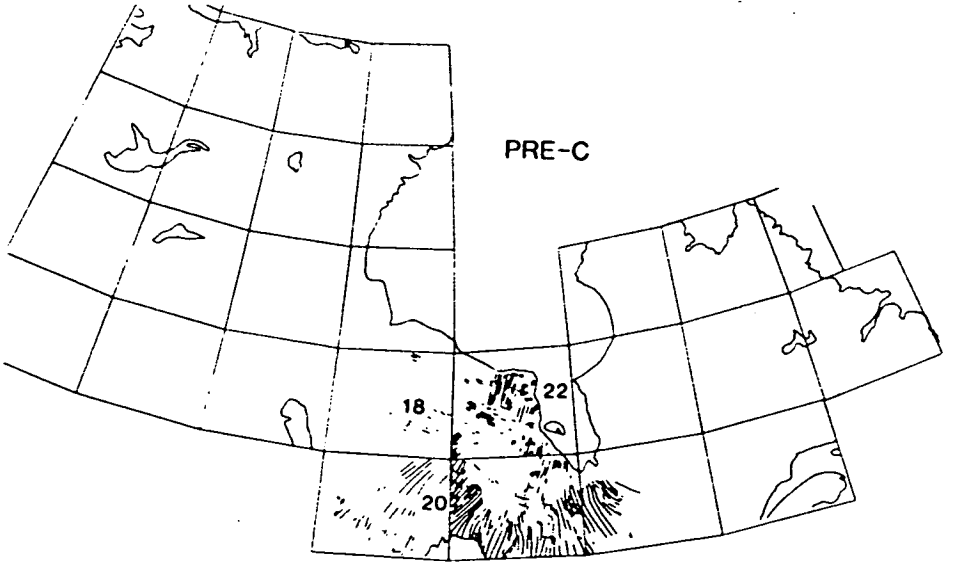

This is not a single, approximately synchronous flow stage, but rather a collection of

discrete flow sets which relative chronology criteria show to pre-date flow stage C. Their relationship to stages A and B is unknown. They may be of pre-Wisconsinan age, although it is more likely that they represent a partial record of shifting ice flow in the Early Wisconsinan.

DF20 and 22 constitute a diverging flow pattern whose explanation may be either, the termination of an ice divide or subsidiary ridge over eastern Hudson Bay, or the typical fan topology of flow lines common in lobate ice margins. Soft, easily deformable sediments in this area could have favoured low basal shear stresses, thus producing thin, lobate ice margins. DF18 documents ice flow into the James Bay Lowlands from a Keewatin centre. If DF20-DF22, and 18 were consecutive, then changing dominance from a Quebec-Hudson Bay ice dispersal centre to a major Keewatin centre can be inferred. This may have occurred immediately prior to coalescence of domes producing the major trans-Laurentide ice divide of Stage C.

<u>Flow Stage C</u> (discrete flow sets 38-39-5-24-16-35)

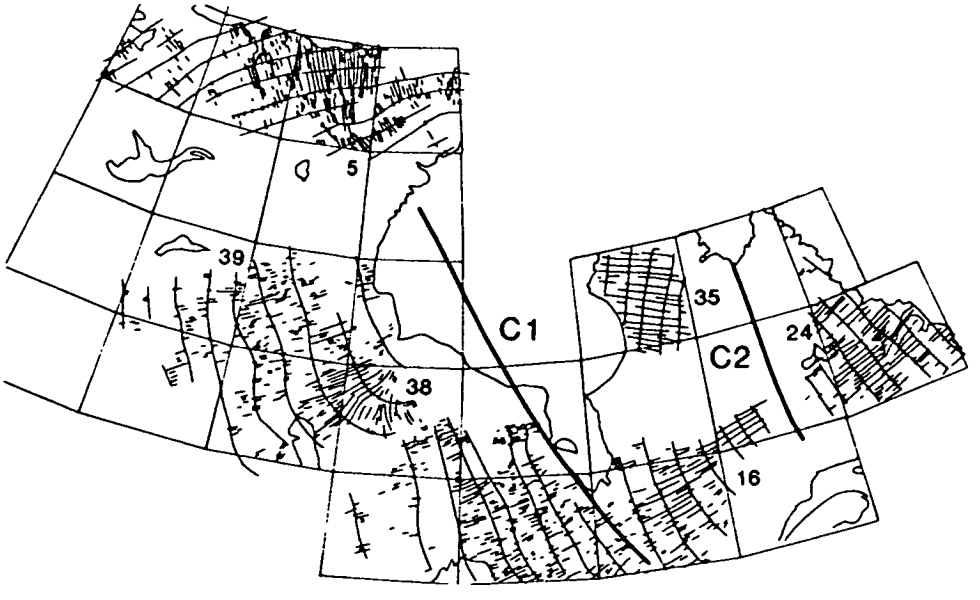

The aforementioned correlations (Section 6.1) between directions of flow in this stage and the Adams Till (Skinner, 1973), Middle till of Dredge and Nielsen (1985), the first till beneath the Owl Creek Beds (DiLabio *et al.* 1988), striae Phase 1 of Veillette (1986), the carbonate dispersal out of Hudson Bay (Dredge, 1988), combined with the dating provided by Andrews *et al.* (1983), strongly suggests that this stage of ice flow occurred in the Early Wisconsinan, between 106 ka and 76 ka. This stage cannot however, represent a single roughly synchronous pattern of flow for whereas normals to flow lines define an ice dispersal centre in Labrador, it is inconceivable that, on an approximately horizontal bed, ice from a Labrador source should penetrate into Alberta some 2500 km to the west, whilst its eastern extension should be limited by the continental shelf edge, a distance of 1100 km. Such an asymmetric ice sheet profile defined by a synchronous lineation pattern must be rejected in favour of a dynamic stage in which the lineation pattern formed diachronously. The lineation pattern, particularly DF16, is thought to reflect the progressive decay of a large ice sheet, which near its maximum, had an ice divide oriented NW-SE over Hudson Bay, and which progressively shifted eastwards as the western portion of the Ice Sheet decayed (divide position C1 to C2 on the above map). As the western ice margin retreated eastwards, the geomorphologically active terminal zone reorganised the bed, producing lineations of progressively younger age. A strongly negative glacier mass balance must have developed in the west whilst a healthy balance was maintained in the east. A possible climatic mechanism producing this effect is presented later.

It seems that the early Stage C Ice Sheet was very extensive and was configured around a trans-Laurentide ice divide (C1). This may have been a divide of constant elevation along its length, but the lineation pattern suggests two ice domes separated by a shallow saddle as a more likely configuration. The early Stage C Ice Sheet is probably equivalent to the

Early Wisconsinan Ice Sheet. This is considered by many to have been more extensive than the Late Wisconsinan Ice Sheet on the eastern Canadian continental shelf (Grant, 1977), in its SW sector in northern USA (Clayton and Moran, 1982), and on its northern margin in Baffin Island and Banks Island (Nelson, 1989; Vincent, 1983; Fulton *et al.* 1986).

The presumed, climatically-induced eastward migration of the centre of mass of the Ice Sheet during Stage C and the associated deglaciation of Keewatin and Hudson Bay was probably contemporary with the period of marine invasion of Hudson Bay at about 76 ka (Andrews *et al.* 1983). Corroboratory evidence for a trans-Laurentide ice divide across Hudson Bay is provided by the major transport of limestone erratics out of Hudson Bay and into Keewatin, reported by Dredge (1988). The migration of this divide may have been detected in Nova Scotia, as Stea *et al.* (1989) report an Early Wisconsinan shift in ice flow for this region. They describe an Early Wisconsinan phase in which ice flowed in a easterly direction across Nova Scotia, followed by a phase in which it flowed southwesterly. This fits with the eastward migration of the major C1 ice divide. Late Stage C (and Stage D) could be of Middle Wisconsinan age, during which a non-glacial period is recognised in western Canada (Fulton *et al.* 1986) where sites in southern Manitoba and central Saskatchewan and Alberta indicate an ice free period from at least 40 ka to 22 ka (Dredge and Thorleifson, 1987).

<u>Flow Stage D</u> (discrete ice flow 9)

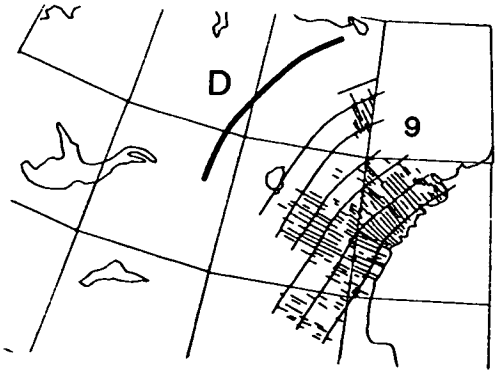

Deglaciation of Keewatin in Late Stage C, the result of a presumed Middle Wisconsinan interstadial, was followed by a build-up of ice perhaps repeating the Stage A and B sequence. A "snapshot" of this emergent Keewatin Ice Sheet is recorded by Stage D lineations. This Flow Stage indicates that ice from a Keewatin source flowed into Hudson Bay, in a direction opposite to that of Stage C. The lineations display convergence into the Bay, defining an ice divide curving from northeast to south. This convergence may be indirect evidence for a calving terminus in a marine-inundated Hudson Bay. If this is so, Stage D must be contemporary with the marine phase of Andrews *et al.* (1983) at around 76 ka.

Flow Stage E (discrete flow set 11)

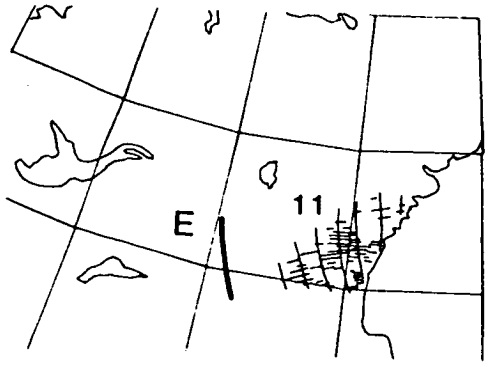

North-easterly ice flow into Hudson Bay defines an approximate ice divide position as shown above. This position represents a 300 km southeastward migration since Stage D. There is no direct evidence for the age of this stage, but it probably represents part of the build-up phase to the Late Wisconsinan maximum.

Flow Stage F (discrete flow sets 1 - 21 - 23)

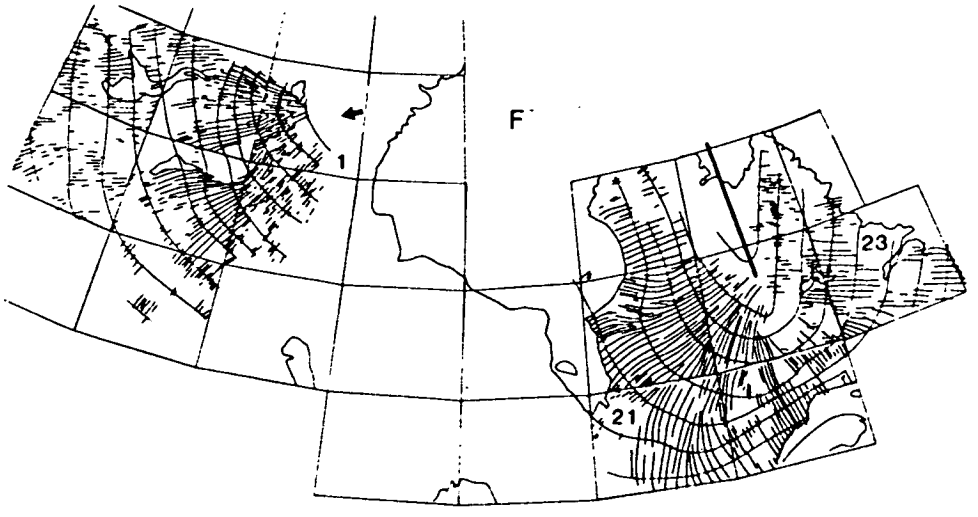

This pattern of bi-nodal flow has been familiar to glacial geologists since the time of Tyrrell (1898). It is widely thought to be the pattern of flow produced by the Laurentide Ice Sheet at its maximum Late Wisconsinan phase at 18 ka (Prest, 1969; Bryson *et al.* 1969; Boulton *et al.* 1985; Dyke and Prest, 1987). The lineation record in Labrador-Quebec defines a north-south trending ice divide. The lineations in Keewatin indicate the existence of an ice dome, or an ice ridge terminating at the origin of the lineation pattern. Nevertheless, the overall configuration is one of twin ice dispersal centres either side of Hudson Bay.

It is probable that the Keewatin Dome was the successor to the growing Stage D and E ice masses in Keewatin, and that the Labrador-Quebec dome grew from the residual Labrador-Quebec dome of Stage C, which many believe persisted there from Early Wisconsinan times (King and Fader, 1986; Piper, 1988).

Flow Stage G (discrete flow sets 3 - 6 - 17 - 29 - 26)

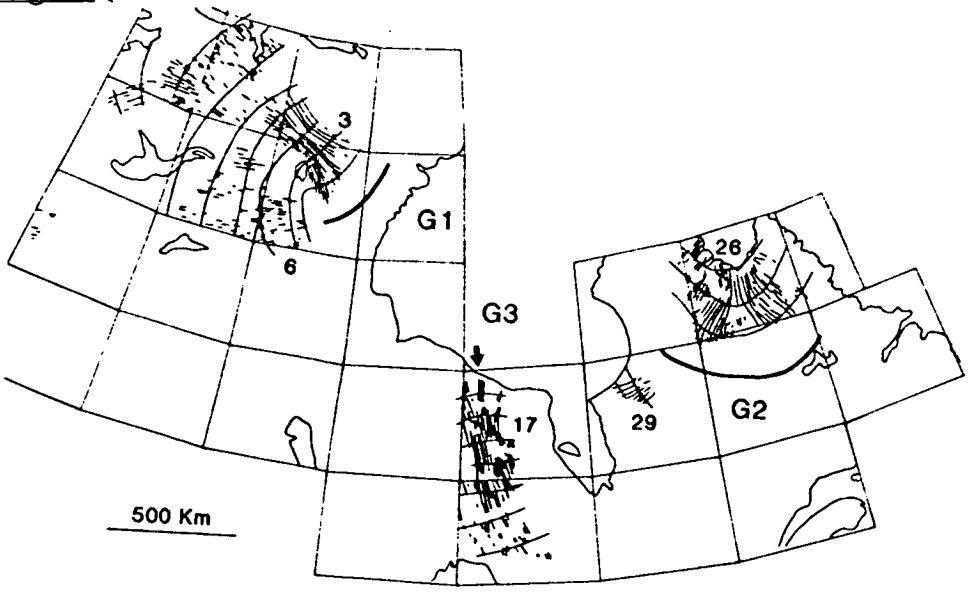

There are three post-F flow stages which have not been related to each other, but which for convenience, are grouped together in Stage G. They all represent final adjustments in the flow of the decaying Ice Sheet.

Sub-stage G1 (DF3 + 6), indicates a slightly reduced Keewatin ice dispersal centre which underwent a minor southeastward shift from the Stage F position. Ice flow appears to have concentrated in a zone of strong convergence, possibly an ice stream, flowing northwestward. This zone of enhanced flow producing strong lineations may be the result of increased ablation in the northwest sector of the Ice Sheet, or a consequence of changing glaciological conditions (basal temperature, porewater-pressures of underlying sediments etc).

Discrete flow sets 26 and 29 define the curving ice divide of sub-stage G2. The radical change of position between the north-south trending ice divide of Stage F to the curving west-east pattern of this stage is evident. This is attributed to the effects of marine drawdown. During deglaciation, rising global sea level led by the melting European Ice Sheet

(Nakada and Lambeck, 1988; James and Keigwin, 1988), destroyed that part of the Stage F divide which extended over Ungava Bay, producing a calving ice front terminating in a marine embayment. Rapid subsequent drawdown of ice, further destroyed the major Stage F divide creating a large ice basin whose limit is the G2 ice divide. The disappearance of the major north-south Ungava ice divide would have permitted the Hudson Strait to act as a major throughway for ice, allowing rapid disintegration of the core of the Laurentide Ice Sheet.

The G3 sub-stage consists of very strong lineations (DF17) which correlate with the Cochrane Readvance, presumed to be a glacier surge interrupting ice margin retreat between 8.5 ka and 8 ka (Dyke and Prest, 1987).

Regarding the whole lineation pattern and flow stage sequence, two further points deserve comment. Firstly, for those cases in which spatially extensive lineation sets exist, it is likely that the downstream limit of lineation is close to the contemporary ice margin. It was noted in Chapter 3 that the longest and strongest lineations were most likely to form in the high basal velocity zone just short of the glacier margin. This supports the above premise.

Secondly it is interesting to note the difference in interpretation between the established views of the so-called Keewatin Ice Divide and those presented here. Following Lee (1959), the concept of a crescent-shaped ice divide has become thoroughly entrenched in the literature (e.g. Shilts *et al.* 1979; Dyke and Prest, 1987; Andrews *et al.* 1983; Andrews, 1987; Shilts *et al.* 1987). Their configuration of ice divide and flow is illustrated in figure 45a. These same patterns of ice flow have been recognised on

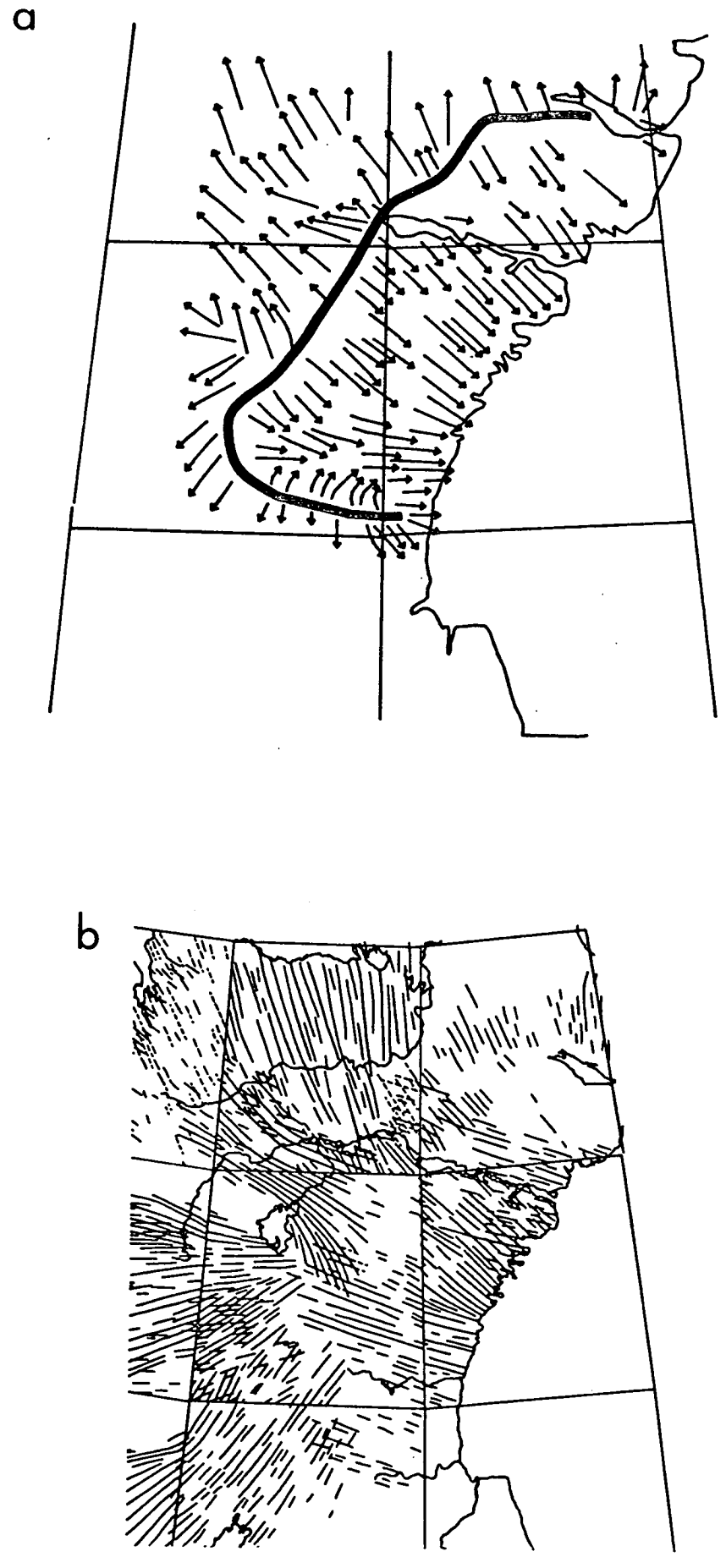

Figure 45 **a:** *The Keewatin Ice Divide as inferred by Shilts et al. (1979). Arrows indicate ice flow reconstructed from striae evidence.*

b: *Flow lines interpreted from Landsat-mapped lineations of the same area.*

remotely sensed images and mapped for this thesis, figure 45b. The lineations used to define their ice divide are in fact of different age, comprising parts of my Flow Stages C, D, F and G1. Furthermore the lineations extend upstream to within a few kilometres of their hypothesized divide, an area in which ice flow velocities were approximately zero. Also, DF9 actually crosses their postulated ice divide. Using cross-cutting lineations to construct relative ages of ice flow patterns, thus shows that the crescent shaped ice divide postulated for Keewatin is an artefact.

6.3 The Mobile Ice Sheet; a summary

Two major sources of uncertainty are inherent in using the mega-scale glacial lineation pattern to reconstruct the behaviour of the Laurentide Ice Sheet through the last glacial cycle. The first is the combining of discrete flows sets to produce Flow Stages. The Flow Stages were simple compilations of discrete flow sets, both compatible in terms of pattern and relative age. For example DF5 and DF38 & DF39 (the western portion of Stage C) could either be synchronous or of different age. Occam's razor has simply been invoked in associating them together.

The second uncertainty is in the dating of flow stages. Evidence that combines ice flow directions and dates thereof, is limited, and comes mostly from the Hudson Bay Lowlands. These have been utilised as much as possible to provide an overall chronology. There may be errors in these dates and in the correlations made. Such errors would produce large changes in the reconstruction presented here. Nevertheless it was felt important to attempt this synthesis in view of the new insights that the recognition of mega-scale glacial lineations represent. Their cross-cutting nature invalidates major

assumptions used in past reconstructions of the history of the Laurentide Ice Sheet. It was therefore important to suggest a fresh synthesis based on the new data. The evolution of the Ice Sheet, described in detail in the last section, is summarised below.

Ice sheet initiation appears to have occurred on northern Baffin Island and, or northeast Keewatin, and may have been concurrent with a similar phase of build-up in Labrador-Quebec. The centre of mass of the growing Keewatin Ice Sheet migrated some 400 km in a southwesterly direction, becoming stable for a while in a location to the north of Dubawnt Lake. Ice spread as far south as northern Manitoba and Saskatchewan. Although no evidence has been presented for an equivalent Labrador-Quebec phase, it is likely that an autonomous ice sheet existed to the east of Hudson Bay. Equivocal evidence from the James Bay Lowlands suggests that a Labrador-Quebec ice centre may have been the more rapidly growing component of the Laurentide Ice Sheet in the earliest Wisconsin. This ice sheet may have occupied the eastern sector of Hudson Bay with ice flowing south into the James Bay Lowlands, but was probably not confluent with the Keewatin Ice Sheet at this time. The Keewatin Ice Sheet is then presumed to have expanded at the expense of the Labrador-Quebec centre, as evidenced by ice flow into the James Bay Lowlands from a Keewatin source. This is expected to be the phase whereby the two ice sheets coalesced to form the major trans-Laurentide ice divide of the Early Wisconsinan. It was in this phase that the Laurentide Ice Sheet attained its maximum thickness (height) and perhaps extent, with a major ridge trending NW-SE across Hudson Bay. Presumed climatic response to this major ice sheet and, or external climatic forcing (Middle Wisconsinan amelioration-interstadial?) produced a negative mass balance in the west. As a result, the trans-Laurentide ice divide migrated eastwards producing partial deglaciation of Keewatin, but leaving a Labrador-Quebec Ice Sheet which is thought to have survived the Middle Wisconsinan stadial. Subsequent Late

Wisconsinan intensification of global cooling produced re-initiation of ice in Keewatin with attendant ice divide migration to the south, as the Ice Sheet grew. Unlike the Early Wisconsinan ice sheet, this Late Wisconsinan phase culminated as two independent ice domes, one in Keewatin and the other in Labrador-Quebec, with an ice saddle or zone of coalescence over Hudson bay. The decay of the Ice Sheet from its maximum phase has been well documented. However, the information provided by cross cutting lineation patterns is able to provide refinements to the established history of decay. The Keewatin Ice Dome readjusted slightly during decay by shifting southeastwards. This seems to have been a result of the development of a major ice stream flowing to the northwest. [Ice divides migrate away from ice streams, as the latter attempt to enlarge their catchment basin]. In Labrador-Quebec the rising sea level during deglaciation produced marine drawdown of ice into Ungava Bay, destroying the major north-south ice divide and producing an enlarged Ungava catchment of ice with a new east-west divide.

This reconstruction shows a dramatically mobile ice sheet whose internal components, ice divides, have migrated 1000's of kilometres. The western margin of the Early Wisconsinan Ice Sheet appears to have receded some 3000 km. Even considering the time-scales involved, this ice sheet behaviour is far more dynamic than hitherto realised. Migration rates of ice divides are of the order of tens to hundreds of metres per year. In the light of published work on ice divide migrations on glaciers (Waddington and Marriott, 1986) these rates seem reasonable.

Estimating ice margin positions for each stage using lineation extent combined with published reconstructions (Andrews, 1987; Vincent and Prest, 1987) has allowed a tentative time-space envelope for the Laurentide Ice Sheet to be compiled. Two-dimensional and three-dimensional representations of this time-space envelope are

presented in figures 46 and 47. They do not attempt to illustrate exact movements in time and space, but are included to provide an easily visualised summary of the behaviour of the Ice Sheet as inferred from the new data presented in this thesis.

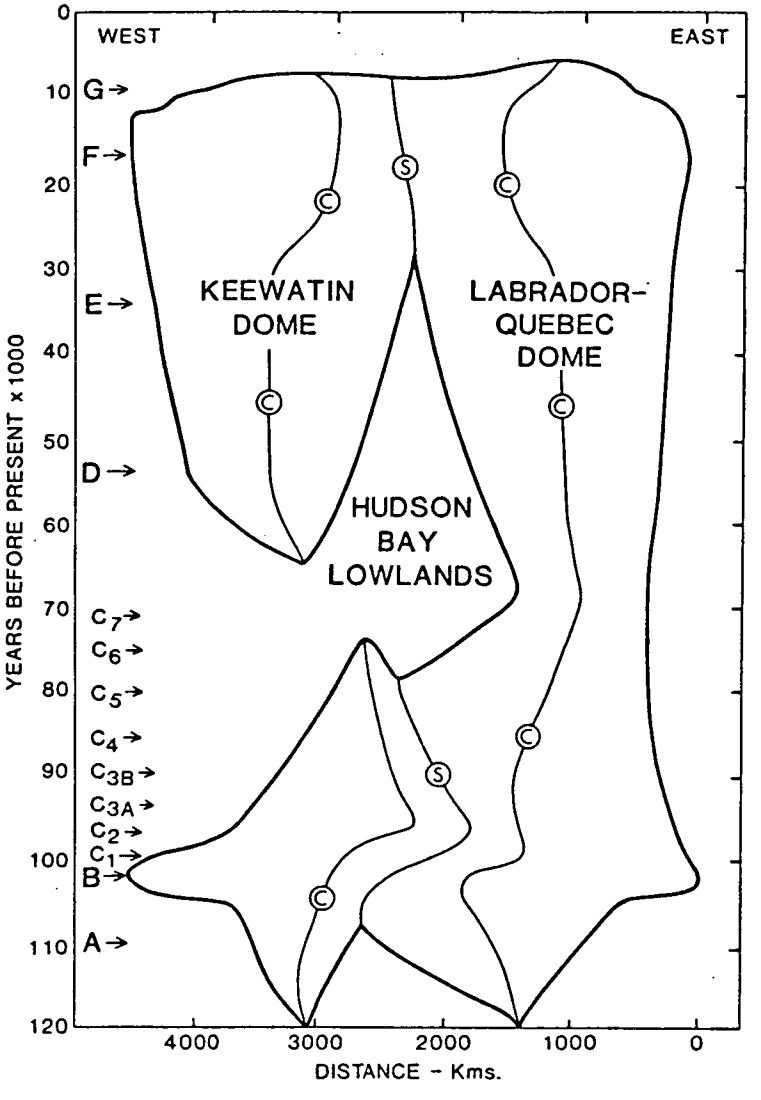

Figure 46 *Two-dimensional time-distance envelope for the Laurentide Ice Sheet along a transect from the East Labrador coast to the MacKenzie Delta area in the northwest. The Heavy line represents ice margins, and other lines mark ice culminations, or divides (C), and saddles (S). Reconstructed Flow Stages (A - G) are marked on the time scale.*

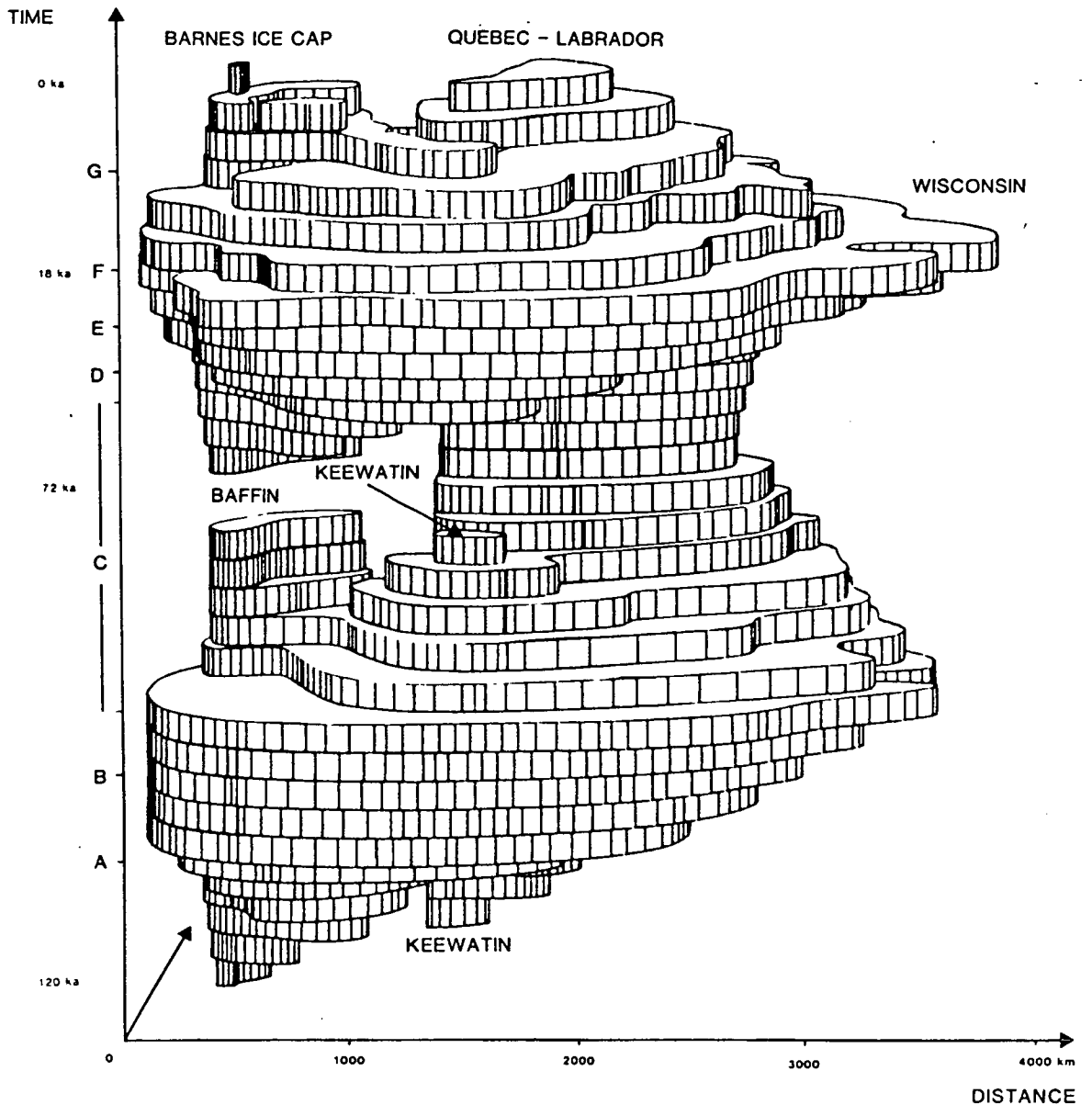

Figure 47 *Postulated three-dimensional time-space envelope for the Laurentide Ice Sheet through the last glacial cycle.*

Chapter 7

Discussion and Conclusions

Chapter 7

Discussion and Conclusions.

A brief history of the changing concepts of the Laurentide Ice Sheet is presented. It is argued, that the discovery that this ice sheet was highly mobile demands that a new paradigm for ice sheet behaviour be adopted. The implications of a mobile ice sheet for isostasy, global climate, sea level and the oceanic oxygen-isotope record are discussed. Overall conclusions are then summarised.

7.1 Historical Development of Models of the Laurentide Ice Sheet.

In an attempt to put the work presented in this thesis into perspective, I briefly document the historical development of the concept of the Laurentide Ice Sheet. This summary is partly drawn from the inspiring paper produced by Shilts (1982).

As is the case for most histories, they can be perceived as a series of steps or minor or major revolutions of thought. I subdivide the history of thought pertaining to the Laurentide Ice Sheet into a number of phases.

PHASE 1: Following the acceptance, in the mid-nineteenth century, of Quaternary continental glaciations, Joseph Tyrrell published a classic paper about the last North American Ice Sheet (Tyrrell, 1898). He suggested two main centres from which ice expanded: Keewatin and Labrador. Three periods of expansion were envisaged for the Keewatin Ice Sheet followed by major expansion of the Labrador Ice Sheet which

produced ice flow across the James Bay Lowlands to as far west as Lake Winnipeg. This conception of the idea of multiple centres of outflow within a Laurentide Ice Sheet held sway until the early 1940's when Flint (1943) published a paper that became a turning point in the development of ideas.

PHASE 2: In Flint's (1943) highly persuasive paper on the "Growth of the North American Ice Sheet during the Wisconsin" he used two arguments to revolutionise the concept of the Laurentide Ice Sheet. Comparison with the more thoroughly studied European Ice Sheet, which was widely regarded as having originated in the mountains of the west and expanded eastwards, and deductions about areas of potential glacierization based upon current climatic theory, formed the basis of his argument. Using these ideas he abandoned Tyrrell's concept of a Keewatin and Labrador Ice Sheet and proposed that the ice sheet initiated in the mountains of the Cordillera, followed by eastward expansion of ice cover, with the eventual stabilisation of an ice centre over Hudson Bay. Flint's synthesis of Laurentide Ice Sheet growth and configuration became widely accepted and was expanded upon in the succeeding decades. Results from the study of isostatic rebound (Walcott, 1972) appeared to support his model.

PHASE 3: This phase of historical development occurred over a period (1950's-1970's) in which the collection of geological information from fieldwork and the study of newly acquired air photographs, played the major role. It increasingly became apparent that most evidence (striae, drumlins, erratic travel, isostasy) indicated that two radial patterns of flow existed. In accommodating this to the influential single-dome model of Flint (1943), the twin-radial pattern was attributed to the very late stages of the Ice Sheet when it was thought to have split into two during final decay (e.g. Taylor, 1956; Bird, 1953; Lee, 1959; Hughes, 1964; Henderson, 1959).

In the 1970's however, two schools of thought simultaneously emerged; one utilised glaciological dynamics to produce mathematical models of the Ice Sheet, and the other formulated a reconstruction based on the latest fieldwork results. The mathematical models were inevitably founded upon a single Hudson Bay dome, stable for most of the Wisconsinan. However, the weight of new palaeo-ice flow evidence suggesting two radial flow patterns eventually swung the balance away from the single dome model. This school of thought was led by the publication of a paper entitled "Re-evaluation of the traditional concept of the Laurentide Ice Sheet" (Shilts *et al.* 1979) and a subsequent paper published in Nature (Shilts, 1980). It was argued that a stable Hudson Bay dome persisting for most of the Wisconsinan cannot be reconciled with the observed pattern of dispersal of distinctive Proterozoic and Palaeozoic erratics. Furthermore it was not just the pattern of dispersal, but the time taken to produce the pattern. The multi-dome decay phase of a Flint-type model was only thought to have existed for 1000-3000 years. This was not thought by Shilts *et al.* (1979) to be a long enough time interval to transport erratics over the hundreds of kilometres observed, and thus a model of a multi-domed ice sheet, that accounted for the erratic dispersal, was adopted.

Having tipped the balance in favour of ice domes positioned either side of Hudson Bay, this new model allowed the mass of field evidence to be interpreted with less contrivance. The pattern of erratic dispersal and the twin radial patterns of flow recorded by drumlins (Prest, 1969; Shilts, 1980, and figure 8) were assumed in this reconstruction to have formed at the maximum stage of the Late Wisconsinan Ice Sheet. Palaeoclimatic research on potential locations of glacierization had also changed viewpoint. The relative lowlands of Keewatin and Labrador were shown to be likely areas for ice sheet initiation (Williams, 1978) making initiation in the Cordillera an unnecessary step in the build-up of the Laurentide Ice Sheet.

The conceptual shift to a multi-domed Laurentide Ice Sheet persisting for a major part of the last glacial is of course a return to the ideas of Tyrrell (1898).

The "nail in the coffin" to the single-domed ice sheet model came when Andrews *et al.* (1983) published a paper citing evidence for multiple deglaciations of the Hudson Bay Lowlands during the last glacial. They found a series of dated marine sediments and tills, in a location that represents the geographical centre or core of the "conventional" single-dome ice sheet. Their stratigraphy allowed them to deduce that there were repeated marine incursions into Hudson Bay associated with phases of deglaciation. This is hard to reconcile with a large, stable, single-domed ice sheet, but is easily explained by Keewatin and Labrador Ice Sheets that were sometimes coalescent and sometimes not. Although these findings did not produce a major conceptual shift in the same way that the papers of Shilts did (single to multi-dome model), they are relevant in that they helped confirm the proposed multi-domed model, and more important, implied that the rate of change of mid-latitude ice sheets had been radically underestimated. In concluding that there had been multiple deglaciations and readvances, Andrews and co-workers (1983) showed that the Laurentide Ice Sheet was far more dynamic than previously thought.

Refinements to the multi-dome model are becoming prolific, and mathematical models incorporating two ice domes have already been presented (Boulton *et al.* 1985; Fisher *et al.* 1985).

The work presented in this thesis shows that a stable, single-domed or multi-domed ice sheet did not exist through the Wisconsinan. Ice domes and divides underwent major migrations of the order of 1000's of kilometres. The Ice Sheet is thus shown to be more dynamic than hitherto thought. Paradoxically, the increased dynamism implied by the

migrating ice divides, allows both the single and multi-dome models to be accommodated. Flow Stage C (Early Wisconsinan) has a large Hudson Bay dome and Stage F a multi-dome configuration.

7.2 Implications of a Mobile Ice Sheet.

Within the Earth and Atmospheric Sciences, systems of global-interaction must have been significantly affected by a mobile Laurentide Ice Sheet. The Ice Sheet acted as a heavy weight (depression of the lithosphere), a mirror (reflection of incoming solar energy), a large wind-deflector (perturbation of mid-latitude westerlies), and a reservoir of water (lowering global sea level). As the Ice Sheet underwent expansion, contraction and continental-scale migration, it must have had consequences on all of these.

7.2.1 Isostasy.

Isostatic depression and flexure of the lithosphere in the region of North America has occurred as a result of the loading of the mass of the Laurentide Ice Sheet. As described in the Introduction (Section 1.2.1) the mapping and dating of raised shorelines has enabled the subsequent recovery of the lithosphere to be recorded. The isobases that document this recovery only reflect average loading integrated over time. Isostatic depression of the lithosphere produces mass-balance feedback to the ice sheet because overall lowering results in a larger area being beneath the equilibrium line (snow-line), to which the ice sheet must respond. A highly mobile Laurentide Ice Sheet is likely to have migrated at rates faster than those of lithospheric response. It is thus likely that time-lags

inherent in the lithosphere-response and mass-balance feedback mechanisms will add to the complexity of the behaviour of the Ice Sheet.

7.2.2 Global Climate.

Although climatic cooling and moisture availability are the triggers for ice sheet initiation, an emergent and growing ice sheet can provide feedbacks capable of providing large changes to the climate system itself. A first effect of growing snow/ice cover is increased albedo, and thus a reduction of temperatures which acts as a strong positive feedback loop further promoting increased snow cover. As the height of the centre of mass of an ice sheet increases (up to 3 km in elevation for the Laurentide Ice Sheet according to Denton and Hughes, 1981) it becomes increasingly capable of perturbing the "normal" (interglacial) pattern of air flow. This can have considerable effects both locally and for thousands of kilometres downstream. The influence of the Laurentide Ice Sheet on northern hemispheric climate of the last glacial, has been investigated using a General Circulation Model (GCM) incorporating a coupled atmosphere-ocean, with a static ice sheet (Manabe and Broccoli, 1985; Broccoli and Manabe, 1987). The ice sheet component of their model was the single-domed ice sheet proposed by Denton and Hughes (1981). The GCM was run with and without the presence of the ice sheet to investigate its influence on northern hemispheric climate. The combined topographic and albedo effect was found to strongly influence the flow pattern and position of atmospheric planetary waves. The ice sheet split the "normal" (interglacial) tropospheric flow field (the mid-latitude westerlies) into two branches, with a strong jet stream forming the southern branch. Their model predicts major changes in the climate of the northern hemisphere as a result of the effect of the Laurentide Ice Sheet. This is

particularly the case for North America and the downwind North Atlantic region, where the northern branch of the tropospheric flow field transports very cold air over the North Atlantic ocean promoting the stabilisation of thick sea ice.

The mid-latitude ice sheets must therefore have been important modulators of climatic change during the Quaternary, and may thus help explain the non-linear response of climate to orbital forcing.

It is assumed that the reconstructed changes of ice sheet configuration and locations of centres of mass are a result of the strong coupling between ice sheets and atmospheric circulation. It is likely that as an ice sheet develops, its increasing influence on atmospheric flow may significantly alter the regional mosaic of accumulation and ablation, to which the ice sheet responds in turn. This mechanism is probably responsible for the major migrations of ice divides of the Laurentide Ice Sheet. It is interesting to note that the GCM of Manabe and Broccoli (1985) predicts the establishment of a strong anticyclone over the western portion (Keewatin sector) of the Laurentide Ice Sheet at its maximum configuration. Their modelled ice sheet component is static and cannot respond to mass balance changes. Although highly speculative, it is tempting to consider how the findings of Broccoli and Manabe (1985; 1987) may affect a developing Laurentide Ice Sheet. It is suggested that as the Laurentide Ice Sheet grew, it perturbed the planetary wave system producing an anticyclone over the Keewatin sector in such a manner as to force major changes upon its own mass balance. Anticyclones are high pressure systems of descending air and consequently precipitation is very low. Perhaps the establishment of such a system over Keewatin starved the western portion of the Ice Sheet of moisture, thus producing a negative mass balance in the west and positive in the

east. This could be the mechanism by which the Stage C (Early Wisconsinan) trans-Laurentide ice divide performed its major eastward shift.

7.2.3 Sea Level and Oxygen Isotope Record.

The Laurentide Ice Sheet at its maximum extent acted as a reservoir of water sufficient to lower global sea level by 40-55 metres (Fulton and Prest, 1987). The Ice Sheet can also be considered as a reservoir of the isotopically lighter O^{16} which has the effect of leaving the oceans enriched in the heavier O^{18}. This is recorded in ocean sediments. A highly mobile Laurentide Ice Sheet, and associated major fluctuations of mass throughout the Wisconsinan, must have produced large fluctuations of global sea level and the oxygen isotope record. If volume changes of the Laurentide Ice Sheet could be computed, it would provide a "metronome" to which other systems may have responded in sympathy. Global sea level, sea surface temperatures, pack-ice extent, other marine-influenced ice sheets, and the oxygen isotope record may be some of these systems.

7.2.4 A Tool for Continental Correlation.

The tempo and pattern of glacier advance and decay is traditionally reconstructed from stratigraphic evidence composed of till and other sediments, which are dated, and then correlated as evidence permits. This provides evidence for or against ice cover at specific points in time and space. However, for the Laurentide Ice Sheet, the number of sections containing such stratigraphic evidence are many fewer in number than would be required to adequately define the time-space envelope through a glacial cycle, even if ice divides

were stable, and advance and retreat rates were similar around the circumference of the Ice Sheet. With shifting ice divides, and non-synchronous growth and decay of different sectors of the Ice Sheet, the number of usable stratigraphic sections are orders of magnitude fewer than would be required to define the time-space envelope. This problem is accentuated by the location of many of the best sections on the periphery of the Ice Sheet.

However, in a manner that is analogous to the use of seismic reflectors for cross-correlations of core sequences in ocean sediments, the use of satellite images to map flow sets can enable us to correlate widely-spaced stratigraphic sections. A foray into this technique was explored in Chapter 6, permitting the elucidation of a tentative time-space envelope for ice sheet evolution. It is expected that the use of continent-wide flow sets may become an important means by which our sparse knowledge of stratigraphy may be utilised to its maximum potential.

7.3 Conclusions:

1) Satellite images reveal a hitherto undiscovered and previously unsuspected pattern of glacial streamlining that is assumed to record palaeo-ice flow.

2) Contrary to established beliefs, the last major events of ice flow did not eradicate all prior evidence. Satellite imagery allows widespread patterns of cross-cutting flow sets to be discerned. These represent different phases of ice flow at different times.

3) The nature of the cross-cutting relationships permit relative ages of flow phases to be determined.

4) The glacial lineation patterns were mapped for most of mainland Canada using six scales of remotely sensed imagery. A digitised database of palaeo-ice flow resulted.

5) Stratigraphic sections containing units of till, for which the direction of ice flow is known, and that have also been dated were sought from the published literature. These provide azimuth-age indicators of ice flow, but only for each, often isolated, location. By a means analogous to the use of seismic reflectors to correlate between widely-spaced cores in ocean sediments, the continent-wide pattern of flow-sets were combined with the stratigraphic data, integrating the sparse azimuth-age indicators into a framework of palaeo-ice flow. From this it appears that the majority of mapped ice flow sets date from the last glacial (Wisconsinan).

6) The decay stages of the Laurentide Ice Sheet are already well known. However, using the mapped continent-wide flow patterns it has been possible to reconstruct the evolution of the Laurentide Ice Sheet prior to its maximum extent. For this Early and Middle Wisconsinan time very little was known about the behaviour of the Laurentide Ice Sheet. It appears that ice sheet initiation occurred in northern Baffin Island, or northeast Keewatin, probably concurrently with ice expansion in Labrador-Quebec. The centre of mass of the emergent Keewatin Ice Sheet migrated 400 km to the southwest. Ice cover at this time extended as far south as northern Manitoba and Saskatchewan. It is likely that an autonomous ice sheet also existed to the east of Hudson Bay. Expansion of these two ice sheets eventually produced a coalescent mass in which a major NW-SE trans-

Laurentide ice divide developed across Hudson Bay. This phase represents the major ice sheet of the Early Wisconsinan. During the warmer, Middle Wisconsinan, this major ice divide underwent considerable eastward migration, resulting in the probable deglaciation of Keewatin. A residual ice mass probably survived this phase in Labrador-Quebec. Subsequent Late Wisconsinan intensification of global cooling produced re-initiation of ice in Keewatin. Unlike the early Wisconsinan Ice Sheet however, this Late Wisconsinan phase culminated as two independent domes with an ice saddle or zone of coalescence over Hudson bay. The decay of the Ice Sheet from this maximum stage is already well known, although some new evidence indicates minor adjustments of configuration occurred during decay.

7) The reconstructed evolution of the Laurentide Ice Sheet reveals that its behaviour was far more dynamic than the presumed long-term behaviour of modern ice sheets and previous views of Quaternary mid-latitude ice sheets.

8) It is proposed that this dynamism of Laurentide Ice Sheet behaviour is intimately linked and partly a result of the interaction with global-scale atmospheric flow. The corollary implies that mid-latitude ice sheets were major modulators of the progression of a glacial climate, and may thus help explain the non-linear response of climate to orbital forcing.

Bibliography

ANDREWS, J.T., 1970, A geomorphological study of post-glacial uplift with particular reference to Arctic Canada. Special Publication, Institute of British geographers, No 2, 156pp.

ANDREWS, J.T., 1982, On the reconstruction of Pleistocene ice sheets; a review. Quaternary Science Reviews, 1, 1-30.

ANDREWS, J.T., 1987, The Late Wisconsin Glaciation and deglaciation of the Laurentide Ice Sheet, in Ruddiman, W.F. & Wright, H.E. Jr, (eds) North America and adjacent oceans during the last deglaciation: Boulder Colorado, Geological Society of America, The geology of North America, v K-3, 13-37.

ANDREWS, J.T., SHILTS, W.W. & MILLER, G., 1983, Multiple deglaciations of the Hudson Bay Lowlands, Canada, since the deposition of the Missinaibi (last interglacial?) Formation. Quaternary Research 19, 18-37.

BIRCHFIELD, G.E. & WEERTMAN, J., 1983, Topography, albedo-temperature feedback, and climate sensitivity. Science, 219:284-285.

BIRD, J.B., 1953, The glaciation of central Keewatin, NWT, Canada. American Journal of Science, 251, 215-230.

BOLIN, B., 1950, On the influence of the Earth's orography on the general character of the westerlies. Tellus, 2 184-195.

BONIFAY, D. & PIPER, D.J.W., 1988, Probable Late Wisconsinan ice margin on the upper continental slope off St. Pierre Bank, eastern Canada. Can. J. Earth Sci, 25, 853-865.

BOUCHARD, M.A. & MARCOTTE, C., 1986, Regional glacial dispersal patterns in Ungava, Nouveau-Quebec, In Current Research, Part B, Geological Survey of Canada, Paper 86-1B, 295-304.

BOUCHARD, M.A. & SALONEN, V.P., 1989, Glacial dispersal of boulders in the James Bay Lowlands of Quebec, Canada. Boreas, 18, 189-199.

BOULTON, G.S., 1971, Till genesis and fabric in Svalbard, Spitsbergen. In R.P. Goldthwaite (ed) Till; a symposium. Ohio State University Press, 47-72.

BOULTON, G.S., 1976, Origin of glacially fluted surfaces. J. Glaciol, 17, 287-301.

BOULTON, G.S., 1979, A model of Weichselian glacier variation in the North Atlantic region. Boreas, 8, 373-395.

BOULTON, G.S., 1982, Subglacial processes and the development of glacial bedforms. In Research in glacial, glacio-fluvial and glacio-lacustrine systems. sixth Guelph symposium on geomorphology 1980 (Geobooks, Norwich, 1982).

BOULTON, G.S., 1987, A theory of drumlin formation by subglacial sediment deformation. In Drumlin symposium (eds) Menzies, J. & Rose, J. Balkeema, Rotterdam / Boston, 360pp.

BOULTON, G.S., SMITH, G.D., JONES, A.S. & NEWSOME, J., 1985, Glacial geology and glaciology of the last mid-latitude ice sheets. J. Geol. Soc. London, 142, 447-474.

BOULTON, G.S., HORSFIELD, B.R., CLARK, C.D. & NEWSOME, J., 1987, Large scale glacial geology and geomorphology of Canada and their implications for the history of the Laurentide Ice Sheet. XXII INQUA '87 abstracts, p135.

BOULTON G.S. & CLARK C.D., 1990, A highly mobile Laurentide Ice Sheet revealed by satellite images of glacial lineations. Nature, *In press*.

BOULTON G.S. & CLARK C.D., 1990, The Laurentide Ice Sheet through the last glacial cycle: drift lineations as a key to the dynamic behaviour of former ice sheets. Trans. Roy. Soc. Edin: Earth Sciences, 81: *In press*.

BROCCOLI, A.J. & MANABE, S., 1987, The effects of the Laurentide Ice Sheet on North American climate during the last glacial maximum. Geographie physique et Quaternaire 1987 XLI no.2, 291-299.

BRYSON, A.R., WENDLAND, W.M., IVES, J.D. & ANDREWS, J.T., 1969, Radiocarbon isochrones on the disintegration of the Laurentide Ice Sheet. Arctic and Alpine research, 1, 1-14..

CHARNEY, J.G. & ELIASSEN, A., 1949, A numerical method for predicting the perturbations of mid-latitude westerlies. Tellus 1, 38-54.

CLARK, C.D. & BOULTON, G.S., 1989, Geomorphic patterns produced by the last Canadian Ice Sheet; matching the scales of remote sensing with the frequency of natural variation. Proceedings IGARSS '89 symposium, Vancouver, Canada, vol 1, 97-100.

CLARK, C.D., 1990, Remote sensing scales related to the frequency of natural variation; an example from palaeo-ice flow in Canada. IEEE Transactions on Geoscience and Remote Sensing, 28, *In press*.

CLARK, J.A., 1980, The reconstruction of the Laurentide Ice Sheet of North America from sea level data: method and primary results. Journal of Geophysical Research, 85, 4307-4323.

CLAYTON, L. & MORAN, S.R., 1982, Chronology of Late Wisconsinan glaciation in middle North America. Quaternary Science Reviews, 1, 55-82.

CUNNINGHAM, C.M. & SHILTS, W.W., 1977, Surficial geology of Baker Lake area. Geological Survey of Canada, Paper 77-1B, 311-314.

DARDIS, G.F. & McCABE, A.M., 1983, Facies of subglacial channel sedimentation in late Pleistocene drumlins, Northern Ireland. Boreas, 12, 263-278.

DEMOREST, M., 1938, Ice flowage as revealed by glacial striae. J. Geol 46, 700-725.

DENTON,G.H. & HUGHES, T.J., 1981, The last great ice sheets. John Wiley and Sons, New York.

DILABIO, R.N.W., MILLER, R.F., MOTT, R.J. & COKER, W.B., 1988, The Quaternary stratigraphy of the Timmins area, Ontario, as an aid to mineral exploration by drift prospecting. Geological Survey of Canada, Paper 88-1C, 61-65.

DREDGE, L.A. & NIELSEN, E., 1985, Glacial and interglacial deposits in the Hudson Bay Lowlands; a summary of sites in Manitoba. Geological Survey of Canada, current research part A: paper 85-1A..

DREDGE, L.A., & THORLEIFSON, L.H., 1987, The Middle Wisconsinan history of the Laurentide Ice Sheet. Geographie Physique et Quaternaire, XLI, No.2, 215-235.

DREDGE, L.A., 1988, Drift carbonate on the Canadian Shield. II: carbonate dispersal and ice flow patterns in northern Manitoba. Can. J. Earth Sci., 25, 783-787.

DREWRY, D.J., 1982, Antarctica unveiled, New Scientist, 244-251.

DYKE, A.S. & PREST, V.K., 1987, Late Wisconsinan and Holocene history of the Laurentide Ice Sheet. Geographie physique et Quaternaire, 1987 XLI no2, 237-263.

FAIRCHILD, H.L., 1907, Drumlins of central western New York. New York State Mus. Bull 111; 391-443.

FASTOOK, J.L., 1984, West Antarctica, the sea level controlled marine instability; past and future. In Hansen, J.E. & Takahashi, T. (eds)- Climate processes and climate sensitivity. Washington D.C. Amer. geophys. Union, 265-274, Geophysical monograph 29.

FISHER, D.A., REEH, N. & LANGLEY, K., 1985, Objective reconstructions of the Late Wisconsinan Laurentide Ice Sheet and the significance of deformable beds. Geographie Physique et Quaternaire, 38: 229-238.

FLINT, R.F., 1943, Growth of the North American Ice Sheet during the Wisconsin age. Bull. Geol. Soc. Amer. 54:325-362.

FLINT, R.F., 1971, Glacial and Quaternary Geology. Wiley, New York, 892pp.

FULLERTON, D.S. & COLTON, R.B., 1986, Stratigraphy and correlation of the glacial deposits of the Montana Plains. Quaternary Science Reviews, 5, No 1-4, 69-82.

FULTON, R.J., 1986, Quaternary stratigraphy of Canada. Quaternary Science Reviews, 5, No 1-4, 207-209.

FULTON, R.J. & PREST, V.K., 1987, The Laurentide Ice Sheet and its significance. Geographie physique et Quaternaire, 1987, XLI No2, 181-186.

FULTON, R.J., FENTON, M.M. & RUTTER, N.W., 1986, Summary of Quaternary stratigraphy and history, western Canada. Quat. Sci. Reviews, 5, 229-241.

GINGERICH, P.D., 1969, Markov analysis of cyclic alluvial sediments. J. Sed. Pet. 39, 330-332.

GLEN , J.W., DONNER, J.J. & WEST, R.G., 1957, On the mechanism by which stones in till become oriented. Amer. J. Sci. 255, 194-205.

GRANT, D.R., 1977, Glacial style and ice limits, the Quaternary stratigraphic record of land and ocean level in the Atlantic provinces, Canada. Geographie physique et Quaternaire, 31, 247-260.

HALL, D.K & ORMSBY, J.P., 1983, Use of Seasat SAR and Landsat MSS subsystem data for Alaskan glaciology studies. Journal of Geophysical Research, 88, 1597-1607.

HARDY, L., 1982, Le Wisconsinein Superieur a 1 est de la Baie James (Quebec). Naturaliste Can. (rev. Ecol. Syst.) 109, 331-351.

HENDERSON, E.P., 1959, A glacial study of central Labrador. Bull. geol. Surv. Canada, 50, 94pp.

HOLMES, C.D., 1941, Till fabric. Bull. Geol. Soc. Amer., 52, 1299-1354.

HOOKE, R de B., 1976, Pleistocene ice at the base of the Barnes Ice Cap, Baffin Island, NWT, Canada. J. Glaciol., 17, 49-59.

HUGHES, O.L., 1964, Surficial geology, Nichicun-Kaniapiska map area, Quebec. Bull. geol. Surv. Canada, 106, 20pp.

JOHNSTON, A.C., CRACKNELL, A.P., VAUGHAN, R.A., BOULTON, G.S., & CLARK, C.D., 1989, Identification of ancient glacier marks using AVHRR imagery. Int. J. Remote Sensing, 10, Nos. 4 & 5, 917-929.

JONES, G.A. & KEIGWIN, L.D., 1988, Evidence from Fram Strait (78^{o}N) for early deglaciation. Nature, 336, 56-59.

KALUSH, R.J., 1979, The problem of resolution in the Landsat imagery. Remote Sensing Quarterly, 1, 38-48.

KING, L.H., & FADER, G.B.J., 1986, Wisconsinan glaciation of the Atlantic continental shelf of S.E. Canada. Geol. Surv. of Canada Bull. 363, 72pp.

KLASSEN, K.G. & THOMPSON, F.J., 1987, Ice flow history and glacial dispersal in the Labrador Trough. Current Research, Part A, Geological Survey of Canada, 61-71.

KLASSEN, K.G. & THOMPSON, F.J., 1989, Ice flow history and glacial dispersal patterns, Labrador. In Drift Prospecting, DiLabio, R.N.W & Coker, W.B, (eds), Geological Survey of Canada, Paper 89-20, 21-29.

KUTZBACH, J.E. & WRIGHT, H.E. (Jr), 1985, Simulation of the climate of 18,000 years before present; results from the N. American/N. Atlantic/European sector, and comparison with the geologic record of North America. Quaternary Science Reviews, 4, 147-188.

LEE, H.A., 1959, Surficial geology of southern District of Keewatin and the Keewatin Ice Divide, Northwest Territories. Bulletin Geological Survey of Canada, 51, 42pp

LYDON, J., 1987, There are no easy answers, to elongated questions, so try and keep an eye out, and be open to suggestion. In Open and Revolving; Happy?, Virgin Records, London.

MacCLINTOCK, P., & DREIMANIS, A., 1964, Reorientation of till fabric by overriding glacier in the St. Lawrence Valley. Amer. J. Science, 262, 133-142.

MANABE, S. & BROCCOLI, A.J., 1985, The influence of continental ice sheets on the climate of an ice age. Journal Geophysical Research, V90D, 2167-2190.

MENZIES, J. & ROSE, J., 1987, Drumlin symposium. Menzies, J. and Rose, J. (eds), 1987, Balkeema.

MILLER, H., 1884, On boulder glaciation. Proc. R. Phys. Soc. Edinburgh, 8, 156-189.

MORGAN, A.V. & MORGAN, A., 1980, Faunal assemblages and distributional shifts of Coleoptera during the Late Pleistocene in Canada and the northern US. Canadian Entomologist, 112, 1105-1128

MUSZYNSKI, I. & BIRCHFIELD, G.E., 1987, A coupled marine ice stream - ice shelf model. J. Glaciol., 33, No.113, 3-15.

NAKADA, M. & LAMBECK, K., 1988, The melting history of the Late Pleistocene Antarctic Ice Sheet. Nature, 333, 36-40.

NELSON, A.R., 1981, Quaternary and marine stratigraphy of the Qivitu Peninsula, northern Cumberland Peninsula, Baffin Island: summary. Geological Society of America, Bulletin 92(I), 512-518, 92(II), 1143-1261.

NEWSOME, J.W., 1986, The Late Wisconsinan Ice Sheet complex. Unpublished PhD. thesis, University of East Anglia.

OERLEMANS, J, & VEEN, C.J. VAN DER, 1984, Ice sheets and climate, D.Reidel, Dordrecht, Holland, 217pp

PEACH, A.M., 1909, Boulder distribution from Lennoxtown, Scotland. Geol. Mag. 46, 26-31.

PELTIER, W.R., 1981, Ice age geodynamics. Annual review of Earth and Planetary Sciences. 9, 199-226.

PELTIER, W.R., FARRELL, W.E. & CLARK, J.A., 1978, Glacial isostasy and relative sea level; a global finite element model. Tectonophysics, 50. 81-110.

PIPER, D.J.W, 1988, Glaciomarine sedimentation on the continental slope off eastern Canada. Geoscience, Canada, 15, 23-28

POWERS, D.W. & EASTERLING, R.G., 1982, Improved method for using embeded Markov chains to describe cyclical sediments. J. Sed. Pet, 52, No.3, 913-923.

PREST, V.K., 1969, Retreat of Wisconsin and recent ice in North America. Geol. Surv. of Canada. Map 1257A, scale 1:5,000,000.

PREST, V.K., 1984, The Late Wisconsinan glacier complex. In Fulton, R.J. (ed) Quaternary stratigraphy of Canada; A Canadian contribution to IGCP project 24; Geol. Surv. of Canada paper 84-10, 21-36.

PREST, V.K., GRANT, D.R. & RAMPTON, V.N., 1968, Glacial map of Canada. Geol. Surv. of Canada. Map 1253A, scale 1:5,000,000.

RAMPTON, V.N., 1982, Quaternary geology of the Yukon coastal plain. Geol. Surv. of Canada Bull. 317, 49pp.

ROSE, J., 1989, Glacier stress patterns and sediment transfer associated with the formation of superimposed flutes. Sedimentary Geology, 62, 151-176.

RUDDIMAN, W.E. & McINTYRE, A., 1981, The mode and mechanism of the last deglaciation. Quaternary Research, 16, 125-134.

RUDDIMAN, W.E. & RAYMO, M.E., 1988, Northern hemisphere climate regimes during the past 3 Ma; possible tectonic connections. Phil. Trans. R. Soc. London. B 318, 411-430.

SALONEN, V.P., 1986, Glacial transport distance distributions of surface boulders in Finland. Geol. Surv. of Finland, Bull. 338, 57pp.

SAUSSURE, H.B.-de, 1779-96, Voyages dans les Alpes, precedes d'un essai sur l'histoire naturelle des environs de Geneve. 4 vols. Neuchatel, S. Fauche.

SHACKLETON, N.J. & OPDYKE, N.D., 1973, Oxygen isotope and palaeomagnetic stratigraphy of equatorial Pacific core V28-238; oxygen isotope temperatures and ice volumes on a 10^5 year and 10^6 year scale. Quaternary Research, 3, 39-55.

SHARPE, D.R., 1985, The stratified nature of deposits in streamlined glacial landforms on southern Victoria Island, District of Franklin. In Current Research part A Geological Survey of Canada paper 85-1A, 365-371.

SHAW, J., 1980, Drumlins and large scale flutings related to glacier folds. Arctic and Alpine Research, 12 (3), 287-298.

SHAW, J., 1983, Drumlin formation related to inverted melt-water erosional marks. J. Glaciol. 29, 461-474.

SHILTS, W.W., 1980, Flow patterns in the central North American Ice Sheet. Nature, 286, 213-218.

SHILTS, W.W., 1982, Quaternary evolution of the Hudson/James Bay region. Naturaliste Can. (Rev. Ecol. Syst.) 109: 309-332.

SHILTS, W.W., 1984, Quaternary events - Hudson Bay Lowlands and southern district of Keewatin. In Fulton, R.J. (ed), Quaternary Stratigraphy of Canada - A Canadian contribution to IGCP project 24, Geological Survey of Canada, Paper 84-10.

SHILTS, W.W., CUNNINGHAM, C.M. & KASZYSKI, C.A., 1979, Keewatin Ice Sheet - re-evaluation of the traditional concept of the Laurentide Ice Sheet. Geology, 7, 537-541.

SHILTS, W.W., AYLSWORTH, J.M., KASZYSKI, C.I. & KLASSEN, R.A. 1987, Canadian Shield, In Graf, W.L., (ed) Geomorphic systems of North America, Boulder Colorado, Geological Society of America, Centennial Special Volume 2, 119-161

SKINNER, R.G., 1973, Quaternary stratigraphy of the Moose River Basin, Ontario. Geological Survey of Canada, Bulletin, 225, 77pp

SMALLEY, I.J. & UNWIN, D.J., 1968, Formation and shape of drumlins and their orientation and distribution. J. Glaciol. 7 (51), 377-480.

STALKER, A.M., 1977, The probable extent of classical Wisconsinan ice in southern and central Alberta. Can. J. Earth Sci., 14, 2614-2619.

STEA, R.R., TURNER, R.G., FINCK, P.W. & GRAVES, R.M, 1989, Glacial dispersal in Nova Scotia: a zonal concept. In Drift Prospecting, DiLabio, R.N.W & Coker, W.B, (eds), Geological Survey of Canada, Paper 89-20, 155-169

STEELE, K.G., BAKER, C.L. & McCLENAGHAN, M.B., 1989, Models of glacial stratigraphy determined from drill core, Matheson area, northeastern Ontario. In Drift Prospecting, DiLabio, R.N.W & Coker, W.B, (eds), Geological Survey of Canada, Paper 89-20, 127-138.

STROMBERG, B., 1972, Glacial striae in southern Hinlopenstrelet and Kong Karls Land, Svalbard. Geogr. Annlr. 54A, 53-65.

SUGDEN, D.E., 1977, Reconstruction of the morphology, dynamics and thermal characteristics of the Laurentide Ice Sheet at its maximum. Arctic and Alpine Research. 9 (1), 21-47.

TAYLOR, R.S., 1956, Glacial geology of north-central Keewatin, NWT, Canada. Geological Society of America Bulletin, 67, 943-956.

TYRRELL, J.B., 1898, The glaciation of north-central Canada. Journal of Geology, 6, 147-160.

VEILLETTE, J.J., 1983, Les polis glaciares au Temiscamingue: une chronologie relative. Geological Survey of Canada, Paper 83-1A, 87-196.

VEILLETTE, J.J., 1986, Formerly southwesterly ice flows in the Abitibi - Timiskaming region (Quebec/Ontario); implications for the configuration of the Late Wisconsinan Ice Sheet. Can. J. Earth Sci. 23(11), 1724-1742.

VEILLETTE, J.J., 1989, Ice movements, till sheets and glacial transport in Abitibi-Timiskaming, Quebec and Ontario. In Drift Prospecting, DiLabio, R.N.W & Coker, W.B, (eds), Geological Survey of Canada, Paper 89-20, 139-154.

VINCENT, J.T., 1983, La geologie du Quaternaire et la geomorphologie de l' ile Banks, Arctique Canadieu. Commission Geologique du Canada, Memoire, 45, 118pp.

VIRKKALA, K., 1960, On the striations and glacier movements in the Tampere region, southern Finland. Bull. Commm. Geol; Finland. 188, 159-176.

VORREN, T.O., 1977, Weichselian ice movement in south Norway and adjacent areas. Boreas, 6, 247-257.

WADDINGTON, E.D. & MARRIOTT, R.T., 1986, Ice divide migration at Blue Glacier, USA. Annals of Glaciology, 8, 175-176.

WALCOTT, R.I., 1972, Late Quaternary vertical movements in eastern North America: quantitative evidence of glacio-isostatic rebound. Rev. Geophys. Space Phys. 10:849-884.

WILLIAMS, L.D., 1978, Ice sheet initiation and climatic influences of expanded snow cover in Arctic Canada. Quaternary Research, 10, 141-149.

WILLIAMS, L.D., 1979, An energy balance model of potential glacierization of northern Canada. Arctic and Alpine Research, 11, No.4, 443-450.

ADDENDUM:

FAIRBRIDGE, R.W., 1968, Indicator boulders. In, Fairbridge, R.W., (ed), Encyclopedia of geomorphology, Reinhold, New York, 550 - 552.

HUGHES, T.J., DENTON, G.H., ANDERSON, G.B., SCHILLING, D.H., FASTOOK, J.L., & LINGLE, C.S., 1981, The last great ice sheets: a global view., In Denton, G.H., & Hughes, T.J., (eds), The last great ice sheets. Wiley and sons, New York, 263-317.

Acknowledgements

Acknowledgements

My gratitude must first extend to Professor Geoffrey Boulton for initiating the project and waiting for me whilst I was late in arriving. I am also grateful for his support, even if it was always a challenge to get to see him! He was especially helpful in transforming my writing to something approaching the English Language.

Dr. Brian Horsefield is gratefully acknowledged for his advice and encouragement in the very early stages of this project. I had many enlightening discussions, sometimes related to my work, with Dr. Richard Hindmarsh. He taught me a great deal about ice sheets on "Planet Vulcan" for which I am very grateful.

I would like to thank Dr. Cliff Ford for his management of the computing facilities and related problem solving, without which the results of this thesis would have been even more mind-boggingly excruciating to produce. I also thank my father for the loan of a personal computer, which allowed me to "word-process" at home to the accompaniment of music, which made it feel less like work.

Apart from expecting postgraduates to carry out research without using up any materials, except oxygen, the support team within the Grant Institute of Geology has been excellent, for which I am grateful. Especial thanks to Dave Preistley, for only sighing quietly when I needed computer tapes etc; Diana Baty, for carto- and photographic advice and help in an always cheerful manner; and Yvonne Cooper for photography (especially the photo of my beloved van).

The Geo-secs, Denise, Heather, and Helena have always been bright and cheerful, for this I am very grateful, it really makes a difference.

Postgraduate colleagues, too numerous to mention, have as always played a part in helping and hindering the production of this thesis. Jon Bull, Ned Pegler and Andy Poole kindly proof-read various chapters.

Escapism has been essential, and so I am extremely grateful to the like-minded colleagues of our white-water hit-squad. The rivers of Scotland provided us with many trips of unadulterated whitewater terror, without which it would have been impossible to face digitising glacial lineations.

Finally, I would like to acknowledge my parents who quite remarkably have always believed in me, even if they haven't always believed me! I could not have asked for better support and encouragement. Thanks are also due to my Grandmother who provided funds with which I bought my van. I feel the power of motor vehicles is often underestimated: apart from getting me from home to work, my van has provided an immense feeling of freedom, not to mention excitement and adrenalin.

Appendix

Interpreted flow lines for each NTS quadrant.

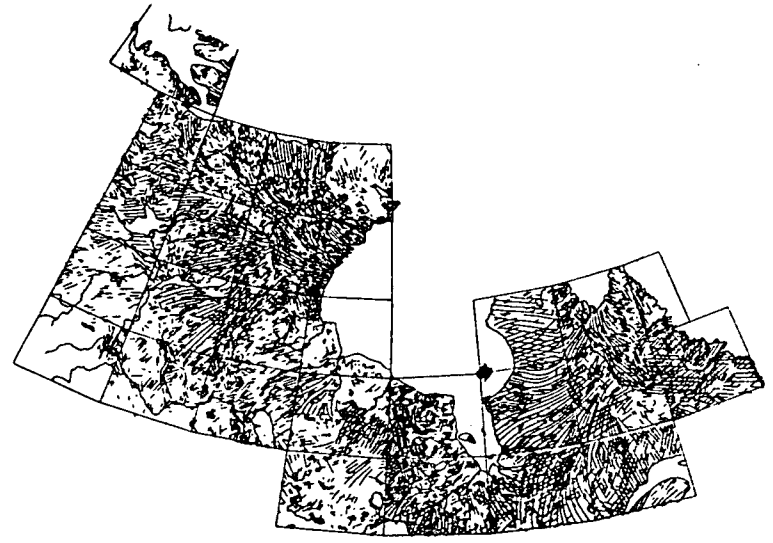

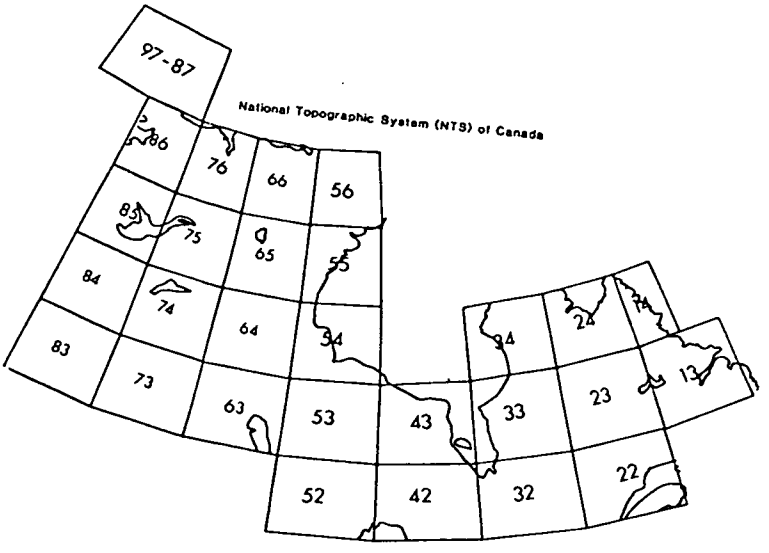

NTS 13

kilometres
0 20 40 60 80 100

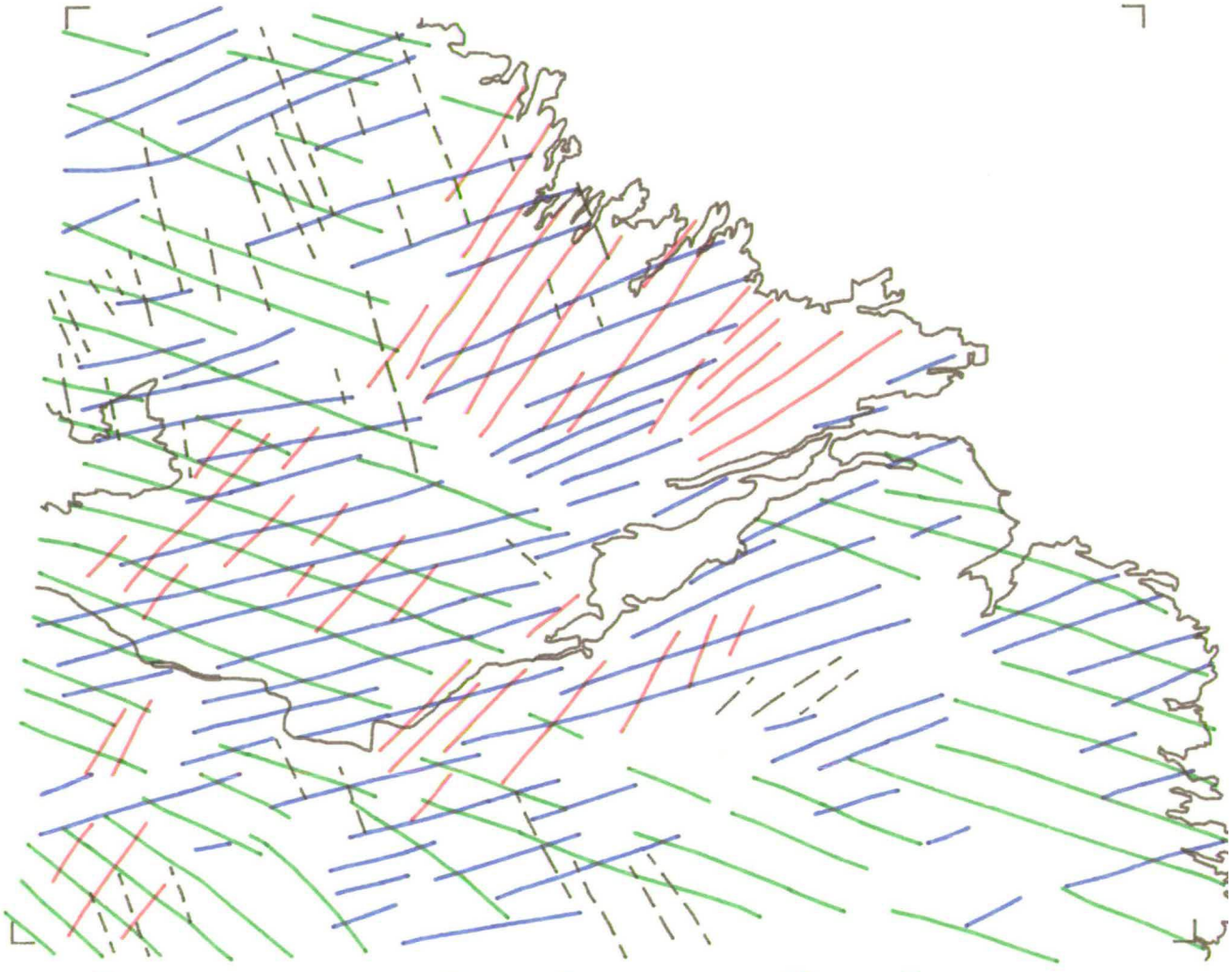

Flow 1 Flow 2 Flow 3

NTS 14

Flow 1 Flow 2 Flow 3

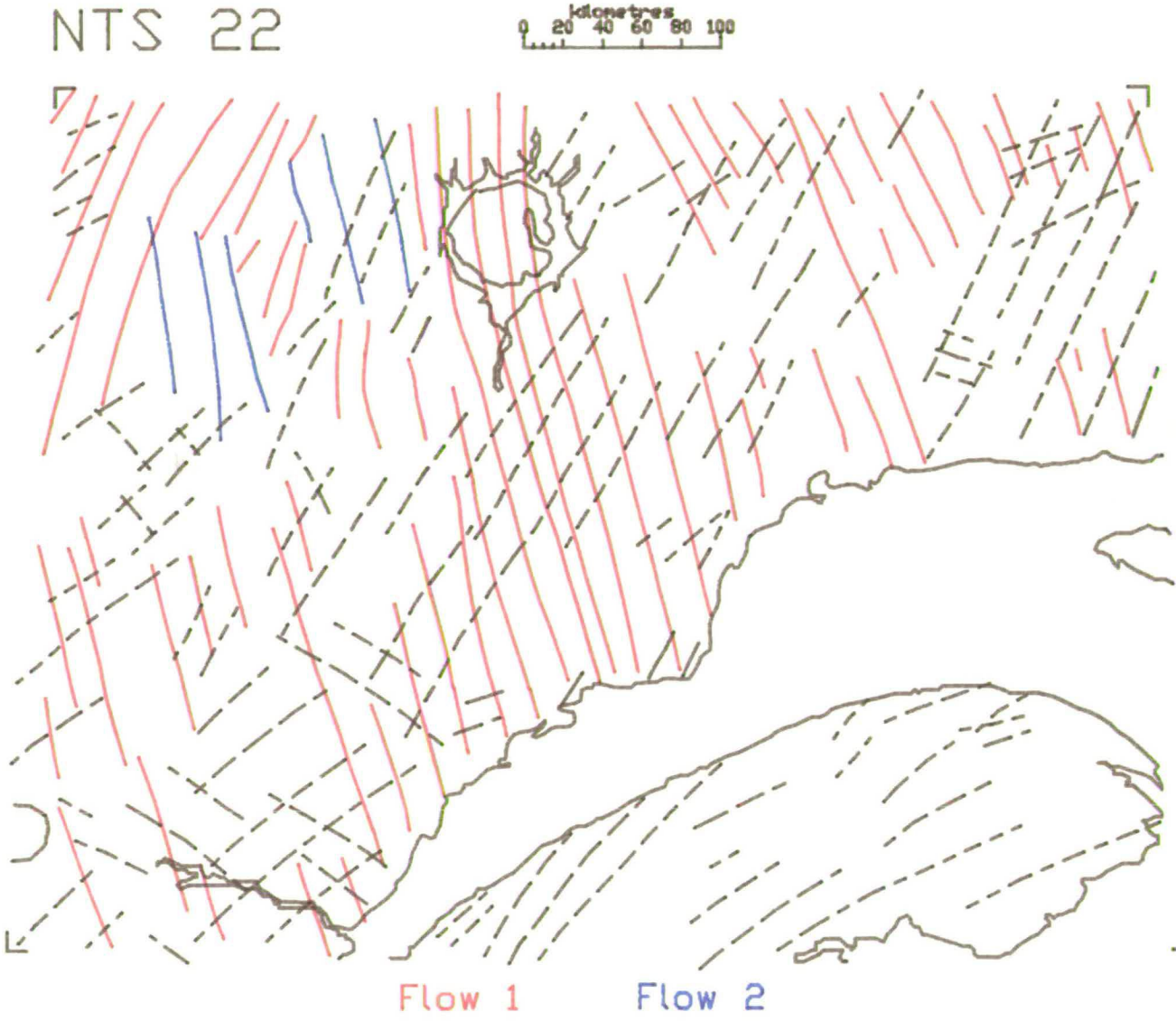
NTS 22
kilometres
0 20 40 60 80 100
Flow 1
Flow 2

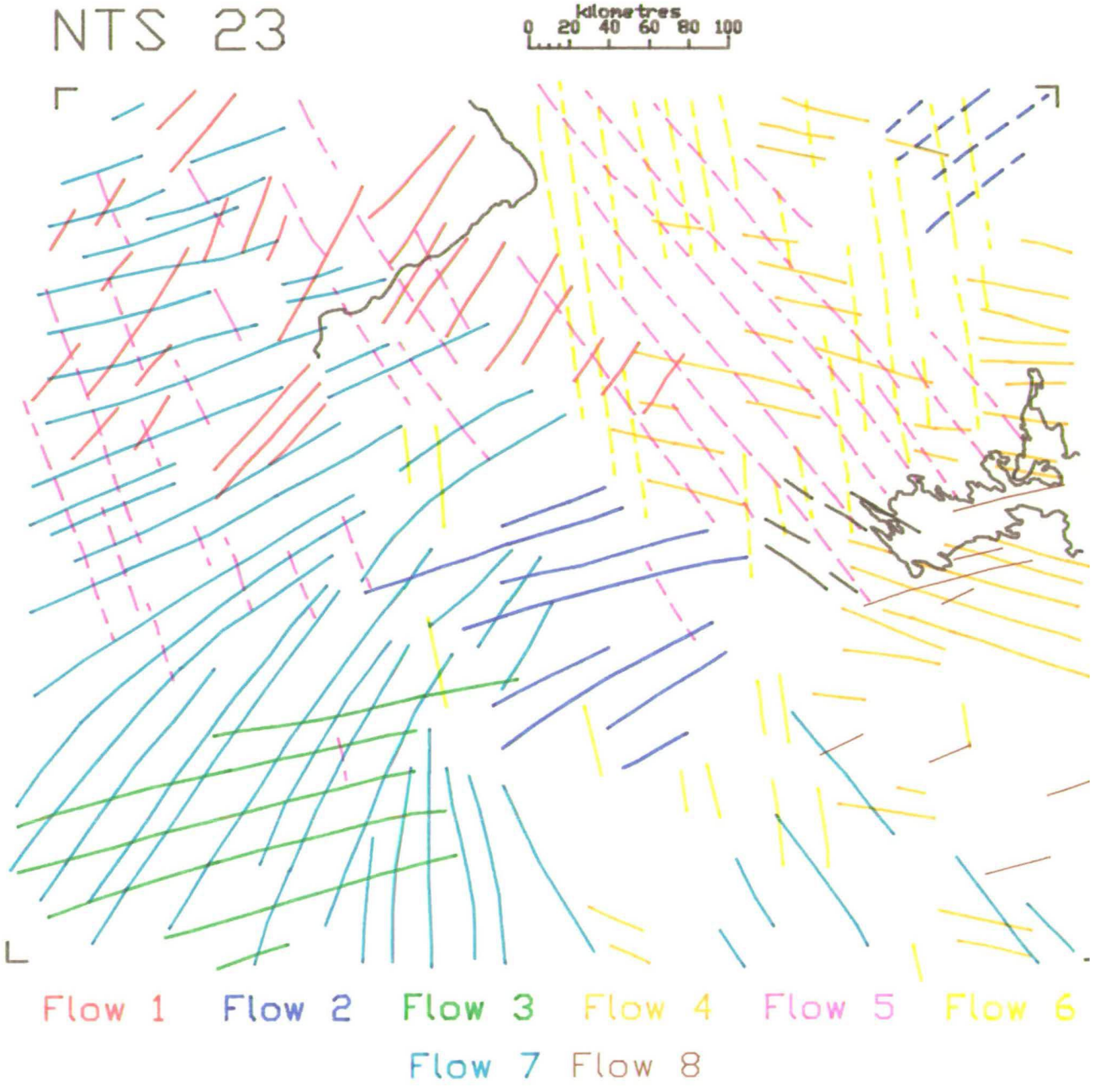
NTS 23
kilometres
0 20 40 60 80 100
Flow 1
Flow 2
Flow 3
Flow 4
Flow 5
Flow 6
Flow 7
Flow 8

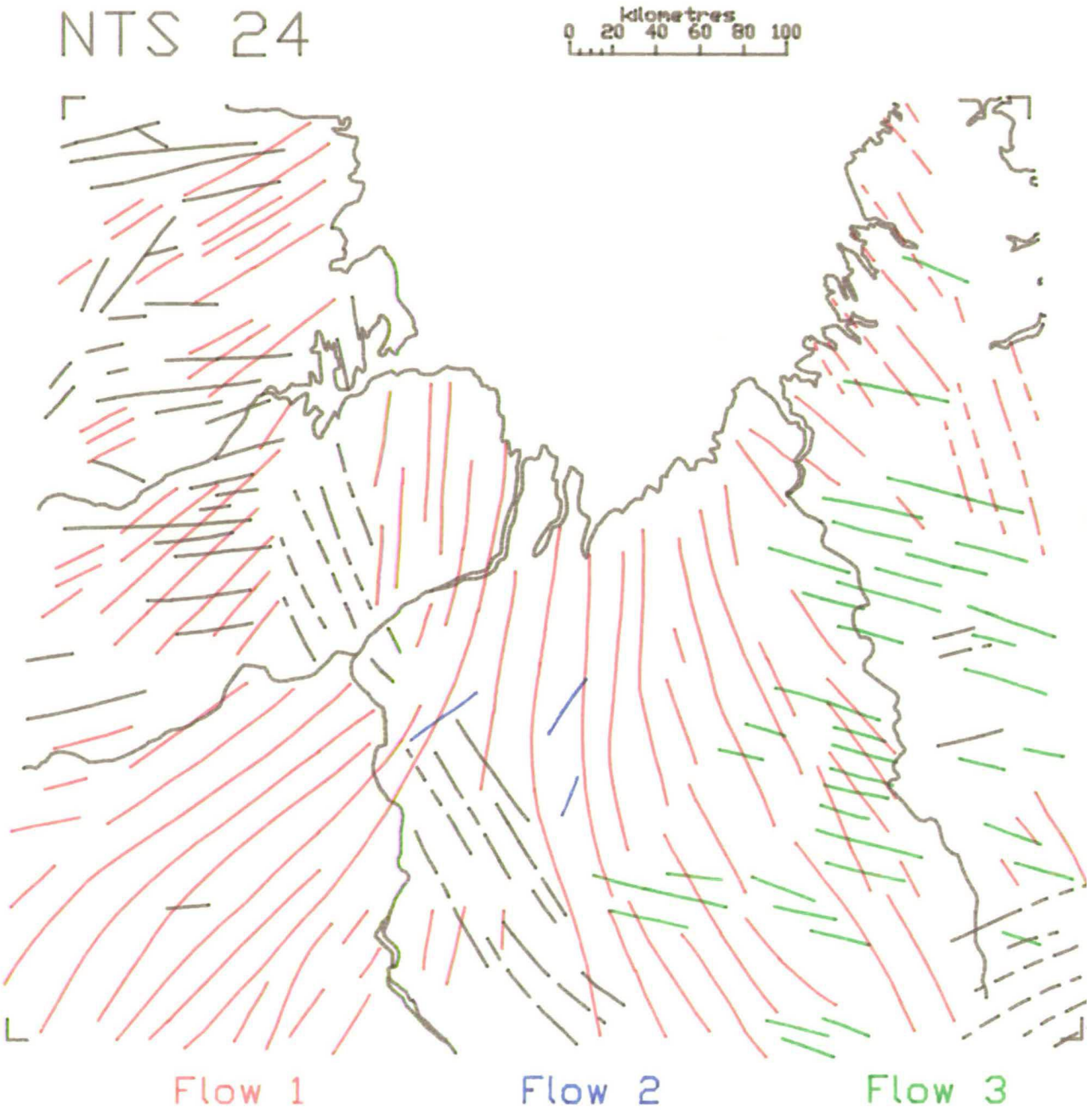
NTS 24
kilometres
0 20 40 60 80 100
Flow 1
Flow 2
Flow 3

NTS 32(a)

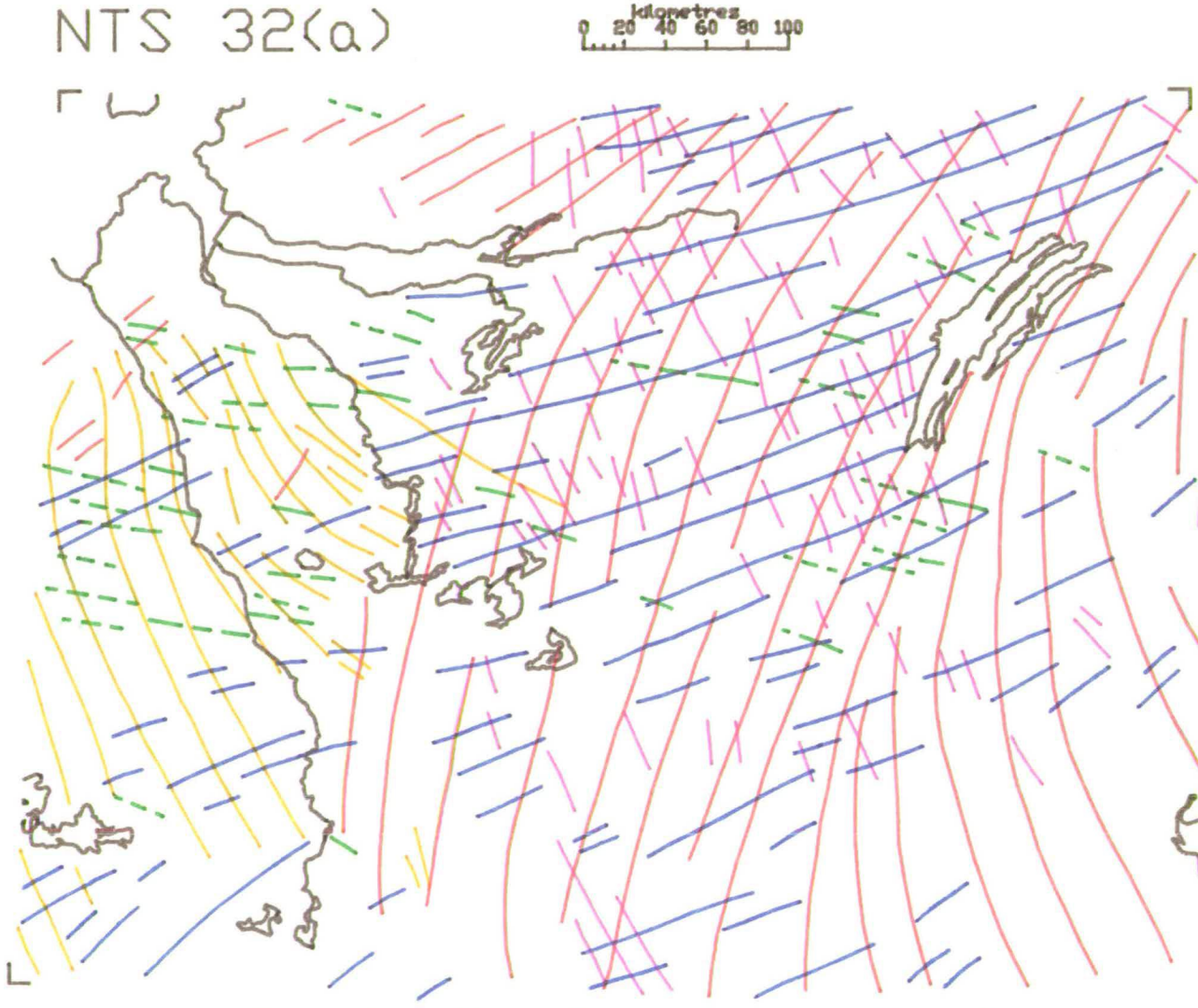

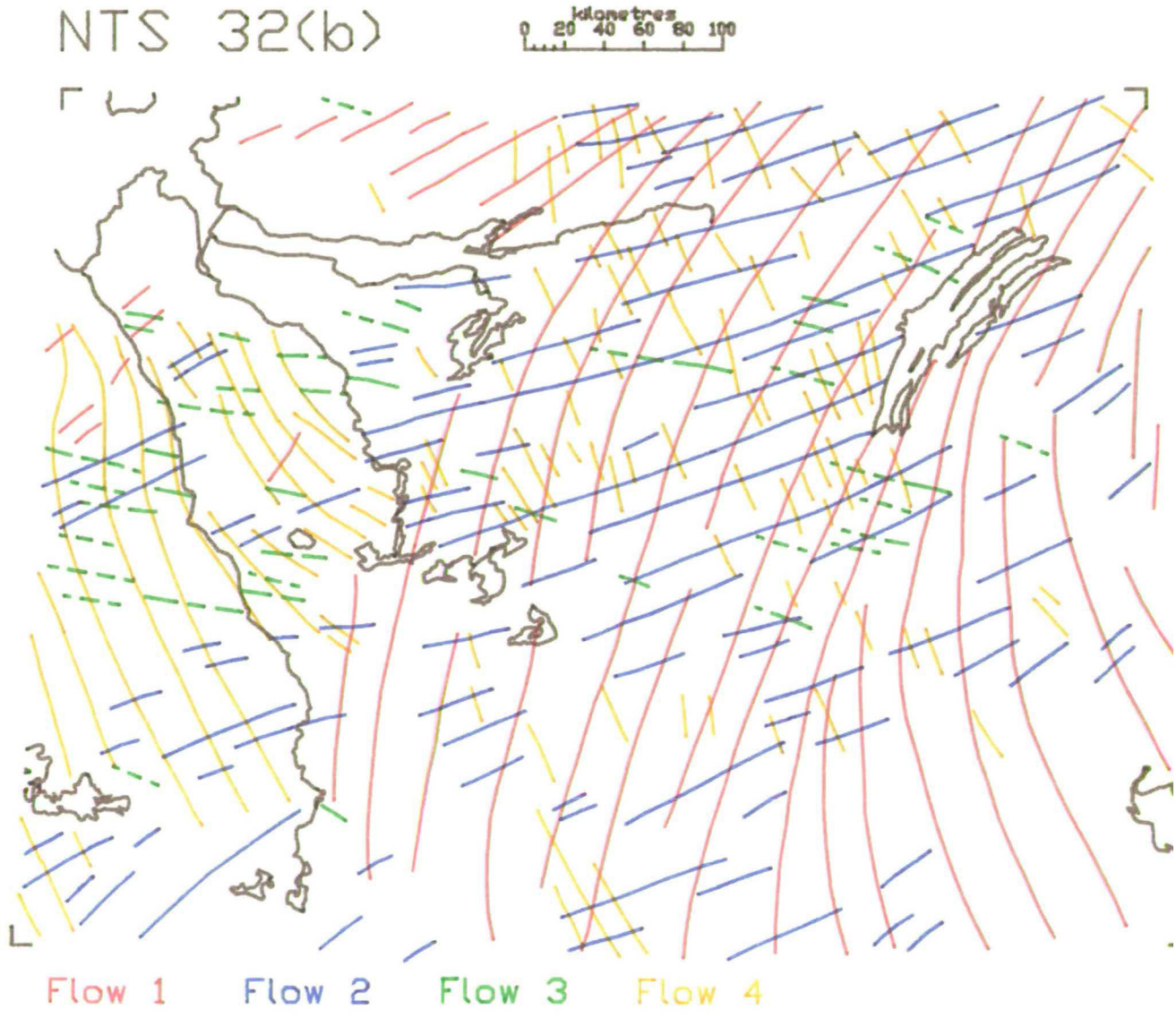
NTS 32(b)
kilometres
0 20 40 60 80 100
Flow 1
Flow 2
Flow 3
Flow 4

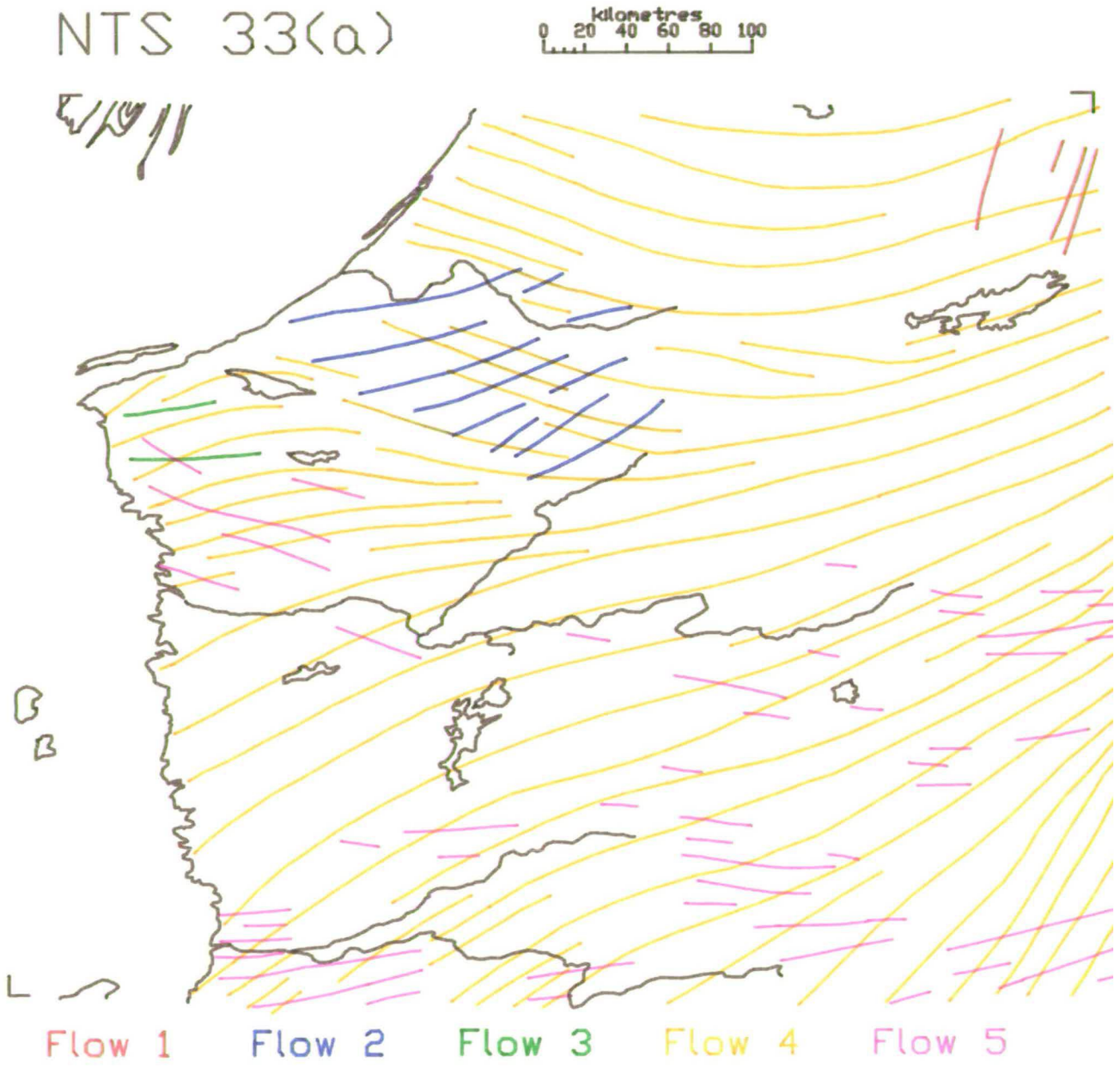
NTS 33(a)
kilometres
0 20 40 60 80 100
Flow 1
Flow 2
Flow 3
Flow 4
Flow 5

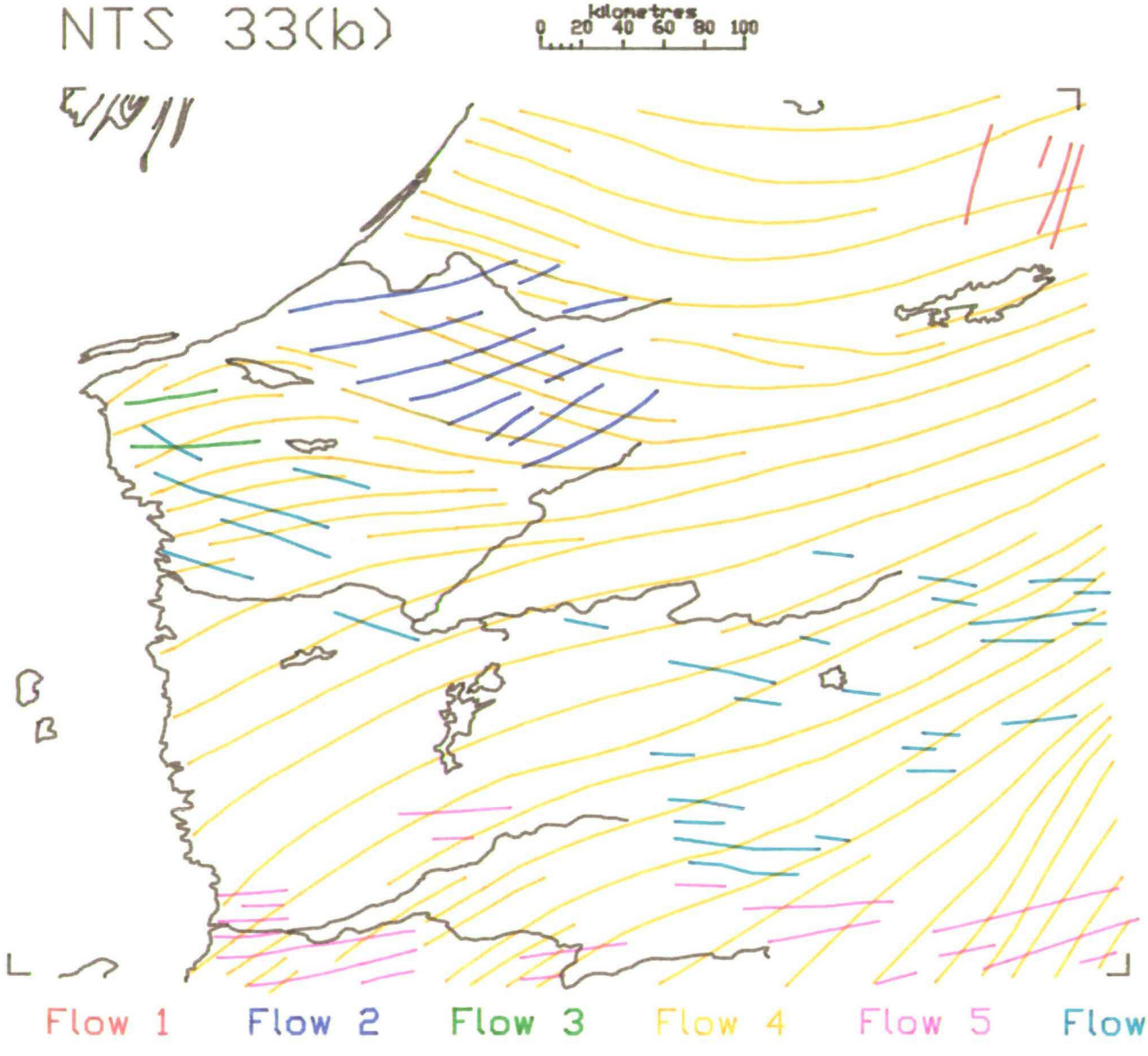
NTS 33(b)
kilometres
0 20 40 60 80 100
Flow 1
Flow 2
Flow 3
Flow 4
Flow 5
Flow

NTS 34

kilometres
0 20 40 60 80 100

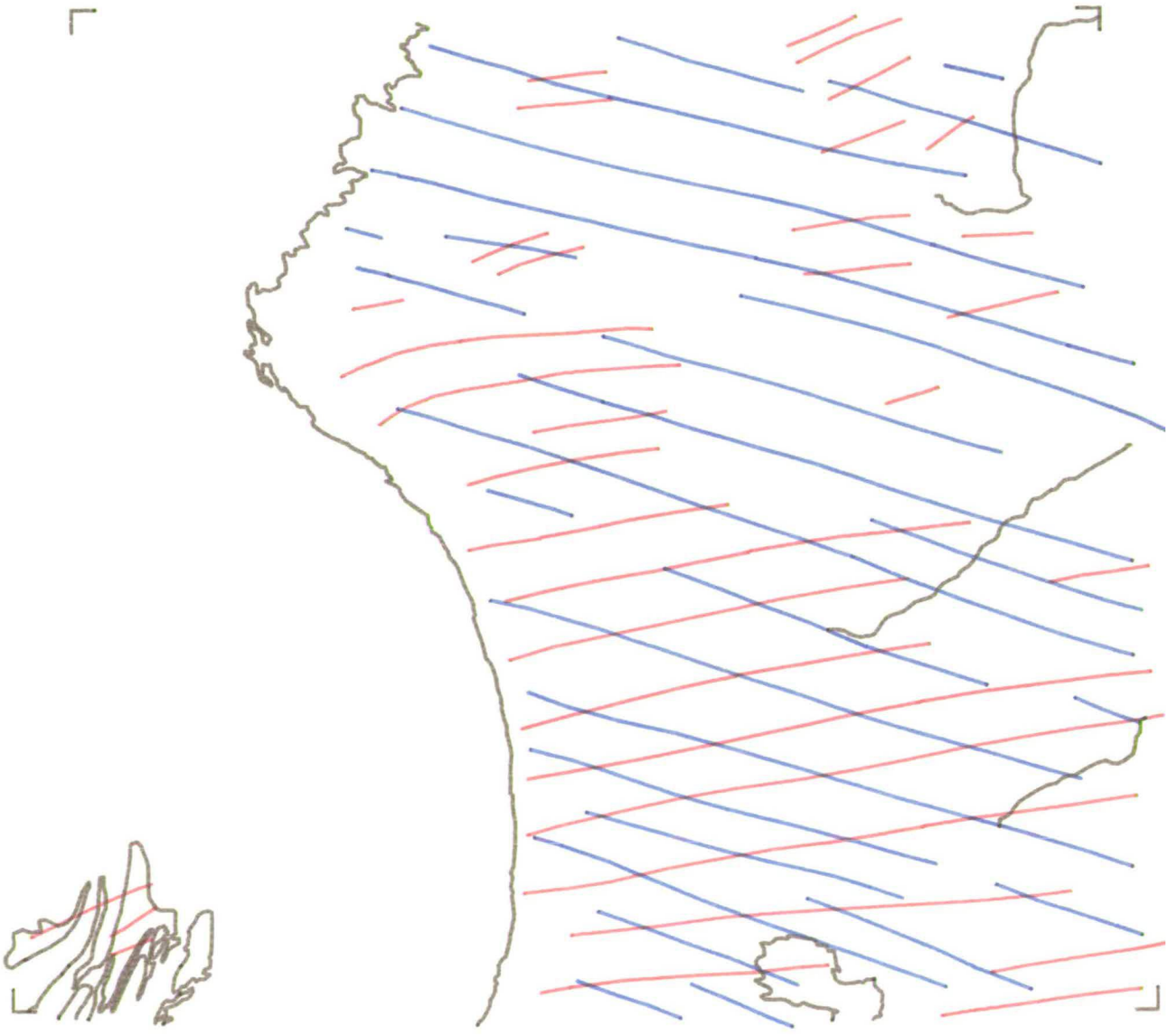

Flow 1

Flow 2

NTS 42(a)

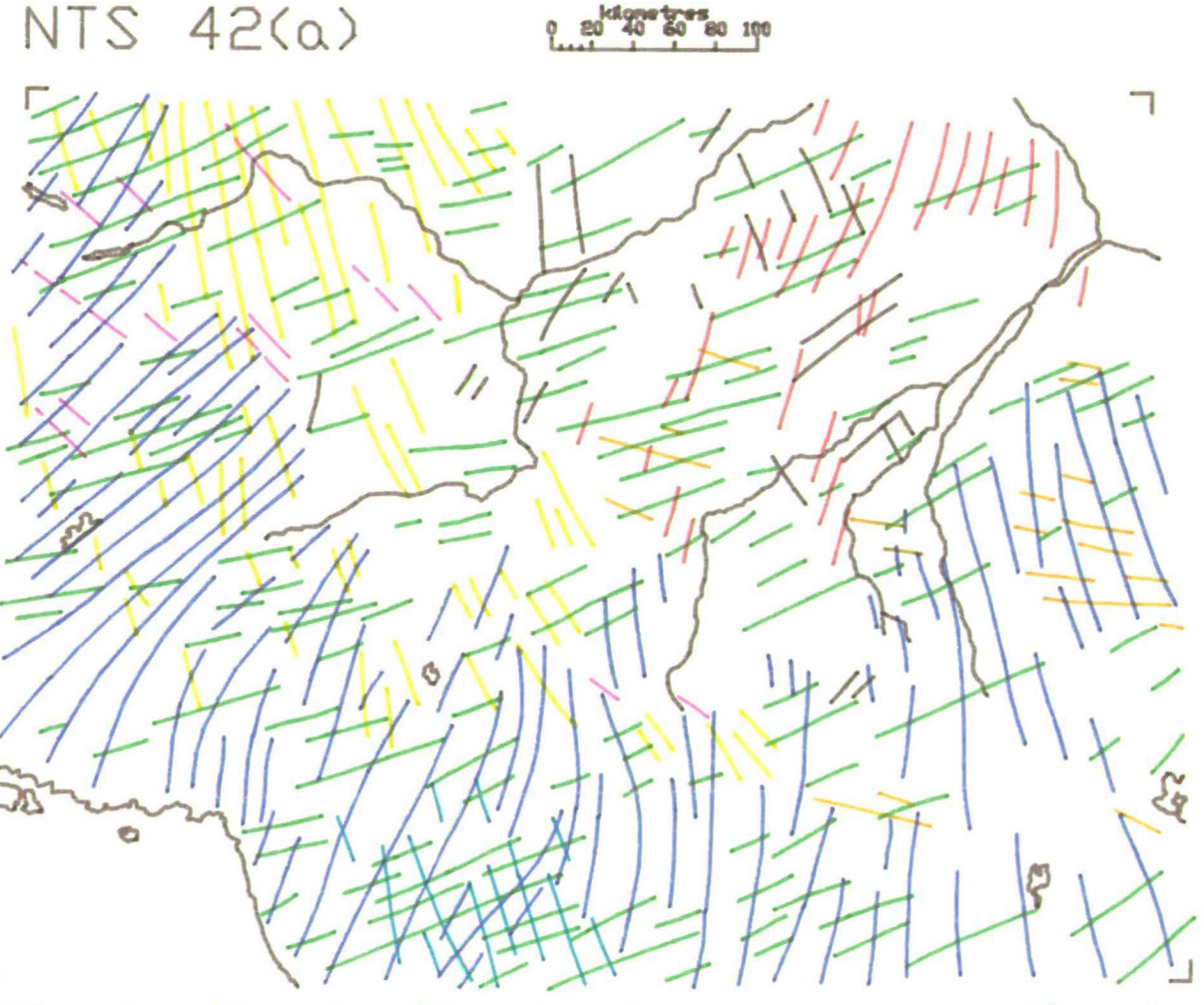

Flow 1 Flow 2 Flow 3 Flow 4 Flow 5 Flow 6

Flow 7

NTS 42(b)

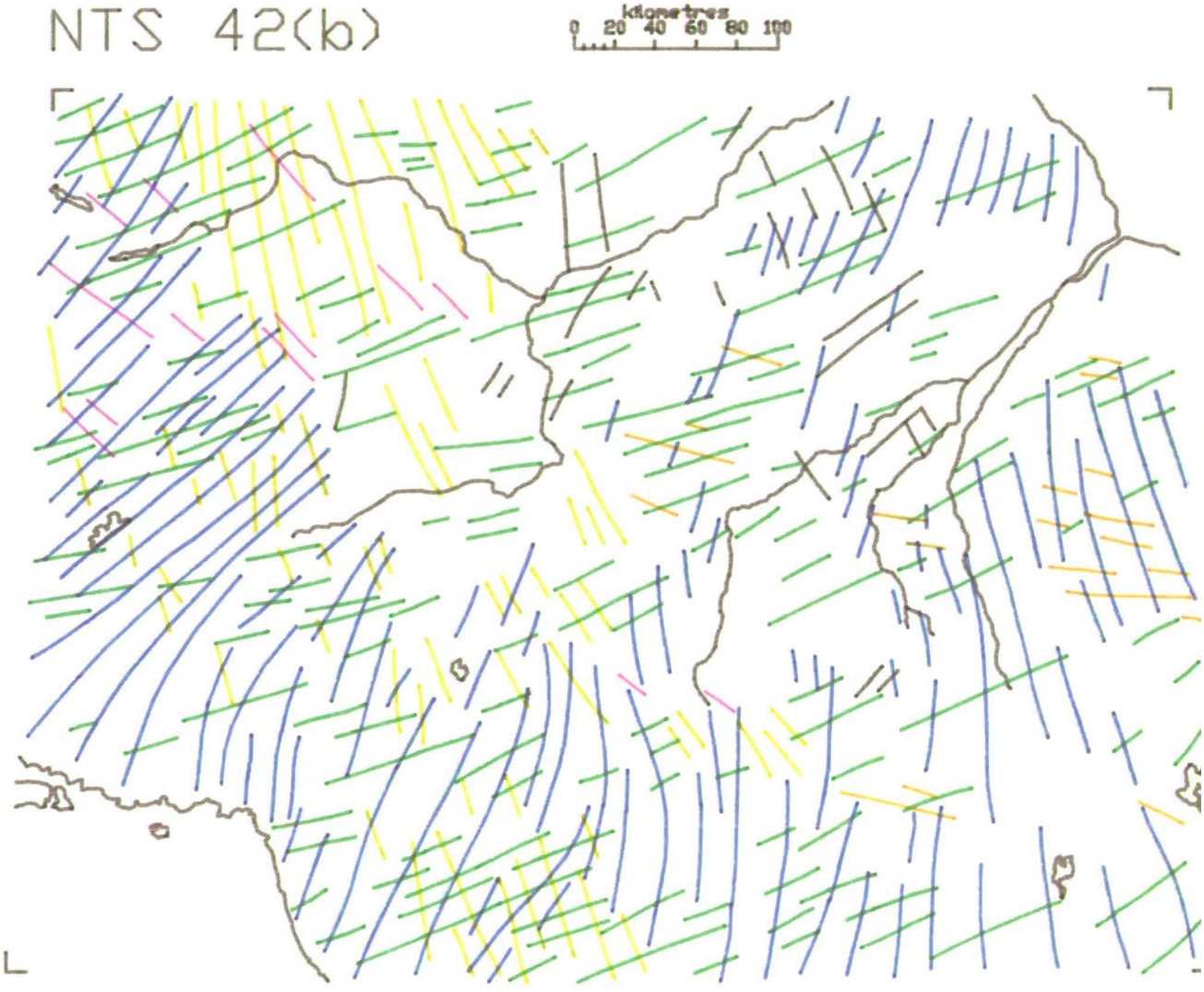

NTS 43(a)

kilometres
0 20 40 60 80 100

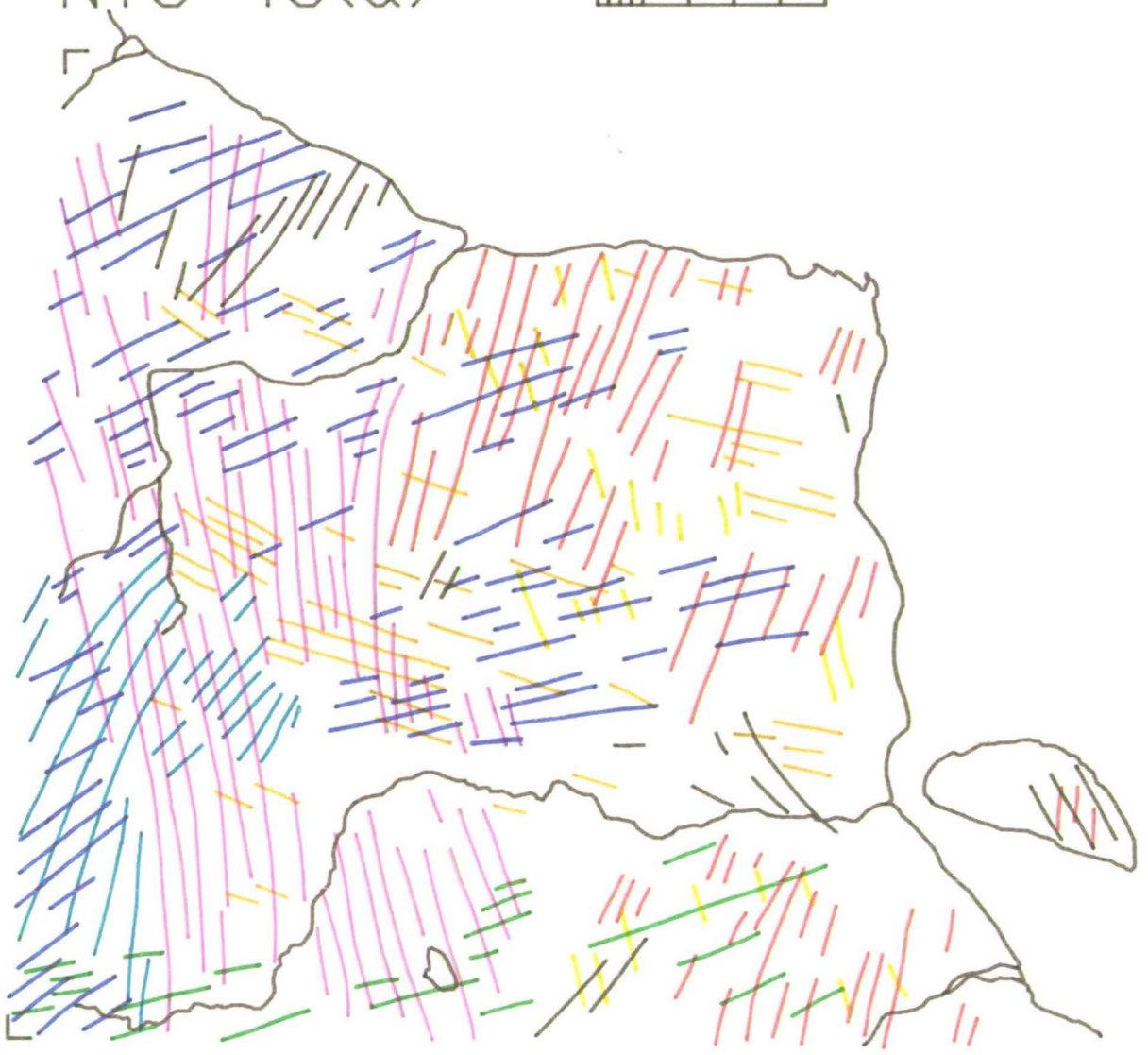

Flow 1 Flow 2 Flow 3 Flow 4 Flow 5
Flow 6 Flow 7

NTS 43(b)

kilometres
0 20 40 60 80 100

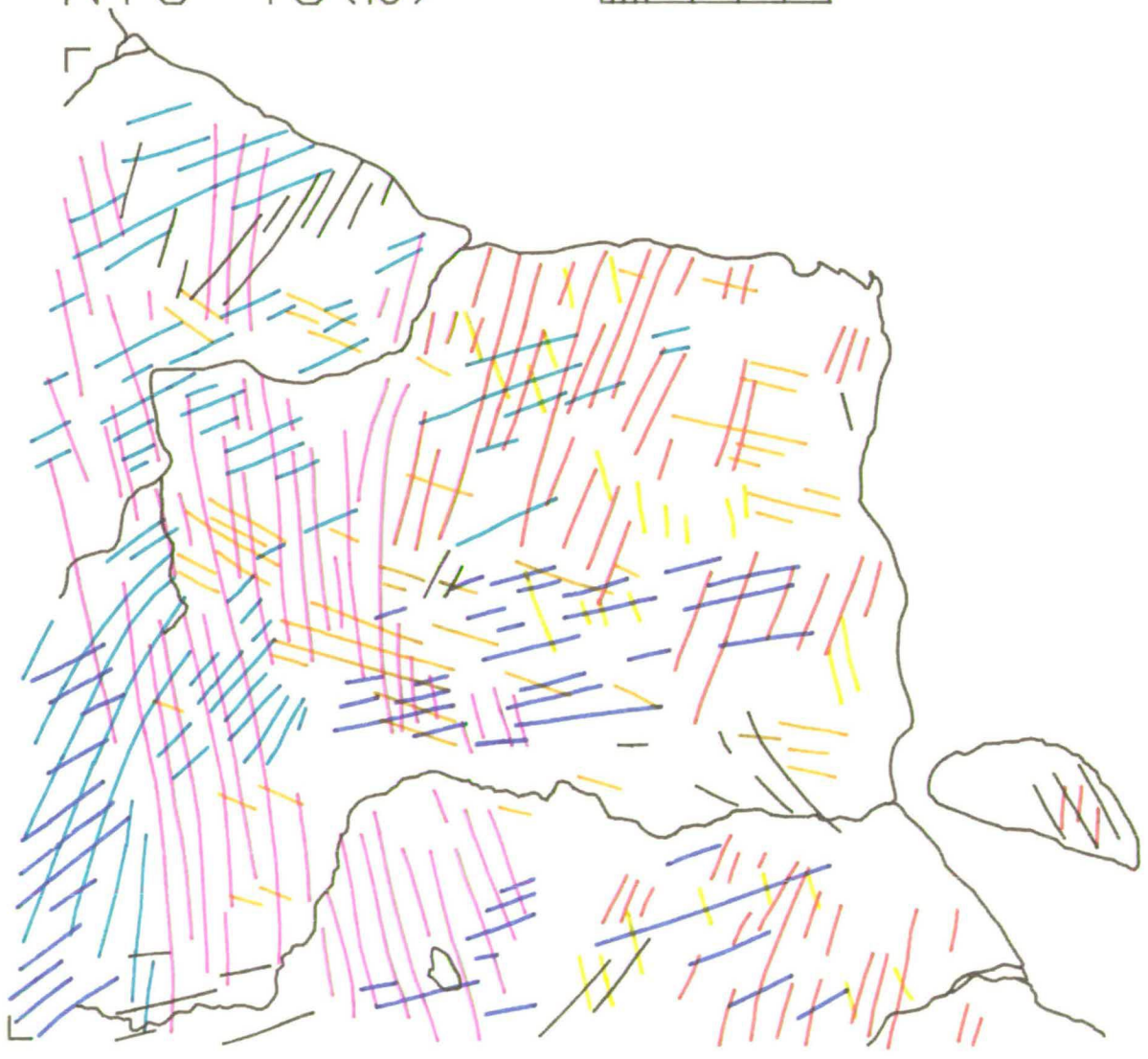

Flow 1 Flow 2 Flow 4 Flow 5
Flow 6 Flow 7

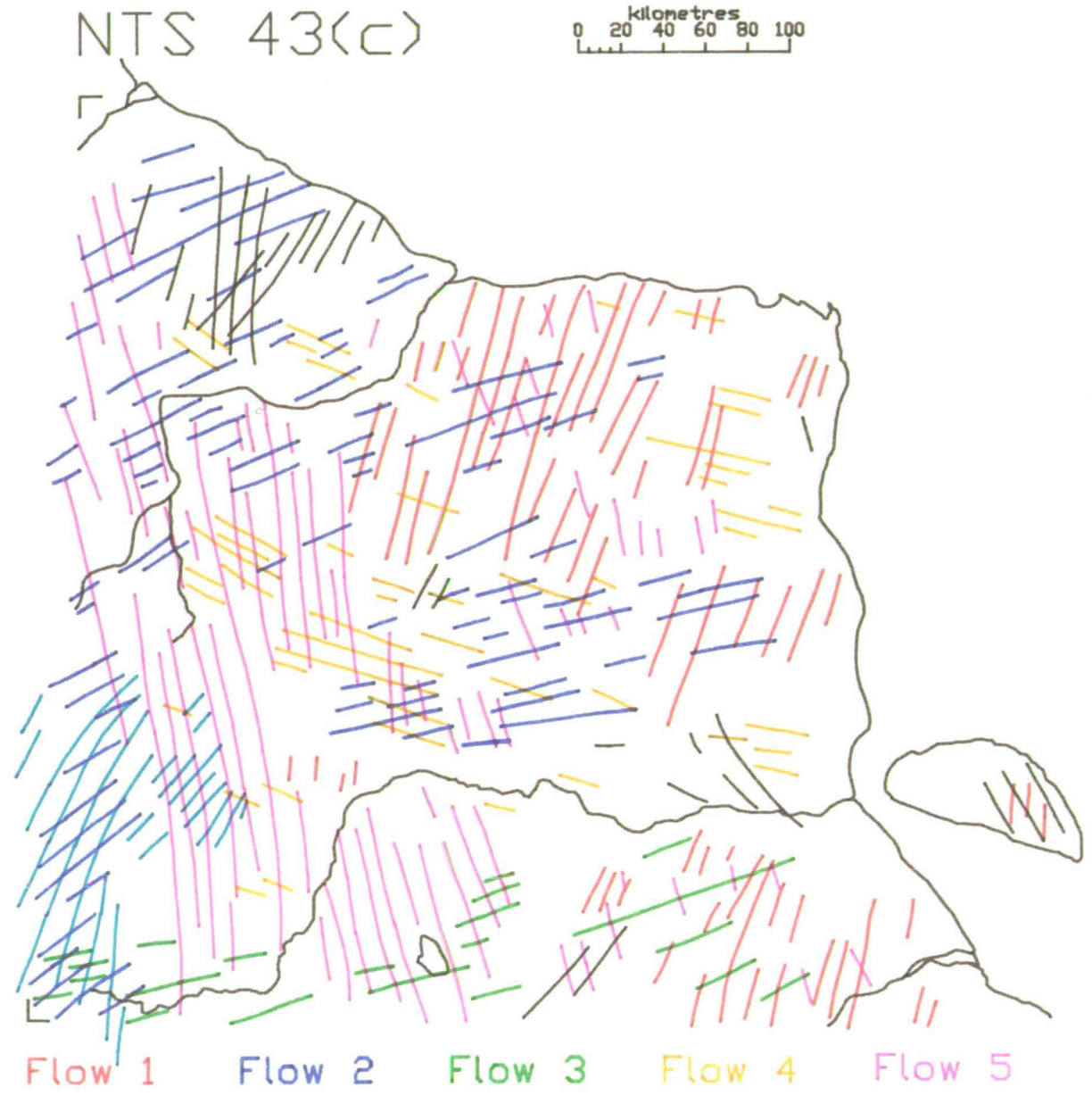
NTS 43(c)
kilometres
0 20 40 60 80 100
Flow 1
Flow 2
Flow 3
Flow 4
Flow 5
Flow 7

NTS 43(d)

kilometres
0 20 40 60 80 100

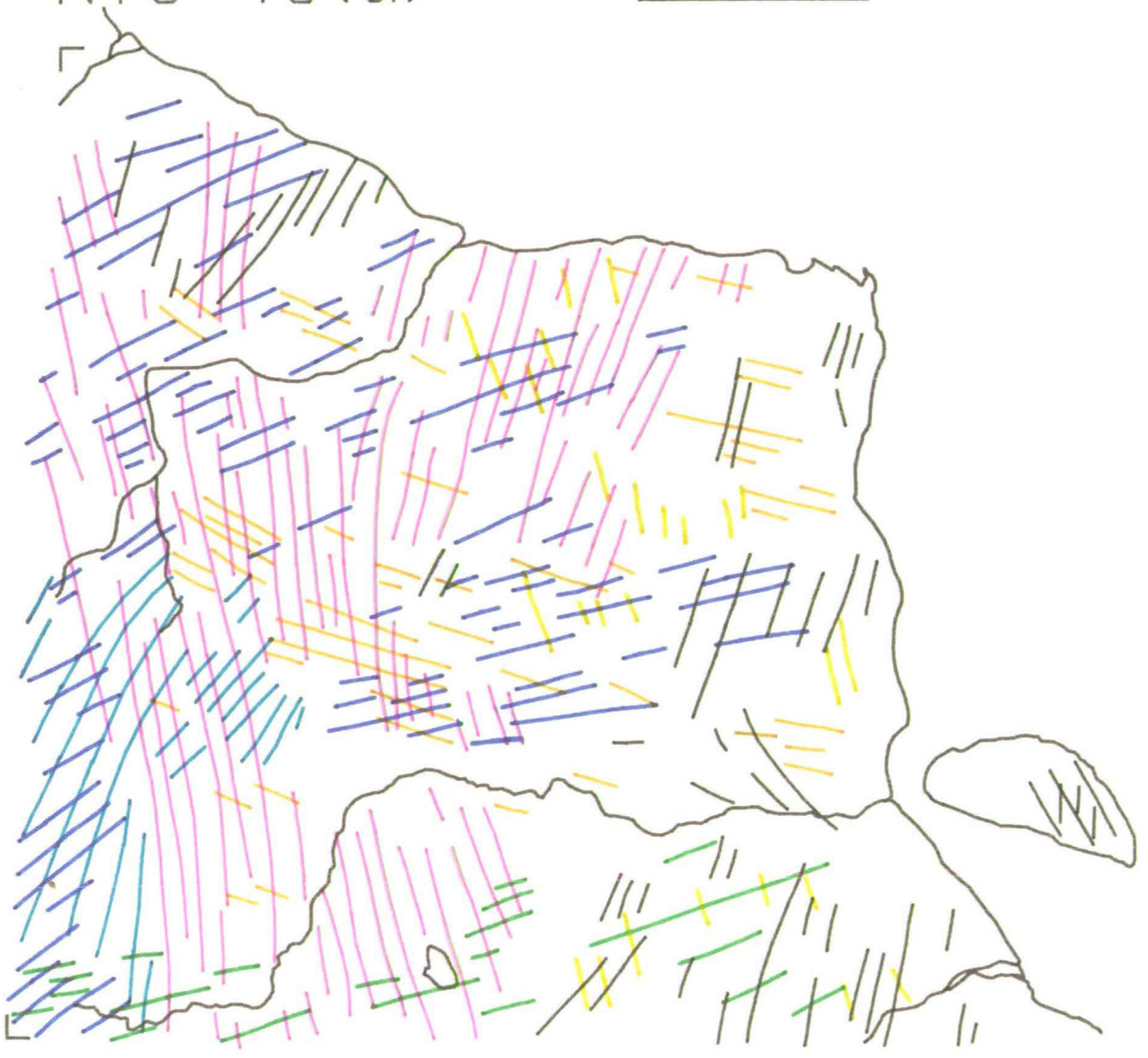

Flow 2 Flow 3 Flow 4 Flow 5

Flow 6 Flow 7

NTS 43(e)

kilometres
0 20 40 60 80 100

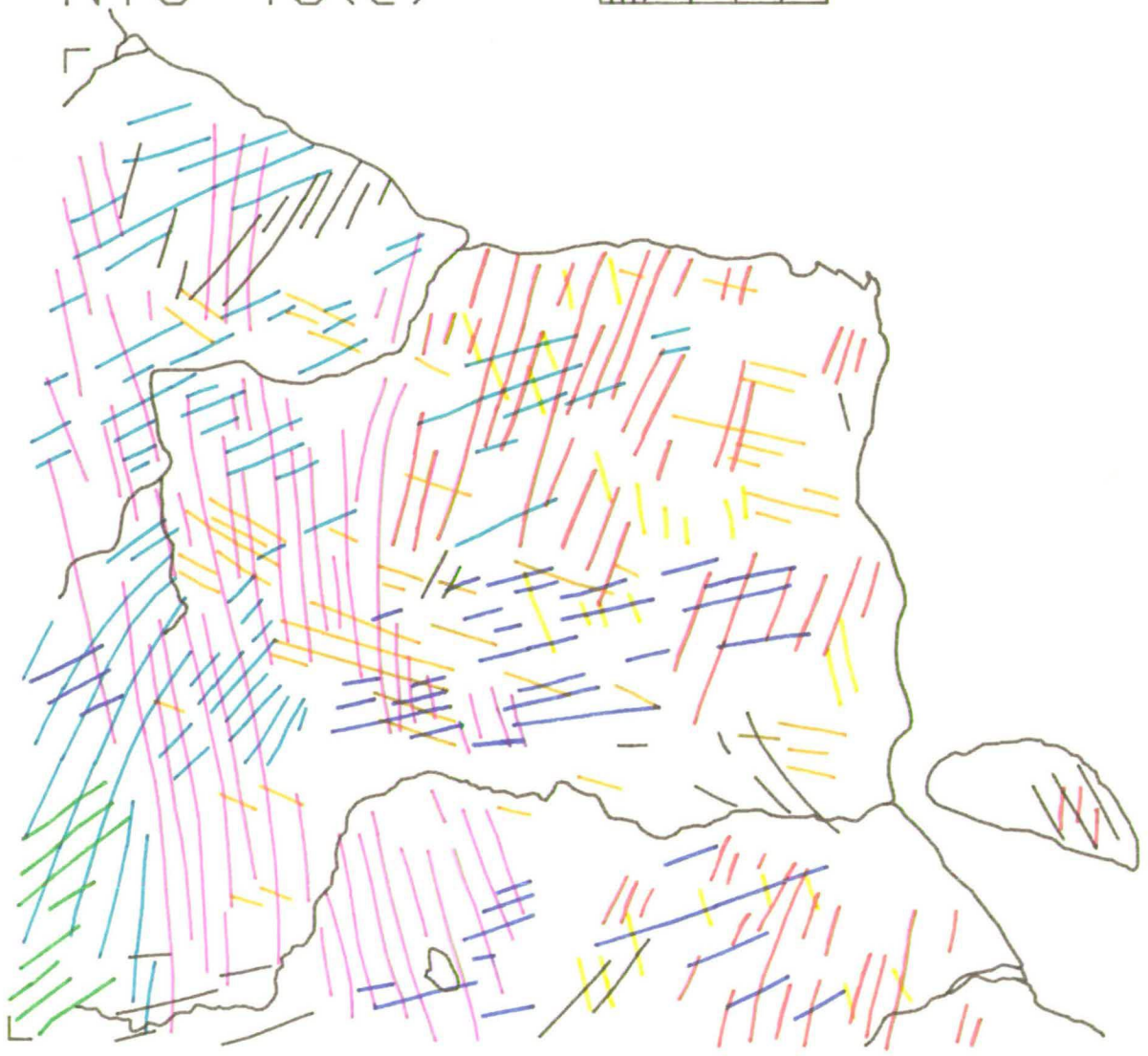

Flow 1 Flow 2 Flow 3 Flow 4 Flow 5

Flow 6 Flow 7

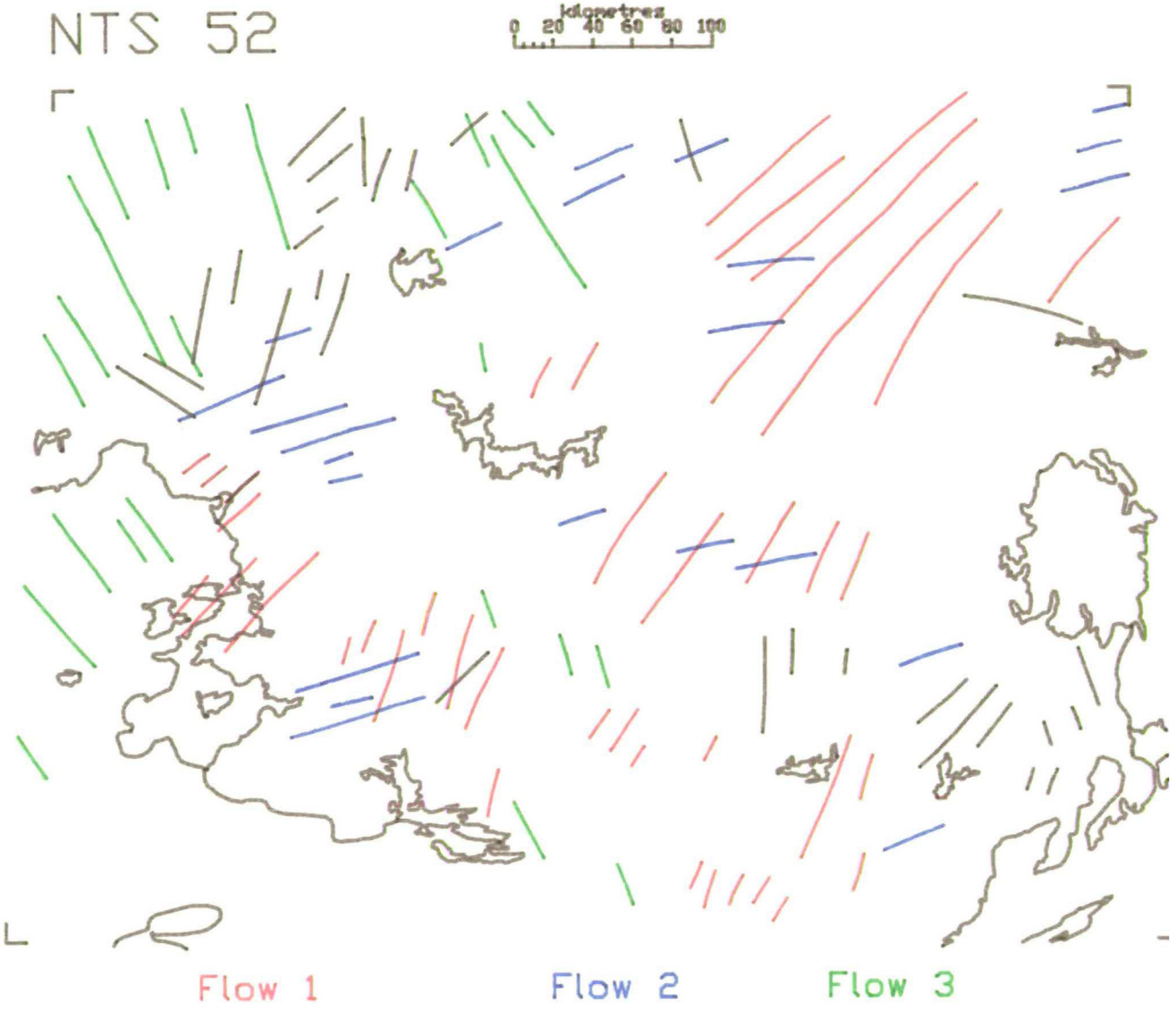
NTS 52
kilometres
0 20 40 60 80 100
Flow 1
Flow 2
Flow 3

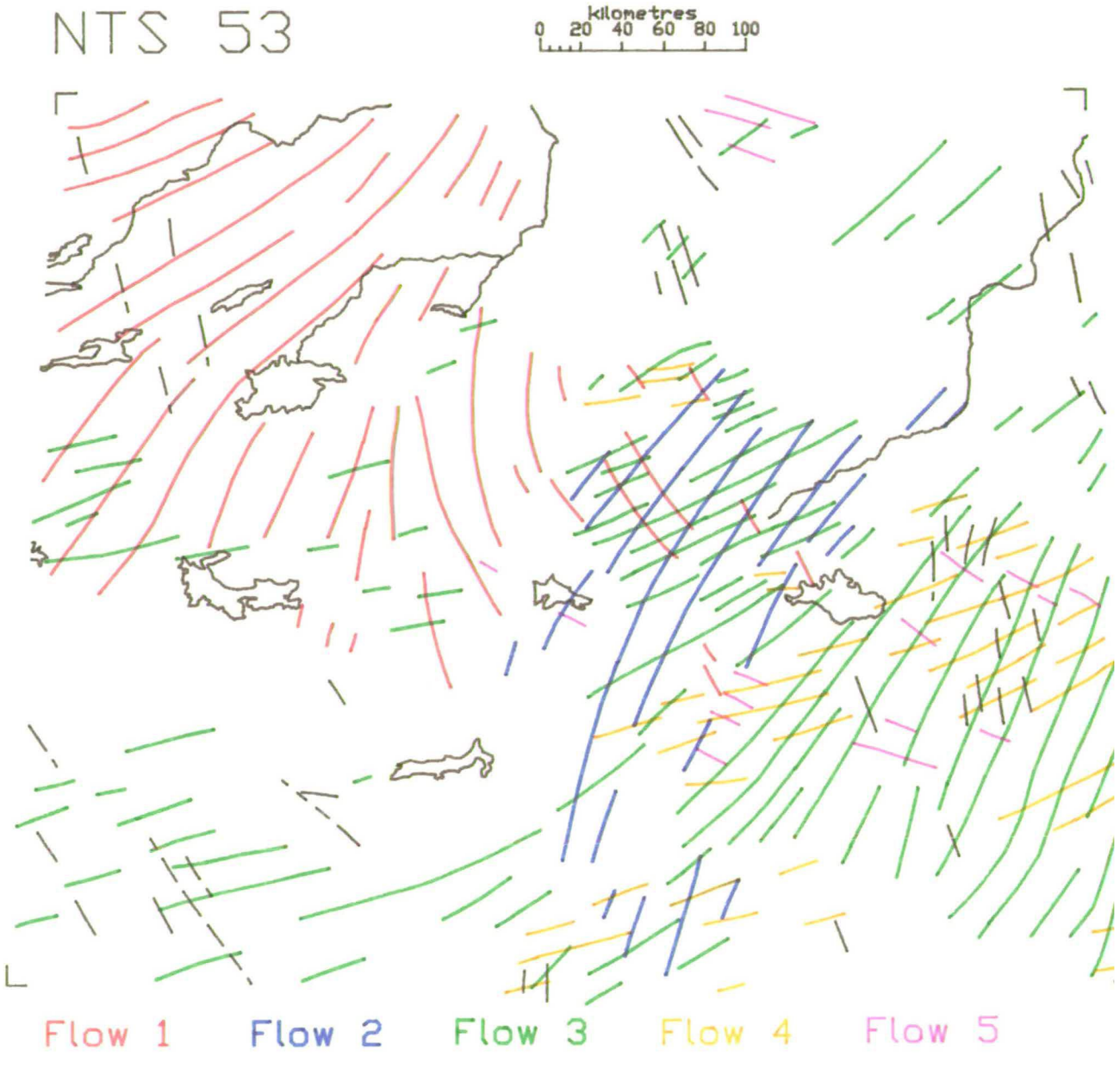
NTS 53
kilometres
0 20 40 60 80 100
Flow 1
Flow 2
Flow 3
Flow 4
Flow 5

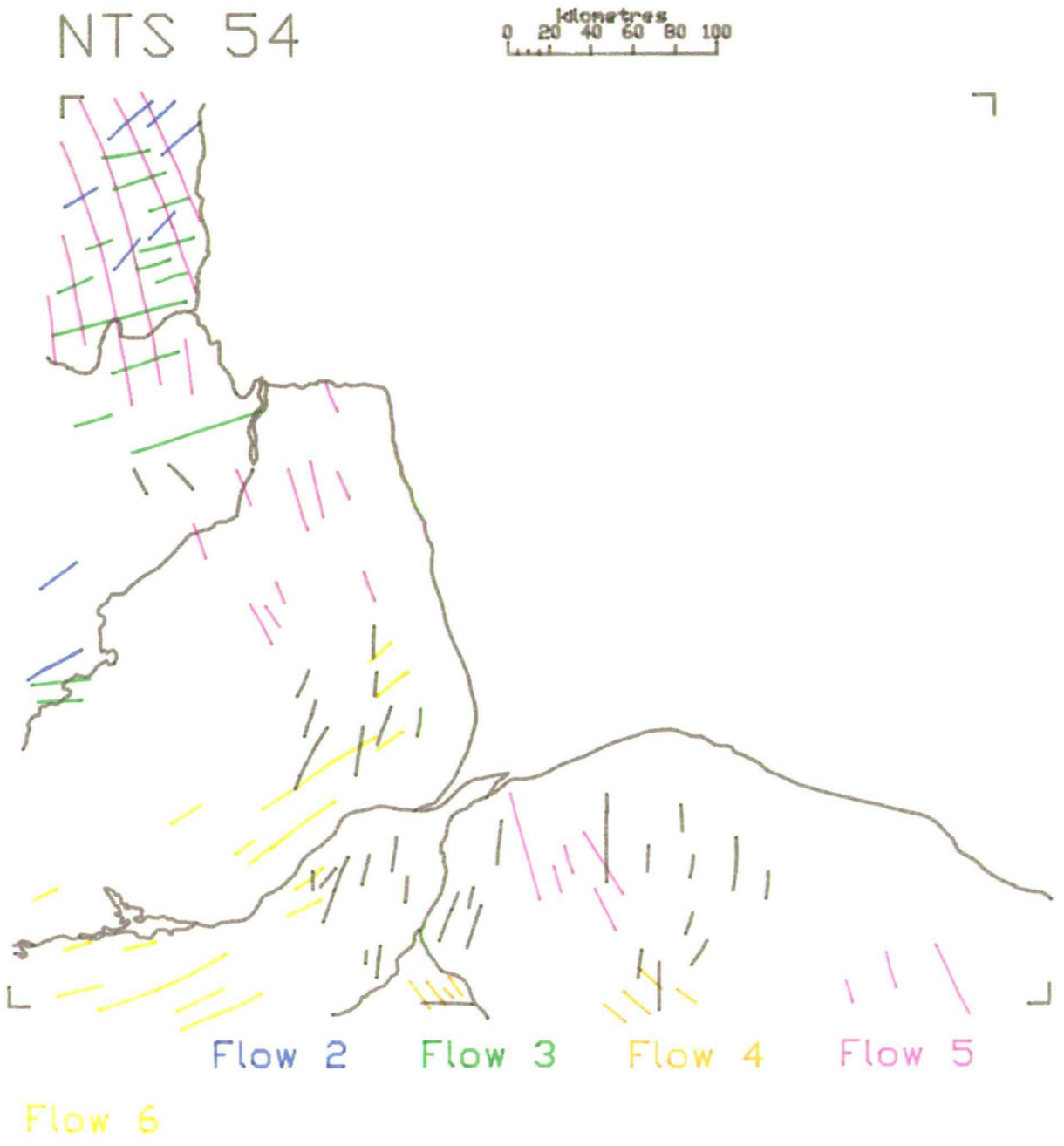
NTS 54
kilometres
0 20 40 60 80 100
Flow 2
Flow 3
Flow 4
Flow 5
Flow 6

NTS 55

kilometres
0 20 40 60 80 100

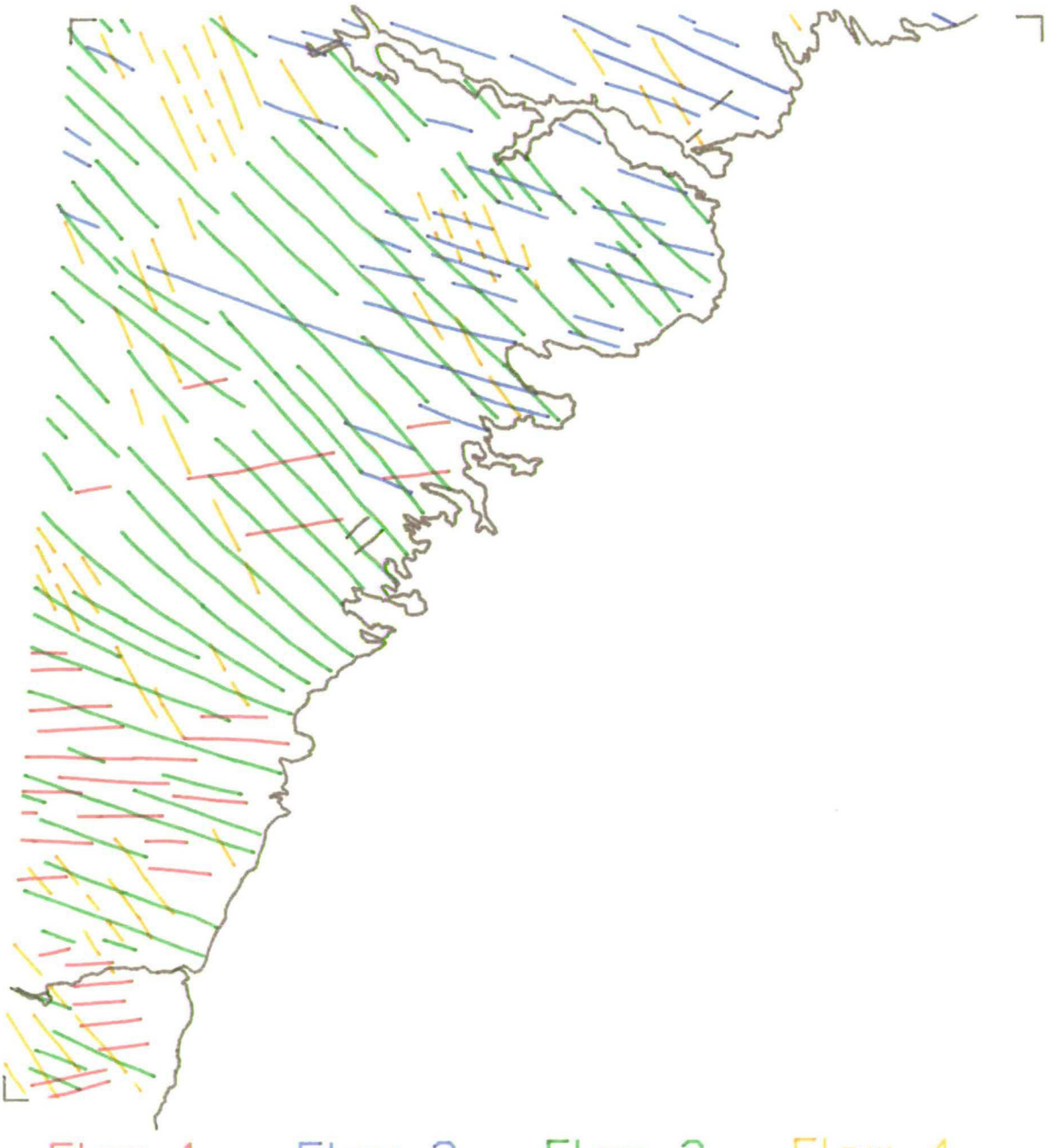

Flow 1 Flow 2 Flow 3 Flow 4

NTS 56

kilometres
0 20 40 60 80 100

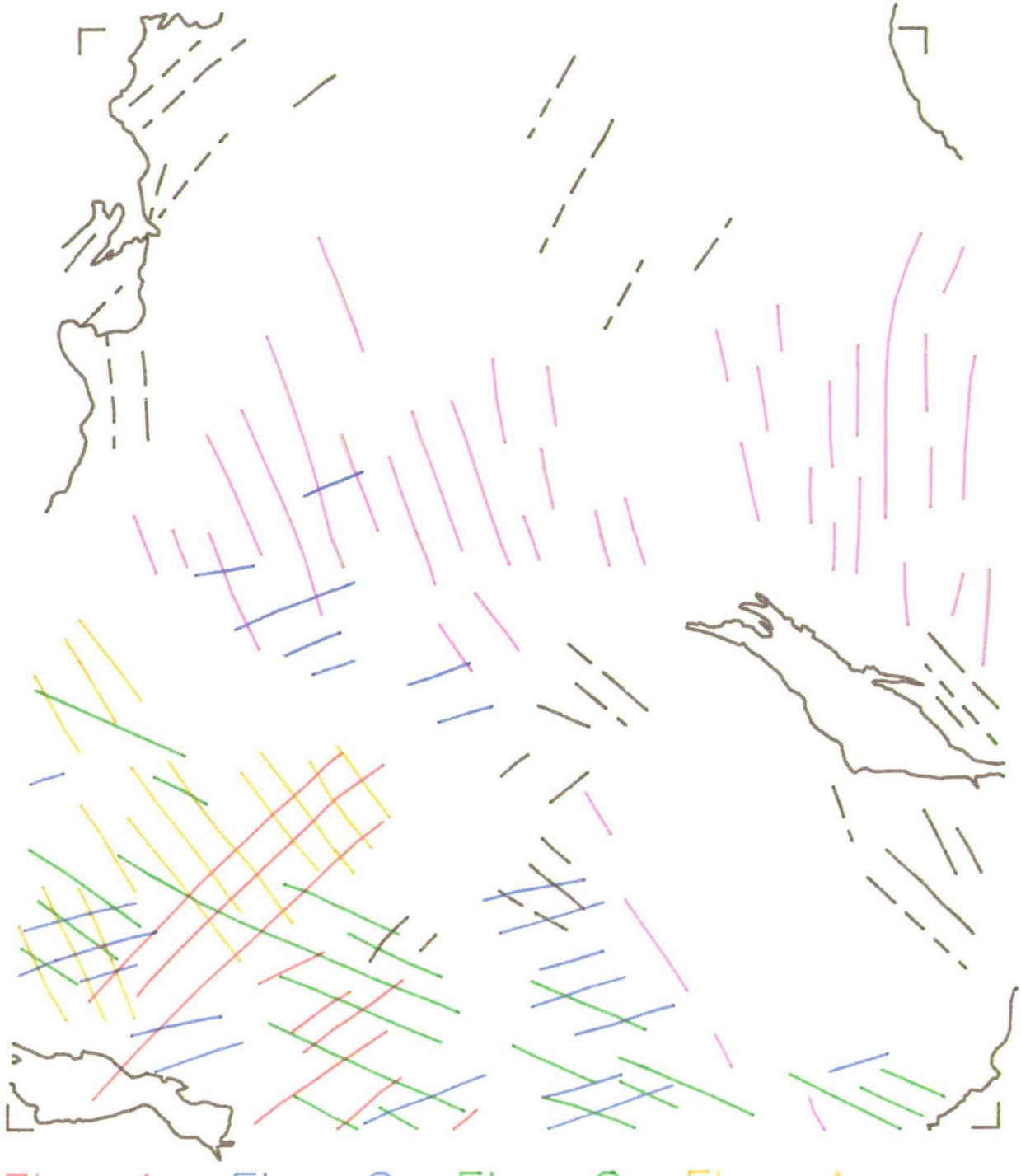

Flow 1 Flow 2 Flow 3 Flow 4

Flow 5

NTS 63a

kilometres
0 20 40 60 80 100

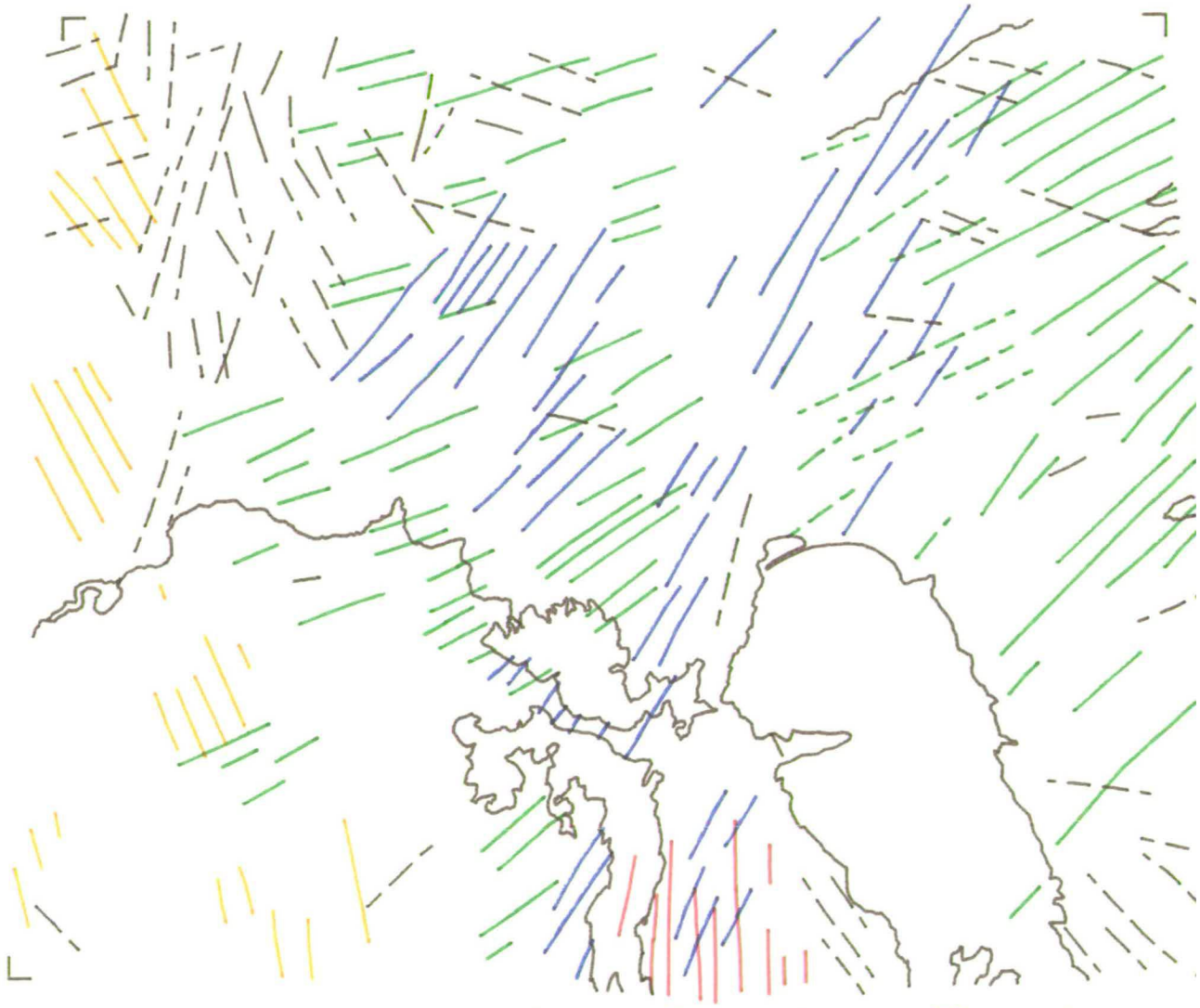

Flow 1 Flow 2 Flow 3 Flow 4

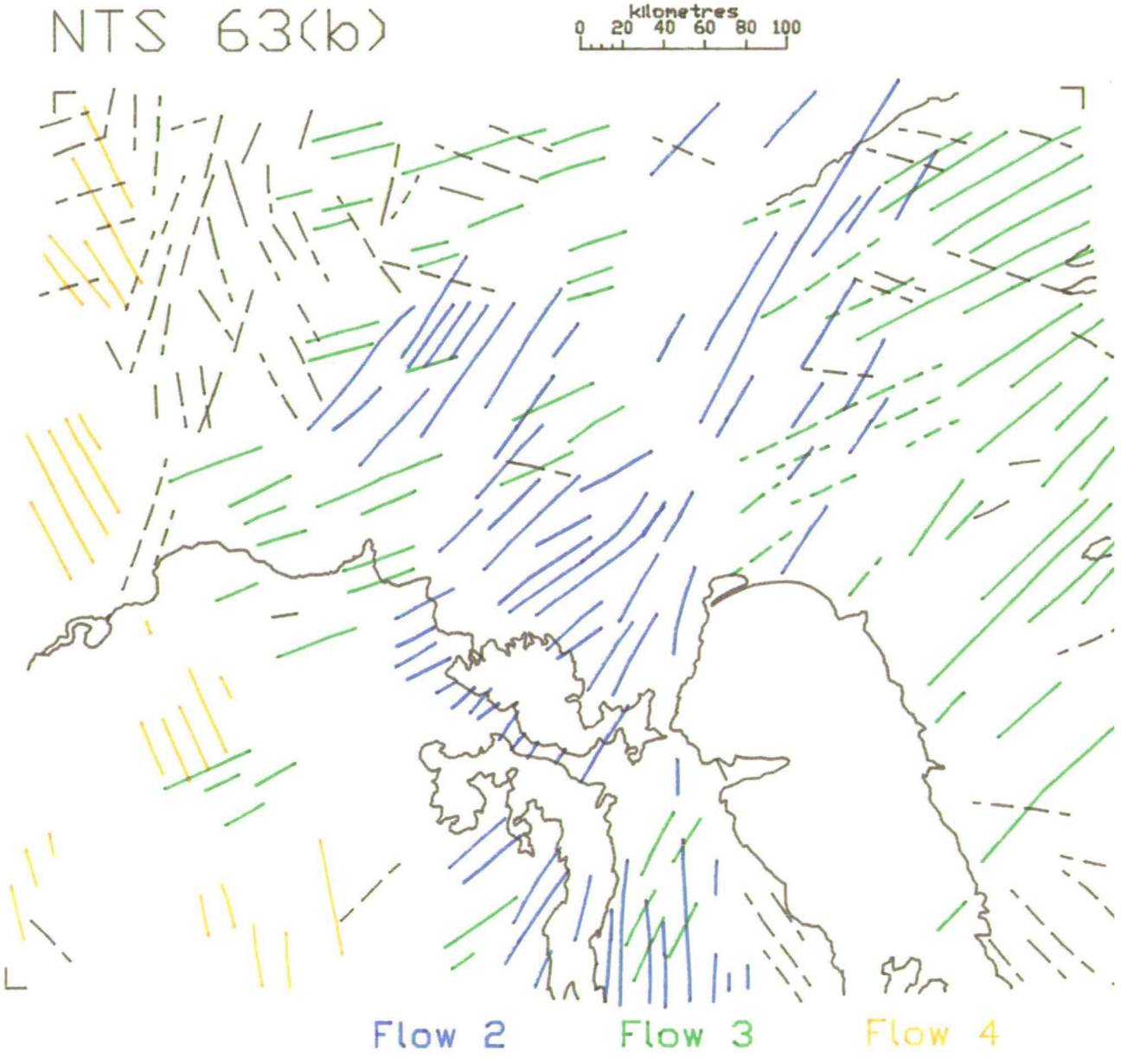
NTS 63(b)
kilometres
0 20 40 60 80 100
Flow 2
Flow 3
Flow 4

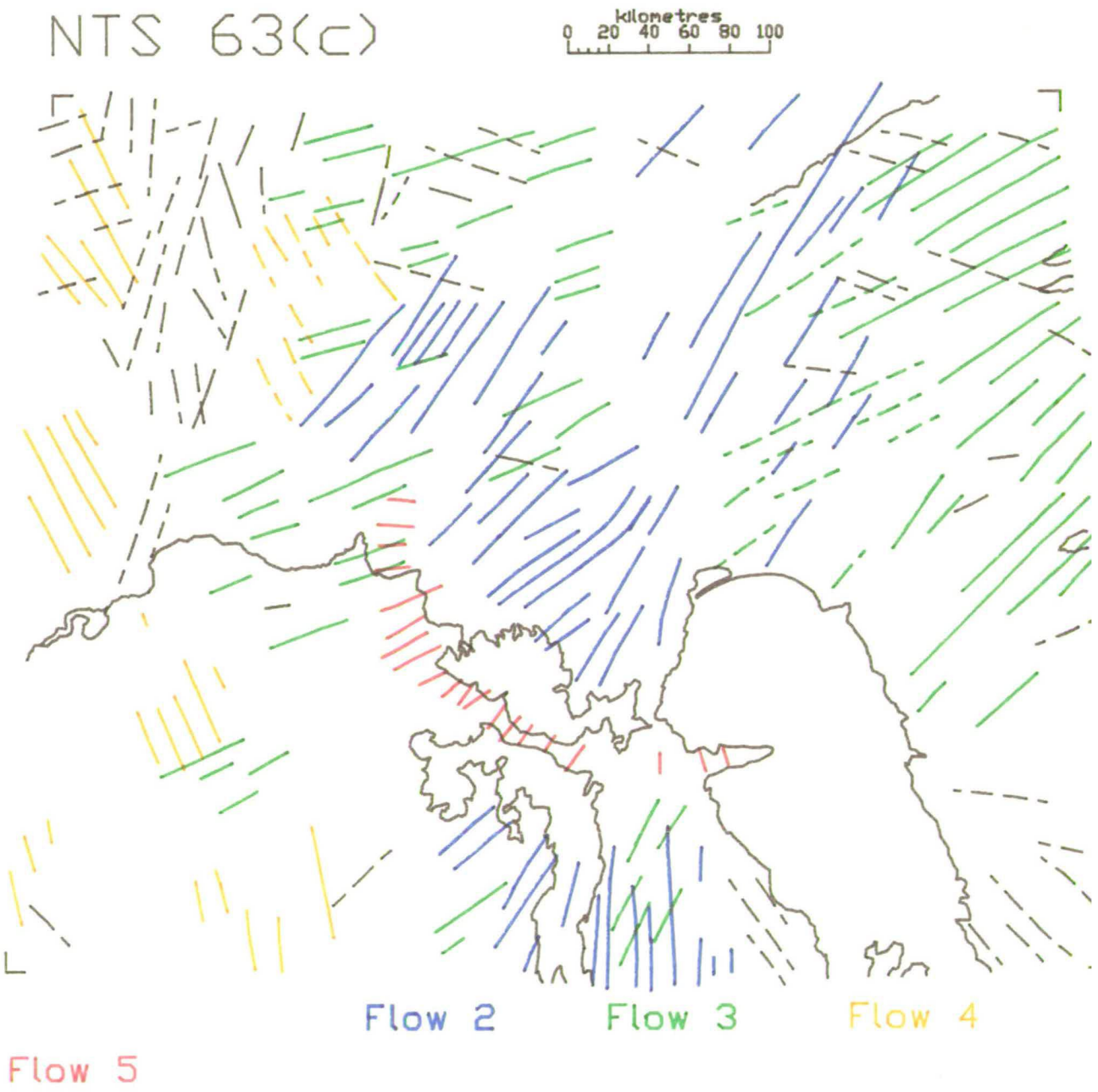
NTS 63(c)
kilometres
0 20 40 60 80 100
Flow 2
Flow 3
Flow 4
Flow 5

NTS 64(a)

kilometres
0 20 40 60 80 100

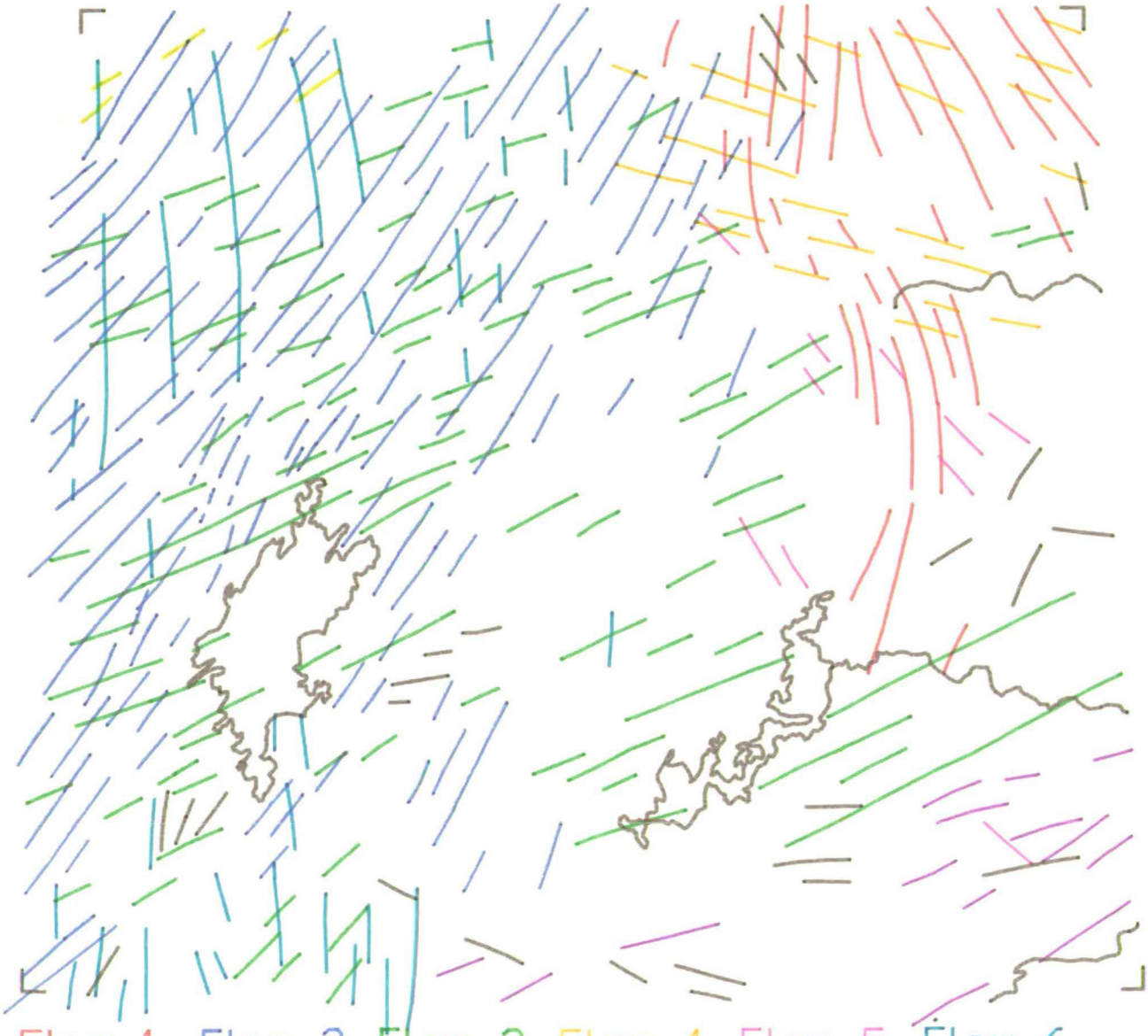

Flow 1 Flow 2 Flow 3 Flow 4 Flow 5 Flow 6

Flow 7 Flow 8

NTS 64(b)

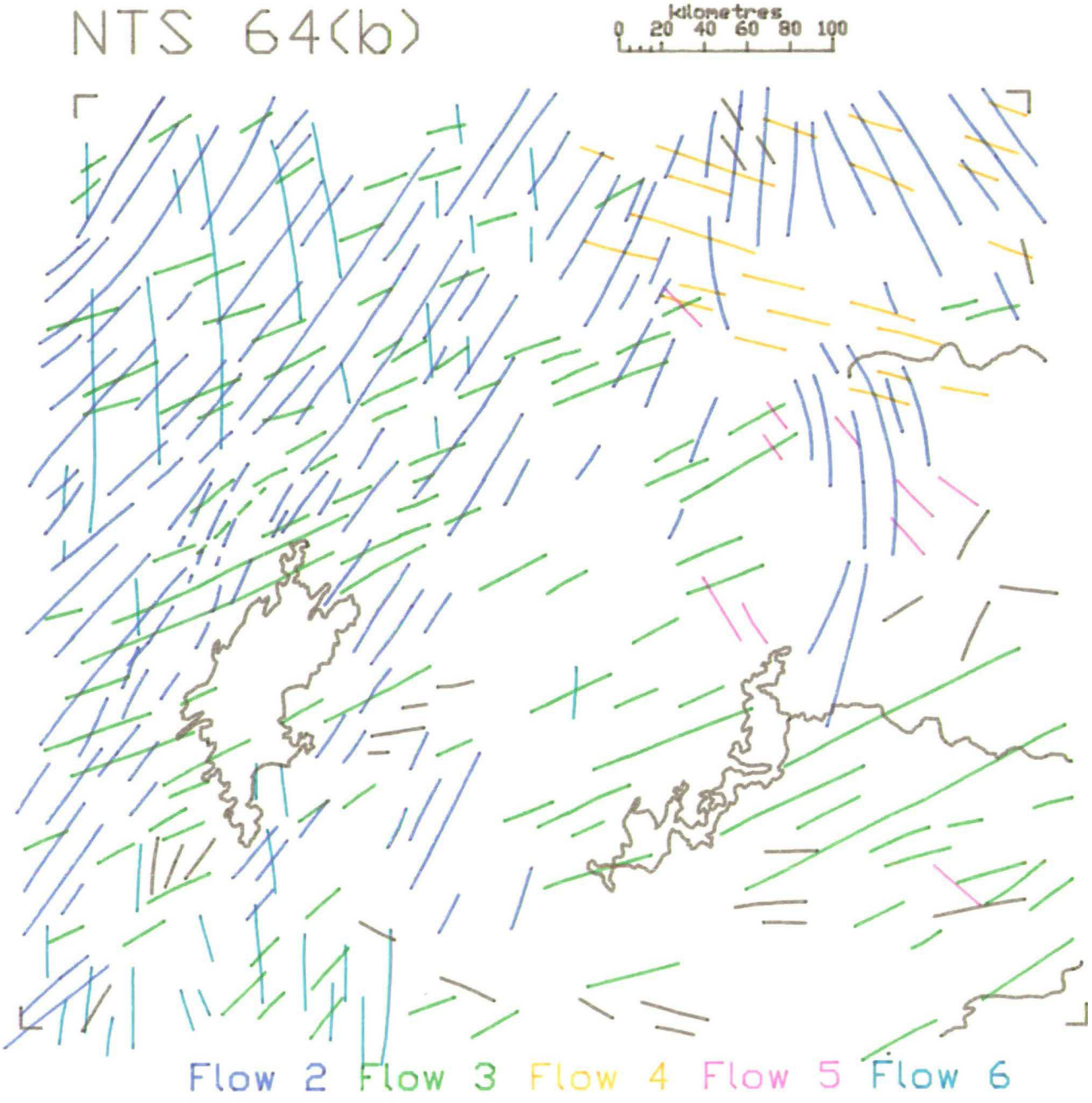

NTS 65(a)

kilometres
0 20 40 60 80 100

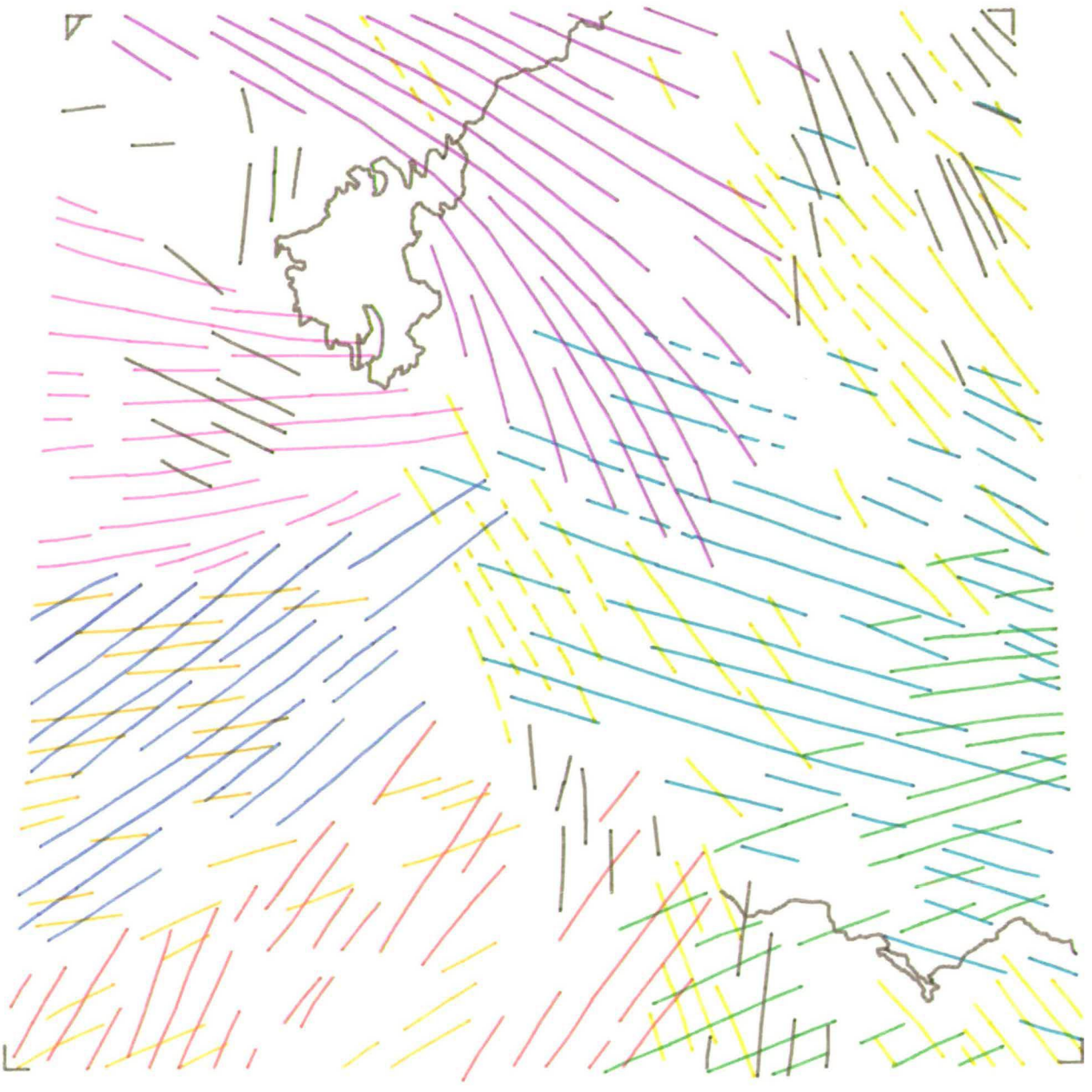

Flow 1 Flow 2 Flow 3 Flow 4 Flow 5
Flow 6 Flow 7 Flow 8

NTS 65(b)

kilometres
0 20 40 60 80 100

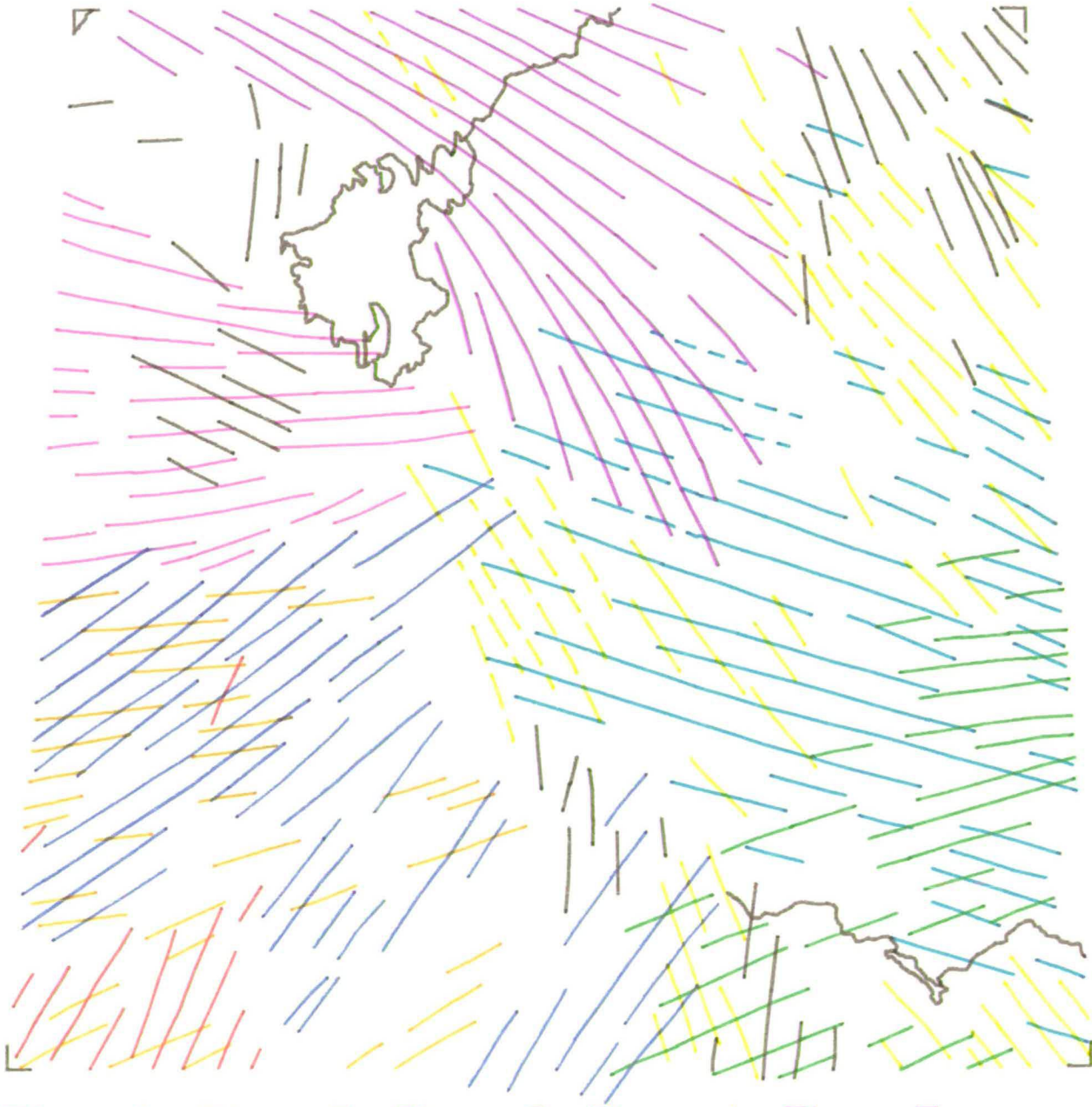

Flow 1 Flow 2 Flow 3 Flow 4 Flow 5

Flow 6 Flow 7 Flow 8

NTS 65(c)

kilometres
0 20 40 60 80 100

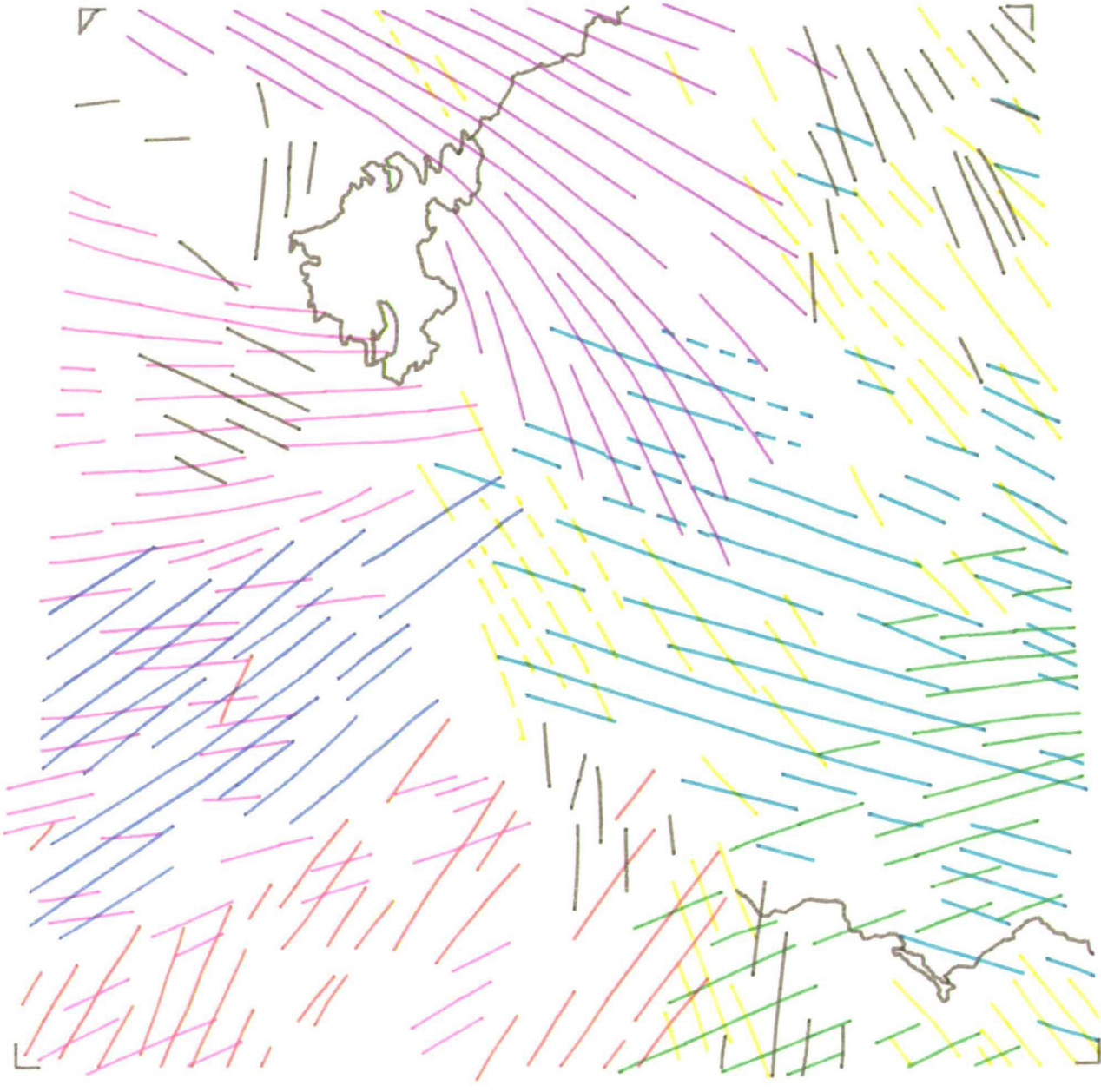

Flow 1 Flow 2 Flow 3 Flow 5

Flow 6 Flow 7 Flow 8

NTS 66

kilometres
0 20 40 60 80 100

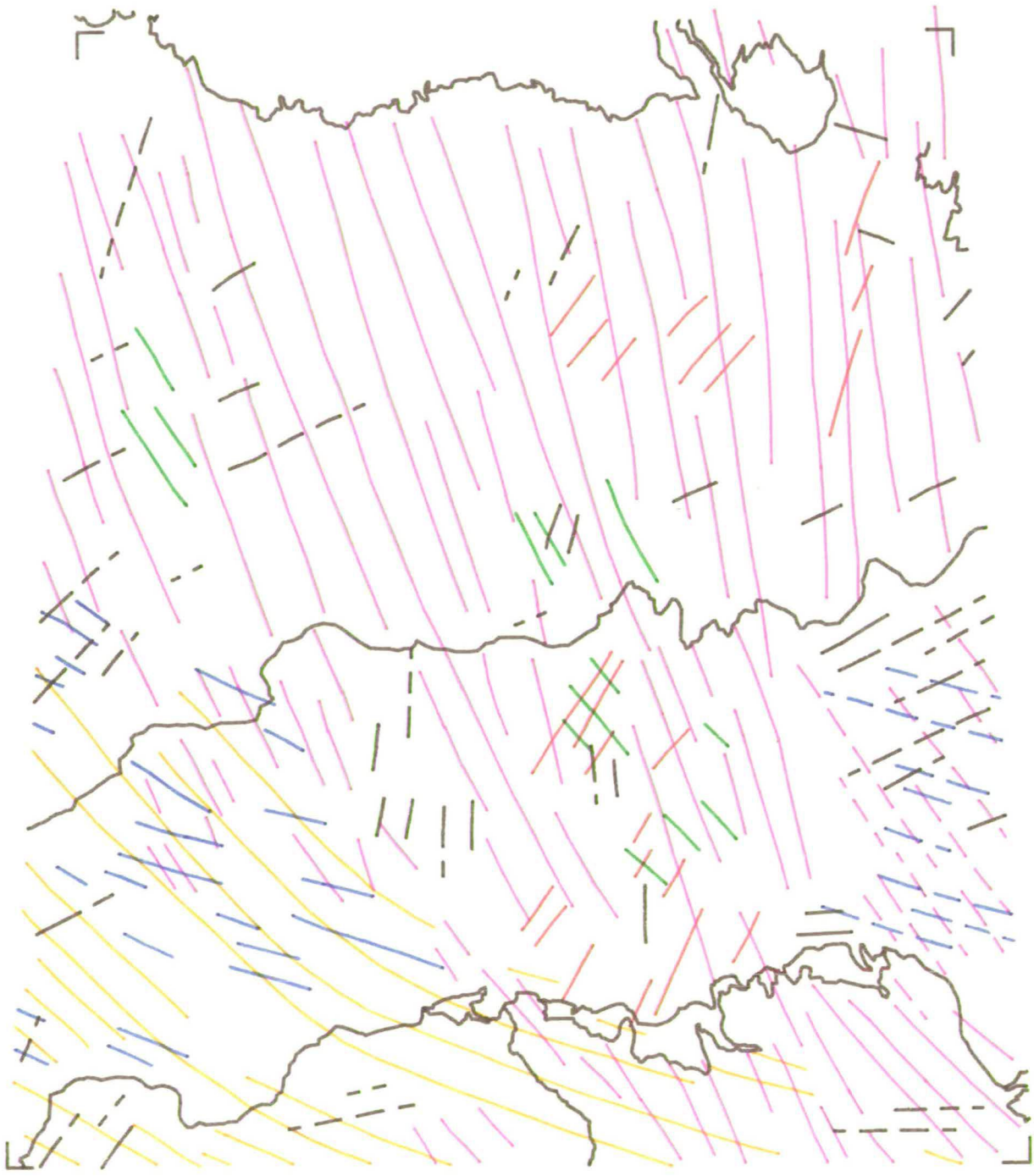

Flow 1 Flow 2 Flow 3 Flow 4
Flow 5

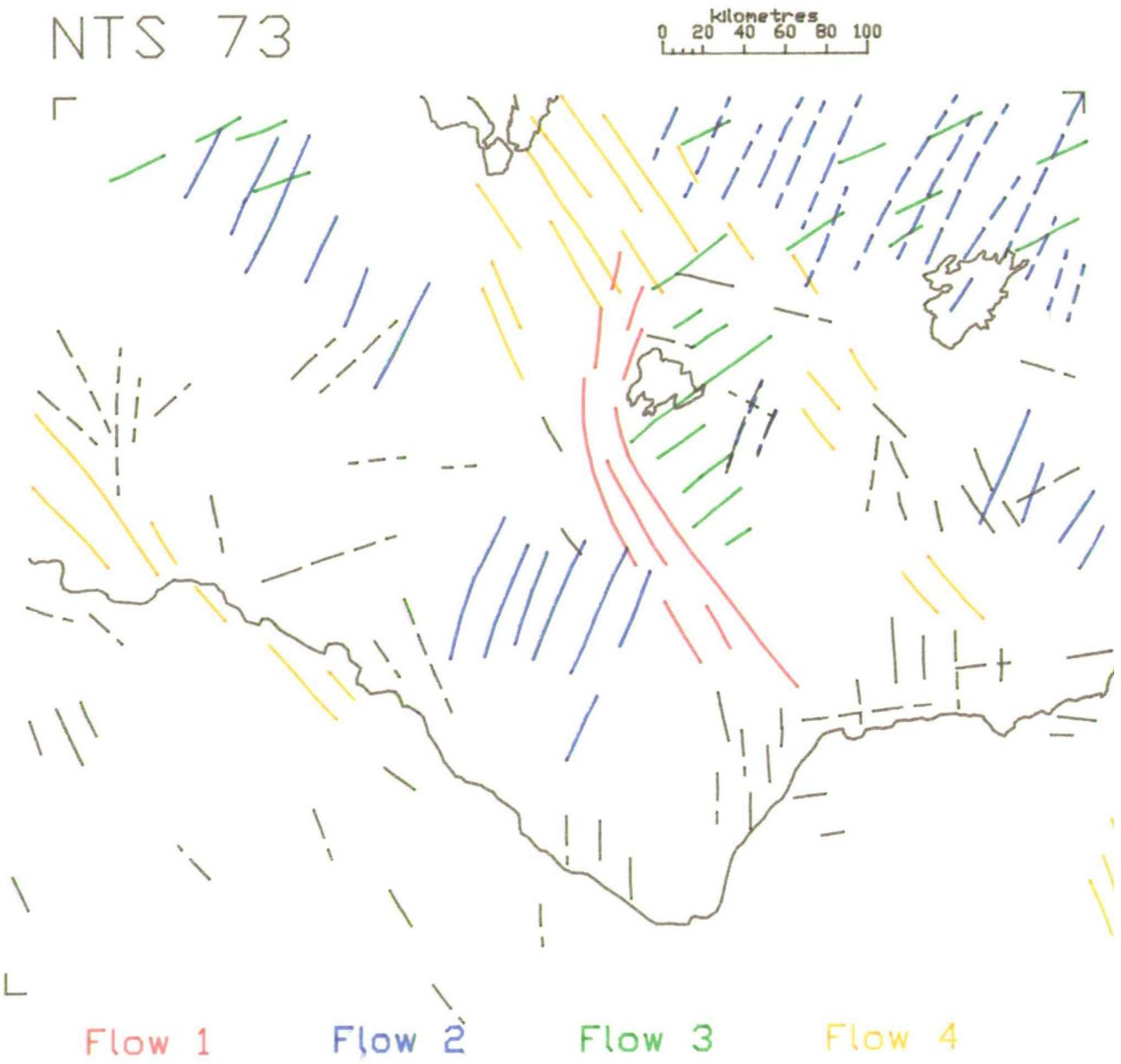
NTS 73
kilometres
0 20 40 60 80 100
Flow 1
Flow 2
Flow 3
Flow 4

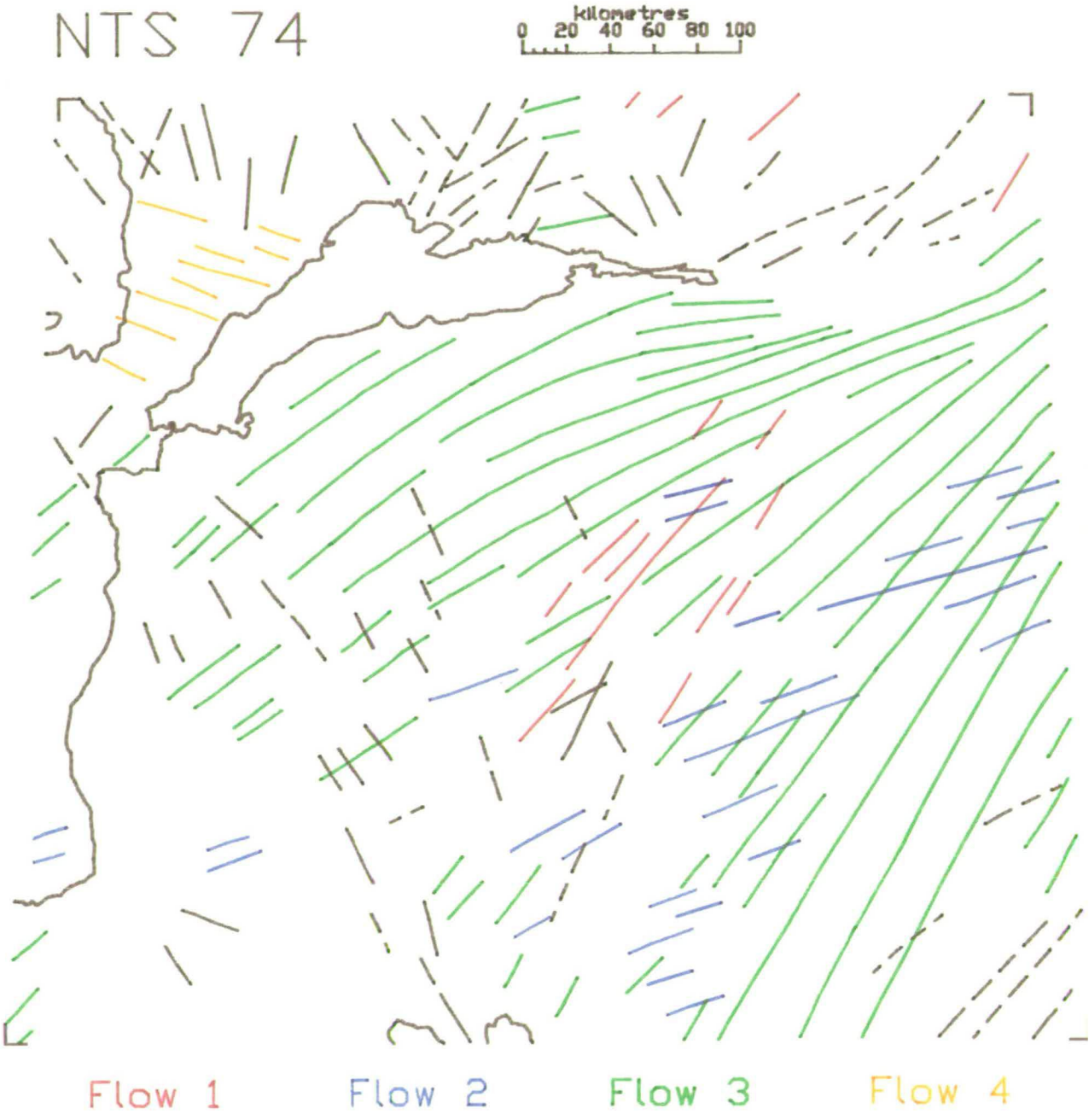
NTS 74
kilometres
0 20 40 60 80 100
Flow 1
Flow 2
Flow 3
Flow 4

NTS 75(a)

kilometres
0 20 40 60 80 100

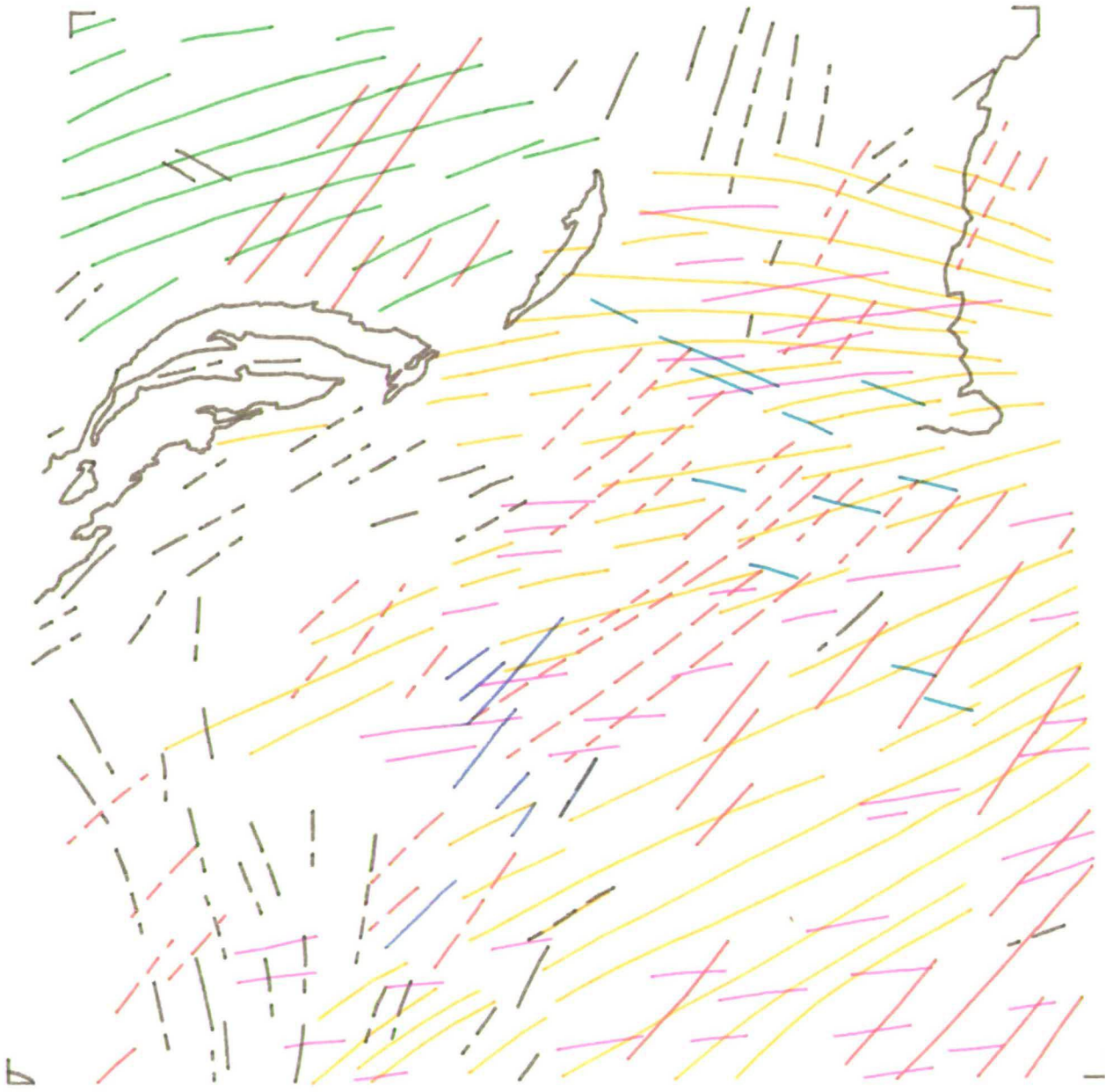

Flow 1 Flow 2 Flow 3 Flow 4 Flow 5 Flow

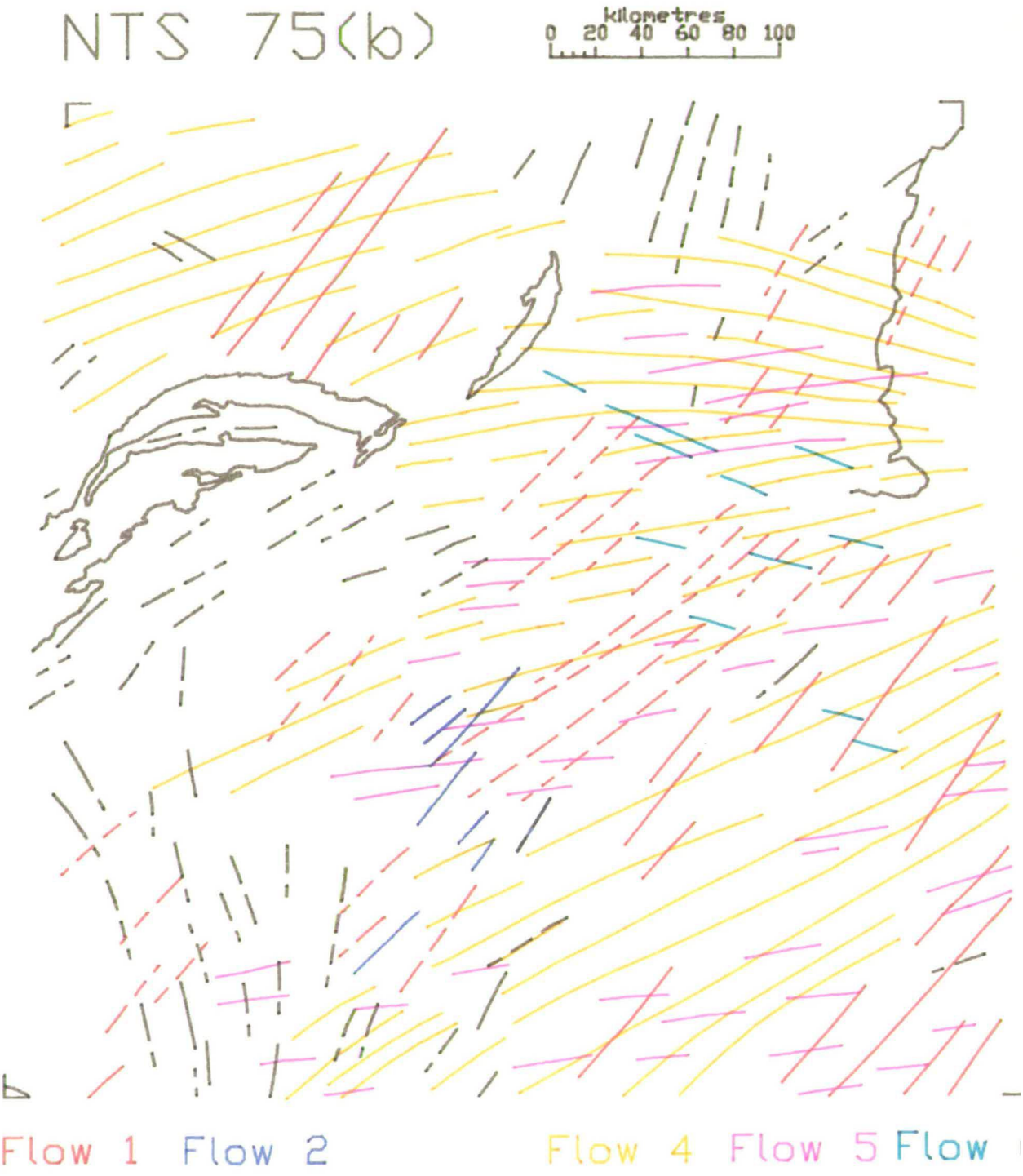
NTS 75(b)
kilometres
0 20 40 60 80 100
Flow 1
Flow 2
Flow 4
Flow 5
Flow

NTS 76

kilometres
0 20 40 60 80 100

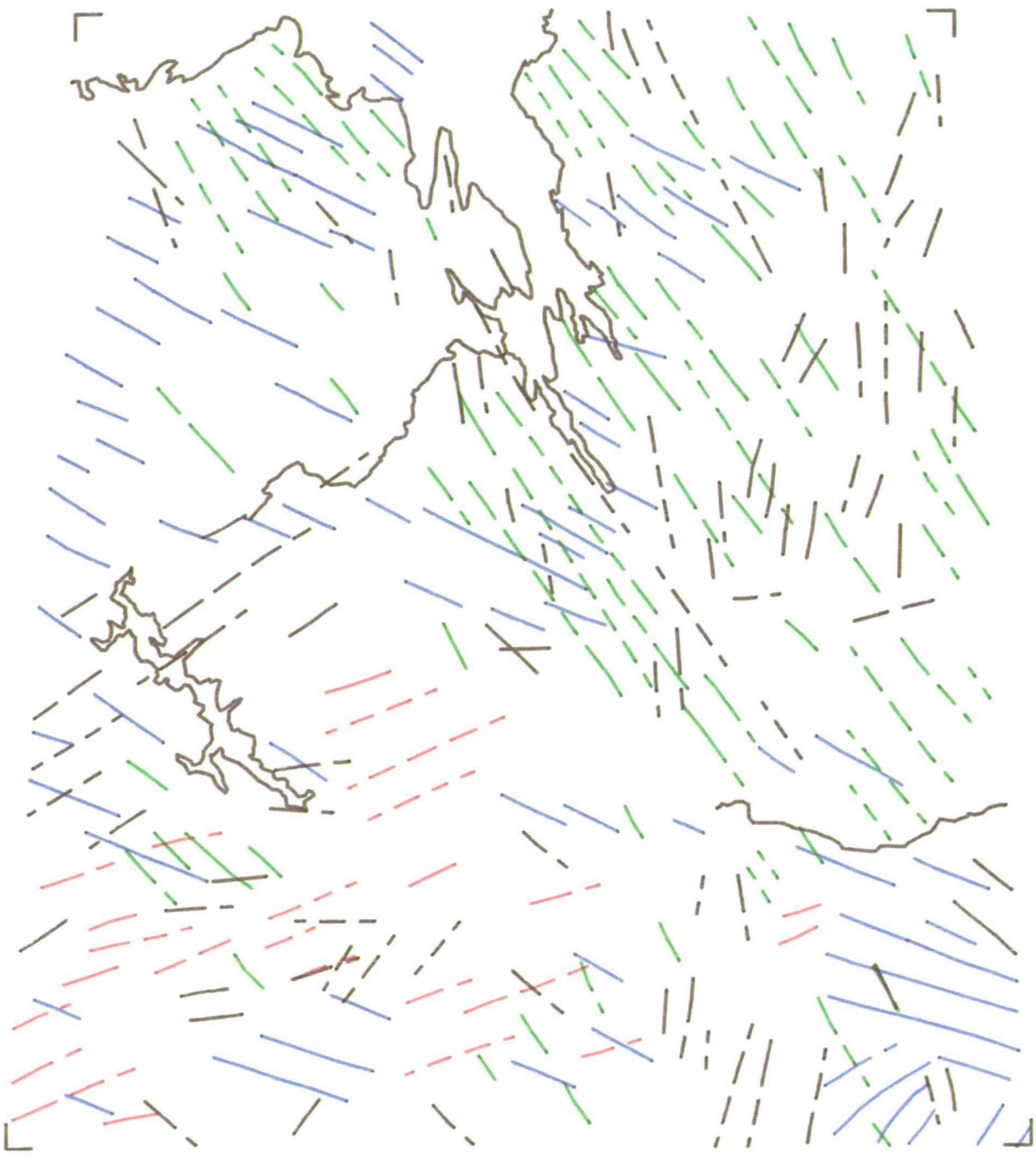

Flow 1 Flow 2 Flow 3

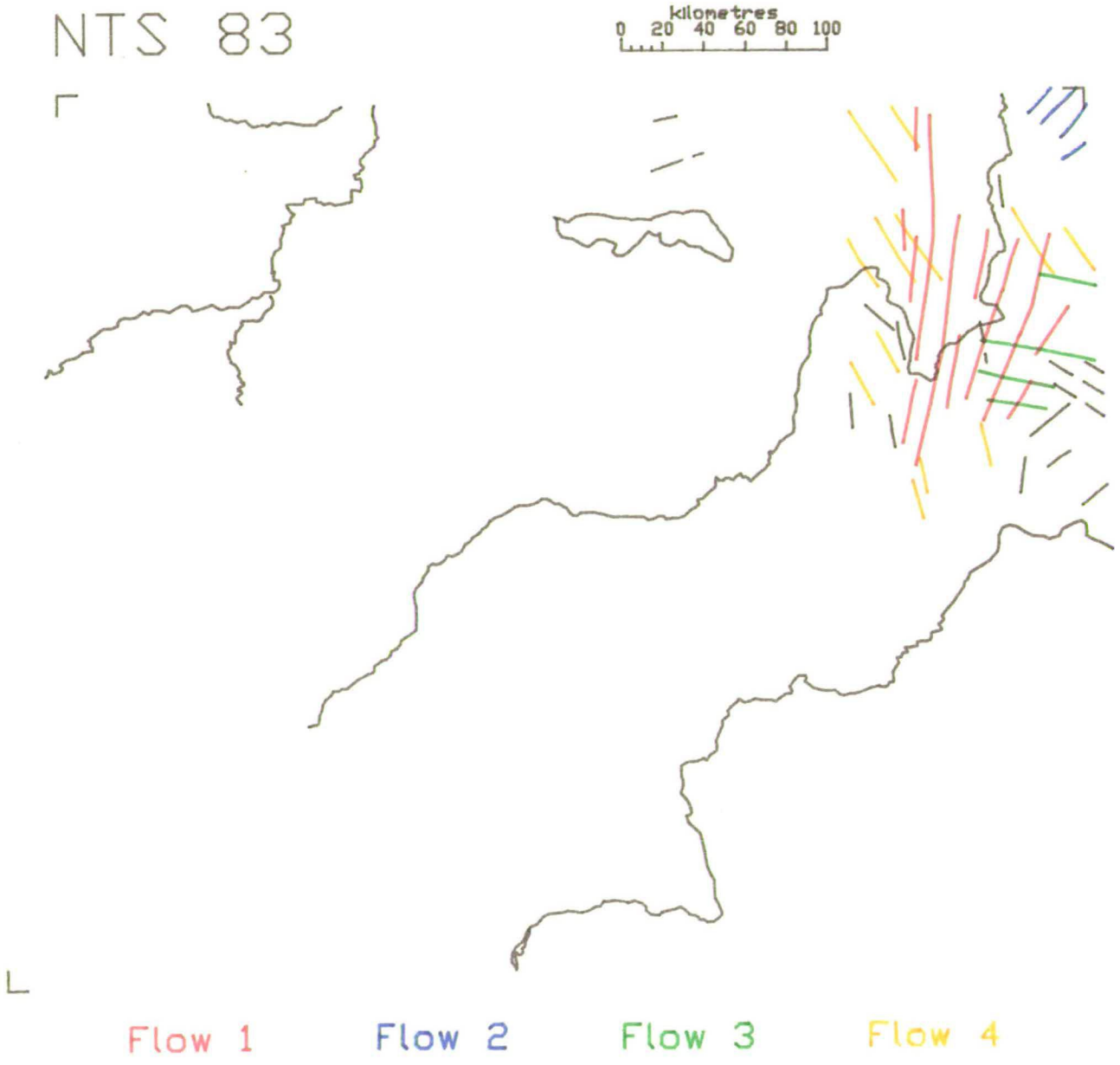
NTS 83
kilometres
0 20 40 60 80 100
Flow 1
Flow 2
Flow 3
Flow 4

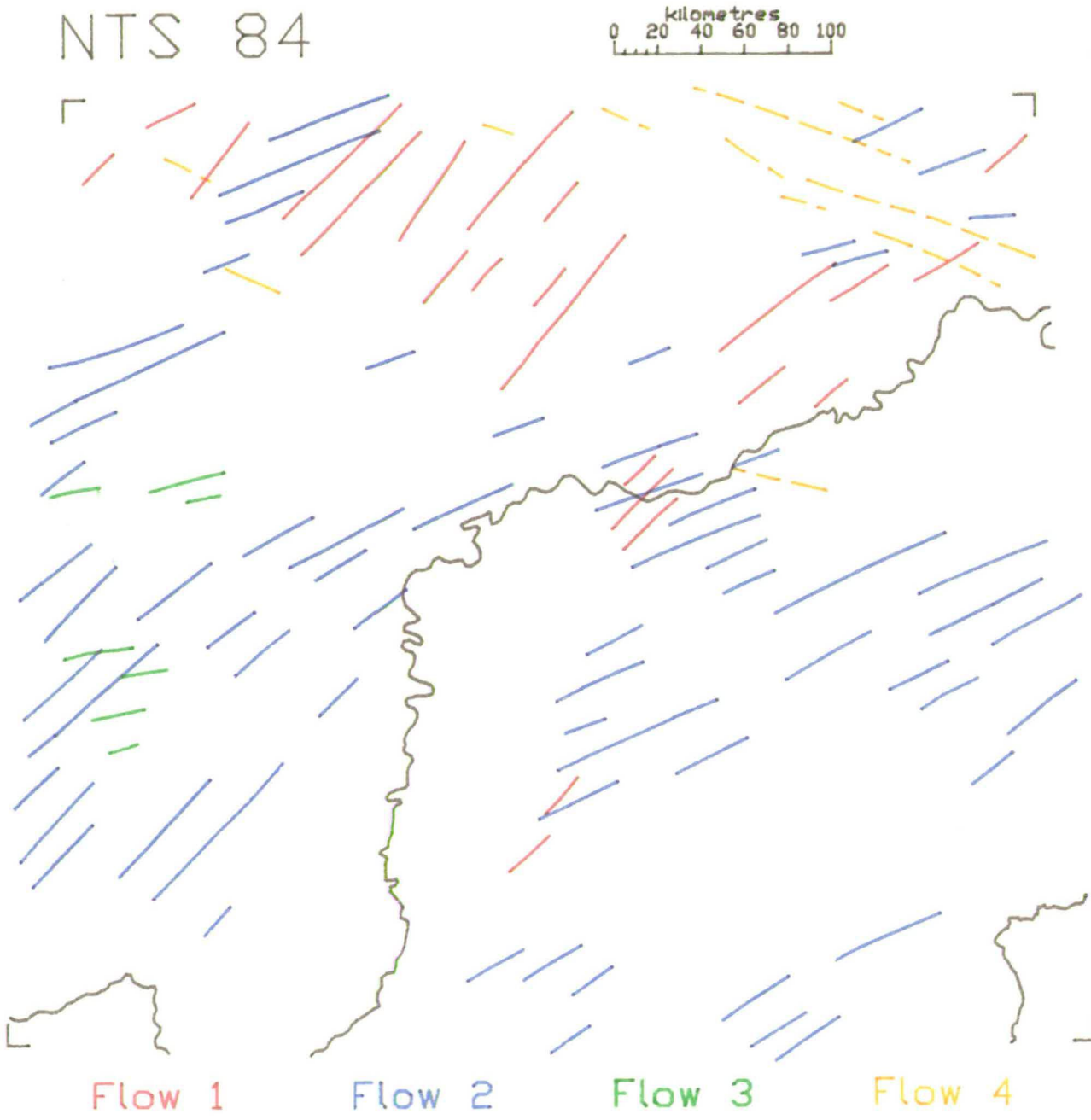
NTS 84
kilometres
0 20 40 60 80 100
Flow 1
Flow 2
Flow 3
Flow 4

NTS 85

kilometres
0 20 40 60 80 100

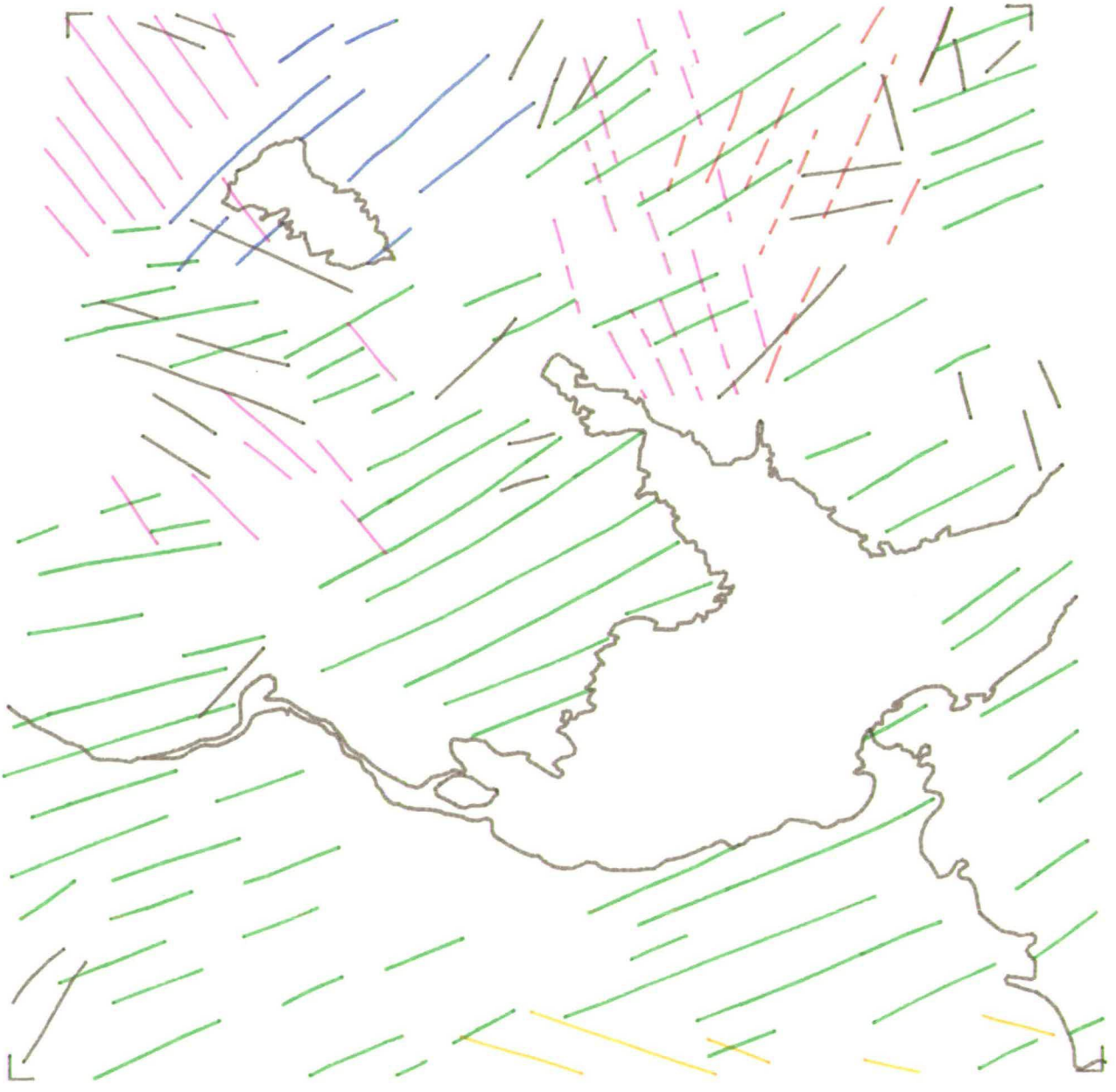

Flow 1 Flow 2 Flow 3 Flow 4 Flow 5

NTS 86

kilometres
0 20 40 60 80 100

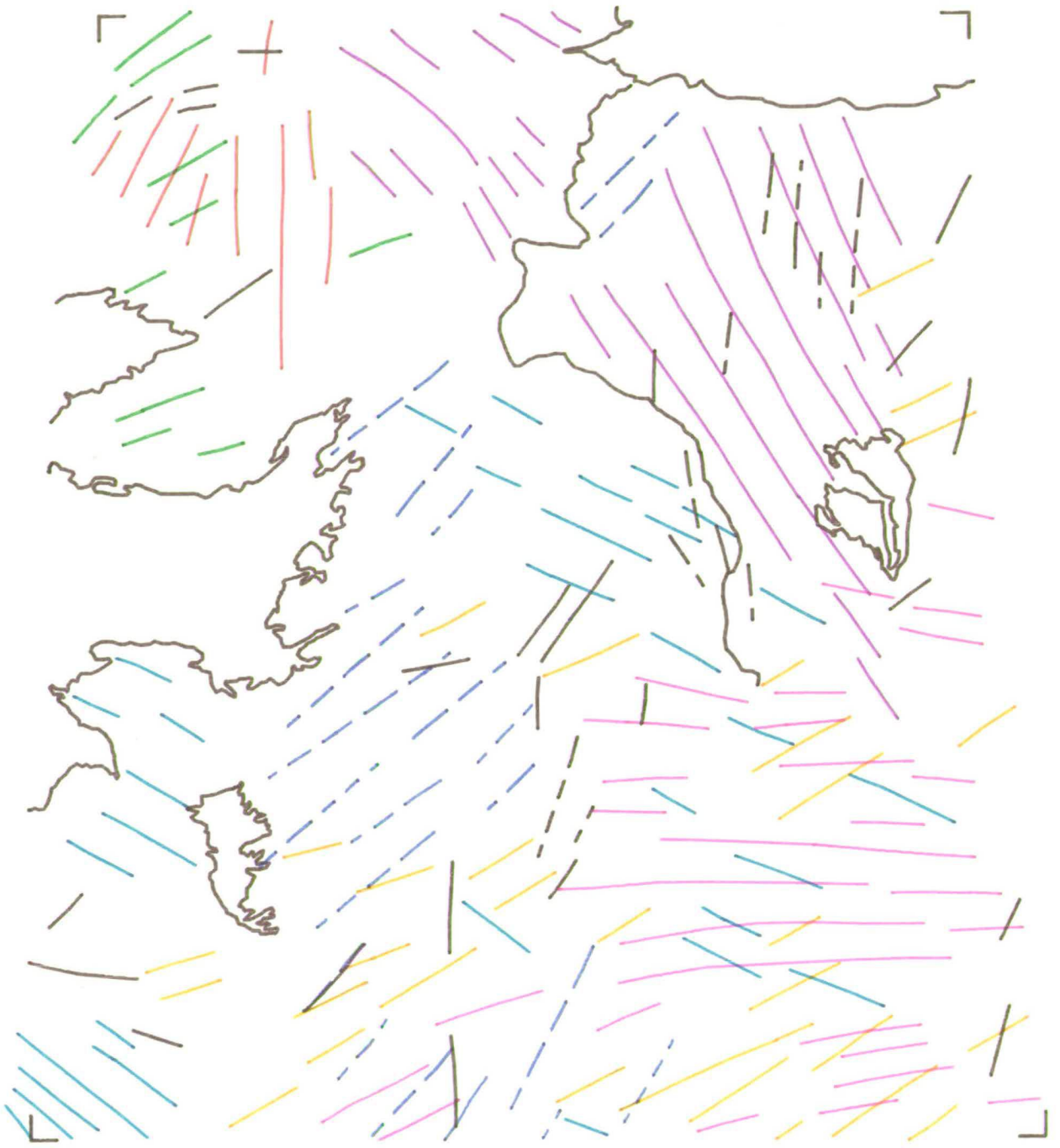

Flow 1 Flow 2 Flow 3 Flow 4 Flow 5
Flow 6 Flow 7

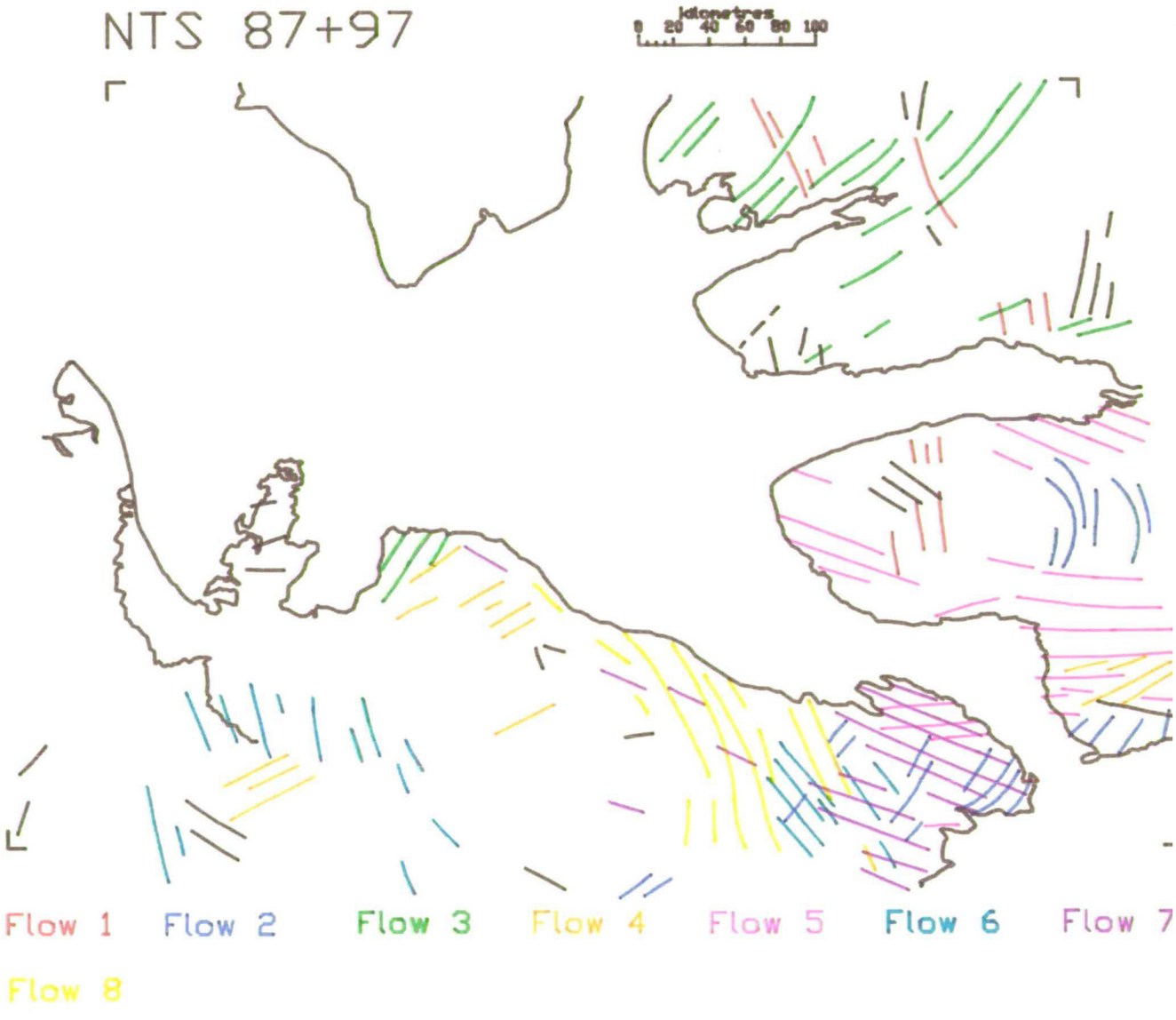
NTS 87+97
kilometres
0 20 40 60 80 100
Flow 1
Flow 2
Flow 3
Flow 4
Flow 5
Flow 6
Flow 7
Flow 8